

**SILANE FUNCTIONALIZED COMPOSITE MATERIALS IN
THE REMEDIATION OF AQUATIC ENVIRONMENT
CONTAMINATED WITH SOME MICRO-POLLUTANTS AND
HEAVY METAL TOXIC IONS**

**A THESIS SUBMITTED IN PARTIAL FULFILLMENT OF THE
REQUIREMENTS FOR THE DEGREE OF DOCTOR OF
PHILOSOPHY**

R.MALSAWMDAWNGZELA

MZU REGISTRATION NUMBER: 882 OF 2007-08

PH.D REGISTRATION NUMBER: MZU/PH.D/848 OF 21.4.2016



**DEPARTMENT OF CHEMISTRY
SCHOOL OF PHYSICAL SCIENCES**

NOVEMBER, 2021

**SILANE FUNCTIONALIZED COMPOSITE MATERIALS IN THE
REMEDICATION OF AQUATIC ENVIRONMENT CONTAMINATED WITH
SOME MICRO-POLLUTANTS AND HEAVY METAL TOXIC IONS**

BY
R. MALSAWMDAWNGZELA
Department of Chemistry

Under the supervision of
Prof. DIWAKAR TIWARI

Submitted

In partial fulfilment of the requirement of the Degree of Doctor of Philosophy in
Chemistry of Mizoram University, Aizawl.



MIZORAM UNIVERSITY
Department of Chemistry
(A DST-FIST Supported Department)
Tanhril, Aizawl, Mizoram. PIN: 796004

Prof. Diwakar Tiwari, Dean (SPS)

Thesis Certificate

This is hereby certified that the research work for the dissertation entitled “*Silane Functionalized Composite Materials in the Remediation of Aquatic Environment Contaminated with Some Micro-Pollutants and Heavy Metal Toxic Ions*” submitted by **R. Malsawmdawngzela** to Mizoram University, Tanhril, Aizawl, for the award of the Degree of Doctor of Philosophy in Chemistry is *bona fide* record of the research work carried by under my supervision. The contents of this dissertation, in full or in parts, have not been submitted to any other Institute or University for the award of any degree or diploma.

Tanhril, Aizawl-04
Date :

(DIWAKAR TIWARI)

Supervisor

Tanhril Campus, Aizawl 796 004
Fax : (0389) 233 0834

Phone : 9862323015
E-mail : diw_tiwari@yahoo.com

Declaration of the Candidate

Mizoram University

November, 2021

I, R. Malsawmdawngzela, hereby declare that the subject matter of this thesis is the record of work done by me, that the contents of this thesis did not form basis of the award of any previous degree to me or to the best of my knowledge to anybody else, and that the thesis has not been submitted by me for any research degree in any other University/Institute.

This is being submitted to the Mizoram University for the degree of Doctor of Philosophy in Chemistry.

(R. Malsawmdawngzela)

Candidate

(Prof. DIWAKAR TIWARI)

Head

(Prof. DIWAKAR TIWARI)

Supervisor

ACKNOWLEDGEMENT

First and foremost, I would like to thank God Almighty for giving me the strength, knowledge, ability and opportunity to undertake this research study. Without his blessings, this achievement would not have been possible.

I would like to express my sincere gratitude to my supervisor, *Prof. Diwakar Tiwari*, Department of Chemistry, Mizoram University, for the patient guidance, encouragement and advice he has provided throughout my time as his student. I have been extremely lucky to have a supervisor who cared so much about my work, and who responded to my questions and queries so promptly

I extend my thanks to *Professor Seung-Mok Lee* and his team, Department of Environmental Engineering, Kwandong University, Gangneung, Korea for inviting me to work in his laboratory and providing me with the facilities during my stay in South Korea. Their valuable help in every possible ways to the success of my research is greatly acknowledged.

I am extremely grateful to *Dr. Lalhmunsiamama*, Department of Industrial Chemistry, Mizoram University for his valuable support, patience and suggestion for the completion of my research work.

I would also like to express my gratitude to *Prof. Muthukumaran, R., Head, Department of Chemistry, MZU, and other faculty members viz., Dr. N. Mohondas Singh, Dr. A. Bimolini Devi, Dr. Zodinpuia Pachuau and Dr. Ved Prakash Singh* for their encouragement, support and innovative suggestions while carrying out my research work.

I am very happy to acknowledge the cooperation and help I received from all my fellow research scholars in the Department of Chemistry. I thank *Ms. J. Lalmalsawmi, Ms. Ngainunsiami, Mr. Sarikokba, Mr. CVL Hmingmawia, Mr. Levia Lalthazuala, Mr. Ricky Lalawmpuia, and Mr. Himangshu Dihingia* for their valuable help and assisting me in my research work. I also thank *Dr. Thanhmingliana, Dr. Lalchhingpuii, Dr. Zirlianggura, Dr. C. Lalhriatpuia and Dr. Lalsaimawia* for their support and encouragement during my research work. It is my pleasure to mention the help of *Mr. Brojendro Singh Shagolsem*, Sr. Laboratory Technician, and *Mr. John Vanlalhraia*, Technical assistant, Chemistry Department. I put forth my deep sense of gratitude to them.

My acknowledgement would be incomplete without thanking the biggest source of my strength, my family. The love and support they gave me throughout my research work.

I would also like to say a big thank you to all those, whose names I may have unintentionally omitted. God bless you all.

R. Malsawmdawngzela

TABLE OF CONTENTS

	<i>Pages</i>
Title of the Thesis	i
Certificate	ii
Declaration of the Candidate	iii
Acknowledgements	iv
Table of Contents	vi
List of Tables	xii
List of Figures	xv

CHAPTER 1

1. INTRODUCTION

1.1. BACKGROUND	1
------------------------	---

1.2. FATE OF POLLUTANTS AND THEIR TOXICITY

1.2.1. HEAVY METALS AND METALLOIDS	4
---	---

1.2.1.1. Arsenic	4
------------------	---

1.2.1.2. Cadmium	5
------------------	---

1.2.1.3. Copper	6
-----------------	---

1.2.2. MICRO-POLLUTANTS

1.2.2.1. Tetracycline(TC)	7
---------------------------	---

1.2.2.2. Triclosan(TCS)	8
-------------------------	---

1.2.2.3 17 α -Ethinylestradiol(EE2)	9
--	---

1.3. REMOVAL OF HEAVY METALS	10
1.4. MICRO-POLLUTANTS REMOVAL TECHNIQUES	13
1.5. ADSORPTION	14
1.5.1. FACTORS AFFECTING ADSORPTION PROCESS	15
1.6. COMMONLY USED ADSORBENTS	17
1.6.1. Activated carbon	17
1.6.2. Agricultural waste/byproducts	18
1.6.3. Industrial byproducts/residues	18
1.6.4. Biomasses and Bio-sorbents	19
1.6.5. Carbon nanotubes	20
1.6.6. Zeolites	21
1.7. REVIEW OF LITERATURE	21
1.8. SCOPE OF THE PRESENT INVESTIGATION	30

CHAPTER – 2

2. METHODOLOGY	
2.1. MATERIALS AND APPARATUSE	32
2.1.1. Ultraviolet–Visible (UV–Vis) spectroscopy	33
2.1.2. Atomic Absorption Spectroscopy (AAS)	35
2.2. METHODS	
2.2.1. Preparation of silane functionalized bentonite clay	38
2.2.2. Characterization of the materials	38
2.2.3. Determination of pH_{PZC} of the solids	39
2.2.4. Speciation studies	39

2.2.5. Batch reactor experiment	
2.2.5.1. Effect of pH	42
2.2.5.2. Effect of sorptive concentration	42
2.2.5.3. Effect of background electrolyte concentration	43
2.2.5.4. Effect of contact time	43
2.2.5.5. Effect of coexisting ions	44
2.2.6. Adsorption isotherm modelling	
2.2.6.1. Langmuir adsorption isotherm	45
2.2.6.2. Freundlich adsorption isotherm	46
2.2.7. Adsorption kinetic modelling	46
2.2.8. Column experiments	47
2.2.9. Applications to real water samples	48
2.2.10. Desorption and reusability study	49

CHAPTER – 3

3. RESULTS AND DISCUSSION	
3.1. CHARACTERIZATION OF MATERIALS	51
3.1.1. Surface morphology and elemental composition of the materials	51
3.1.2. X-ray <i>diffraction</i> (XRD) analysis	57
3.1.3. Fourier–transform infra–red analyses of solid solids	58
3.1.4. Point of zero charge (pH_{PZC}) of the samples	59
3.1.5. BET analysis of solids samples	60

3.2. SPECIATION STUDIES

3.2.1. Speciation of arsenic(III) and arsenic(V)	63
3.2.2. Speciation of copper(II)	64
3.2.3. Speciation of cadmium(II)	65

3.3. BATCH REACTOR STUDIES

3.3.1. Effect of pH	66
3.3.1.1. Removal of arsenic(III) and arsenic(V)	66
3.3.1.2. Removal of copper(II)	69
3.3.1.3. Removal of cadmium(II)	70
3.3.1.4. Mechanism of copper(II) and cadmium(II) sorption by BNMPTS	72
3.3.1.5. Removal of tetracycline(TC)	76
3.3.1.6. Removal of triclosan(TCS)	80
3.3.1.7. Removal of 17 α -ethinylestradiol (EE2)	82
3.3.2. Effect of sorptive concentration	
3.3.2.1. Arsenic(III) and arsenic(V)	84
3.3.2.2. Copper(II)	86
3.3.2.3. Cadmium(II)	87
3.3.2.4. Tetracycline(TC)	88
3.3.2.5. Triclosan(TCS)	89
3.2.2.6. 17 α -ethinylestradiol (EE2)	90

3.3.3. Adsorption isotherm modeling	
3.3.3.1. Adsorption isotherm modelling for arsenic(III) and arsenic(V)	91
3.3.3.2. Adsorption isotherm modelling for copper(II) and cadmium(II)	93
3.3.3.3. Adsorption isotherm modelling for tetracycline, triclosan and EE2	96
3.3.4. Effect of contact time	
3.3.4.1. Arsenic(III) and arsenic(V)	102
3.3.4.2. Copper(II)	104
3.3.4.3. Cadmium(II)	105
3.3.4.4. Tetracycline(TC)	106
3.3.4.5. Triclosan(TCS)	107
3.3.4.6. 17 α -ethinylestradiol (EE2)	108
3.3.5. Kinetic modelling studies	
3.3.5.1. Arsenic(III) and arsenic(V)	109
3.3.5.2. Copper(II)	111
3.3.5.3. Cadmium(II)	113
3.3.5.4. Tetracycline(TC)	114
3.3.5.5. Triclosan(TCS)	116
3.3.5.6. 17 α -ethinylestradiol (EE2)	118

3.3.6. Effect of background electrolyte concentrations	
3.3.6.1. Arsenic(III) and Arsenic(V)	121
3.3.6.2. Copper(II)	123
3.3.6.3. Cadmium(II)	124
3.3.6.4. Tetracycline(TC)	125
3.3.6.5. Triclosan(TCS)	126
3.3.6.6. 17 α -ethinylestradiol (EE2)	127
3.3.7. Effect of co-existing ions in the removal of arsenic(III) and arsenic(V)	129
3.3.8. Effect of co-existing ions in the removal of copper(II) and cadmium(II)	131
3.3.9. Effect of co-existing ions in the removal of tetracycline, triclosan and EE2	135
3.4. COLUMN REACTOR STUDIES	
3.4.1. Copper(II)	140
3.4.2. Cadmium(II)	142
3.4.3. Tetracycline, triclosan and EE2	145
3.5. Applications of BNMPTS and BNAPTES in real water sample	153
3.6. Desorption and reusability of the solids	156

CHAPTER-4

4. CONCLUSIONS 161

REFERENCES

Bio Data

List of Publications

Conferences and Seminar

LIST OF TABLES

Tables	Page
2.1 Various equilibrium constants used for the speciation of As(III) in aqueous solutions at 25 °C.	40
2.2 Various equilibrium constants used for the speciation of As(V) in aqueous solutions at 25 °C.	40
2.3 Various equilibrium constants used for the speciation of Cu(II) in aqueous solutions at 25 °C.	40
2.4 Various equilibrium constants used for the speciation of Cd(II) in aqueous solutions at 25 °C.	41
3.1 The pH_{PZC} values obtained for the BN, BNMPTS and BNAPTES solids.	60
3.2 BET pore size, specific pore volume and specific surface area values of pristine bentonite (BN), BNMPTS and BNAPTES solids.	62
3.3 Langmuir and Freundlich constants estimated for the adsorption of As(III) and As(V) using functionalized materials.	92

List of Tables (continued)	Page
3.4 Langmuir and Freundlich adsorption isotherm constants along with the R^2 values obtained for the adsorption of Cu(II) and Cd(II) using BNMPTS material.	94
3.5 Langmuir and Freundlich constants estimated for sorption of tetracycline using BNMPTS and BNAPTES solids.	97
3.6 Langmuir and Freundlich isotherm constants estimated for the sorption of triclosan using BNMPTS and BNAPTES solids.	99
3.7 Langmuir and Freundlich isotherm constants estimated for the sorption of EE2 using BNMPTS and BNAPTES solids.	101
3.8 Predicted kinetic parameters for pseudo-first order (PFO) and pseudo-second order (PSO) kinetic models in the sorption of As(III) by BNMPTS and As(V) by BNAPTES.	110
3.9 Predicted kinetic parameters for pseudo-first order (PFO) and pseudo-second order (PSO) kinetic models in the sorption of Cu(II) by the BNMPTS solid.	112
3.10 Predicted kinetic parameters for pseudo-first order (PFO) and pseudo-second order (PSO) kinetic models in the sorption of Cd(II) by the BNMPTS solid.	113
3.11 Predicted kinetic parameters for pseudo-first order (PFO) and pseudo-second order (PSO) kinetic models in the sorption of tetracycline by the BNMPTS and BNAPTES solids.	115

List of Tables (continued)	Page
3.12 Predicted kinetic parameters for pseudo-first order (PFO) and pseudo-second order (PSO) kinetic models in the sorption of triclosan by the BNMPTS and BNAPTES solids.	117
3.13 Predicted kinetic parameters for pseudo-first order (PFO) and pseudo-second order (PSO) kinetic models in the sorption of EE2 by the BNMPTS and BNAPTES solids.	119
3.14 Thomas constants estimated for the removal of Cu(II) by BNMPTS material. ([Cu(II)]: 10.0 mg/L; Flow rate: 1.0 mL/min; pH: 4.0; Amount of solid loaded: 0.25/or 0.50 g; Temperature: 25°C).	141
3.15 Thomas constants estimated for the removal of Cd(II) by BNMPTS material ([Cd(II)]: 5.0 mg/L; Flow rate: 1.0 mL/min; pH: 5.0; Amount of solid loaded: 0.25/or 0.50 g; Temperature: 25°C).	143
3.16 Thomas constants estimated for the removal of tetracycline by BNMPTS and BNAPTES ([TC]: 10.0 mg/L; Flow rate: 1.0 mL/min; pH: 4.0; Amount of solid loaded: 0.25/0.50 g; Temperature: 25°C).	146
3.17 Thomas constants estimated for the removal of triclosan by BNMPTS and BNAPTES ([TCS]: 10.0 mg/L; Flow rate: 1.0 mL/min; pH: 4.0; Amount of solid loaded: 0.25/0.50 g; Temperature: 25°C).	149
3.18 Thomas constants estimated for the removal of EE2 by BNMPTS and BNAPTES ([EE2]: 10.0 mg/L; Flow rate: 1.0 mL/min; pH: 4.0; Amount of solid loaded: 0.25/0.50 g; Temperature: 25°C).	151
3.19 Different parameters result obtained from real water sample.	154

LISTS OF FIGURES

Fig. No.	Title	Page
1.1	Structure of tetracycline	7
1.2	Structure of triclosan.	8
1.3	Structure of EE2.	9
3.1	SEM images of (a) pristine bentonite (BN); (b) BNMPTS; and (c) BNAPTES.	53
3.2	EDX mapping of (a) pristine bentonite (BN); (b) BNMPTS; and (c) BNAPTES.	54
3.3	TEM images of (a) BN; (b) BNMPTS; and (c) BNAPTES	56
3.4	X-ray diffraction pattern of BN, BNMPTS and BNAPTES.	57
3.5	Fourier transform-infrared spectra of bentonite (BN), BNMPTS and BNAPTES solids.	59
3.6	Plots of initial pH vs final pH of various solid materials viz., pristine bentonite (BN), BNMPTS and BNAPTES.	60
3.7	Nitrogen adsorption-desorption isotherms for (a) pristine bentonite (BN); (b) BNMPTS; and (c) BNAPTES solids.	62
3.8	Percentage distribution of various species of (a) As(III) and; (b) As(V) as a function of pH ([As(III)/ or As(V)]: 10.0 mg/L; Temperature: 25°C).	64
3.8(c)	Percentage distribution of various species of Cu(II) as a function of pH ([Cu(II)]: 10.0 mg/L; Temperature: 25°C).	65
3.8(d)	Percentage distribution of various species of Cd(II) as a function of pH ([Cd(II)]: 10.0 mg/L; Temperature: 25°C).	65

Lists of Figures (continued)	Page
3.9 Effect of pH in the removal of (a) As(III) by the BNMPTS; and (b) As(V) by the BNAPTES solids ([As(III)/ or As(V)]: 10.0 mg/L; Solid dose: 2.0 g/L; Temperature: 25°C).	68
3.10 Effect of pH in the removal of Cu(II) by BNMPTS ([Cu(II)]: 10.0 mg/L; Solid dose: 2.0 g/L; Temperature: 25°C).	70
3.11 Effect of pH in the removal of Cd(II) by BNMPTS ([Cd(II)]: 10.0 mg/L; Solid dose: 2.0 g/L; Temperature: 25°C).	72
3.12 (a) XPS spectra of BNMPTS before adsorption of Cu(II) and Cd(II); (b) XPS spectra of BNMPTS after adsorption of Cd(II); and (c) XPS spectra of BNMPTS after adsorption of Cu(II).	75
3.13 (a) O1s spectra before and after adsorption of Cu(II) and Cd(II) using BNMPTS; (b) S2p spectra before and after adsorption of Cu(II) and Cd(II) using BNMPTS; and (c) Schematic of sorption of Cu ²⁺ and Cd ²⁺ by the BNMPTS solid.	76
3.14 Percentage removal of tetracycline by pristine bentonite and functionalized bentonite (BNMPTS and BNAPTES) as a function of pH ([TC]: 10.0 mg/L; Solid dose: 2.0 g/L; Temperature: 25°C).	76
3.15 Percentage distribution of tetracycline (TC) as a function of pH ([TC]: 10.0 mg/L; Temperature: 25°C).	76

Lists of Figures (continued)	Page
3.16 Percentage removal of triclosan (TCS) by pristine bentonite and functionalized materials (BNMPTS and BNAPTES) as a function of pH ([TCS]: 10.0 mg/L; Solid dose: 2.0 g/L; Temperature: 25°C).	81
3.17 Percentage distribution of triclosan (TCS) as a function of pH ([TCS]: 10.0 mg/L; Temperature: 25°C).	81
3.18 Percentage removal of EE2 by pristine bentonite and functionalized bentonite solids (BNMPTS and BNAPTES) as a function of pH ([EE2]: 10.0 mg/L; Solid dose: 2.0 g/L; Temperature: 25°C).	83
3.19 Percentage distribution of 17 α -ethinylestradiol (EE2) as a function of pH ([EE2]: 10.0 mg/L; Temperature: 25°C).	84
3.20 Effect of initial sorptive concentration in the removal of (a) As(III) by BNMPTS; and (b) As(V) by BNAPTES (pH: 3.5; Solid dose: 2.0 g/L; Temperature: 25°C).	85
3.21 Effect of initial sorptive concentration in the removal of Cu(II) by BNMPTS (pH: 4.0; Solid dose: 2.0 g/L; Temperature: 25°C).	86
3.22 Effect of initial sorptive concentration in the removal of Cd(II) by BNMPTS solid (pH: 5.0; Solid dose: 2.0 g/L; Temperature: 25°C).	87
3.23 Percentage removal of tetracycline by the BNMPTS and BNAPTES materials as a function of initial tetracycline concentrations (pH: 4.0; Solid dose: 2.0 g/L; Temperature: 25°C).	88

Lists of Figures (continued)	Page
3.24 Percentage removal of triclosan by the BNMPTS and BNAPTES solids as a function of initial triclosan concentrations (pH: 4.0; Solid dose: 2.0 g/L; Temperature: 25°C).	89
3.25 Percentage removal of EE2 by the BNMPTS and BNAPTES solids as a function of initial EE2 concentrations (pH: 4.0; Solid dose: 2.0 g/L; Temperature: 25°C).	90
3.26 Fitting of (a) Langmuir adsorption isotherm for the adsorption of As(III) onto BNMPTS and As(V) onto the BNAPTES; and (b) Freundlich adsorption isotherms for As(III) onto BNMPTS and As(V) onto BNAPTES solids.	93
3.27 Fitting of (a) Langmuir adsorption; and (b) Freundlich adsorption isotherms in the sorption of Cu(II) and Cd(II) by BNMPTS material.	95
3.28 Fitting of concentration dependence data to the (a) Langmuir adsorption; and (b) Freundlich adsorption isotherms in the sorption of tetracycline by BNMPTS and BNAPTES solids.	98
3.29 Fitting of concentration dependence data to the (a) Langmuir adsorption; and (b) Freundlich adsorption isotherms in the sorption of triclosan by the BNMPTS and BNAPTES solids.	100
3.30 Fitting of concentration dependence data to the (a) Langmuir adsorption; and (b) Freundlich adsorption isotherms in the sorption of EE2 by the BNMPTS and BNAPTES materials.	102

Lists of Figures (continued)	Page
3.31 Effect of contact time in the removal of (a) As(III) by BNMPTS and; (b) As(V) by BNAPTES solids ([As(III)/or As(V)]: 10.0 mg/L; pH: 3.5; Solid dose: 2.0 g/L; Temperature: 25°C).	103
3.32 Effect of contact time in the removal of Cu(II) by the BNMPTS solid ([Cu(II)]: 10.0 mg/L; pH: 4.0; Solid dose: 2.0 g/L; Temperature: 25°C).	104
3.33 Effect of contact time in the removal of Cd(II) by the BNMPTS solid ([Cd(II)]: 5.0 mg/L; pH: 5.0; Solid dose: 2.0 g/L; Temperature: 25°C).	105
3.34 Effect of contact time in the removal of tetracycline by the BNMPTS and BNAPTES solids ([TC]: 10.0 mg/L; pH: 4.0; Solid dose: 2.0 g/L; Temperature: 25°C).	106
3.35 Effect of contact time in the removal of triclosan by the BNMPTS and BNAPTES solids ([TCS]: 10.0 mg/L; pH: 4.0; Solid dose: 2.0 g/L; Temperature: 25°C).	107
3.36 Effect of contact time in the removal of EE2 by the BNMPTS and BNAPTES solids ([EE2]: 10.0 mg/L; pH: 4.0; Solid dose: 2.0 g/L; Temperature: 25°C).	108
3.37 Plots of PFO and PSO kinetic models for the sorption of (a) As(III) by BNMPTS; and (b) As(V) by BNAPTES ([As(III)/ or As(V)]: 10.0 mg/L; pH: 3.5; Solid dose: 2.0 g/L; Temperature: 25°C).	111

Lists of Figures (continued)	Page
3.38 Plots of PFO and PSO kinetic models for the sorption of Cu(II) by the BNMPTS solid ([Cu(II)]: 10.0 mg/L; pH: 4.0; Solid dose: 2.0 g/L; Temperature: 25°C).	112
3.39 Plots of PFO and PSO kinetic models for the sorption of Cd(II) by the BNMPTS solid ([Cd(II)]: 5.0 mg/L; pH: 5.0; Solid dose: 2.0 g/L; Temperature: 25°C).	114
3.40 Plots of PFO and PSO kinetic models for the sorption of tetracycline by (a) BNMPTS and; (b) BNAPTES solids ([TC]: 10.0 mg/L; pH: 4.0; Solid dose: 2.0 g/L; Temperature: 25°C).	116
3.41 Plots of PFO and PSO kinetic models for the sorption of triclosan by (a) BNMPTS; and (b) BNAPTES solids ([TCS]: 10.0 mg/L; pH: 4.0; Solid dose: 2.0 g/L; Temperature: 25°C).	118
3.42 Plots of the PFO and PSO kinetic models for the sorption of EE2 by (a) BNMPTS; and (b) BNAPTES solids ([EE2]: 10.0 mg/L; pH: 4.0; Solid dose: 2.0 g/L; Temperature: 25°C).	120
3.43 Effect of background electrolyte concentrations in the removal of (a) As(III) by the BNMPTS solid and; (b) As(V) by the BNAPTES Solid ([As(III)/ or As(V)]: 10.0 mg/L; pH: 3.5; Solid dose: 2.0 g/L; Temperature: 25°C).	122
3.44 Effect of background electrolyte concentrations (NaCl) in the removal of Cu(II) by the BNMPTS solid ([Cu(II)]: 10.0 mg/L; pH: 4.0; Solid dose: 2.0 g/L; Temperature: 25°C).	123

Lists of Figures (continued)	Page
3.45 Effect of background electrolyte concentrations (NaCl) in the removal of Cd(II) by the BNMPTS solids ([Cd(II)]: 5.0 mg/L; pH: 5.0; Solid dose: 2.0 g/L; Temperature: 25°C).	124
3.46 Effect of background electrolyte concentrations (NaCl) in the removal of tetracycline by the BNMPTS and BNAPTES solids ([TC]: 10.0 mg/L; pH: 4.0; Solid dose: 2.0 g/L; Temperature: 25°C).	126
3.47 Effect of background electrolyte concentrations (NaCl) in the removal of triclosan by the BNMPTS and BNAPTES solids ([TCS]: 10.0 mg/L; pH: 4.0; Solid dose: 2.0 g/L; Temperature: 25°C).	127
3.48 Effect of background electrolyte concentrations in the removal of EE2 by the BNMPTS and BNAPTES solids ([EE2]: 10.0 mg/L; pH: 4.0; Solid dose: 2.0 g/L; Temperature: 25°C).	128
3.49 Effect of co-existing cations in the removal of As(III) by the BNMPTS solid ([As(III)]: 10.0 mg/L; [Cations]: 50.0 mg/L; pH: 3.5; Solid dose: 2.0 g/L; Temperature: 25°C).	130
3.50 Effect of co-existing anions in the removal of As(V) by the BNAPTES solid ([As(V)]: 10.0 mg/L; [Anions]: 50.0 mg/L; pH: 3.5; Solid dose: 2.0 g/L; Temperature: 25°C).	131

Lists of Figures (continued)	Page
3.51 Effect of co-existing cations in the removal of Cu(II) by the BNMPTS solid ([Cu(II)]: 10.0 mg/L; [Cations]: 50.0 mg/L; pH: 4.0; Solid dose: 2.0 g/L; Temperature: 25°C).	132
3.52 Effect of co-existing anions in the removal of Cu(II) by the BNMPTS solid ([Cu(II)]: 10.0 mg/L; [Anions]: 50.0 mg/L; pH: 4.0; Solid dose: 2.0 g/L; Temperature: 25°C).	133
3.53 Effect of co-existing cations in the removal of Cd(II) by BNMPTS solid ([Cd(II)]: 5.0 mg/L; [Cations]: 50.0 mg/L; pH: 5.0; Solid dose: 2.0 g/L; Temperature: 25°C).	134
3.54 Effect of co-existing anions in the removal of Cd(II) by BNMPTS solid ([Cd(II)]: 5.0 mg/L; [Anions]: 50.0 mg/L; pH: 5.0; Solid dose: 2.0 g/L; Temperature: 25°C).	135
3.55 Effect of co-existing cations in the removal of tetracycline by BNMPTS and BNAPTES solids ([TC]: 10.0 mg/L; [Cations]: 50.0 mg/L; pH: 4.0; Solid dose: 2.0 g/L; Temperature: 25°C).	136
3.56 Effect of co-existing anions in the removal of tetracycline by BNMPTS and BNAPTES solids ([TC]: 10.0 mg/L; [Anions]: 50.0 mg/L; pH: 4.0; Solid dose: 2.0 g/L; Temperature: 25°C).	137

Lists of Figures (continued)	Page
3.57 Effect of co-existing cations in the removal of triclosan by BNMPTS and BNAPTES solids ([TCS]: 10.0 mg/L; [Cations]: 50.0 mg/L; pH: 4.0; Solid dose: 2.0 g/L; Temperature: 25°C).	138
3.58 Effect of co-existing anions in the removal of triclosan by BNMPTS and BNAPTES solids ([TCS]: 10.0 mg/L; [Anions]: 50.0 mg/L; pH: 4.0; Solid dose: 2.0 g/L; Temperature: 25°C).	138
3.59 Effect of co-existing cations in the removal of EE2 by BNMPTS and BNAPTES solids ([EE2]: 10.0 mg/L; [Cations]: 50.0 mg/L; pH: 4.0; Solid dose: 2.0 g/L; Temperature: 25°C).	139
3.60 Effect of co-existing anions in the removal of EE2 by BNMPTS and BNAPTES solids ([EE2]: 10.0 mg/L; [Anions]: 50.0 mg/L; pH: 4.0; Solid dose: 2.0 g/L; Temperature: 25°C).	140
3.61 Breakthrough curves obtained for the removal of Cu(II) by BNMPTS ([Cu(II)]: 10.0 mg/L; Flow rate: 1.0 mL/min; pH: 4.0; Amount of solid loaded: 0.25/or 0.50 g; Temperature: 25°C).	142
3.62 Breakthrough curves obtained for the removal of Cd(II) by BNMPTS solid ([Cd(II)]: 5.0 mg/L; Flow rate: 1.0 mL/min; pH: 5.0; Amount of solid loaded: 0.25/or 0.50 g; Temperature: 25°C).	144

Lists of Figures (continued)	Page
<p>3.63 Breakthrough curves obtained for the removal of tetracycline by BNMPTS and BNAPTES solids ([TC]: 10.0 mg/L; Flow rate: 1.0 mL/min; pH: 4.0; Amount of solid loaded: 0.25/0.50 g; Temperature: 25°C).</p>	147
<p>3.64 Breakthrough curves obtained for the removal of triclosan by BNMPTS and BNAPTES solids ([TCS]: 10.0 mg/L; Flow rate: 1.0 mL/min; pH: 4.0; Amount of solid loaded: 0.25/or 0.50 g; Temperature: 25°C).</p>	150
<p>3.65 Breakthrough curves obtained for the removal of EE2 by BNMPTS and BNAPTES materials ([EE2]: 10.0 mg/L; Flow rate: 1.0 mL/min; pH: 4.0; Amount of solid loaded: 0.25/or 0.50 g; Temperature: 25°C).</p>	152
<p>3.66 Removal of tetracycline in purified water (PW) and real water (RW) using BNMPTS and BNAPTES materials as a function of pH ([TC]: 10.0 mg/L; Solid dose: 2.0 g/L; Temperature: 25°C).</p>	155
<p>3.67 Removal of triclosan in purified water (PW) and real water (RW) using BNMPTS and BNAPTES materials as a function of pH ([TCS]: 10.0 mg/L; Solid dose: 2.0 g/L; Temperature: 25°C).</p>	155
<p>3.68 Removal of EE2 in purified water (PW) and real water (RW) using BNMPTS and BNAPTES materials as a function of pH ([EE2]: 10.0 mg/L; Solid dose: 2.0 g/L; Temperature: 25°C).</p>	156

Lists of Figures (continued)	Page
3.69 Reusability of BNMPTS for the removal of Cu(II) ([Cu(II)]:10.0 mg/L; Solid dose: 2.0 g/L; [HCL]: 0.01 mol/L; pH: 4.0).	159
3.70 Reusability of BNMPTS and BNAPTES for the removal of tetracycline ([TC]:10.0 mg/L; Solid dose: 2.0 g/L; [HCL]: 0.01 mol/L; pH: 6.0).	159
3.71 Reusability of BNMPTS and BNAPTES for the removal of triclosan ([TCS]:10.0 mg/L; Solid dose: 2.0 g/L; [HCL]: 0.01 mol/L; pH: 4.0).	160
3.72 Reusability of BNMPTS and BNAPTES for the removal of EE2 ([EE2]:10.0 mg/L; Solid dose: 2.0 g/L; [HCL]: 0.01 mol/L; pH: 4.0).	160

CHAPTER -1

INTRODUCTION

1. INTRODUCTION

1.1. BACKGROUND

Water is a basic need of living organisms and the supply of clean water is important for healthy life; however, the shortage of clean water has become a serious concern around the globe (Dwivedi, 2017; Kunduru *et al.*, 2017). In recent past, human civilization and climate change showed a huge negative impact on water cycle around the world which threatened the security of water for human thereby disturbing the ecological balance of the environment (Xi *et al.*, 2017). Around 1.41 billion km³ of water is present on the earth's surface. The oceans and seas constitute *Ca* 97.51% of the world's water but because of high concentration of salt, it is not suitable for the human consumption. Fresh water on earth constitutes only *Ca* 2.5%, out of which *Ca* 70% of this fresh water is frozen as ice caps and 30% is present in the soil and underground. Therefore, only 1.01% of fresh water on the earth is readily available for human consumption (El-Ghonemy, 2012; Gleick, 1993; Shanmugam *et al.*, 2004). Therefore, the lack of clean water has become a global concern. Several strategies such as building of dam, conservation of water and transporting of water do not meet or satisfy the high demand of fresh water supply and sometimes supply is seemingly decreased due to several physical or socio-economic constraints. Conventional sources of fresh water viz., streams, rivers and reservoirs are over utilized and often used excessively or even misused; as a result, fresh water sources are under tremendous stress.

The cities are expanding with exponential increase in industrialization needs exceedingly high demand of water but the existing sources are limited which impacted greatly the ecological imbalance (Greenlee *et al.*, 2009). The U.N. has predicted that 2-7 billion peoples around the world are likely to suffer with shortage of water supply by 2050. This implies that *Ca.* 80 nations, having 20% of the global populations may greatly be affected with fresh water supply (United Nations, 2006). The requirement and equal distribution of water in a particular region is influenced by various factors including increased population, unpredictable climate change, public issues, enhanced urbanization/industrialization etc. (Plappally and Lienhard, 2012). Insufficient availability of fresh water and inadequate healthcare system is perhaps one of the main public health concerns in developed or developing nations,

which may deteriorate even more in the upcoming years. About 21% of India's population are provided with wastewater treatment plants and around 79% of the population is suffering from waterborne diseases (Fosshage, 2014).

A rapid growth of industry, increasing population and rapid urbanization resulted with enhanced level of water contamination. Discharge of unprocessed or even partially treated sewage and hazardous industrial effluent, disposal of industrial waste and drainage from farmlands are mainly contaminating the water bodies. Additionally, the improper dumping of solid waste is contributing the contamination of aquatic environment. Further, an analysis results showed that around 14 billion pounds of trashes are dumped into the oceans around the world (Bhatnagar and Sillanpaa, 2010). Water contaminated by human activities is often termed as polluted water and having less suitability for supporting life or living organisms. The natural changes viz., volcanic eruptions, algal blooms, hurricanes and earthquakes lead to deleterious of water quality and impacting greatly the natural ecosystem. Organic and inorganic pollutants are the two major pollutants contaminating water bodies on the surface and the ground waters. Hydrocarbons, polychlorinated biphenyls, cleansing agent, pesticides, lubricants, fats, plasticizers, medicines, fertilizers, etc. are potential organic contaminants (Ali *et al.*, 2012; Schell *et al.*, 2012). Whereas, the inorganic contaminants are typically mineral-based compounds, the most significant forms of inorganic water contaminants are heavy metals and salts (Hu *et al.*, 2010; Wasewar *et al.*, 2020). The fundamental needs for wastewater treatment (WWT) are quality of treated water, low cost, vitality effectiveness and mineral discharge/restoration. Government and policymakers intended to enhance the health of local environment using innovative ideas in wastewater treatment. In order to enhance the long-term reliability of the required treatment capability, the installation of adequate waste water treatment systems are essential (Hassard *et al.*, 2015; Kumar *et al.*, 2020).

It was reported that a significant amount of contaminants are present at concentrations that surpass the permissible levels, creating an imminent danger to the effectiveness of existing waste management systems (Ahmed *et al.*, 2020). The wastewater treatment plants are examined for various parametric studies in order to optimize the suitability and efficacy of these WWTs (Kosek *et al.*, 2020) However, it

is important to ensure that the existing WWTs must provide the environmental safety and efficient to maintain the socio-economic development in large (Ainger *et al.*, 2009). Various technologies are introduced to obtain required efficacy of existing wastewater treatment plants which includes *viz.*, membrane filtration, electrolytic processes, coagulation, oxidation process, froth flotation, ion exchange, activated sludge etc. However, most of these technologies required high cost and sometime less environmentally benign (Jiang *et al.*, 2020; Mahouachi *et al.*, 2020; Sophia and Lima, 2018). Therefore, up to certain level, treatment of waste water using conventional procedures seems to be effective, but these methods are having several disadvantages in terms of high energy requirement, high cost, production of massive side products and production of huge amount of sludges (Mook *et al.*, 2014; Taha *et al.*, 2017). Adsorption is considered to be most versatile method for the treatment of polluted water due to its low cost, easy operation, toxic free, desirable for batch and dynamic operations, reusability and regeneration (Han *et al.*, 2019; Sophia and Lima, 2018)). Moreover, adsorption can eliminate/remove huge amount of contaminants, leading to broader applicability in controlling pollution of water. It is, therefore, suitable for the elimination of variety of water pollutants and finding greater scope of implications in the countries where water pollution is a major concern (Unuabonah and Taubert, 2014).

The adsorption process is greatly investigated using wide range of materials employed as adsorbents. However, the important aspect of material selection is the selectivity and suitability of materials towards the specific water contaminants. The adsorption capacity and effectiveness/expense ratio of the material is additional key factor to be assessed in selecting a sorbent material. On the other hand, the chemical nature and speciation of water pollutants greatly depend upon the nature and concentration of pollutants in the contaminated water. Since the amount of polluted water for treatment mostly carried out in bulk quantities, hence, the highly selective materials are to be chosen for the strategic treatment processes. Moreover, the adsorbent materials, preferably be non-toxic, efficiently retrievable from filters, regenerable, low-cost and abundance in nature (Bhattacharyya and Gupta, 2008). Several cost-effective adsorbents are investigated and employed which include clays and modified clays, activated carbon, silica gel, polymeric resins, activated alumina,

zeolites, low-cost adsorbents from industrial wastes like fly ash, blast furnace slag, dust, sludge, red mud, etc. and agricultural by-products and biomasses (Fu and Wang, 2011; Vardhan *et al.*, 2019). Among these materials the natural clay and modified clay materials received greater attention in recent time because of the natural abundance of clay minerals. Moreover, based on the cation exchange capacity of clay materials, it enables suitable modification for achieving the required selectivity in wastewater treatment strategy. Additionally, the terminal hydroxyl groups allows to functionalize clay with suitable organic silanes and the functionalized materials are found to be highly efficient in the treatment of wastewater of specific concerns (Lazaratou *et al.*, 2020; Yadav *et al.*, 2019; Zhu *et al.*, 2016).

1.2. FATE OF POLLUTANTS AND THEIR TOXICITY

1.2.1. HEAVY METALS AND METALLOIDS

The term ‘Heavy Metals’ generally refers to the group of metals and metalloids with high atomic density above 4 g/cm³ and are found toxic at low metal concentrations (Aprile and De Bellis, 2020; Edelstein and Ben-Hur, 2018). Arsenic, copper, cadmium, lead, zinc, mercury, boron, titanium, strontium, tin, vanadium, nickel, molybdenum, cobalt, chromium and manganese are posing serious environmental concerns due to their persistency, non-biodegradability and associated with high biological toxicity (Abbas *et al.*, 2014; Engwa *et al.*, 2019).

1.2.1.1. Arsenic

Arsenic is extremely toxic element and is released into the environment from human activities along with several natural sources. Presence of arsenic, even at low level, in water is not suitable for human intake and agricultural purposes. Arsenic is the 20th most common element in geosphere, 12th in human body and 14th in sea water (Renu *et al.*, 2018). Arsenic is tasteless, odourless, silver-grey and usually associated with an element carbon (Mora *et al.*, 2019). Arsenic exists both in organic and inorganic forms in the environment in which inorganic form of arsenic (As(V) and As(III)) is prevalent in the environment (Luo *et al.*, 2012). The mobility and toxicity of arsenite (As(III)) in aqueous solutions is higher than arsenate (As(V)) and

the removal of these species from the aquatic environment is a daunting task (Maji *et al.*, 2018). Human and natural activities are responsible for increased concentrations of arsenic in the aqueous solutions (Vithanage *et al.*, 2017). International Agency for Research on Cancer (IARC), has listed arsenic as Group 1 carcinogen (Dong *et al.*, 2019; IARC, 2016). The maximum permissible level of arsenic in drinking water according to World Health Organization (WHO) and United States Environmental Protection Agency (US-EPA) is 10 µg/L (Karim, 2000). Contamination of water bodies with arsenic has become severe health issue in different parts of the world. Acute promyelocytic leukemia was cured by arsenic in humans but at the same time, it also causes serious health hazard (Sun *et al.*, 2014). Human exposure to arsenic mainly occurs through drinking water and food ingestion. Prolonged exposure to arsenic leads to several diseases including skin, cancer, kidney, black-foot, diabetes, endocrine disorders, arsenicosis, etc. (Medda *et al.*, 2021).

1.2.1.2. Cadmium

Cadmium belongs to transition metals, slightly bluish and silver white metal having atomic weight 112.4. Cadmium mostly exists as +2 oxidation state in solution. The chemical properties of cadmium resembles with zinc. Hence, cadmium has the potential to replace Zn(II) ions in certain enzymes, and thus disturbing the activity of enzyme in biological systems (Amari *et al.*, 2017; Lalhmunsiamama *et al.*, 2016c). Cadmium enters the environment through natural and anthropogenic activities. It is used for steel protection, electroplating, blending, colour paint, manures, and weld metals in alloy, polyvinyl chloride plastics and other industrial operations. It is also regarded as endocrine disrupting chemical (EDC's). The minimal risk level (MRL) for acute inhalation is 0.00003 mg/m³, for chronic inhalation 0.00001 mg/m³, for intermediate oral exposure 0.0005 mg/kg/day and for chronic oral exposure it is 0.0001 mg/kg/day (Tinkov *et al.*, 2017). Cadmium has high mobility as compared to other heavy metals (Cd>Ni>Zn>Mn>Cu>Pb=Cr>Hg) and damages and inhibits DNA mechanisms (Mortensen *et al.*, 2018). Cadmium mostly presents in wastewater and is highly toxic in any of its chemical forms. Consumption of cadmium causes vomiting, dysentery, muscular ache, prolonged respiratory problems, kidney stone formation, skeletal distortion, high blood

pressure, etc., in human body. Cadmium is classified as group I carcinogen for humans by IARC (International Agency for Research on Cancer) (Genchi *et al.*, 2020; Hayat *et al.*, 2019). The *Itai-Itai* disease in Japan is due to the intake of rice contaminated with cadmium (Khan *et al.*, 2017). The maximum permissible limit in drinking water for cadmium is 3.0 µg/L as per the WHO guidelines (WHO, 2008). Cadmium and its compounds are soluble over wide range of pH in water compared to other metals; therefore, enters easily into bio-system where it accumulates readily. Cadmium is also known as strong teratogen which causes fatal deformity and hampers growth during pregnancy as well (Lalchhingpui *et al.*, 2017).

1.2.1.3. Copper

Copper is extensively used in several industries including the electroplating, artificial fertilizers, paper industries, tanneries, metal finishing, manufacturing of electrical goods etc. (Meseldzija *et al.*, 2019; Zafar *et al.*, 2020). The effluent of these industries contained varied concentrations of copper (Dogan *et al.*, 2009; Kumar *et al.*, 2011). Although copper is an essential element required in small content in the biological system as to sustain life and development of human and animals (Bost *et al.*, 2016; Madsen and Gitlin, 2007); however, an elevated level of copper is toxic and causes several biological disorders (Ameh and Sayes, 2019; Arbabi and Golshani, 2016; Hasfalina *et al.*, 2012). The maximum permissible limit of copper in drinking water set by WHO is 1.5 mg/L (Nebagha *et al.*, 2015). Copper causes homeostasis and lead to the harmful Menkes and Wilson's diseases (de Romana *et al.*, 2011; Shaligram and Campbell, 2013). Prolonged consumption of water contaminated with elevated level of copper causes permanent liver damage, loss of hair, increased heart rate, brain malfunction, depression and schizophrenia (Belhadri *et al.*, 2019; Zafar *et al.*, 2020).

1.2.2. MICRO-POLLUTANTS

1.2.2.1. Tetracycline(TC)

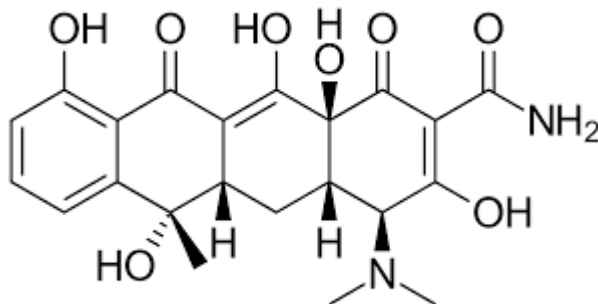


Figure 1.1. Structure of tetracycline.

Tetracycline is a crystalline compound with yellow in colour and the structure is shown as Figure 1.1. It is slightly soluble in water, lesser soluble in alcohol and not soluble in organic solvents. Tetracycline is made up of four rings fused together in which hydro naphthalene act as a backbone of the molecule (Dai *et al.*, 2020b). Tetracycline molecule consists of amino and enone groups which lack electron and also phenolic group which is rich with electron. Tetracycline possesses three different pK_a values having the values of 3.30, 7.7 and 9.7, respectively for pK_a^1 , pK_a^2 and pK_a^3 (Chang *et al.*, 2014; Yi *et al.*, 2020). Tetracycline is a widely used antibiotic for treatment of various infectious diseases in humans, aquatic animals and livestock (Gopal *et al.*, 2020). The consumption of tetracycline for veterinary is significantly high compared to other classes of antibiotics (Kim *et al.*, 2014; Niu *et al.*, 2013). The digestive tract of human and animals absorbs the tetracycline maximum of *Ca* 50% and more than half of it is excreted through faeces and urine which enters into sewage and hence in the aquatic environment (Brinzila *et al.*, 2011; Sarmah *et al.*, 2006). The concentration of tetracycline in the aquatic environment is relatively high (i.e., $\mu\text{g/L}$) due to continuous input through various sources (Lindsey *et al.*, 2001). The prolonged exposure of tetracycline by bacteria resulted in the bacterial antibiotic resistance which is directly or indirectly harmful for human and animal health (Levy *et al.*, 2002). Moreover, intensive studies performed on rats have shown that tetracycline reduces the antioxidant enzymes and glutathione levels which further causes the oxidative stress in liver and pancreas of rats (Asha *et al.*, 2007).

Tetracycline is persistence is nature and partly degraded in the conventional treatment plants hence, escaped through the effluents of treatment plants and enters into the aquatic environment. Hence, the residual tetracycline is distributed to surrounding water sources and soil, leading to non-point contamination in several areas (Sassman *et al.*, 2005; Tanis *et al.*, 2008; Westerhoff *et al.*, 2005). Gastrointestinal distress and skin reactions are the major side effects of tetracycline (Antonini and Luder, 2011). Moreover, the long term exposure or high affected the liver and kidney functions (Silva *et al.*, 2003; Szalowska *et al.*, 2014). Tetracycline is believed to induce the acute hepato-nephrotoxicity (Nada and Mahmoud, 2004).

1.2.2.2. Triclosan(TCS)

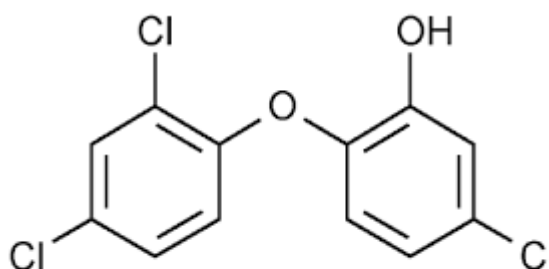


Figure 1.2. Structure of triclosan.

Triclosan [5-chloro-2-(2,4-dichlorophenoxy)-phenol] is often employed as antibacterial and antifungal compound in various personal care products (PPCPs) such as washing powder, toothpastes, shampoos, soaps, deodorants, etc. (Fiss *et al.*, 2007). In aqueous medium, triclosan is having solubility less than 10^{-6} g/mL but the solubility is increased at higher pH values. The acid dissociation constant (pK_a) of triclosan lies between 7.9 and 8.1. The growth of terrestrial and aquatic species might be affected by the presence of triclosan since the triclosan get dissolved in fats and lipids of living organisms in water (Tiwari *et al.*, 2020). Moreover, the aquatic organisms are indirectly affected by triclosan since enzymes carrying the proteins are blocked by triclosan which may eventually develop bacterial resistance to that particular species (McMurry *et al.*, 1998).

Triclosan is an antimicrobial agent which binds the ligase of fatty acids forming stable FAS-NAD⁺-TCS complex. This blocks effectively biosynthesis of lipid in cell-membrane and inhibiting the growth of microbe (Wang *et al.*, 2018). Triclosan is a widespread used personal care products (PPCPs) and more than 700 types of PPCPs are made with triclosan (Dhillion *et al.*, 2015; Lee *et al.*, 2012a; Nfodzo *et al.*, 2012). Triclosan is an emerging water contaminant because of its geno- and cytotoxicity as studied in aquatic organisms (Zorrilla *et al.*, 2009). Moreover, it damages the DNA, hemocyte function with enhanced oxidation stress (Aranami and Readman, 2007). The soil nitrogen cycle is extremely impaired when the concentration of triclosan is at higher level i.e., 5 mg/g (Svenningsen *et al.*, 2011). Human urine samples as randomly collected in USA and Asia, indicated that 83% samples are contained with high value of triclosan (Iyer *et al.*, 2018). Triclosan is potential water contaminant and occurred in the streams, lakes and seawater at higher levels (Wang *et al.*, 2018). Therefore, in order to maintain a safe and stable natural environment, it is important and inevitable to devise the newer technologies for safe and efficient removal of these emerging micro-pollutants from effluents of existing water treatment plants (Dai *et al.*, 2012; Durán-Álvarez *et al.*, 2012; Kiran and Venkata, 2012; Sipma *et al.*, 2010).

1.2.2.3. 17 α -Ethinylestradiol (EE2)

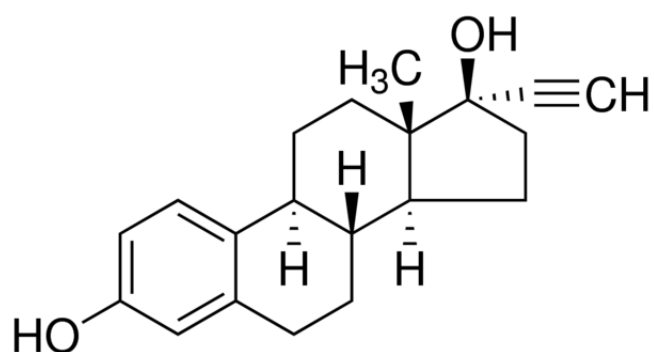


Figure 1.3. Structure of EE2.

The most harmful endocrine disruptor is known to be 17 α -ethynylestradiol (EE2), the major primary substance used in contraceptive pills and postmenopausal hormone supplement used in human and animal therapies (Larcher *et al.*, 2012; Han *et al.*, 2013; Silva *et al.*, 2012). EE2 is commonly discharged in domestic sewages and some industrial wastewaters (Larcher *et al.*, 2012; Oliveira *et al.*, 2015). Hormones are excreted at large quantities by humans hence, from domestic/sewage wastes. The major source of EE2 is from the urine of human (Pauwels *et al.*, 2008). Previous studies reported that significant amount of free EE2 is identified in wastewater at a concentration 7 to 42 ng/L from the effluent wastewater treatment plants (Cargouet *et al.*, 2004). It is also reported that treated water for drinking in Germany contain significant amount of EE2 at 0.5 ng/L (Atkinson *et al.*, 2012). According to several reports, human and living beings are significantly affected by EE2 and cause several diseases such as disorders of the reproductive system, cancer and impotence (Assis *et al.*, 2012; Komesli *et al.*, 2015; Vandenberg *et al.*, 2013). Comparing with other natural estrogens, the half-life of EE2 is longer and is more harmful (Scala-Benuzzi *et al.*, 2018). In addition, EE2 is readily assembles in silt and ecosystems (De Wit *et al.*, 2010). The concentrations of EE2 ranging from 0.1–10 ng/L may pose threat to the fish and other aquatic life (Feng *et al.*, 2010). Research conducted by spiking a lake in Canada with EE2 concentration 5-6 ng/L resulting in the death of entire fish population (Kidd *et al.*, 2007).

1.3. REMOVAL OF HEAVY METALS

Elevated concentrations of heavy metals in the environment are of great concern due to its potential threat to all living beings. Human activities and natural phenomenon are the main reasons involved in the release of heavy metals into the environment (Bendezu and Fuentes, 2019; Briffa *et al.*, 2020). Ion exchange, chemical precipitation, coagulation/flocculation, adsorption, membrane filtration, solvent extraction, cementation, electrochemical methods and flotation are the most accessible technique employed for the removal of heavy metals from wastewater samples (Saravanan *et al.*, 2013; Wolowiec *et al.*, 2019).

Ion exchange is a phenomenon in which ions are interchange between liquid media and solid material and usually it is a reversible chemical reaction (Bashir *et al.*, 2019). Heavy metals in wastewater are removed efficiently using the ion exchange process and are easily retrieved and recycled. The ionic exchange materials are natural and synthetic resins. Ion-exchange resins could be employed for variety of heavy metals removal depending on the type of functional groups present on its surface (Fernandez *et al.*, 2005). Furthermore, extraction of heavy metals from sludge are promoted using ion-exchange resin thereby changing the thermodynamic equilibrium of $M(OH)_2(s) \leftrightarrow M^{2+} + 2OH^-$ (Budak, 2013).

Cementation is a process in which additional electropositive metal is employed to precipitate metals from a solution of its salts thereby reducing to its elemental metallic form electrochemically and resulting in the loss of electron from sacrificial metal (Nassef and El-Taweel, 2015). Valuable or hazardous metals are retrieved from industrial effluents using cementation process. It is also employed in the purification of contaminated water other than hydrometallurgy (Konsowa, 2010). Cementation is pH dependent and greatly affected with change in solution pH. At pH < 7.0, corrosion of reactor and dissolution of reducing metal occurs. On the other hand, at pH > 7.0, the hydroxide is predominantly precipitated (Noubactep, 2010). The cementation process is heterogeneous in nature and is governed by electrochemical reaction and mass transport (Youssef *et al.*, 2020).

Coagulation-flocculation technique is used to remove heavy metals to form low soluble compounds including hydroxides (OH^-), sulfides (S^{2-}), carbonates (CO_3^{2-}) (Visa *et al.*, 2016). Coagulation is a process in which the colloidal particles are destabilized by suitable coagulants resulting in sedimentation. Coagulation is usually accompanied by flocculation in which the flocculants are added which accumulates the destabilized colloidal particles to form larger flocs which is separated by filtration (Teh *et al.*, 2016). Aluminium sulphate ($Al_2(SO_4)_3$), ferrous sulphate ($Fe_2(SO_4)_3$) and ferric chloride ($FeCl_3$) are widely used coagulants. The temperature, nature of coagulant, quantity of coagulant, blending method and pH plays important roles in the efficiency of coagulation (Renault *et al.*, 2009). Polyaluminum chloride, polyacrylamide and polyferric sulphates are often used as

flocculants for treating heavy metals in wastewater (Duan *et al.*, 2010; Jaafarzadeh *et al.*, 2016; Mwewa *et al.*, 2019).

Chemical precipitation is very common method used for the removal of heavy metals due to its low cost and simple operation. In an alkaline condition, precipitating reagent is added which precipitates the heavy metal ions which is easily removed by sedimentation or filtration (Hashim *et al.*, 2011). The precipitates are further sequestered and the remaining solution is utilized for next cycle of operation (Fu and Wang, 2011). Hydroxide and sulphide precipitation are two methods commonly employed in chemical precipitation (Huisman *et al.*, 2006). It was reported that Cu(II), Cd(II), Mn(II), Zn(II) are efficiently removed using chemical precipitation process (Bilal *et al.*, 2013). Calcium hydroxide, lime, sodium hydroxide are accessible to create hydroxide precipitates. Detailed study in the removal of fluoride in waste stream showed that, among the precipitates, magnesium hydroxide ($Mg(OH)_2$), calcium hydroxide ($Ca(OH)_2$) and calcium chloride ($CaCl_2$), calcium salt showed highest removal efficiency for fluoride in the pH range 4.0-14.0 (Jadhav *et al.*, 2014). Solid (FeS), aqueous (NH_4S) or gaseous sulphide sources (H_2S) are mostly employed as sulphide precipitants (Lewis, 2010).

Membrane is composed of definite permeable substances which is responsible for the attenuation of heavy metal toxic ions from polluted water (Patil *et al.*, 2016). In membrane filtration, particles are separated according to their size, concentration of the solution, pH and pressure applied. The physical and chemical properties of the membrane is an important parameter for the easy penetration of water and hence, the removal/rejection of contaminants. The filtration process is further accelerated by the suitable addition of chemical reagents (Barakat and Schmidt, 2010). Reverse osmosis, ultrafiltration, electrodialysis and nanofiltration are the common membrane filtration methods used for the removal of heavy metals in aqueous medium.

1.4. MICRO-POLLUTANTS REMOVAL TECHNIQUES

Physicochemical techniques such as coagulation-flocculation processes are not sufficient to eliminate pharmaceuticals and personal care products (PPCPs) and endocrine disrupting compounds (EDCs) from wastewater treatment plants. Therefore, several techniques including advanced oxidation processes (AOPs) (Ribeiro *et al.*, 2019), membrane technologies (Bodzek *et al.*, 2015), biological processes (Kanaujiya *et al.*, 2019) are employed in the elimination of these micro-pollutants from aqueous solutions.

Advanced oxidation processes (AOPs) are the most attractive and favourable methods employed for the elimination of hazardous and recalcitrant organic pollutants in wastewater. These methods include the *in-situ* generation of extremely reactive and nonselective hydroxyl radicals ($\bullet\text{OH}$) (Singh and Garg, 2021). Hydrogen peroxide (H_2O_2), ozone (O_3), iron salts and ultraviolet radiation are used for the generation of ($\bullet\text{OH}$) radicals. Mineralization of contaminants to its end product (CO_2) or conversion of pollutant compounds to its intermediate by-products using strong oxidant via oxidation-reduction methods are important mechanisms of associated with AOPs (Verma *et al.*, 2021). Several pollutants including endocrine disrupters, pesticides, dyes and emerging contaminants are degraded using AOP methods (Rayaroth *et al.*, 2020). However, it is also reported that in some instances, AOPs generates some recalcitrant by-products which possesses enhanced toxicity compared to the parent compounds (Kumar *et al.*, 2021).

Membranes are having selective boundaries that partition two phases and inhibit the movement of pollutant substances in aqueous solutions (Nath, 2008). Membrane separation method is extensively studied for the rejection of micro-pollutants, mainly reverse osmosis (RO) and nanofiltration (NF) membranes, which holds suspended salts and solutes and are efficient for the micro-pollutants having molecular weights from 200 and 400 Da (Sui *et al.*, 2010). Reverse osmosis holds higher amount of micro-pollutants due to the presence of small size of pores compared to the nanofiltration. But the retention efficiency of NF is very close to RO and it has an ability to operate under higher flow and low pressures. It showed lesser fouling rates and found cost effective (Silva *et al.*, 2017). Therefore, in membrane

processes, several parameters *viz.*, physico-chemical features of target pollutants, transport, properties of membrane and matrix effect need to be considered for effective and efficient decontamination processes (Chon *et al.*, 2012).

Conventional treatment plants such as activated sludge, fixed bed and trickling bed bioreactors, and innovative treatment processes including membrane-based bioprocesses, two-phase portioning bioreactors, and cell-immobilized systems, are among the biological treatment methods implicating through the potential microorganisms. The most common process for the treatment of polluted water using biological treatment plants is activated sludge technique (Kanaujiya *et al.*, 2019). This process depends on the activity of microbes for the removal of nutrients and oxidizing high carbon containing substances (Eckenfelder and Clearly, 2013). Microbial degradation or sorption by microbial flocs is responsible for the major degradation of pollutants by microbes (Maeng *et al.*, 2013).

1.5. ADSORPTION

Adsorption is a mass conversion technique in which an adsorbate is transported by chemical or physical processes onto the active binding sites of an adsorbent and it is primarily a surface phenomenon (Ojedokun and Bello, 2016). Adsorbent refers to the material/substances on which adsorption occurs, whereas adsorbate refers to the molecular or atomic/or ionic species that are being adsorbed. The adsorption procedure is versatile in terms of design and performance and it provides superior treated effluent in many conditions. Adsorption is, mostly, a reversible process and therefore adsorbents are recycled using appropriate desorption method and the recycled adsorbent can be further reused for different purposes. The commonly used recycling processes are pressure swing method, electrochemical and thermal regeneration methods (Demirbas, 2008). The efficacy of the adsorption technique is determined by the specific surface area, distribution of pore size, polarity and functional groups of the adsorbent (Bernal *et al.*, 2018).

Adsorption is categorized into two types *viz.*, chemisorption and physisorption. In physisorption, the adsorbate binds to the surface of the adsorbent through physical forces including Van der Waals forces, hydrophobicity, hydrogen bonding, dipole-dipole, π - π interactions, etc. (Sen, 2013). It is reversible process, fast

and spontaneous and decreases with the increase in temperature hence, required less energy for activation. Sorption equilibrium is rapidly attained and does not undergo molecular structure change for physisorption (Butt *et al.*, 2013).

Chemisorption is formed when the adsorbent and adsorbates are forming covalent bond through electron exchange in monolayer coverage onto the surface of the adsorbent. The adsorbates are immobilized in an irreversible manner to the binding sites of the adsorbates in chemisorption. It depends on temperature and increases with the increase in temperature indicating the existence of activation energy barrier. Further, both the processes can occur together or one after another under appropriate situations (De Gisi *et al.*, 2016).

1.5.1. FACTORS AFFECTING ADSORPTION PROCESS

There are different parameters which govern the process of adsorption at solid-solution boundary *viz.*, nature of adsorbent and adsorbate, temperature, pH and sorptive concentrations.

a) Nature of adsorbent and adsorbate

Generally, adsorption is enhanced on increasing the surface area of the adsorbent resulting in the increased availability of binding sites on the surface of the adsorbents. Opposite charged species are attracted on to the adsorbent surface having high surface charge while like charged species are adsorbed with lesser extent. The increased in the sorption of cationic dyes using ZnO impregnated natural clay is due to the increased in surface area and pore volume compared to natural and calcined clay (Behilil *et al.*, 2020).

The shape, size and chemical properties of the adsorbate also play an important role in the process of adsorption. Adsorption is determined by the charge present on the sorbate species and the existence of active binding sites on the surface of the adsorbent. The competitive sorption of heavy metals towards adsorbates revealed that adsorption process is strongly dependent on the nature of the adsorbate species (Martin-Lara *et al.*, 2020; Xu and McKay, 2017).

b) pH of the solution

The change in pH of a solution greatly influenced the adsorption process of the adsorbents. The difference in the sorption capacity is mostly due to the effect of pH on the adsorption properties of the adsorbent's surface (Vijayalakshmi *et al.*, 2016). Furthermore, the structure and features of the adsorbent surface are affected by the acidity and basicity of the solution hence, affected the adsorption processes (Gundersen and Steinnes, 2003).

c) Temperature

Temperature is one of the most important parameter in the adsorption process and usually affected the rate of adsorption. The rate of diffusion of adsorbate molecules increased on increasing the solution temperature (Mekatel *et al.*, 2015). Increasing temperature results in higher mobility of adsorbate species leading to desorption which further shows that the adsorption process is spontaneous and exothermic in nature (Barkat *et al.*, 2014).

d) Initial sorptive concentration

The sorptive concentration is an important factor in adsorption process since it governs the adsorbent adsorption capacity for particular initial adsorbate concentrations (Banerjee and Chattopadhyaya, 2017). Therefore, increasing the initial concentration of adsorbate caused an increase in extent of removal (Mnasri-Ghnimi and Frini-Srasra, 2019). The isotherms *viz.*, Freundlich, Langmuir, Dubinin-Radushkevich, Redlich-Paterson, Halsey, and Sips are among the isotherms utilised and each equilibrium model discussed several characteristics of the adsorption process. However, Langmuir and Freundlich are the most appropriate isotherms mainly employed in adsorption studies (Kausar and Bhatti, 2013).

1.6 COMMONLY USED ADSORBENTS

Various adsorbents are employed for the removal of contaminants in aqueous environment. Some of very common adsorbents are discussed briefly here.

1.6.1 Activated carbon

Activated carbon (AC) showed high potential towards the treatment of wastewater due to its high specific surface area, large meso- and micropore volumes (Mezohegyi *et al.*, 2012). Activated carbons are of two types *viz.*, powder activated carbon (PAC) and granular activated carbon (GAC). The removal efficiency of PAC for micro-pollutants is higher than GAC (Odabasi and Buyukgungor, 2016). Generally, activated carbon is employed for the elimination of organic pollutants but it also efficient in the removal of several heavy metals. Activated carbon is made in such a way that raw materials are dried first and then carbonized using high temperature followed by activation leading to large surface area varying from 600 to 2000 m²/g. Therefore, different contaminants including heavy metal toxic ions, anions, organic pollutants etc. are removed efficiently (Bhatnagar and Sillanpää, 2010). Al-Lagtah *et al.* (2011) studied the adsorption of Cr(VI), Cu(II), Cd(II) and Zn(II) on commercial activated carbon. The Langmuir adsorption capacity was found to be 62.857, 44.56, 43.33 and 53.98 mg/g for Cr(VI), Cu(II), Cd(II), Zn(II), respectively and followed pseudo-second order kinetics. Cu(II), Cd(II), Zn(II) are primarily adsorbed through the ion exchange mechanism. Prokic *et al.* (2020) utilized unmodified and chemically modified activated carbon for the adsorption of estrone, 17 β -estradiol, and 17 α -ethinylestradiol. They reported that physisorption is the main mechanism of adsorption. Further, an increased in the amount of oxygen functional group enhanced the adsorption while increased in the surface area did not show significant effect in elimination of these pollutants. A high adsorption capacity of arsenic (2860 mg/g) is achieved from copper electrorefining solutions using commercial activated carbon (Navarro and Alguacil, 2002).

Tounsadi *et al.* (2016) prepared activated carbon (AC) from *Glebionis Coronaria* L and reported that carbonization temperature, activation temperature and time, ratio of impregnation are important factors for the production of AC. Further, the removal of Cd(II) and Co(II) using AC showed that the contact between the

carbonization temperature and impregnation ratio increased the removal capacity of Cd(II) and Co(II) with 57.87 and 45.75 mg/g, respectively. Manganese coated activated carbon materials produced from areca nut waste and rice hulls were employed for the removal of arsenic in aqueous media (Lalhmunsiana *et al.*, 2012). The sorption of As(III) and As(V) by these solid materials in the presence of background electrolytes concentration (NaNO₃) almost remain unaffected due to the formation of 'inner-sphere' complexes through strong chemical bond.

1.6.2 Agricultural waste/byproducts

Agricultural wastes/by-products are produced from the agricultural and forest activities and are often discarded in the environment as waste materials. Agricultural waste materials are considered to be economical and eco-friendly due to their distinctive chemical properties, low cost, natural abundance and renewable in nature. These materials are favourable to be used practically in water purification system (Ahmed, 2016; Anastopoulos *et al.*, 2017; Anastopoulos and Kyzas, 2014; Chen *et al.*, 2019a). Agricultural by-products mostly consist of cellulose and lignin and thus their unique features and chemical composition, presence of different functional groups makes them good alternative adsorbents in wastewater treatment (Bhatnagar *et al.*, 2015). A huge amount of agricultural residues including lemon peel (Kannan and Veemaraj, 2010), peat soil and rice husk (Mohamad *et al.*, 2018), wheat straw, corncob (Amen *et al.*, 2020), *Eucalyptus* leaves (Alimohammadi *et al.*, 2017), groundnut shell (N'diaye *et al.*, 2019), rice husk ash (Chen *et al.*, 2016b), white pine (*Pinus durangensis*) sawdust (Salazar-Rabago *et al.*, 2017) etc. are employed for the decontamination of water.

1.6.3 Industrial by-products/residues

The by-products/residues from industries are utilized as low-priced adsorbents in the removal heavy metals, dyes and organic compounds in aqueous waste waters. These materials are not required additional treatment and easily be employed for the decontamination of water (Vardhan *et al.*, 2019). Numerous industrial waste solids including paper mill waste (Suryan and Ahluwalia, 2012), khangar (carbon waste) (Nagpal *et al.*, 2016), modified blast furnace slag (Gao *et al.*,

2016), rice straw fly ash (El-Bindary *et al.*, 2015) and modified sugarcane bagasse (Akl *et al.*, 2014) etc. are used in the removal of contaminants from wastewater/water.

Huge quantity of fly ash is produced from thermal power plants due to burning of coal. Carbon, alumina, ferric oxide etc. are the major constituents of fly ash (Montalvo *et al.*, 2017). Fly ash was employed for the adsorption of Crystal Violet (CV) in water. Results show that 98.3% of Crystal Violet (CV) was removed with 90 minutes of contact. However, regeneration of adsorbent is practically difficult (Ghosh and Bandyopadhyay, 2016).

Bauxite residue, often known as red mud, is an industrial byproduct produced during the production of bauxite into aluminium. The percentage removal of As(III) and As(V) using activated red mud (ARM) was found to be 87.54 and 96.52%, respectively. The isotherm model followed Langmuir model with adsorption capacities of 1.80 $\mu\text{mol/g}$ for As(III) and 12.57 $\mu\text{mol/g}$ for As(V) (Altundogan *et al.*, 2002). The mechanically activated fly ash showed higher removal percentage (96%) of Zn(II), Ni(II), Pb(II), Mn(II) and Cu(II) than the raw fly ash under identical experimental conditions (Xiyili *et al.*, 2017). The maximum sorption capacity of Pb(II) using oxygen furnace slag is 92.5 mg/g (Naiya *et al.*, 2009).

1.6.4 Biomasses and Bio-sorbents

Trace quantity of contaminants are often removed from wastewater using variety of bio-sorbents. Several biomasses, living and non-living including algae (Ali *et al.*, 2018; Rubin *et al.*, 2010), fungi (Abbasi, 2017; Anayurt *et al.*, 2009), bacteria (Abbas *et al.*, 2014; Aragaw, 2020) and yeast (Danouche *et al.*, 2021; Ferdous *et al.*, 2016), chitosan (Nechita, 2016; Vidal and Moraes, 2019) are used for the decontamination of wastewater. Algae are promising bio-sorbents due to its high adsorption capacity and are easily available in huge quantity in water bodies (Trinelli *et al.*, 2013).

Adsorption of Cd^{2+} , Cr^{3+} , Pb^{2+} and Cu^{2+} on algae *Ulva lactuca* powder (AP) and activated carbon (obtained from *Ulva lactuca*) (AAC) was carried out and results showed that *Ulva lactuca* (AAC) possessed higher adsorption capacity than *Ulva lactuca* powder (AP) (Ibrahim *et al.* 2016). Chitosan is produced from chitin,

consisting of polysaccharide structure of deacetylated- β -glucosamine and is widely used in the removal of various contaminants from waste water (Escudero-Onate and Martinez-Frances, 2018). The maximum uptake of Cr(VI) using *Bacillus sp* immobilized waste tea biomass is 741.389 mg/g (Gupta and Balomajumder, 2015) and the maximum uptake of Cr(VI) using *Arthrobacter viscous* biomass is 1161.3 mg/g (Hlihor *et al.*, 2016). Inorganic organic iron chitosan nanoparticles (CIN) showed high adsorption capacity of 94 ± 1.5 and 119.0 ± 2.6 mg/g towards As(V) and As(III), respectively. No significant change in the adsorption capacity of adsorbent is observed after five cycle of adsorption-desorption operations (Gupta *et al.*, 2012). Ahamad *et al.* (2020) employed fabricated nanocomposite (CTM@Fe₃O₄) for the removal of tetracycline and the maximum adsorption capacity was 215.31 mg/g. Further, π - π and hydrogen bonding interaction are revealed in the sorption of tetracycline by the material.

1.6.5 Carbon nanotubes

Iijima discovered carbon nanotubes (CNTs) in 1991 (Iijima, 1991). Carbon nanotubes (CNTs) are composed of carbon with cylindrical shape having a tube-like structure. CNTs are classified into three types (1) single-walled CNTs (SWCNTs) (2) multi-walled CNTs (MWCNTs) and (3) functionalized CNTs (f-CNTs). Several pollutants are effectively removed using carbon nanotubes (Ma *et al.*, 2011; Anjum *et al.*, 2019). The mechanical, magnetic, heat resistance and high varied chemical properties of CNTs makes it a good adsorbent in wastewater treatment. Chemical interactions, electrostatic attractions, sorption- precipitation and ion-exchange are the main process involved between the CNTs and metal ions (Al-Khalidi *et al.*, 2015).

Adsorption-desorption results of As(V) and As(III) using zerovalent iron doped MWCNT (ZCNT) showed that the material lost its sorption efficiency by 25% and 13%, respectively for As(V) and As(III) after five cycles of adsorption experiments (Sankararamkrishnan *et al.*, 2014). Adsorption of 4-chloro-2-nitrophenol using SWCNTs and MWCNTs under identical experimental conditions showed that MWCNTs adsorption capacity was two-fold higher than SWCNTs. This is primarily due to the presence of additional sorption sites even the SWCNTs exhibited larger specific surface area (Mehrizad *et al.*, 2012; Salam and Burk, 2010).

The adsorption of 17 α -ethinylestradiol and bisphenol A using SWCNTs in artificial seawater, brackish water or their combination showed removal efficiency of 95–98% and 75–80%, respectively (Joseph *et al.*, 2011a).

1.6.6. Zeolites

Zeolites are porous hydrated aluminosilicates with anionic skeleton and are used as an adsorbent over the past several years in separation and/or purification method (Pérez-Botella *et al.*, 2019). The removal process of natural zeolite for contaminants occurred as: (a) distinct pores inside the crystal structure (Hoang *et al.* 2012); (b) presence of negative charge which are exchangeable by cations in solutions (Ghasemi *et al.*, 2016). Mordenite, chabazite, analcime, phillipsite, clinoptilolite, etc. are the different types of zeolites in which clinoptilolite is the most common among zeolites which is studied extensively (Wang and Peng, 2010).

The removal efficiency of copper, chromium and iron by natural zeolite was reported as 96.0% in 180 minutes, 85.1% in 300 minutes and 95.4%, in 360 minutes, respectively (Zanin *et al.*, 2017). Aluminium-loaded shirasu-zeolite showed effective removal of As(V) in drinking water within a wide pH range (3-10). The presence of interfering ions *viz.*, chloride, nitrate, sulfate, etc. is insignificant but the presence of phosphate significantly reduced the adsorption of As(V) (Xu *et al.*, 2002). Natural zeolites NZ01, NZ02 and NZ03 are used in the removal of tetracycline (TC) and oxytetracycline (OTC) in which NZ02 achieved highest sorption capacity for TC and OTC. Further, regeneration after five cycles showed that the performance of NZ02 is reduced by about 50% for TC and 30% for OTC (Lye *et al.*, 2017).

1.7. REVIEW OF LITERATURE

Clay minerals are fine particles, occurred naturally on the earth's crust which consist mostly silica, water, alumina, and dissolved rocks. Clay has the ability to expand according to the amount of water content and becomes harden when dried or apply heat (Uddin, 2017). Clay minerals are crystalline structures and are composed of layers mainly tetrahedral $[\text{SiO}_4]^{4-}$ and octahedral $[\text{AlO}_3(\text{OH})_3]^{6-}$ sheets. The metal cations are located inside the tetrahedrons and octahedrons, the oxygen atom occupy the tip from which some are linked with protons (as OH). Thus, hexagonal system is

organized with each sheet by fundamental structural elements. The charge on the layer depends upon the ratio and number of sheets in the fundamental structural units (Lee and Tiwari, 2012).

Clay minerals are roughly divided into seven groups: (i) The two sheet silicates, serpentine and kaolinite group, where the two-sheet layer (unit cell) T:O is in the ratio 1:1 (ii) The micas group, three-sheet phyllosilicates, where T:O ratio is 2:1 (iii) The group of vermiculite, having expanding three sheet silicates with T:O ratio 2:1. (iv) The smectite group, three sheet silicates which expand strongly, where the three-sheet layer T:O ratio is 2:1. (v) The non-swelling three-sheet phyllosilicates, pyrophyllite and the talc group, in which three-sheet layer T:O ratio is 2:1. (vi) The chlorites group with four-sheet silicates, in which the charge of the four-sheet layer is 1.1 with T:O:O ratio 2:1:1. (vii) The palygorskite and sepiolite group are having the layer-fibrous structure (Huggett, 2021; Mukhopadhyay *et al.*, 2020). Bentonite is having clay natural abundance which consists of layered phyllosilicates, where tetrahedral and octahedral sheets (T:O) are interchanged in the ratio of 2:1. Bentonite is having a net negative charge due to the replacement of aluminium and silicon by lower metal cation such as magnesium, sodium, calcium, etc. Bentonite possessed high cation exchange capacity (CEC), large specific surface and well distinct porous structure which makes bentonite as an efficient adsorbent for various pollutants (Bergaya *et al.*, 2006; Prabhu and Prabhu, 2018). The adsorption ability of bentonite is primarily defined by their pore structure and the cation exchange capacity (CEC) (Kul and Koyuncu, 2010).

Therefore, numerous studies are conducted to demonstrate the efficiency of clay minerals towards Pb(II), Cr(VI), Ni(II) and Cu(II) in aqueous medium using attapulgite. Results show that over 60% adsorption efficiency was achieved for all the metals and the amount adsorbed were found to be 62.1, 33.4, 58.5 and 30.7 mg/g for Pb(II), Cr(VI), Ni(II) and Cu(II), respectively (Potgieter *et al.*, 2006). The removal of Cd(II), Cu(II), Ni(II), Pb(II) and Zn(II) using montmorillonite showed that at lower pH, outer sphere complex formation occurred at permanently charged basal sites and is affected by ionic strength and at higher pH. The inner-sphere-complex formation took place at variable charged sites and is less affected by ionic strength. The permanent charge site affinity for metal cations was $Pb > Cu > Ni \approx Zn$

$\approx \text{Cd}$ and for variable charged edge sites was $\text{Pb} \approx \text{Cu} > \text{Zn} > \text{Cd} > \text{Ni}$ (Gu *et al.*, 2010). Kaolinite clay was employed for the sorption of Cu(II), Cd(II), Ni(II) and Pb(II) in single and multi-metal ion systems. Results show that interaction between the clay surface and metal-ions was chemical in nature and the adsorption sites are non-uniform and non-specific (Jiang *et al.*, 2010). In other study, adsorption of Cu(II), Ni(II), Cd(II) and Pb(II) onto natural bentonite in mono- and multi-metal systems was conducted. It was found that the amount of metal uptake by bentonite in multi-component system are lower than those obtained for the particular single metal system and the equilibrium uptake amounts of each metal in the multi-component system was decreased on increasing the concentrations of the other metals due to their antagonistic effect (Bourliva *et al.*, 2015).

Clay minerals are efficient in the removal of several metal cations however, the clay materials are not found efficient towards variety of oxyanion impurities such as As(V), As(III), Cr(VI) along with several micro-pollutants (Lee and Tiwari, 2012; Paiva *et al.*, 2008; Unuabonah and Taubert, 2014). The hydrophilic nature and charges on the surface of the pristine clay makes it ineffective for the adsorption of anionic contaminants and hydrophobic or non-polar organic pollutants (Park *et al.*, 2011). Therefore, the pristine clay mineral needs to be modified in order to make it efficient in the removal of low- or non-polar organic and anionic water pollutants. Organic cations with short or long chain are introduced within the interlayer space of clay network by the available exchangeable cations (Thanhmingliana and Tiwari, 2015). The introduced organic moiety greatly enhances the hydrophobic nature with more organophilic nature which enabled the materials more effective and efficient in the removal of several non-polar and polar organic or even anionic water pollutants (Alkaram *et al.*, 2009). Moreover, clay minerals are also pillared with polyoxycations and then intercalated with organic cations at the same time to obtain organo-inorgano materials which are then utilized for the removal of inorganic and organic impurities in water bodies (Zermane *et al.*, 2010). However, materials showed its inherent limitations since the surfactants and clay minerals interacted through weak electrostatic forces, therefore, the intercalated surfactant possibly leached out into the aqueous phase and causing secondary pollution (Qin *et al.*, 2014).

Clay minerals are physically modified through thermal activation which removes intercrystallite water thereby increasing porosity and surface area (Chen *et al.*, 2011). While chemically modified clay minerals consist of grafting with amine, activation with acid and doping/impregnation with surfactant or metal (Loganathan *et al.*, 2013). Therefore, advanced and functionalized materials precursors to the natural clays are suitable options for its wide range of implications (Buruga *et al.*, 2019; Kotal and Bhowmick, 2015). Silane grafted clay has recently attracted researchers attention since the silylated clay results in stable confinement of organic functional groups with the formation of strong bond between clay and organic moieties which further restricted the leaching of organic moieties into the environment (Bertuoli *et al.*, 2014; Fonseca and Airoidi, 2003). Several factors are responsible for the effective immobilisation of silane, including the concentration, type of surface, properties of organosilane and the hydrolytic stability of the bonds formed. However, broken edges of clay minerals is most reactive sites for grafting of silane. Grafting of silane compound within the clay network is, however, challenging (Queiroga *et al.*, 2019; Tao *et al.*, 2016). The structure of silylated compounds are governed by the presence of solvent molecules. Solvents with comparatively low surface energy but having higher surface energy than montmorillonite results in large average basal spacing of silylated products. This shows that the basal spacing is influenced by the polar components and dispersive surface energy (Wamba *et al.*, 2018). The silylated products include internal-surface grafted silane, intercalated silane and physically adsorbed silanes. Grafting of silane onto clay minerals proceeded in two steps, i.e., intercalation and adsorption, and then condensation reaction. Further, the total surface energy is an important factor governing the overall yield of silane grafted materials (Shanmugharaj *et al.*, 2006). The grafting of silane was not obtained in the nonpolar solvent (e.g., toluene) (Daniel *et al.*, 2008; Herrera *et al.*, 2005), however, the polar solvents (e.g., water/ethanol mixture and ethanol) enabled the intercalation of silane as due to proper dispersing medium (He *et al.*, 2005). Silylation of montmorillonites with long chain of aminosilane molecule exhibit smaller basal spacing. The basal spacing is governed by an important factor viz., interactions between functional group present with silane (e.g., -NH₂ group) and type of clay mineral (Piscitelli *et al.*, 2010). Low dielectric constant of nonpolar

solvents enables hydrolysis, condensation and intercalation of silane molecules which results in the production of high loaded silane and polysiloxane oligomers in the interlayer spaces of montmorillonite. The neighbouring montmorillonite layers is linked with polysiloxane oligomers via covalent bond which leads to 'locking' effect and the silylated products loses the ability to swell. Whereas the high dielectric constant of polar-protic solvents causes the less hydrolysis decreasing hence, the loaded silane and degree of condensation is low which is due to hydrogen bonding between the $-NH_2$ groups of APTES and solvents. The silylated products synthesized in polar-protic solvent showed swelling ability as pristine montmorillonite (Su *et al.*, 2013). The surface of bentonite clay was grafted with 3-aminopropyltriethoxysilane (APTES) and the material thus prepared allowing its micro-mesopores for removal of cations, bio-molecules, polymeric materials, drug molecule, etc. (Abeywardena *et al.*, 2017). Zhu *et al.* (2007a) pillared bentonite clay with Keggin ion (hydroxyaluminum polycation) and the material (PILCs) is further silylated with octadecyltrichlorosilane (OTS) and trimethylchlorosilane (TMCS) producing organo-inorgano composite material (SPILC). The composite material is employed for the sorption of organic pollutants in air and waste water. SPILC showed much higher sorption capacity for pollutants than the CTMAB-bentonite.

Activation of montmorillonite increases the sorption active sites and thus lead to higher loading of silane (Shen *et al.*, 2009; He *et al.*, 2002). Bentonite is modified using different strategies: cationic exchange, silylation and acid activation. The uptake percentage of water in the silylated bentonite is substantially reduced compared to the pristine bentonite even at less loading of silane. However, the silylation is carried out on acid-activated bentonite clay, the organic content is not changed significantly. This result showed that silylation reaction depends on the limited geometrical condition and movement forced by the interlayer of clay rather than the number of $-OH$ group accessible for the reaction. But, when cation exchange reaction is applied on silylated bentonite and activated bentonite, the previous process results in increasing the uptake of number of surfactant cations. Moreover, the combination of the three treatments (acid-activation, silylation and cationic exchange) gave place to the modified bentonite with higher basal spacings and lower equilibrium water uptake percentage. Undoubtedly, acid-activation,

silylation and cationic exchange treatments resulted in lower uptake percentage of water at equilibrium and higher basal spacing is obtained with the modified bentonite clay (D'Amico *et al.*, 2014). Nano silica surface was grafted with 3-mercaptopropyltrimethoxy (MPTS), DFT method provide the grafting modes between the MPTMS and nano silica surface in four different modes. Results show that when concentration of MPTMS is lower, mono- and di-grafting modes are favourable and when MPTMS concentration is higher, ladder-like grafting mode is favourable. Using the feed ratio 75 mL MPTS to 10 g nano silica, the grafting ratio is reached to 16.8% with the incorporated –SH concentration of 0.9 mmol/g (Wu *et al.*, 2014). Natural smectite clay was silylated with 3-aminopropyltriethoxysilane and 3-mercaptopropyltrimethoxysilane for the adsorption of mercury. Results showed that the basal spacing of natural smectite clay is increased from 0.99 to 2.01 nm and 1.84 nm for 3-aminopropyltriethoxysilane and 3-mercaptopropyltrimethoxysilane silylation, respectively. Moreover, the surface area was also increased from 48 to 79 m²/g and 781 m²/g, respectively, for both the modified clays (Guerra *et al.*, 2009). The diatom silica was chemically modified with 3-mercaptopropyltrimethoxy (MPTMS), 3-aminopropyl-trimethoxysilane (APTES) and n-(2-aminoethyl)-3-aminopropyl-trimethoxysilane (AEAPTMS) for the removal of Hg(II). Diatom silica modified with MPTMS showed higher removal efficiency due to the strong bond between –SH group and Hg(II). The maximum sorption capacities are 169.5, 131.7 and 185.2 mg/g for AEAPTMS, APTES and MPTMS, respectively within 60 minutes of contact (Yu *et al.*, 2012). Pre-treatment of bentonite clay with acid and then functionalized with 3-mercaptopropyltrimethoxy (MPTMS) silane leads to increase the basal spacing of clay from 1.4 (activated clay) to 1.6 nm (functionalized bentonite clay). Moreover, a remarkable binding capacity was obtained for Ag⁺ ions using functionalized bentonite clay (Guimaraez *et al.*, 2009).

Marjanovic *et al.* (2011) modified natural and acid-activated sepiolite with 3-mercaptopropyl trimethoxy silane and employed for the adsorption of Cr(VI). It was found that grafting occurs mainly on the surface of sepiolite without changing the crystal structure of sepiolite. The removal efficiency for Cr(VI) is higher for functionalized acid-activated sepiolite than functionalized natural sepiolite due to higher content of silanol groups. There are two possible mechanisms for the

adsorption of Cr(VI) onto the materials, one is electrostatic attraction between Cr(VI) anionic species and the proton from mercapto group. Second is the electrostatic interaction of the sulfonate group ($-\text{SO}_2\text{O}^-$) attained by oxidation of the mercapto groups with the reduced Cr(III) from Cr(VI) ions by mercapto groups. It was also reported that pH plays an important role in the adsorption mechanisms for both the materials. The removal of Cr(VI) by functionalized sepiolites is mainly physical adsorption obtained from the thermodynamic data. Dogan *et al.* (2008) performed functionalization of sepiolite with [3-(2-aminoethylamino)propyl] trimethoxysilane and employed for the removal of metal ions Cd(II), Co(II), Cu(II), Fe (III), Mn(II) and Zn(II). The modification result showed that the methoxy group from silane is bonded with oxygen atoms or hydroxyl groups within the sepiolite structure. It was also found that increasing the temperature and equilibrium pH, modified sepiolite adsorbed more metal ion. The adsorption capacity of modified sepiolite followed the order Zn(II) > Cu(II) ~ Co(II) > Fe(III) > Mn(II) > Cd(II) . Cui *et al.* (2013) modified natural attapulgite (ATP) with (3-Aminopropyl)triethoxysilane (APTES) and then employed for the efficient sorption of Hg(II) from aqueous media. Over a wide pH range (3-11), the adsorbent efficiency remained constant. The adsorption capacities of raw ATP increased from 5 mg/g to 90 mg/g after modification. The uptake of Hg(II) was rapid and reached equilibrium within 60 minutes of contact. This was demonstrated due to the complex formation between functional groups (i.e., amino group) and mercury. Desorption was carried out effectively in 1:1 (m/m) chlorohydric acid/thiourea solution which further showed that the adsorbent is renewable material for repetitive operations in the removal of Hg(II). Mesoporous SBA-15 was grafted with aminosilane without destroying the meso-structure of solid. One NCO group from diisocyanate (TDI) employed as bridging molecule was linked with the silanol surface of SBA-15 and the other one was linked with ethylenediamine (EDA). The grafting can avoid amino/amino interactions and amino/silanol interactions for the achievement of high loading of NH_2 groups on SBA-15. The NH_2 -SBA-15 was employed for the adsorption of Cd^{2+} , Ni^{2+} , Cr^{2+} , Zn^{2+} and Cu^{2+} with high adsorption rates 99.9, 98.7, 99.7, 100 and 99.4%, respectively. The high adsorption rates are due to the metal ions and grafted NH_2 groups forming strong complex (Zhao *et al.*, 2011). The adsorption of chromate and

arsenate on three amino-functionalized (hexadecylamine, dodecylamine, and dimethyldodecylamine) mesoporous silicas (MCM-41 and MCM-48) was conducted. The cubic structure of MCM-48 and hexagonal structure of MCM-41 remain unchanged as confirmed with the XRD patterns. Larger amount of chromate is adsorbed by amino-functionalized MCM-41 compared to the expanded MCM-48 samples. The arsenate adsorption capacity is higher for mesoporous silicas modified by dimethyldodecylamine (Benhamou *et al.*, 2013). The removal of 5-chloro-2-(2,4-dichlorophenoxy) phenol (Triclosan) and 2,4-dichlorophenoxyacetic acid (2,4-D) was performed using modified SBA-15 and MCF mesoporous silicas with 3-aminopropyltriethoxysilane (APTES). Results show that both the modified materials showed high removal of 2,4-D and the maximum adsorption capacity were 286 and 278 mg/g for amine-MCF and amine-SBA-15, respectively. The ionic interaction between the adsorbent and 2,4-D seems to play a major role in the adsorption process of the pollutant on APTES-modified siliceous matrices. While the adsorption of triclosan on these materials show efficiency around 38.2 – 44.2 mg/g. On the other hand, the -OH functional group of (triclosan) and the H-bond interaction between amine functional group and 2, 4-D molecules are responsible for the process of adsorption (Moritz and Geszke-Moritz, 2014). Paul *et al.*, (2011) first treated beidellite clay with acid and then grafted with triethoxy silane (OTES) and chloropropyltrimethoxy silane (CPTES). The material prepared is utilized in the efficient removal of anionic (imazaquin) and neutral (alachlor) herbicides. Hydrophobic sites are predominantly responsible for an enhanced uptake of these pollutants. Bui *et al.*, (2011) studied the adsorption of twelve pharmaceutical compounds in a complex solution using the SBA-15 and SBA-15 modified with tetraethylorthosilicate (TEOS), (3-aminopropyl)triethoxysilane APTES, hexamethyldisilazane (HMDS). It was shown that for the hydrophobic compounds and amino-containing pharmaceuticals, the adsorption affinity of SBA -15 is moderate, but no significant adsorption for hydrophilic compounds was recorded. Similar adsorption capacity of all pharmaceuticals was observed for SBA-15, HMSBA-15 and AP-SBA-15, the adsorption efficiency of diclofenac and clofibric acid on AP-SBA-15 was increased but decreased for two cationic compound and estrone compared to SBA-15. At pH 5.5, TMS-SBA-15 possessed maximum adsorption efficiency for almost all

pharmaceuticals with the removal efficiency of more than 70% for several pollutants. Therefore, TMS-SBA-15 is regarded as an efficient adsorbent for the decontamination of pharmaceuticals in wastewater treatment processes. Xiong *et al*, (2018) synthesized novel composite adsorbent by combining multi-walled carbon nanotubes (MWCNT) with amino-functionalized MIL-53 (Fe) and employed for the adsorption of chlortetracycline hydrochloride (CTC) and tetracycline hydrochloride (TCN) in aqueous solutions. Results show that the adsorption process was due to the hydrogen bonding between -OH of the TCN (CTC) and -NH₂ of the modified MWCNT/NH₂-MIL-53(Fe), the π - π interaction and pore-filling effect. Further, the major factor for the adsorption of CTC and TCN is due to the π - π interactions between adsorbent and adsorbate species. Yu *et al*, (2015) functionalized natural diatomite with phenyltriethoxysilane (PTES) and assessed the removal efficiency of benzene using the functionalized material. Results show that the benzene adsorption capacity on the functionalized diatomite is 28.1 mg/g which is 4-fold higher than the unmodified diatomite. Further, the adsorption isotherm followed Langmuir isotherm. A strong π - π interaction are occurred between the benzene and the phenyl groups present with solid in addition to the macro-porosity of functionalized diatomite resulted extremely high removal capacity of benzene by the functionalized material. Sepiolite was grafted with γ -aminopropyletriethoxy silane, 3-chloropropyltriethoxysilane (CPTES), triethoxy (octyl) silane (OTES) and phenyltrichlorosilane (TFS) and employed for the adsorption of atenolol, ranitidine, and carbamazepine. Functionalization of sepiolite with CPTES showed higher removal of atenolol and ranitidine while functionalized sepiolite with triphenyl groups showed higher sorption of carbamazepine. The mechanism of sorption process followed with donor-acceptor complexes between electronegative atoms and protonated groups. Moreover, hydrophobic interactions between alkyl chains and π - π^* interactions between the phenyl rings are responsible for uptake of micro-pollutant (Undabeytia *et al.*, 2019). Silica nano particles was grafted with vinyltrimethoxysilane (VTMSO) and the copolymerized with acryloxyethyl-trimethylammonium chloride (Q). Results show that the hybrid particles Q/VTMSO-SiO₂ could remove efficiently the arsenic in aqueous solutions. Further, it was also reported that the material exhibits better removal efficiency for copper, zinc,

chromium, uranium, vanadium, and lead than commercial water filter (Valdes *et al.*, 2018). Gilberto *et al.* (2016) functionalized bentonite with (3-aminopropyl)triethoxysilane (APTS), N -[3-(trimethoxysilyl)propyl] diethylenetriamine (TMPT), and N -[3-(trimethoxysilyl)propyl] ethylenediamine (TMPO) and are employed for the sorption of Cr(III) ions. The adsorption capacity is not significantly affected by increasing quantity of amino groups. The maximum adsorption capacities were 0.088, 0.096, 0.097 and 0.097 mg/g for bentonite, APTS, TMPO and TMPT, respectively. Further, the result showed that the number of amino groups bonded to bentonite does not affect the sorption capacity of the functionalized solids.

1.8. SCOPE OF THE PRESENT INVESTIGATION

Contamination of aquatic environment with heavy metals, metalloids and micro-pollutants has become a serious environmental concerns around the globe. Therefore, in order to safeguard the aquatic and terrestrial life, the decontamination of potential pollutants from aquatic environment is a greater concern for the environmentalists. Conventional wastewater treatment plants are expected to provide the required efficiency as to remove the pollutants completely or even to the permissible level as laid down by the regulatory bodies. However, the existing wastewater treatment plants are not efficient enough to remove the potential heavy metal toxic ions or the emerging and persistence micro-pollutants including pharmaceutical, personal care products, endocrine disrupting chemicals etc. Therefore, advanced treatment is prerequisite in order to enhance the efficacy and efficiency of existing treatment plants. In a line, the adsorption is considered to be simple and cost-effective technique since it offers the possible utilization of naturally abundant materials for removing various water pollutants. The solution/surface chemistry is regulated using the novel and functionalized materials which could be useful in the low level removal of specific pollutants from aqueous solutions.

Several materials are widely studied and employed as adsorbents for treating polluted water. Among these adsorbents, clays and modified clays have received greater attention in the wastewater treatment strategy particularly in the removal of

heavy metals, micro-pollutants and arsenic oxyanions. Clays are porous materials, employed widely towards the elimination of water pollutants since it possesses a large surface area, expandability, high cation exchange capacity, porosity at micro levels, low cost and ubiquitous in nature. Moreover, clay minerals are found useful in large-scale operations because of its abundance and environmental benign. However, clays are having its limitations since highly hydrophilic in nature hence, ineffective towards the removal of organic pollutants, oxyanionic and anionic species. However, the suitable modifications/functionalizations of natural clay materials could show wide range of applicability in particular the environmental studies. Therefore, advanced and functionalized materials precursors to the natural clays are having suitable options for its wide range of implications. Silane grafted clay has shown potential materials, since the silylated clay results from stable confinement of organic functional groups with the formation of strong bonds between clay and organic moieties which further restricted the leaching of organic moieties into the environment and preventing the secondary contamination of water bodies. Several factors are responsible for the effective immobilization of silane, including the concentration, type of surface, properties of organosilane and the hydrolytic stability of the bonds formed. However, broken edges of clay minerals is most reactive sites for grafting of silane. Grafting of silane compound within the clay network is, however, challenging in the material synthesis.

Therefore, the present work intended to graft indigenously the two different silanes *viz.*, 3-mercaptopropyl trimethoxysilane and 3-aminopropyl triethoxysilane with the bentonite network in a facile and one step synthetic route. The functionalized materials were then extensively utilized in the efficient elimination of As(III), As(V), Cu(II), Cd(II), tetracycline (TC), triclosan (TCS) and 17 α -ethynylestradiol (EE2) from aqueous solutions under the batch and column reactor operations. The batch reactor operations conducted with several parametric studies could enable us to propose a plausible mechanism involved at solid/solution interface. Moreover, the column reactor operations provides the loading capacity of solids for these pollutants under the dynamic conditions which is useful for real implications of materials in the wastewater treatment strategy or even to help in scaling up the laboratory data to large scale treatment.

CHAPTER -2

METHODOLOGY

2. METHODOLOGY

2.1. MATERIALS AND APPARATUS

Bentonite clay (BN) was purchased from a commercial supplier which was mined near Bhuj, Gujarat, India. 3-mercaptopropyletrimethoxy silane, 3-aminopropyletriethoxy silane, sodium arsenate dibasic heptahydrate, 17 α -ethynylestradiol, tetracycline hydrochloride were obtained from Sigma–Aldrich, USA. Copper (II) sulfate pentahydrate and cadmium sulfate were obtained from Kanto Chemical Co. Inc., Japan. Ethylenediaminetetraacetic acid (EDTA) was obtained from Qualigens, India. Magnesium sulphate heptahydrate was purchased from Loba Chemie, India. Calcium chloride dihydrate powder, manganese (II) chloride, oxalic acid, di-sodium hydrogen phosphate anhydrous purified, sodium hydroxide and nickel chloride were purchased from Merck, India. Sodium chloride (Extrapure), sodium meta arsenite, glycine and triclosan were obtained from HiMedia, India.

Satorius (Arium Mini Plus UV Lab) water purification system was used for purifying the water. The purified water was used for preparing all the solutions. Electronic balance (HPB220, Wensar, India) was used for taking weights of chemicals and clay materials. A pH–meter (Thermo Scientific, Model: Orion 2 Star, pH Benchtop) was utilized for the entire pH measurements. The pH meter was calibrated using standard buffer solution having pH 4.0, 7.0 and 12.0.

For column experiments, glass bead (0.5 to 1 mm) obtained from HiMedia was used for packing of glass column (1 cm inner diameter and 30 cm long; Spectra/Chrom Aqueous Column, USA). Peristaltic pump (KrosFlo Research I Peristaltic Pump, Spectrum Laboratories Inc., California, USA) was used to pump the sorptive solution of pollutant upward and the fraction collector (Spectra/Chrom CF–2 Fraction Collector, Spectrum Laboratories Inc., California, USA) was employed for collecting the effluent solution. Syringe filter (PVDF filter membrane, 25 mm diameter and porosity of 0.45 μ m) was obtained from Whatman, USA, which was used for filtration of samples in batch experiments. Fast Sequential Atomic Absorption Spectrometer (FS-FAAS) (Model AA240FS, Varian, Australia) was employed for analysing As(III), As(V), Cu(II) and Cd(II). The calibration curve was obtained with the standard sorptive solutions having concentrations 1.0, 5.0, 10.0 and

15.0 mg/L of As(III)/As(V)/Cu(II) or Cd(II). Tetracycline(TC), triclosan(TCS) and 17 α -ethynylestradiol (EE2) were analysed using UV–Visible Spectrophotometer (Shimadzu Model: UV 1800, Japan). The calibration curve was obtained with the standard sorptive solutions having concentrations 1.0, 5.0, 10.0, 15.0, 20.0 and 25.0 mg/L of tetracycline, triclosan or EE2. The absorbance was measured at 280 nm for EE2, triclosan and 275 nm for tetracycline.

Real water sample was collected from Kawnpui, Kolasib district, Mizoram and water sample was filtered using Whatman filter paper (pore size 20 μ m) before utilizing it for experiments and then subjected for quality assessment. The presence of sulphate, phosphate, fluoride and nitrate in real water sample were analysed using multiphotometer instrument (Hanna Instruments, USA; Model: HI98194). The reagent used in the analysis of sulphate, phosphate, fluoride and nitrate were sulphate reagent (HI9751-0), phosphate reagent (HI93713-0), fluoride LR reagent and nitrate reagent (HI93728-0), respectively which were obtained from (Hanna Instruments, USA). Atomic Absorption Spectrometer instrument (AAS) (Model: AA-7000 Series, Shimadzu) was employed for analyzing the metal content in the real water sample. Total organic carbon analyzer (TOC) (Model: TOC-VCPH/CPN; Shimadzu, Japan) instrument was used to determine the amount of NPOC (Non-purgeable Organic Carbon) and IC (inorganic carbon). The UV-Vis Spectrophotometer was used for measuring the absorbance of solutions.

2.1.1. Ultraviolet–Visible (UV–Vis) spectroscopy

Spectrophotometry is the analytical method used for determining the quantity of light absorbed by chemical substances at a certain wavelength. The UV–Vis Spectroscopy utilized electromagnetic radiations between 190 to 800 nm and is categorized into the ultraviolet (UV, 190–400 nm) and visible (VIS, 400–800 nm) regions. This method is different from fluorescence spectroscopy, fluorescence concern with transitions of electron in molecules from the excited state to the ground state, while absorption deals with transitions of electron in molecules from the ground state to the excited state (Skoog *et al.*, 2007). Since molecule absorbs ultraviolet or visible radiation leading to the transitions among electronic energy states of the molecule, it is frequently termed as electronic spectroscopy. The term

infers that the distribution of electron in a molecule is interrupted by these remarkably high energy photons. Since molecules absorb UV–visible energy at diverse wavelength, spectroscopy is frequently employed in chemistry for distinguishing compounds through the spectrum emitted from or absorbed by them. The larger the number of atoms/molecules that absorb light at particular wavelength, the larger the quantity of absorbed light and peak intensity is increased significantly in the absorption spectrum. If radiation is absorbed by a smaller number of molecules, the total energy being absorbed is low and eventually lower intensity peak is achieved (Kumar, 2008). This marks the foundation of Beer–Lambert law which expresses that the portion of incident energy absorbed is proportional to the amount of absorbing molecules/ions in its direction.

The quantity of light absorbed or transferred when radiation travels through a solution is an exponential function of the molecular concentration of the solute as well as the path length of the radiation as it travels through the solution. It can be denoted as (Equation 2.1):

$$\log \frac{I_o}{I} = \varepsilon c l = A \quad \dots(2.1)$$

where I_o = Intensity of the incident light (or the light intensity passing through a reference cell)

I = Intensity of light transmitted through the sample solution.

c = concentration of the solute in mol/L.

l = path length of the sample in cm.

ε = molar absorptivity or the molar extinction coefficient of the substance.

ε is a constant and its value depends upon the nature of a given absorbing molecules in a specific solvent at a specific wavelength. ε is numerically equal to the absorbance of a solution of unit molar concentration ($c = 1$) in a cell of unit length ($l = 1$) and its unit is L/mol/cm. However, it is customary practice to omit the units. Thus, if the path length and the molar absorptivity are known and the absorbance is measured, the concentration of the substance can be deduced.

The inner arrangement of a molecule responds to radiation energy not only by electronic transitions. Molecular vibration and rotation is often observed in some molecules due to their natural resonant frequencies of bonding electrons. The variations in energy states related to rotation and vibration are very less in comparison with energy involved in electronic transitions; thus, excitation will take place only at longer wavelengths. In a solution for several absorbing molecules or ions, sharp lines are not observed in absorption peaks at extremely distinguished wavelengths; instead they appeared as absorption band over a range of wavelengths. This is due to the fact that electronic transition is normally followed by vibrational transitions between electronic states (Hollas, 2005). Likewise, each vibrational level is accompanied with rotational levels so that an absorption spectrum on account of an electronic transition might be a composite structure, with providing constituents from vibrational and rotational absorption.

A typical spectrophotometer consists of a light source, sample holder, diffraction grating or monochromator for separating the different wavelengths of light and detector. The radiation source is often a tungsten filament lamp (300–2500nm), a deuterium arc lamp which is continuous over the ultraviolet region (190–400nm), and more recently light emitting diodes (LED) and Xenon Arc Lamps for the visible wavelengths. The detector is typically a photodiode or a charge–coupled device (CCD). Photodiodes are used with monochromators, which allow them only light of a single wavelength reaches the detector. Diffraction gratings are used with CCDs, which collects light of different wavelengths on different pixels. In the present investigation, UV–Visible Spectrophotometer (Shimadzu Model: UV 1800, Japan) was employed to determine the absorbance of solutions containing tetracycline, triclosan and EE2 so as to obtain the concentration of these pollutants.

2.1.2. Atomic Absorption Spectroscopy (AAS)

Atomic Absorption Spectroscopy (AAS) is a Spectro-analytical technique employed for the quantitative and qualitative determination of chemical elements that exist in several samples. It is based on absorption of light by free metallic atoms. Alan Walsh in the middle of 1950 developed AAS. In AAS, atoms are converted to gaseous state from the ground state by absorbing the energy. Fumes of metallic

species are obtained when solution comprising of metallic species/ions are aspirated into a flame. Some of the metal atoms elevated the energy level adequately high to produce the property of the metal. The lowest energy state atoms of a specific element are accessible of light energy of their individual distinct resonance wavelength. As a result, when radiation of this particular wavelength travels through the flame, a portion of it is absorbed, and the absorption is proportional to the concentration of the atoms in the flame. Therefore, in AAS, one regulates the quantity of light captivated. Further, when the amount of this absorption is established, the quantity of the metallic species is quantified.

In 1955, Walsh proposed the utilization of cathode lamps to produce the desired wavelength of light (Walsh, 1955); as well as the employment of a flame to create neutral species that will absorb the emission as they passed through the path. Flame is used to convert metal ions in solution into atomic level. The amount of light absorbed is measured against a standard curve once the proper wavelength of light is provided. Flame Atomic Absorption Spectrometer (FAAS) technique need a liquid sample to be aspirated, aerosolized, and combined with flammable gases, including acetylene and air or acetylene and nitrous oxide. The mixture is light up in a flame at temperature varying from 2100 to 2800°C. During ignition, atoms of the desired elements in the sample are brought down to the ground state free atoms, which absorb light at definite wavelengths which are element explicit and precise to 0.01–0.1 nm. A beam of light from a lamp whose cathode is made of the element being measured is transmitted through the flame to produce element definite wavelengths. A photon multiplier can identify the concentration of light intensity decrease caused due to absorption by the sample, which may be linked directly to the concentration of the analyte in the sample.

Flame atomic absorption spectrometer (FAAS) is a very common method used for detecting metals and metalloids in environmental samples. For most analytes, FAAS is a highly suitable, consistent, manageable and widely used method with an admissible degree of accuracy. Light at definite wavelengths is employed to excite metals at ground state by using absorption spectroscopy to measure the analyte concentration in the sample. To determine the relationship between the observed absorbance and the concentration of analyte, it requires standard solutions with

known analyte concentration and based on the Beer–Lambert law, the analyte concentration is measured accurately. In short, the electrons of the atoms in the atomizer can be promoted to higher orbitals (excited state) for a short period of time (nanoseconds) by absorbing a defined quantity of energy (radiation of a given wavelength). This amount of energy, i.e., wavelength, is specific to a particular electronic transition in a particular element. Each wavelength relates to just single element, and the range of an absorption line is only a few picometers (pm), providing the method of selectivity of the element. The radiation flux without a sample and with a sample in the atomizer is measured using a detector, and the ratio between the two values (the absorbance) is converted to analyte concentration or mass using Beer–Lambert’s law stating that the absorbance of an absorbing analyte is proportional to its concentration. Fast Sequential Atomic Absorption Spectrometer (FS-FAAS) (Model AA240FS, Varian, Australia) was employed in the present study for the quantitative estimation of As(III), As(V), Cu(II), and Cd(II) concentrations. FS–FAAS is a consecutive multi-element procedure that has the benefits of conventional FAAS. FS–FAAS is a successive multi-element technique that has the benefits of conventional Flame Atomic Absorption Spectrometer (FAAS); for example easy in operation. The continuous mode of this instrument permits the calculation of the order of analytes in decreasing order of wavelengths in one monochromator scan. The overall analysis time is minimized by measuring all components in one solution before moving on to the next, and the data are available as soon as the sample investigation is completed. It is also feasible to utilize the reference–element approach in such a manner that the instrument software applies the correction factors automatically (Miranda and Pereira–Filho, 2009).

2.2. METHODS

2.2.1. Preparation of silane functionalized bentonite clay

Bentonite clay was used after simple washing with purified water without any further purification, dried in an oven at 90°C and crushed to obtain 100 BSS (British Standard Sieve). Bentonite clay was functionalized with silane using simple one pot synthetic route. 15 g of dried bentonite (BN) was dispersed in 300 mL of toluene in 1000 mL three neck round bottom flask. Further, under stirring the suspension was refluxed for 30 minutes at 70°C under nitrogen atmosphere. To the above suspension, 15 mL of 3-mercaptopropyletrimethoxy silane was added drop-wise and it was further refluxed for 24 hours. The suspension was filtered and washed with 250 mL of toluene to remove excess silane and again washed with 250 mL of ethanol. The sample was dried at 90°C overnight in an oven. The dried synthesized material was named as BNMPTS and stored in a polyethylene bottle at room temperature for further used.

Further, in a separate 1000 mL three neck round bottom flask containing 300 mL of toluene, 15 g of dried bentonite was introduced and the mixture was refluxed and mechanically stirred for 30 minutes at 70°C under N₂ atmosphere. And then 15 mL of 3-aminopropyletriethoxy silane was added drop-wise to this suspension and was further refluxed for 24 hours. The slurry was filtered and washed with 250 mL toluene to eliminate unreacted silane and further washed with 250 mL of ethanol and dried in an oven at 90°C overnight. The silane functionalized bentonite clay was kept in a sealed polyethylene bottle at room temperature and named as BNAPTES.

2.2.2. Characterization of the materials

The functional groups present in bentonite (BN), BNMPTS and BNAPTES are obtained by using FT-IR (IR Affinity Shimadzu, Japan) analysis. Surface morphologies of bentonite, BNMPTS and BNAPTES are obtained by Scanning Electron Microscope (SEM) (Oxform max), Transmission Electron Microscope (TEM) (Oxford xtreme) and the elemental mapping of solids is carried out using the Energy-dispersive X-ray spectroscopy (EDX). The structural property of the materials is evaluated by the X-ray diffraction method (Philips X'pert MPD System). Further, the specific surface area, pore size and pore volume of the materials are

acquired by using BET Surface Area Analyzer (Micromeritics, ASAP 2010, France). Moreover, the X-ray photoelectron spectroscopy (XPS) (ESCALAB-250Xi+, Thermo Fisher Scientific, U.K) was utilized for obtaining the XPS data of the modified materials before and after the sorption of Cu(II) and Cd(II). This enables to obtain greater insights of the interaction of sorbate ions with the BNMPTS and BNAPTES solids.

2.2.3. Determination of pH_{PZC} of the solids

The pH at which the total charge on the solid surface becomes zero is termed as the point of zero charge (pH_{PZC}). Therefore, at $pH < pH_{PZC}$, the surface of the solid is considered to have a positive charge while at $pH > pH_{PZC}$, the solid surface is possessed with negative charge (Kragovic *et al.*, 2019). Drift method was used for the determination of pH_{PZC} (Lalhmunsiana *et al.*, 2013). The procedure is followed as; in 1000 mL Erlenmeyer flask, 500 mL of purified water was added, capped with cotton and was slowly and continuously heated until boiling for 20 minutes to remove the dissolved CO_2 . The flask was capped immediately to prevent re-absorption of atmospheric CO_2 by water. Then, 50 mL of 0.01 mol/L NaCl solutions was prepared from CO_2 free water and the pH of each solution in each flask was adjusted to pH values of 2.0, 4.0, 6.0, 8.0, 10.0 and 12.0 by adding 0.1 mol/L HCl or 0.1 mol/L NaOH, solutions. In each bottle, 100 mg of the solid sample was added and the bottles were closed firmly and put in the shaker for 24 hours at 25°C. The final pH of the solutions was noted and a graph was plotted between $pH_{Initial}$ and pH_{Final} . The point of intersection of these curves where the $pH_{Initial} = pH_{Final}$ gave the point of zero charge.

2.2.4. Speciation studies

The speciation studies was conducted for As(III), As(V), Cu(II) and Cd(II) using the Visual MINTEQ (Version 3.1), a freeware chemical equilibrium model for the calculation of metal speciation, solubility equilibria, sorption etc. for natural waters. The input parameters were taken as initial concentration of As(III), As(V), Cu(II) Cd(II) at 10 mg/L at a constant temperature 25°C. The thermodynamic equilibrium constants used were given in Table 2.1, 2.2, 2.3 and 2.4. The species

distribution of these metal ions as a function of pH are further obtained and graphically presented in the results and discussion. Moreover, the speciation study was also conducted for tetracycline, triclosan and EE2 from their pKa values using Microsoft Excel. The species distribution of tetracycline, triclosan and EE2 as a function of pH are graphically presented in the results and discussion.

Table 2.1: Various equilibrium constants used for the speciation of As(III) in aqueous solutions at 25 °C.

Equilibrium	Log K
$\text{AsO}_3^{3-} + \text{H}^+ \leftrightarrow \text{HAsO}_3^{2-}$	13.414
$\text{AsO}_3^{3-} + 3\text{H}^+ \leftrightarrow \text{H}_3\text{AsO}_3$	34.744
$\text{AsO}_3^{3-} + 2\text{H}^+ \leftrightarrow \text{H}_2\text{AsO}_3^-$	25.454
$\text{AsO}_3^{3-} + 4\text{H}^+ \leftrightarrow \text{H}_4\text{AsO}_3^+$	34.439

Table 2.2: Various equilibrium constants used for the speciation of As(V) in aqueous solutions at 25 °C.

Equilibrium	Log K
$\text{AsO}_4^{3-} + \text{H}^+ \leftrightarrow \text{HAsO}_4^{2-}$	11.80
$\text{AsO}_4^{3-} + 2\text{H}^+ \leftrightarrow \text{H}_2\text{AsO}_4^-$	18.79
$\text{AsO}_4^{3-} + 3\text{H}^+ \leftrightarrow \text{H}_3\text{AsO}_4$	21.09

Table 2.3: Various equilibrium constants used for the speciation of Cu(II) in aqueous solutions at 25 °C.

Equilibrium	Log K
$2\text{Cu}^{2+} + 2\text{H}_2\text{O} \leftrightarrow \text{Cu}_2(\text{OH})_2^{2+} + 2\text{H}^+$	-10.49
$\text{Cu}^{2+} + 3\text{H}_2\text{O} \leftrightarrow \text{Cu}(\text{OH})_3^-$	-26.64
$\text{Cu}^{2+} + 4\text{H}_2\text{O} \leftrightarrow \text{Cu}(\text{OH})_4^{2-} + 4\text{H}^+$	-39.73
$\text{Cu}^{2+} + \text{H}_2\text{O} \leftrightarrow \text{Cu}(\text{OH})^+ + \text{H}^+$	-7.49
$\text{Cu}^{2+} + 2\text{H}_2\text{O} \leftrightarrow \text{Cu}(\text{OH})_2(\text{aq.}) + 2\text{H}^+$	-16.23

Table 2.4: Various equilibrium constants used for the speciation of Cd(II) in aqueous solutions at 25 °C.

Equilibrium	Log K
$\text{Cd}^{2+} + 3\text{H}_2\text{O} \leftrightarrow \text{Cd}(\text{OH})_3^- + 3\text{H}^+$	-33.30
$\text{Cd}^{2+} + 4\text{H}_2\text{O} \leftrightarrow \text{Cd}(\text{OH})_4^{2-} + 4\text{H}^+$	-47.28
$\text{Cd}^{2+} + \text{H}_2\text{O} \leftrightarrow \text{Cd}(\text{OH})^+ + \text{H}^+$	-10.09
$\text{Cd}^{2+} + 2\text{H}_2\text{O} \leftrightarrow \text{Cd}(\text{OH})_2 (\text{aq}) + \text{H}^+$	-20.29
$2\text{Cd}^{2+} + \text{H}_2\text{O} \leftrightarrow \text{Cd}_2(\text{OH})^{3+} + \text{H}^+$	-9.39

2.2.5. Batch reactor experiment

The stock solutions of 100 mg/L of As(III), As(V), Cu(II) and Cd(II) were prepared by dissolving sodium meta arsenite (173.39 mg), sodium arsenate dibasic heptahydrate (416.44 mg), copper (II) sulfate pentahydrate (392.91 mg) and cadmium sulphate (185.45 mg), respectively in 1.0 L of purified water in 1000 mL volumetric flask. Similarly, the stock solutions of 100 mg/L of tetracycline, triclosan and EE2 were prepared by dissolving 100 mg of tetracycline hydrochloride, triclosan and 17 α -ethynylestradiol in 1.0 L of purified water in 1000 mL volumetric flask. 100 mL of As(III), As(V), Cu(II), Cd(II), tetracycline, triclosan and EE2 stock solutions were taken out in 1000 mL volumetric flask and filled with purified water up to the mark to obtain 10 mg/L of these pollutants. A 50 mL aliquot of 10.0 mg/L of these pollutants solution was taken into different polyethylene bottles and the pH was adjusted adding the 0.1 HCl/NaOH mol/L solutions drop-wise. 100 mg of the solid sample were then introduced into these bottles contained with pollutants. A 50 mL aliquot of 10.0 mg/L of these pollutants solution was taken into different polyethylene bottles and the pH was adjusted adding the 0.1 HCl/NaOH mol/L solutions drop-wise. 100 mg of the solid sample were then introduced into these bottles contained with pollutants. The solution mixture was equilibrated using an automatic shaker (KUKJE, Shaking Incubator, Korea model 36-SIN-125 or Incubator Shaker, TM Weiber, ACMAS Technologies Pvt. Ltd., India) for 24 hours at 25°C. The equilibrated solution was filtered using 0.45 μm syringe filter. The bulk sorptive concentration was measured using Fast Sequential Atomic Absorption

Spectrometer (Model AA240FS, Varian) for As(III), As(V), Cd(II) and Cu(II); and UV–Vis spectrophotometer (Shimadzu Model: UV 1800, Japan) for tetracycline, triclosan and EE2,. The percentage removal was calculated using Equation 2.2:

$$\% \text{ Removal} = \frac{C_0 - C_e}{C_0} \times 100 \quad \dots(2.2)$$

where C_0 and C_e are the initial and final sorptive concentrations, respectively.

2.2.5.1. Effect of pH

The solution pH is an important parameter in adsorption processes. The charge on the surface of the adsorbent, the degree of ionization of several contaminants and the dissociation of functional groups present in the adsorbent are greatly affected by the change in pH of the solution. The pH of the solution would have an impact on both the aqueous chemistry and the binding sites on the surface of the adsorbents (Bazrafshan *et al.*, 2013). Therefore, the adsorption process is effective/and efficient at a particular pH or some pH range. The effect of pH was performed by keeping the sorptive equilibrium solution pH of As(III), As(V) and Cd(II) between pH 2.0 to 10.0; sorptive equilibrium solution pH between 2.0 to 7.0 for Cu(II) and sorptive equilibrium solution pH between 4.0 to 10.0 for tetracycline, triclosan and EE2; with the sorptive concentrations of 10.0 mg/L for As(III), As(V), Cu(II), tetracycline, triclosan or EE2, and 5.0 mg/L for Cd(II). The solutions were equilibrated for 24 hours at a constant temperature of 25°C. Further, the sorption experiments were performed as demonstrated previously vide Chapter 2.2.5. The results obtained were presented as percentage removal of pollutants as a function of sorptive pH.

2.2.5.2. Effect of sorptive concentration

The initial sorptive concentrations are changed in batch adsorption studies because the driving factor in surpassing the mass transfer barrier between the solution and solid media depends greatly on sorptive concentration (Mustaqeem *et al.*, 2013). Moreover, the rate and uptake of contaminants by a sorbent are dependent upon its initial concentration in solution. The data obtained is further utilized for the

application of sorption isotherm models (Dawodu and Akpomie, 2014). Therefore, the effect of initial sorptive concentrations were conducted between 1.0 to 25.0 mg/L for As(III), As(V), Cu(II), Cd(II), tetracycline, triclosan, and 1.0 to 10.0 mg/L for EE2; at the pH 3.5 for As(III) and As(V), pH 4.0 for tetracycline, triclosan, EE2 and Cu(II); and pH 5.0 for Cd(II) with 24 hours as equilibrium time at 25°C. The sorption experiments were conducted as demonstrated previously in Chapter 2.2.5. The results were reported as percentage removal of pollutants as a function of initial sorptive concentrations.

2.2.5.3. Effect of background electrolyte concentrations

The extent of sorption is greatly affected by the existence of background electrolyte in aqueous medium. However, the impact relies on the concentration and nature of the electrolytes (Lalhmunsiana *et al.*, 2016b). The study often employed to observe the ‘specific’ and ‘non-specific’ adsorption between the target pollutants and the adsorbent. The ‘specific’ adsorption is not primarily affected by an increase in the concentration of background electrolytes whereas the ‘non-specific’ adsorption is greatly affected due to increased competition with counter ions for the adsorption site (Foo and Hameed, 2010). Therefore, by taking into account the background electrolyte (NaCl) concentrations was increased from 0.0001 to 0.1 mol/L in the solution maintaining the initial As(III), As(V), Cu(II), tetracycline, triclosan and EE2 concentrations of 10.0 mg/L; and Cd(II) at 5.0 mg/L. The solution pH of As(III) and As(V) were maintained at 3.5, Cu(II), tetracycline, triclosan and EE2 at pH 4.0 and for Cd(II), pH was maintained at 5.0. The sorptive solutions were equilibrated for 24 hours with a solid dose of 2.0 g/L. The results were shown as percentage removal as a function of background electrolyte concentrations.

2.2.5.4. Effect of contact time

The analysis of adsorption kinetics in treating wastewater is essential because it gives useful information about reaction pathways and permits to deduce the process of adsorption reactions. Furthermore, the kinetic studies discuss the rate at which the solute is adsorbed as well as governs the time of solute uptake at the solid–solution boundary. Therefore, it is essential to estimate the rate at which the

contaminant is eliminated from aqueous medium so as to develop suitable wastewater treatment plants (Ho and McKay, 1999). The effect of contact time was conducted at different intervals of time keeping the initial sorptive concentrations of As(III), As(V), Cu(II), tetracycline, triclosan and EE2 concentrations at 10.0 mg/L; Cd(II) at 5.0 mg/L. The solution pH of As(III) and As(V) were maintained at 3.5, Cu(II), tetracycline, triclosan and EE2 at pH 4.0 and for Cd(II), pH was maintained at 5.0. The results were reported as percentage removal as a function of time.

2.2.5.5. Effect of co-existing ions

The sorption of As(III), As(V), Cu(II), Cd(II), tetracycline, triclosan and EE2 by BNMPTS and BNAPTES were performed in presence of various coexisting ions. The cations chosen were Mn(II), Mg(II), Ca(II) and Ni(II); whereas the anions chosen were ethylenediaminetetraacetic acid (EDTA), oxalic acid, glycine and phosphate. The concentrations of co-ions were taken as 50.0 mg/L while the initial sorptive concentration of As(III), As(V), tetracycline, triclosan and EE2 were maintained at 10.0 mg/L; and Cd(II) at 5.0 mg/L. The solution pH of As(III) and As(V) were maintained at 3.5, Cu(II), tetracycline, triclosan and EE2 at pH 4.0 and for Cd(II), pH was maintained at 5.0. The sorptive solutions were equilibrated for 24 hours with a solid dose of 2.0 g/L. The results were then presented as percentage removal as a function of various coexisting ions.

2.2.6. Adsorption isotherm modelling

Different equilibrium isotherm models such as Langmuir, Freundlich, Brunauer-Emmett-Teller, Redlich-Peterson, Dubinin-Radushkevich, Temkin, Toth, Koble-Corrigan, Sips, Khan, Hill, Flory-Huggins and Radke-Prausnitz are specified depending on the several fundamental assumptions. Several models have received more attention than others because of their convenience in specified conditions and universal suitability. The quantity of independent factors included with an isotherm model determines its accuracy, but its acceptability in relation to process application is determined by its mathematical simplicity (Malek and Farooq, 1996). When the adsorbent and sorptive solution interact with an adequate amount of time, adsorption equilibrium is established, and the concentration of adsorbate in the bulk solution is

possibly in a dynamic balance with the concentration at the interface. Usually, the mathematical correlation which represents a significant contribution to the modelling survey, technical plan and practical application of the adsorption method, is typically represented by graphical illustration of the solid state concentration against its bulk sorbate concentrations. Its physical and chemical factors along with the essential thermodynamic supposition offered the idea of the sorption mechanism, properties of the adsorbent surface and the extent of attraction of the adsorbents (Foo and Hameed, 2010).

Therefore, among the several adsorption Isotherm models, these two models are the most common models to formulate adsorption equilibrium data.

2.2.6.1. Langmuir adsorption isotherm

Langmuir adsorption isotherms are based on the assumption that adsorbate are homogeneously dispersed on the surface of the adsorbent and that there is no lateral interactions and steric hindrance between the adsorbed molecules, even on adjacent sites. In its derivation, Langmuir isotherm refers to homogeneous adsorption; each molecule has constant enthalpies and sorption kinetic energy, and all sites have identical affinity for the adsorbate (Kundu and Gupta, 2006). The linearized form of Langmuir adsorption model (Tiwari *et al.*, 2007) is used for the evaluation of maximum uptake (q_o) at varied initial concentrations (Equation 2.3):

$$\frac{C_e}{q_e} = \frac{1}{q_o b} + \frac{C_e}{q_o} \quad \dots(2.3)$$

where q_e is the amount of solute adsorbed per unit weight of adsorbent (mg/g) at equilibrium; C_e is the equilibrium bulk sorptive concentration (mg/L); q_o is the Langmuir monolayer adsorption capacity, i.e., the amount of solute required to occupy all the available sites in unit mass of solid sample (mg/g) and b is the Langmuir constant (L/g).

2.2.6.2. Freundlich adsorption isotherm

Freundlich adsorption isotherm illustrates the relationship between the non-ideal and reversible adsorption, with no restriction to the organization of monolayer. Freundlich isotherm assumed multilayer adsorption, with uneven dispersion of adsorption heat and attractions over the heterogeneous surface. Currently, Freundlich isotherm is broadly employed in heterogeneous surfaces and binding sites with discrete energies relying on multilayer adsorption and equilibrium (Balouch *et al.*, 2013). The linearized form of Freundlich equation (Tiwari *et al.*, 2007) is shown in Equation 2.4:

$$\log q_e = \frac{1}{n} \log C_e + \log K_f \quad \dots(2.4)$$

where q_e and C_e are the amount adsorbed (mg/g) and bulk sorptive concentration (mg/L) at equilibrium, respectively, and K_f and $\frac{1}{n}$ are the Freundlich constants referring to adsorption capacity (mg/g) and adsorption intensity or surface heterogeneity, respectively.

2.2.7. Adsorption kinetic modelling

Several adsorption processes for pollutants are investigated in an effort to find an appropriate mechanisms taking place in the uptake of pollutants by the employed materials. Therefore, kinetic models are employed to examine the sorption mechanism. Several kinetic models previously explained the reaction order of adsorption technique based on concentration of solution, as well as the reaction orders depending on adsorbent capacity (Ho, 2006).

The time dependence sorption data are utilized to study the kinetics of sorption by employing kinetic modeling for two different kinetic models, *viz.*, pseudo-first order (PFO) (Azizian, 2004), pseudo-second order (PSO) (Ho and McKay, 1998) in its non-linear forms as given in Equations 2.5 and 2.6 respectively, so as to demonstrate the best fitted model for the studied systems:

$$q_t = q_e (1 - \exp(-k_1 t)) \quad \dots(2.5)$$

$$q_t = \frac{k_2 q_e^2 t}{1 + k_2 q_e t} \quad \dots(2.6)$$

where q_t and q_e are the amount of sorbate removed at time t and removal capacity at equilibrium, respectively. k_1 and k_2 are the pseudo-first and pseudo-second order rate constants, respectively. The pseudo-first-order kinetic model which is theoretically derived by the Lagergren could show the properties of the Langmuir rate at initial times of adsorption or close to equilibrium. Similarly, theoretical studies indicate that the rate coefficient of pseudo-second-order model, i.e., k_2 is a complex function of the initial concentration of the sorbing species (Azizian, 2004). A non-linear least square fitting is conducted for the estimation of these unknown parameters. For the purpose the Microsoft Excel add-ins ‘Solver’ is employed with user-defined functions to minimize the residuals between the model-calculated and model-measured values.

2.2.8. Column experiments

A glass column was employed to conduct fixed-bed column studies. 0.25 g or 0.50 g of BNMPPTS/or BNAPTES solid was taken at the middle of the column and the remaining part of the column was packed with glass beads. The initial sorptive concentrations of Cu(II), tetracycline, triclosan and EE2 were maintained at 10.0 mg/L, pH 4.0 and Cd(II) at 5.0 mg/L and pH 5.0. The sorptive solution was pumped upward from the bottom of the column using a peristaltic pump at a constant flow rate of 1.0 mL/min, and at a constant temperature of 25°C. The effluent from column was collected by fraction collector and then analysed for pollutant concentrations using the Fast Sequential Atomic Absorption Spectrometer for Cu(II) and Cd(II); and UV-Visible spectrophotometer for tetracycline, triclosan and EE2.

The loading capacity of the two solids BNMPTS/or BNAPTES under continuous flow system for various pollutants was obtained using the Thomas equation (Equation 2.8) (Thomas, 1944):

$$\frac{C_e}{C_o} = \frac{1}{1+e^{(K_T(q_o m - C_o V))/Q}} \quad \dots(2.8)$$

where C_e and C_o are the concentrations of effluents and influent solution of Cu(II), Cd(II), tetracycline, triclosan and EE2 (mg/L), respectively; K_T refer to the Thomas rate constant (L/min/mg); q_o is the maximum amount of Cu(II), Cd(II), tetracycline, triclosan and EE2 loaded (mg/g) under the specified column conditions; m is the mass of hybrid materials taken in column (g); V is the throughput volume (L); and Q is the flow rate of pumped Cu(II), Cd(II), tetracycline, triclosan and EE2 solution (L/min). The column data were then fitted to a non-linear Thomas equation using the least square fitting method to estimate two unknown variables, i.e., K_T and q_o . Microsoft Excel add-ins ‘Solver’ is used with user-defined functions to minimize the residuals between the model-calculated and model-measured values.

2.2.9. Applications to real water samples

To evaluate the practical implacability of the synthesized material in the removal of tetracycline, triclosan and EE2 from real water matrix, the sorption experiment was performed using the real water sample collected from Kawnpui river, Kolasib District, Mizoram, India (Global Positioning System: N24.00676, E092.67032) for the removal of tetracycline, triclosan and EE2. This could enable to simulate the sorption process to a real water matrix. The upper middle portion of river water was taken in a polyethylene water container, filtered and subjected for its parametric analysis before performing the experiment. The initial pH of river water was found to be 7.23. Various water quality parameters *viz.*, pH, conductivity, resistivity, salinity, total dissolved solids, phosphate, sulfate, nitrate and fluoride were measured using multiphotometer instrument. Atomic Absorption Spectrometer was employed to obtain the metal contents *viz.*, Fe, Zn, Mn, Ca, Pb and Cu. TOC

analyzer was employed to obtain the NPOC and inorganic carbon values of real water sample. The stock solutions of 100 mg/L of tetracycline, triclosan and EE2 were prepared by dissolving 100 mg of tetracycline hydrochloride, triclosan and 17 α -ethynylestradiol in 1.0 L of real water sample in 1000 mL volumetric flask. 100 mL of tetracycline, triclosan and EE2 stock solutions were taken out in 1000 mL volumetric flask and filled with real water sample up to the mark to obtain 10 mg/L of these pollutants. 50 mL of tetracycline, triclosan and EE2 (each 10 mg/L) were taken in polyethylene bottles and the pH was adjusted by addition of 0.1 mol/L HCl or 0.1 mol/L NaOH solutions from pH 4.0 to 10.0 for each of the pollutants. And then 100 mg of BNMPTS/BNAPTES was added to each of the pollutants solution and kept in the automatic shaker for 24 hours. The equilibrated solutions were then taken out and filtered using Whatman syringe filter (PVDF filter membrane, 25 mm diameter and porosity of 0.45 μ m) and further analysed using UV-Visible Spectrophotometer. The absorbance was measured at 280 nm for EE2, triclosan and 275 nm for tetracycline.

2.3.10. Desorption study

The desorption studies of Cu(II) using BNMPTS, tetracycline, triclosan and EE2 using BNMPTS and BNAPTES were performed using hydrochloric acid (HCl) at room temperature and the concentration of the acid was varied between 0.005 to 0.1 mol/L in order to find out the most suitable concentration of HCl to desorb the pre-adsorbed Cu(II) from BNMPTS, tetracycline, triclosan and EE2 from BNMPTS and BNAPTES. The sorption experiment was first carried out as described in batch experiment section 2.2.5. The sorption experiment was first carried out for Cu(II) at the concentration of 10 mg/L at pH 4.0 using BNMPTS, 10 mg/L for tetracycline and triclosan at pH 6.0 and the concentration of EE2 was kept at 10 mg/L by maintaining pH at 4.0 using BNMPTS and BNAPTES. 100 mg of BNMPTS was introduced in different polyethylene bottles containing 50 mL of Cu(II) solution and kept in automatic shaker for 24 hours. It was then centrifuge and the equilibrated solutions were analysed using Atomic Absorption Spectrometer. The same procedure was followed for tetracycline, triclosan and EE2 using BNMPTS and BNAPTES and the equilibrated solutions were analysed using UV-Visible Spectrophotometer. 50

mL of HCl having various concentrations (i.e., 0.005, 0.01, 0.05 and 0.1 mol/L) were introduced into different polyethylene bottles to desorb the pre-adsorbed Cu(II), tetracycline, triclosan and EE2. The desorption was performed in automatic shaker for 60 minutes to desorb the pre-adsorbed Cu(II) from BNMPTS solid, and tetracycline, triclosan and EE2 from BNMPTS and BNAPTES solids. It was then centrifuged and the supernatant solution was analyzed using Atomic Absorption Spectrometer for Cu(II) and UV-Visible Spectrophotometer for tetracycline, triclosan and EE2. The percentage desorption was calculated using equation 2.9. It was found that 0.01 mol/L HCl was most suitable to desorb the studied pollutants from BNMPTS or BNAPTES. The regenerated materials were washed with purified water for several times to attain neutral pH and then dried in an oven at 60°C. Further, the next adsorption-desorption studies were performed for Cu(II) using BNMPTS solid and tetracycline, triclosan and EE2 using BNMPTS and BNAPTES solids. The reusability test was conducted for six adsorption-desorption cycles.

$$\% \text{ Desorbed} = \frac{\text{Concentration of pollutant desorbed}}{\text{Concentration of pollutant adsorbed}} \times 100 \quad \dots(2.9)$$

CHAPTER -3

RESULTS AND DISCUSSION

3. RESULTS AND DISCUSSION

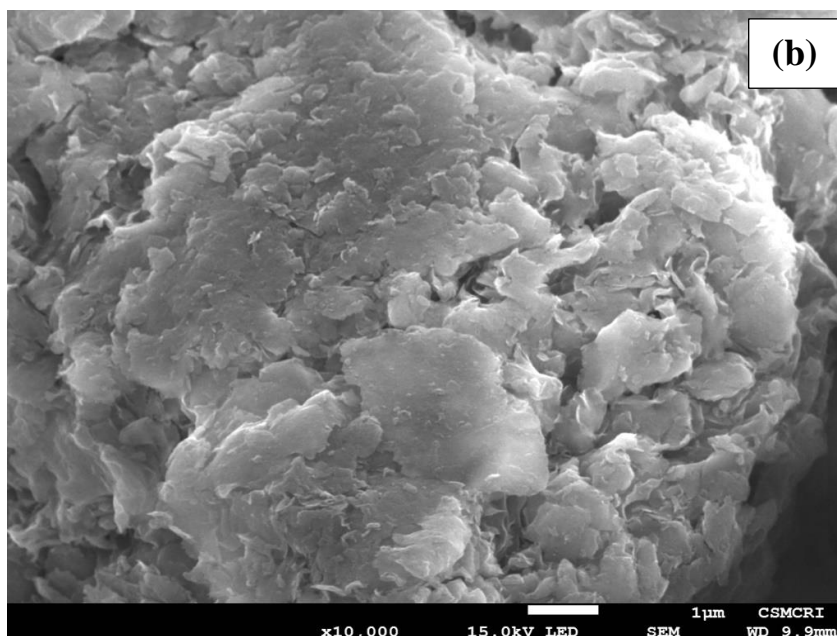
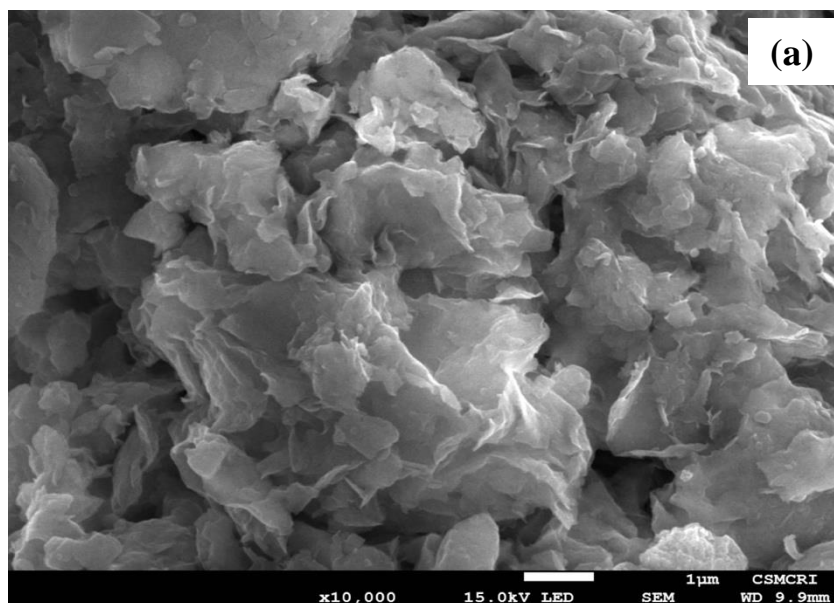
3.1. CHARACTERISATION OF MATERIALS

3.1.1. Surface morphology and elemental composition of the materials

The SEM images of pristine bentonite (BN), and silane grafted bentonite viz., BNMPTS and BNAPTES are shown in Figure 3.1 (a-c). Morphological images of showed that these solids possessed with heterogeneous and disordered surface structures. Pristine bentonite exhibits fairly good porosity which is significantly reduced with the solids BNMPTS and BNAPTES. This is due to the grafting of MPTS/or APTES molecules within the pores of bentonite. The materials are denser and more compact but possessed with high hydrophobic and organophilic nature. Natural attapulgite possessed loose aggregate structure but after grafting with (3-aminopropyltriethoxysilane) the modified material possessed compact aggregate structure (Cui *et al.*, 2013). These results are in consistent to the textural properties obtained by the BET analyses.

Further, the energy-dispersive X-ray spectroscopy (EDX) results were obtained for the solids BN, BNMPTS and BNAPTES and shown in Figure 3.2 (a-c). Figure clearly inferred that the BN solid is contained with the elements viz., K, C, O, Ti, Fe, Al and Si. These elements are often present with clay samples at varied percentages. Further, in addition to these elements, the presence of sulphur and nitrogen is present with the solids BNMPTS and BNAPTES, respectively. Results confirmed the grafting of MPTS and APTES with the bentonite in the samples of BNMPTS and BNAPTES, respectively. These results are further entailed the successful grafting of MPTS/or APTES molecules within the bentonite network. It was reported previously that the silicon (Si) and sulphur (S) peaks are observed in the EDX mapping on mercaptopropyl-coated SiO₂ particles (Kořak *et al.*, 2015). Modification of bentonite with 3-aminopropyletrimethoxy silane showed the predominant peaks of nitrogen (N) and carbon (C) in the EDX analysis (Abeywardena *et al.*, 2017). Result obtained using CHN elemental analysis in the modification of mesoporous SBA-15 with amino-propyl silane showed the presence of nitrogen along with enhanced carbon percentage (Bui *et al.*, 2011). EDX analysis of natural clay grafted with 3-aminopropyletrimethoxy silane show a significant increase in the percentage of carbon (C) and nitrogen (N) from 0.582% and 0.0814%

to 7.714% and 2.594%, respectively. Moreover, the amount of hydrogen in the grafted product is also increased significantly. EDX data further confirms successful grafting of natural clay with organosilane (Thue *et al.*, 2018).



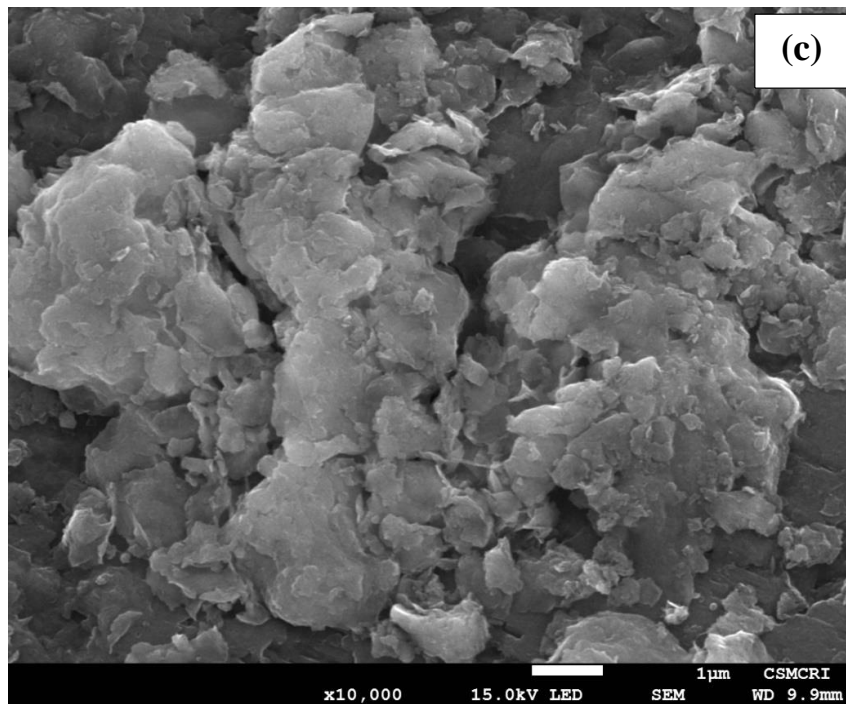
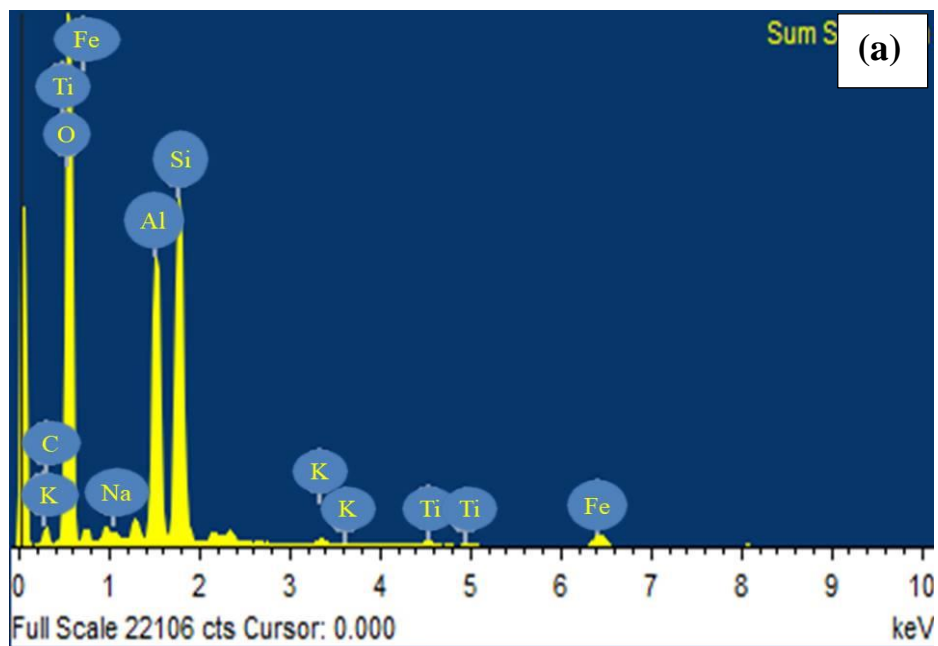


Figure 3.1: Scanning electron microscopic (SEM) images of (a) pristine bentonite (BN); (b) BNMPPTS; and (c) BNAPTES solids.



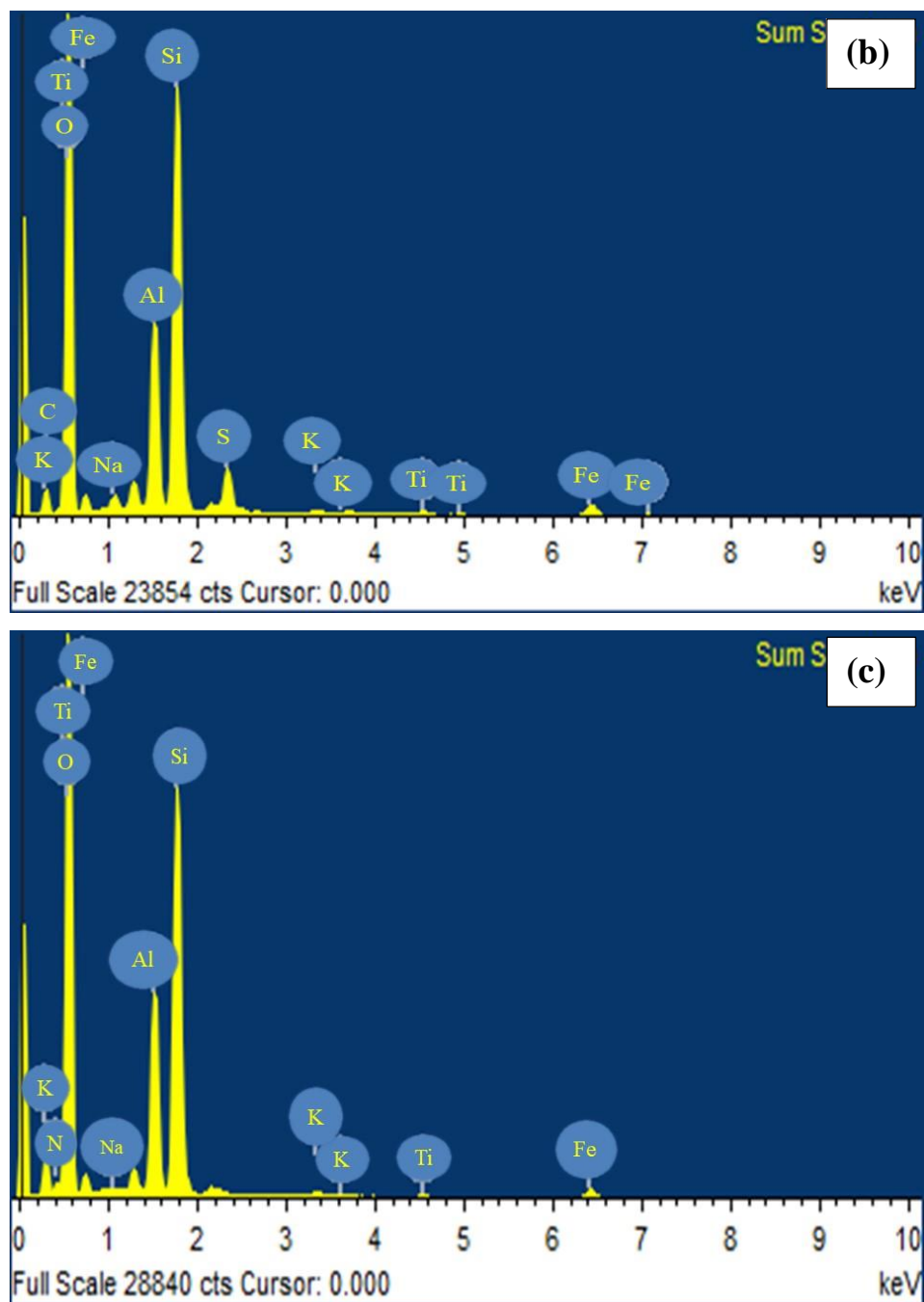
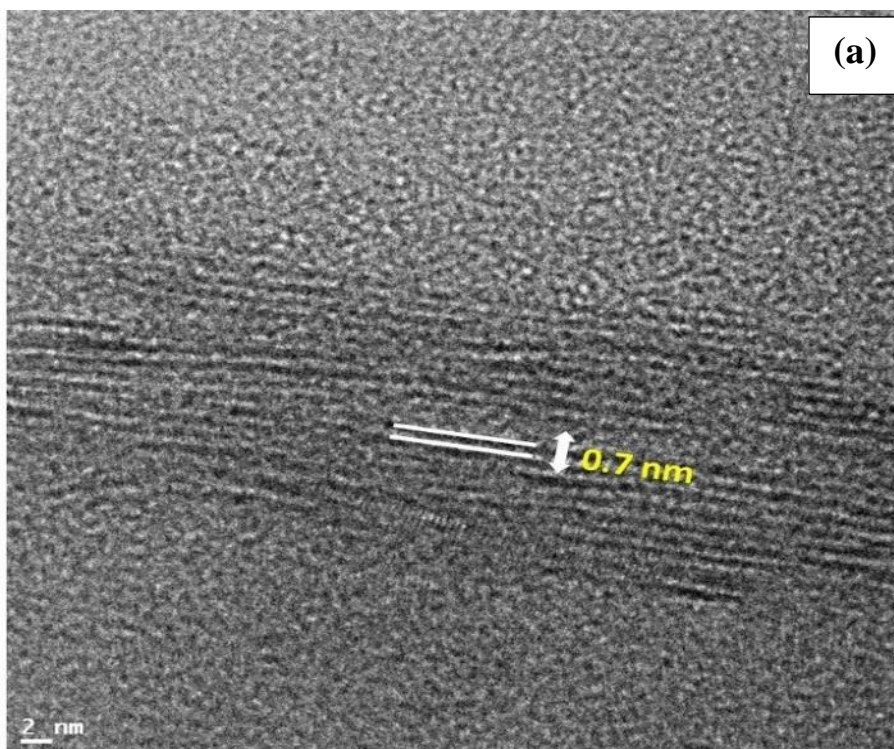


Figure 3.2: Energy dispersive spectra of (a) pristine bentonite (BN); (b) BNMPTS; and (c) BNAPTES solids.

The transmission electron microscopy (TEM) of the pristine bentonite and the functionalized bentonite (BNMPTS and BNAPTES) are given in Figure 3.4 (a-c). The TEM images showed a straight lattice fringe without deflection for pristine bentonite, BNMPTS and BNAPTES solids. It is interesting to observe that the basal spacing obtained for pristine clay and functionalized clay using TEM analyses were same as that obtained by XRD analysis. Previous report showed that the layered structure of bentonite and microwave silylated bentonite was clearly observed in TEM analysis showing a straight lattice fringe for bare bentonite as well as silylated bentonite (Queiroga *et al.*, 2019).



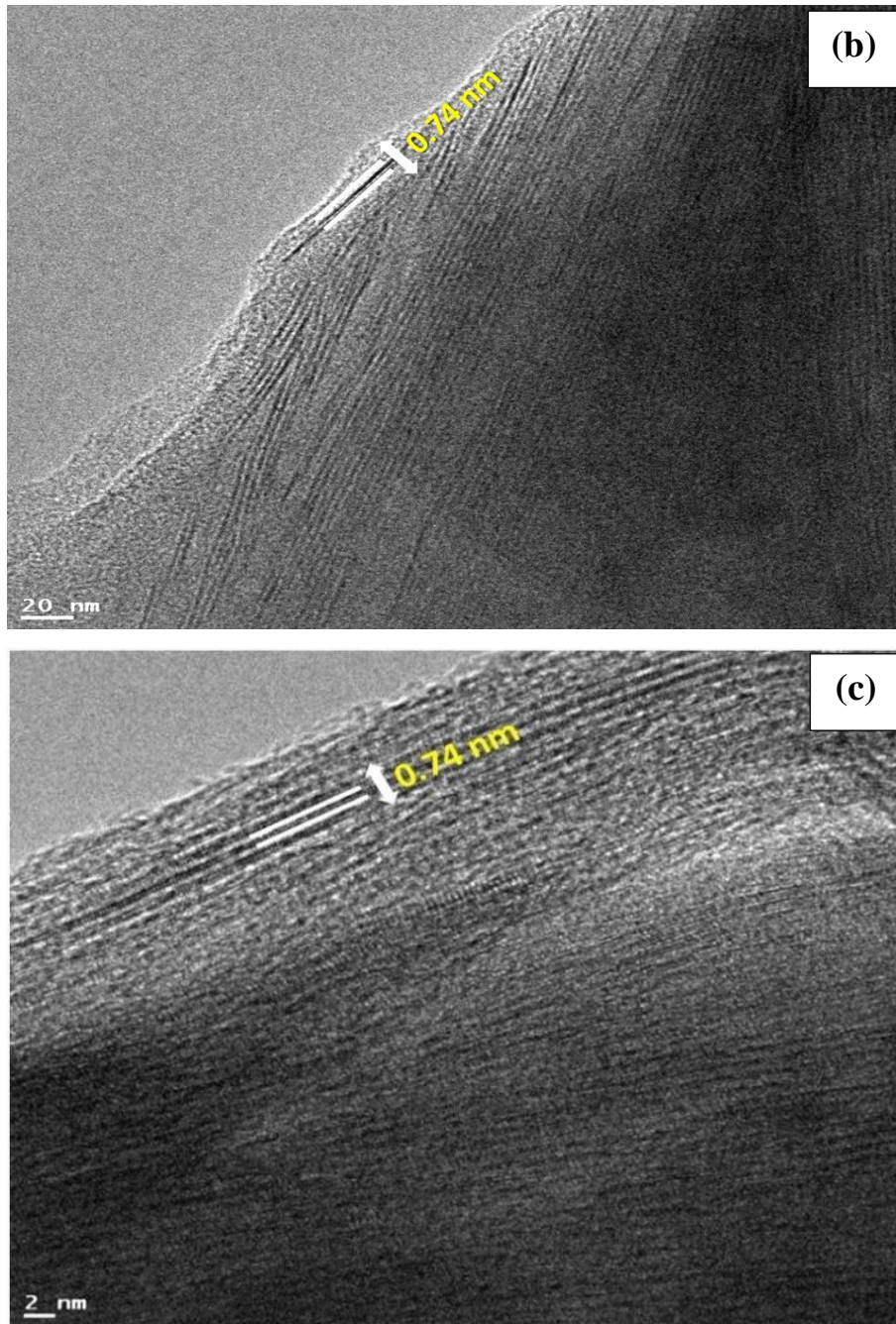


Figure 3.3: TEM images of (a) BN; (b) BNMPTS; and (c) BNAPTES

3.1.2. X-ray diffraction (XRD) analysis

The XRD diffraction pattern of BN, BNMPTS and BNAPTES are given in Figure 3.4. The XRD data collected for pristine bentonite and functionalized bentonite were identified and the data matched well with the standard ICDD (International Centre for Diffraction Data) reference pattern. The presence of typical montmorillonite (M), kaolinite (K), and quartz (Q) diffraction pattern are present in bare bentonite and modified samples. The main characteristic pattern of the montmorillonite peak was identified at 2θ value of 6.03° . The montmorillonite peaks are also observed at 2θ value of 19.85° , 36.62° and 50° (Burham and Sayed, 2016). Therefore, the XRD pattern obtained clearly showed the existence of the smectite phases in all the solid samples (Maged *et al.*, 2020; Terzic *et al.*, 2016). Moreover, other minerals were also detected at 2θ value of 12.40° for kaolinite (Sdiri *et al.*, 2016), 20.93° , 26.76° and 29.31° for quartz (Maged *et al.*, 2020, Wahab *et al.*, 2019). Further, it was observed that, in bare bentonite, the peak corresponding to '001' plane showed the d-spacing of 14.02 \AA which was decreased to 12.97 and 11.30 \AA after the incorporation of MPTS and APTES, respectively. On the other hand, d-spacing obtained for '020' plane remain almost unchanged, i.e., 4.24 , 4.27 and 4.32 \AA for BN, BNMPTS and BNAPTES, respectively.

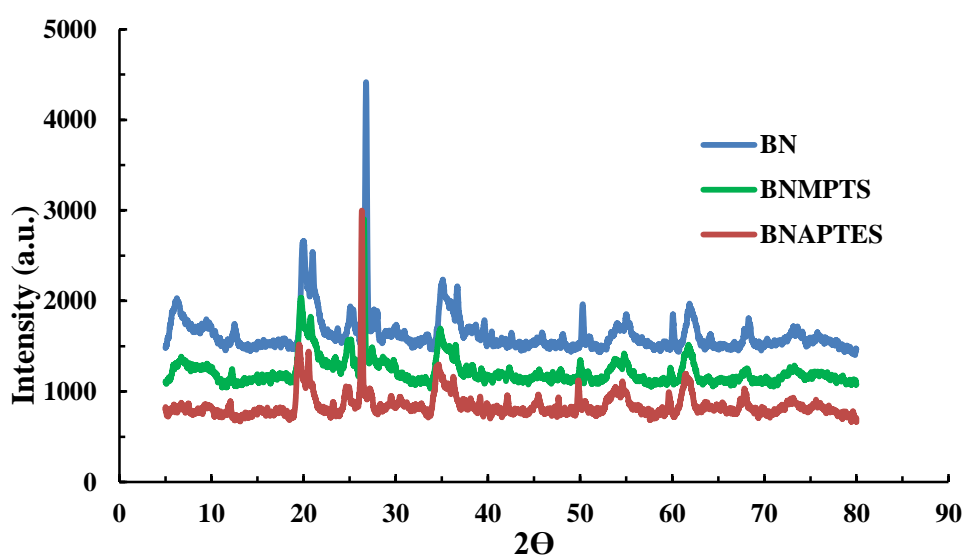


Figure 3.4: X-ray diffraction pattern of BN, BNMPTS and BNAPTES solids.

3.1.3. Fourier–transform infra–red analyses of solids

The FT-IR spectrum of pristine bentonite (BN), BNMPTS and BNAPTES are shown in Figure 3.5. A characteristic stretching vibration of Al_2OH was occurred at 3626 cm^{-1} (Aroke and El-Nafaty, 2014). The prominent but broad peak at 3420 cm^{-1} is ascribed due to the stretching vibrations of hydroxyl group of water. The Al–Al–OH hydroxyl bending vibrations is occurred at 911 cm^{-1} (Aroke and El-Nafaty, 2014; Petit and Madejova, 2013). The BNMPTS solid showed additional weak peaks at the wave numbers 2927 cm^{-1} and 2858 cm^{-1} which are attributed to the stretching vibrations of $-\text{CH}_3$ and $-\text{CH}_2$, respectively (Sahan *et al.*, 2018; Tonle *et al.*, 2003). Similarly, a characteristic peak of methoxy group of silane (MPTS) is appeared at 2927 cm^{-1} (Sahan *et al.*, 2018; Yilmaz *et al.*, 2017). The stretching vibration of $-\text{SH}$ group from MPTS is observed at 2550 cm^{-1} (weak vibrations) (Liang *et al.*, 2014). The vibrational peaks at 682 and 1402 cm^{-1} are, perhaps, attributed to the C-H deformation vibration and the C-S stretching of thiol group from MPTS, respectively (Carvalho *et al.*, 2008). These results clearly indicated that the MPTS is successfully grafted with the bentonite clay.

On the other hand, the BNAPTES showed a small peak at 1485 cm^{-1} is due to the CH_2 bending mode of vibration (Jovic-Jovicic *et al.*, 2010) and a subtle peak at $\sim 1319\text{ cm}^{-1}$ is ascribed to the stretching vibration of C-N bond which further inferred the successful grafting of organosilane to the bentonite network (Asgari and Sundararaj, 2017). Weak but distinguishable peak is obtained at 2894 cm^{-1} in BNAPTES solid, is attributed to the symmetric stretching vibrations of CH group which is possibly due to the CH_2 group of organosilane (Bertuoli *et al.*, 2014).

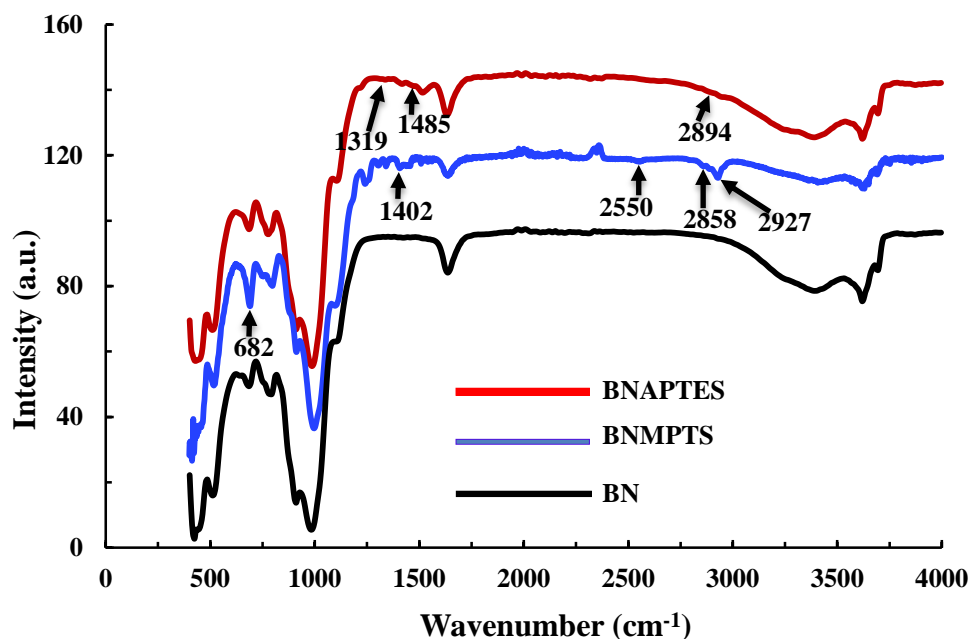


Figure 3.5: Fourier transform-infrared spectra of bentonite (BN), BNMPTS and BNAPTES solids.

3.1.4. Point of zero charge (pH_{PZC}) of solid samples

The point of zero charge (pH_{PZC}) is defined as the pH value at which the total charge on the surface of the solid is zero, i.e., the surface of the solid material possesses neither positive nor negative charges (Khormaei *et al.*, 2007). The mechanism of adsorption taking place at solid solution boundary is illustrated from the determination of point of zero charge. Below pH_{PZC} , the materials exhibit total net positive charge, and above to the pH_{PZC} , the materials surface possesses total net negative charge because. This is due to the acidic dissociation/association of surface functional groups. The pH_{PZC} obtained for the raw bentonite and BNMPTS and BNAPTES are presented in Table 3.1. and the plots are shown in Figure 3.6. Table 3.1 clearly indicated that the functionalized materials and raw bentonite showed almost identical pH_{PZC} values.

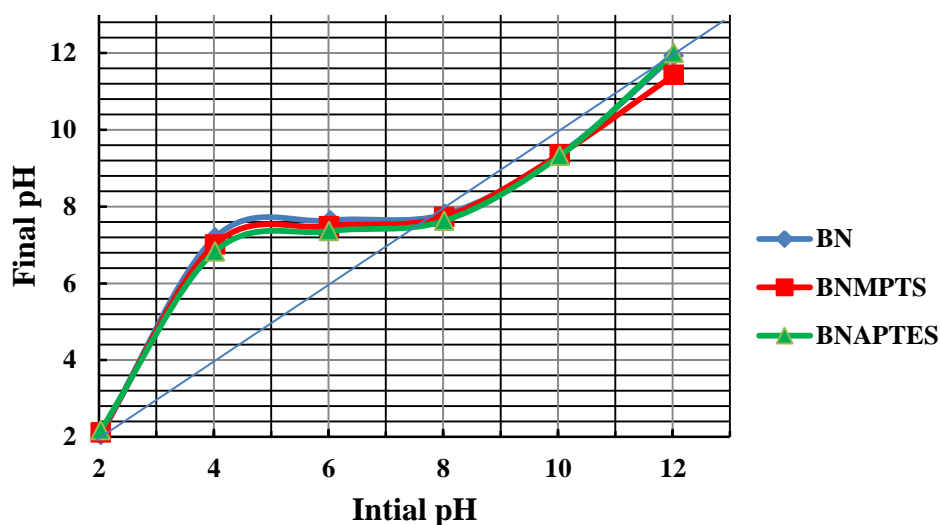


Figure 3.6: Plots of initial pH vs final pH of various solid materials viz., pristine bentonite (BN), BNMPTS and BNAPTES.

Table 3.1. The pH_{PZC} values obtained for the BN, BNMPTS and BNAPTES solids.

Sl. No.	Solid samples	pH_{pzc}
1	BN	7.81
2	BNMPTS	7.73
3	BNAPTES	7.63

3.1.5. BET analyses of solids samples

The Brunauer, Emmett, and Teller (BET) method was employed for obtaining the specific surface area, pore volume, and pore size of raw bentonite (BN), BNMPTS and BNAPTES solids and results are presented in Table 3.2. Moreover, the nitrogen adsorption-desorption isotherms of these solids are presented in Figure 3.7. It is clear from the figure that all the solid materials possessed type IV isotherm with H3 type hysteresis loop. This indicated that the solid materials are exhibiting mesoporous structure (Paul *et al.*, 2011; Qin *et al.*, 2014). Additionally,

the N₂ adsorption-desorption isotherm reveals that a larger hysteresis loop was obtained for raw bentonite with the pore size of 68.39 Å and pore volumes of 0.07 cm³/g. On the other hand, the pore size and pore volume of BNMPTS and BNAPTES were found to be 237.91 Å, 0.03 cm³/g and 165.12 Å, 0.05 cm³/g, respectively. The BET specific surface area of BN, BNMPTS and BNAPTES were found to be 41.14, 4.64 and 12.50 m²/g, respectively. It is interesting to note that BNMPTS and BNAPTES showed significant reduction in the specific surface area once the bentonite was functionalized with organo silane. The results confirmed that the pores on the surface of bentonite were occupied by the MPTS/APTES molecules hence, caused for reduction specific area of solids. Previously, it was reported that hybrid material obtained by the intercalation with gemini surfactant showed a significant decrease in the specific surface area from 155 m²/g to 6 m²/g, (Tcheumi *et al.*, 2010). Similarly, acid activation of raw bentonite resulted in the increase in specific surface area, however, the grafting of bentonite with amino-propyl (AP) and diethylene-triamine (DT) resulted with a significant decrease in specific surface area (Horri *et al.*, 2019). A significant decrease in the specific surface area of SBA-15 was observed after the incorporation of amino propyl or mercapto group (Liu *et al.*, 2000). In a line, the grafting of 3-aminopropyltriethoxysilane (APTES) and 3-mercaptopropyltrimethoxysilane (MPTMS) onto silica gels caused for significant decrease in the surface area of materials (Walcarius *et al.*, 2002).

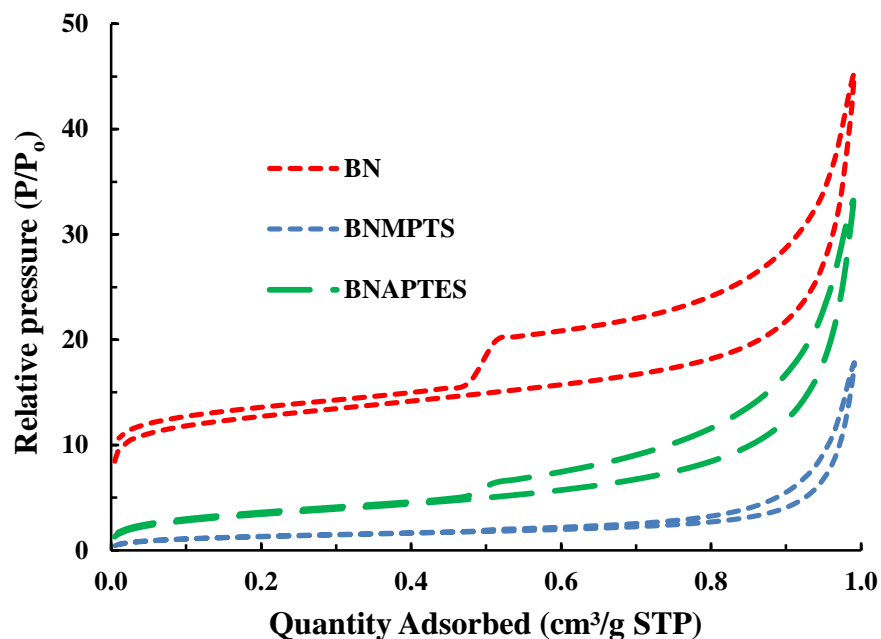


Figure 3.7: Nitrogen adsorption-desorption isotherms for (a) pristine bentonite (BN); (b) BNMPTS; and (c) BNAPTES solids.

Table 3.2. BET pore size, specific pore volume and specific surface area values of pristine bentonite (BN), BNMPTS and BNAPTES solids.

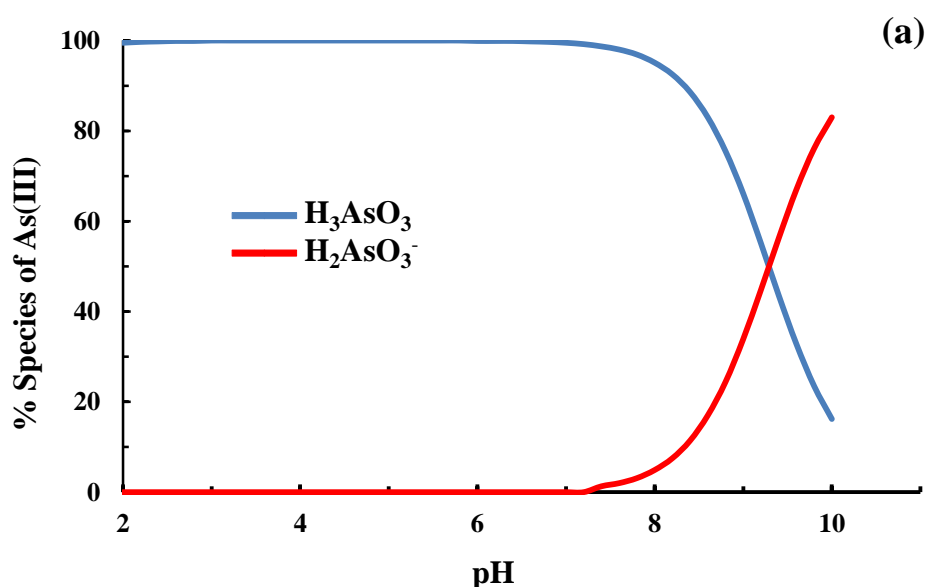
Materials	Pore size (Å)	Specific pore volume (cm ³ /g)	BET specific surface area (cm ² /g)
BN	68.39	0.07	41.14
BNMPTS	237.91	0.03	4.64
BNAPTES	165.14	0.05	12.5

3.2. Speciation studies

The speciation studies were conducted by using Visual MINTEQ (Version 3.1) freeware chemical equilibrium software and the equilibrium constants used were given in the previous Chapter and Section 2.2.4. The results achieved with speciation studies could enable to understand the sorption studies or to deduce the mechanism involved at solid/solution interface. Therefore, a complete speciation studies were carried out in a wide range of pH i.e., pH 2.0 to 10.0.

3.2.1. Speciation of arsenic(III) and arsenic(V)

The speciation of As(III) and As(V) in aqueous solution at different pH values are studied and results are presented in Figure 3.8(a) and 3.8(b), respectively for As(III) and As(V). It is observed that up to pH ~8.0, As(III) exists as H_3AsO_3 uncharged species and beyond pH ~8.0, it dissociates and the anionic H_2AsO_3^- species are dominant. On the other hand, at lower pH i.e., up to pH ~6.8, As(V) exists predominantly as H_2AsO_4^- and H_3AsO_4 species and the anionic species HAsO_4^{2-} species is fully dominant above pH 6.8.



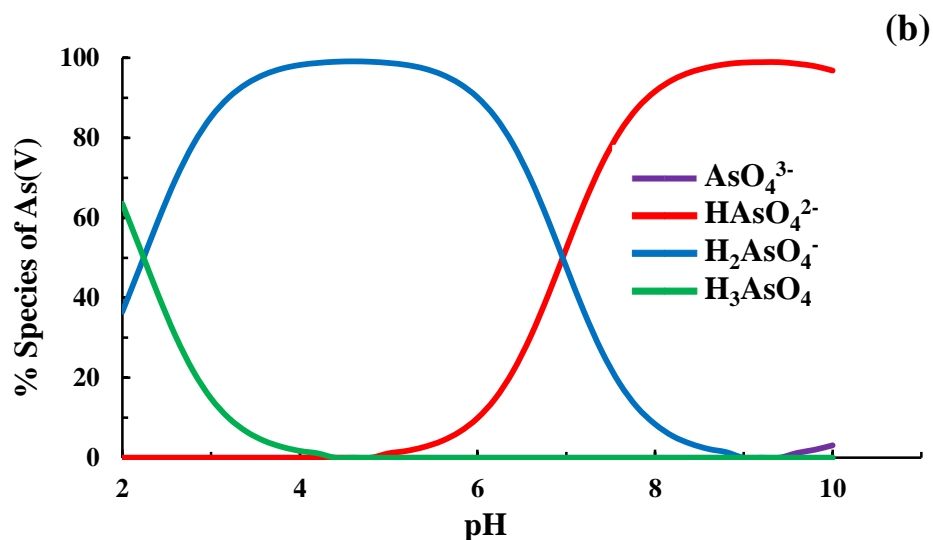


Figure 3.8: Percentage distribution of various species of (a) As(III) and; (b) As(V) as a function of pH ([As(III)/ or As(V)]: 10.0 mg/L; Temperature: 25°C).

3.2.2. Speciation of copper(II)

The speciation results (Figure 3.8(c)) obtained for Cu(II) show that copper exists as the ionic form of Cu^{2+} up to pH ~5.5, beyond that it starts precipitating as insoluble tenorite species. The insignificant $\text{Cu}(\text{OH})^+$ species was formed between pH 5.0-7.0 with a maximum of 1.4 % only. Cu(II) shows formation of insoluble tenorite species at lower pH comparing to other metal ions. Therefore, in order to carry out the adsorption experiments without precipitation for Cu(II), it was suggested to perform the sorption studies at lower pH values i.e., ~pH 4.0.

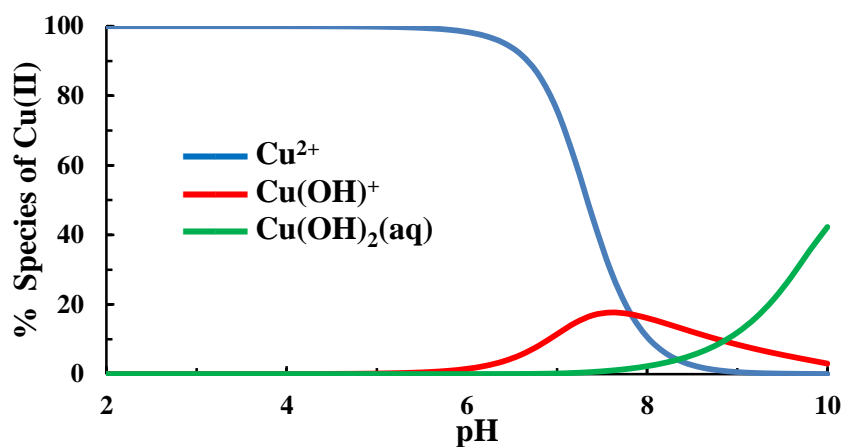


Figure 3.8(c): Percentage distribution of various species of Cu(II) as a function of pH ([Cu(II)]: 10.0 mg/L; Temperature: 25°C).

3.2.3. Speciation of cadmium(II)

The speciation data obtained for Cd(II) is presented graphically in Figure 3.8(d). The results show that cadmium exists as Cd²⁺ soluble cationic species exist up to pH 8.8. Beyond the pH 9.0 the cadmium turns into insoluble Cd(OH)₂ species and above the pH 10.0, the Cd(OH)₂ is the only dominant species. In between pH 8.0 to 10.0; maximum of 5.1 % of cadmium exists as Cd(OH)⁺ species.

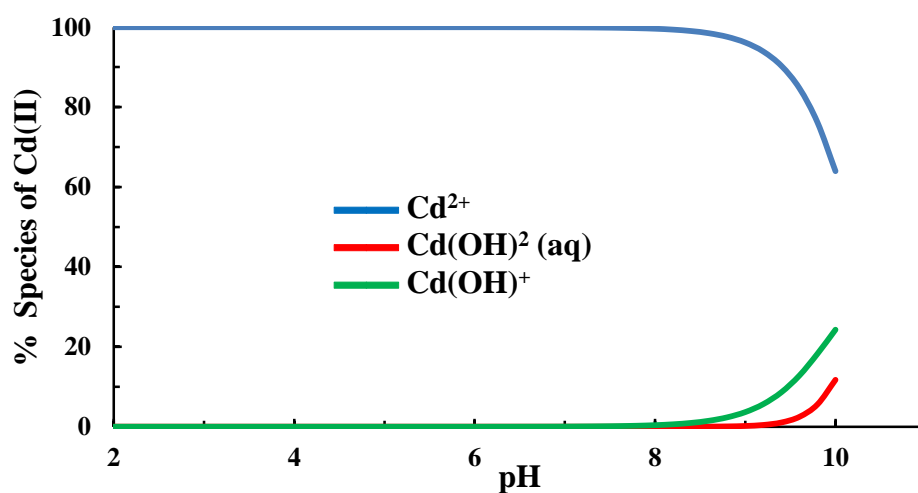


Figure 3.8(d): Percentage distribution of various species of Cd(II) as a function of pH ([Cd(II)]: 10.0 mg/L; Temperature: 25°C).

3.3. BATCH REACTOR STUDIES

3.3.1. Effect of pH

3.3.1.1. Removal of arsenic(III) and arsenic(V)

The effect of pH on the sorption of As(III) and As(V) using the functionalized materials BNMPTS and BNAPTES was conducted at wide range of solution pH (pH 2.0 to 10.0), taking ~10.0 mg/L As(III)/or As(V) solution and at a solid dose of 2.0 g/L. Results are presented graphically in Figure 3.9 (a and b). The speciation of arsenic, pH_{PZC} and functional groups on the surface of the adsorbents are useful parameters demonstrating the mechanism of sorbate ions onto the surface of solid. The pH_{PZC} of the solids BN, BNMPTS and BNAPTES were found to be 7.81, 7.73 and 7.63, respectively. Therefore, below the value of pH_{PZC} , the materials are having net positive charge and beyond pH_{PZC} , the materials are possessed with the net negatively charge. On the other hand, the speciation of As(III) and As(V) was conducted and shown in Figure 3.8 (a and b). The speciation results clearly reveal that up to pH 8.0, the As(III) exists as neutral H_3AsO_3 species and beyond this pH, the As(III) is predominantly having the negatively charged species $H_2AsO_3^-$. The lower percentage removal of As(III) at lower pH was due to the excess of H^+ ions which results in strong competition between neutral arsenic species and the H^+ ions towards the surface of the adsorbent which restricts the attraction of arsenic species toward the surface of the solid material. However, on increasing the pH of the solution, higher percentage removal of As(III) was observed. This is due to the strong chelation between As(III) and thiol group of BNMPTS. Further increasing the solution pH (6.42 to 10.11) resulted a significant decrease in percentage removal of As(III). This is due to the strong repulsive forces between the negatively charged solid surface due to the dissociation of thiol group as thiolates and negatively charged sorbate species of As(III) (Hao *et al.*, 2009; Li *et al.*, 2014; Zhang *et al.*, 2015).

On the other hand, the pristine bentonite (BN) showed almost insignificant removal of As(III) as compared to the BNMPTS functionalized solid. This clearly inferred that the functionalized material BNMPTS found promising material in the removal of As(III) from aqueous solutions.

Moreover, the percentage removal of As(V) by the BNAPTES is shown in Figure 3.9 (b). The results indicated that increasing the pH from 2.67 to 5.21, the percentage removal of As(V) was increased and attained a maximum percentage of adsorption at pH 5.21. Further increase in pH 5.21 to 10.29, a gradual but sharp decrease in percentage removal of As(V) was recorded. The speciation studies which was conducted separately for As(V) is shown in Figure 3.8 (b). It is evident from the speciation studies that the As(V) is predominantly existed in the anionic species $\text{pH} > 3.4$. $\text{pH} < 3.4$, the neutral species H_3AsO_4 was predominantly present. Therefore, the low percentage uptake of As(V) at lower pH value (pH 2.67) is due to the presence of neutral As(V) species and positively charged solid surface. This, perhaps, restricted slightly the uptake of As(V) by the solid surface. However, relatively high uptake of As(V) was recorded between the 4.36 to 6.58 is due to the increased in the anionic species H_2AsO_4^- as well as the protonated amino group from APTES through strong electrostatic interaction which promotes the adsorption of As(V) (Boyacı *et al.*, 2011; Chen *et al.*, 2008). The decreased in the percent removal of As(V) by BNAPTES beyond pH 6.58 is due to the electrostatic repulsion between the negatively charged solid surface and presence of anionic species of sorbate ions i.e., the H_2AsO_4^- and AsO_3^- species (Lee *et al.*, 2015).

Further, it was also recorded that very low uptake of As(V) was obtained using the BN solid i.e., pristine bentonite as compared to the BNAPTES. This clearly inferred that the functionalized material BNAPTES possessed much enhanced removal efficiency compared to the pristine bentonite solid.

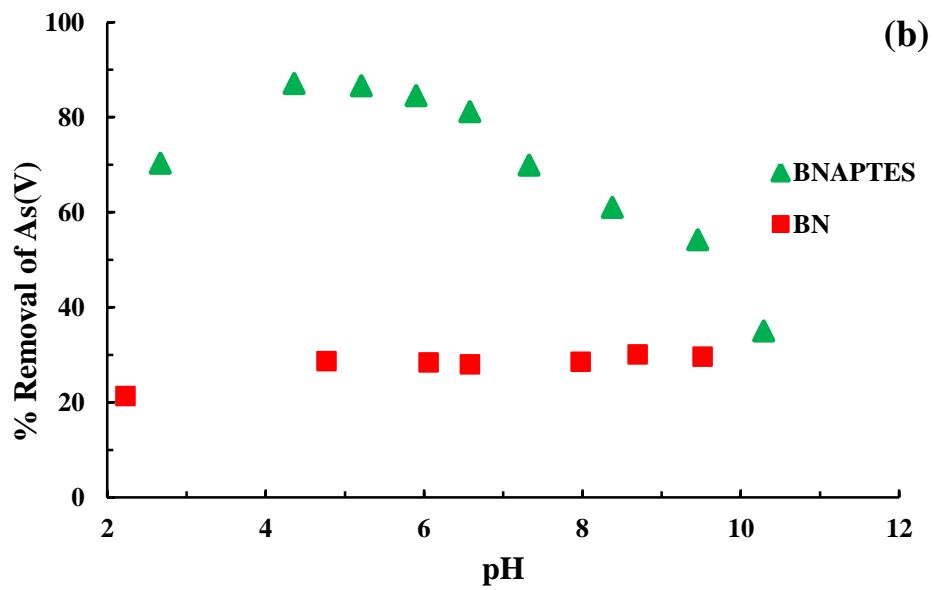
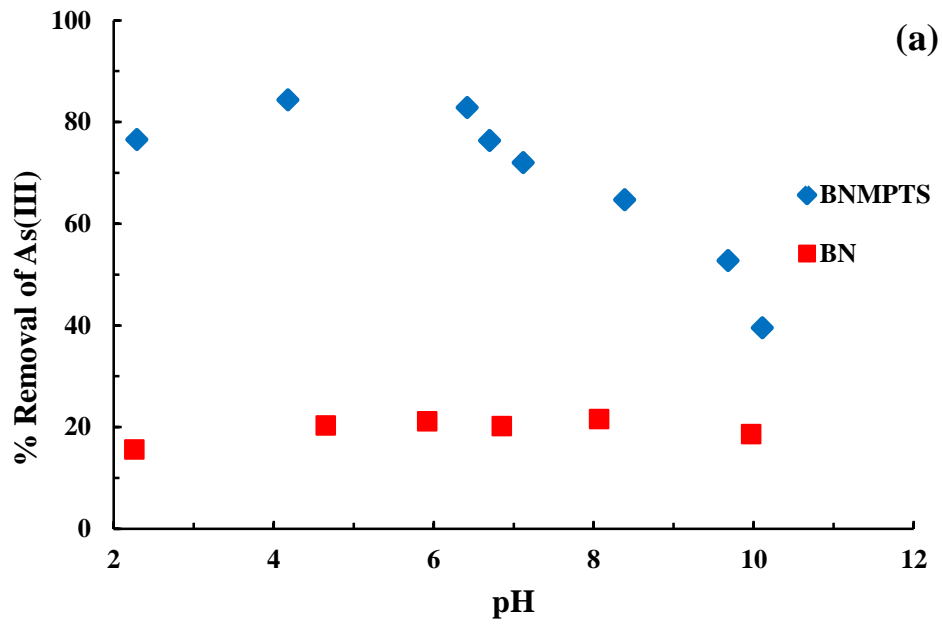


Figure 3.9: Effect of pH in the removal of (a) As(III) by the BNMPTS; and (b) As(V) by the BNAPTES solids ([As(III)/ or As(V)]: 10.0 mg/L; Solid dose: 2.0 g/L; Temperature: 25°C).

3.3.1.2. Removal of copper(II)

The pH dependence removal of Cu(II) by the pristine bentonite and BNMPTS was studied in the solution pH (2.0 to 7.0), taking ~10.0 mg/L Cu(II) solution, and with a solid dose of 2.0 g/L. The percentage removal of Cu(II) as a function of pH is shown Figure 3.10. It is interesting to observe that the grafting of MPTS with bentonite network has enabled to achieve the percentage removal of Cu(II) of almost 100% within the pH range of 2.0 to 7.0. Therefore, the pH dependent study revealed that BNMPTS possessed very high affinity towards Cu(II) at wide range of pH and showed potential applicability in remediation of wastewater contaminated with toxic Cu(II) ions. The pH_{PZC} of the BNMPTS was determined and found to be 7.73. This indicated that BNMPTS possessed net positive charge below pH 7.73 and it is having net negative charge above to this pH. On the other hand, the speciation studies of Cu(II) is conducted and shown in Figure 3.8 (c). The speciation studies indicated that the Cu(II) exists as Cu^{2+} species up to pH 5.5. Between pH 5.0 to 7.0, Cu(II) exists as insignificant species of $Cu(OH)^+$ with a maximum of 1.4% only. Further, Cu(II) starts to form insoluble tenorite species beyond pH~5.5. The high percentage removal of Cu(II) beyond 5.5 could be the mixed effect of adsorption and co-precipitation of Cu(II) onto the surfaces of the BNMPTS material (Tiwari *et al.*, 2007). However, the high removal of Cu(II) even at lower pH values clearly indicated the high affinity of solid towards the Cu(II). Moreover, it was revealed that Cu(II) was bound with strong chemical forces rather the weaker physical forces. The availability of -SH or -OH groups, possibly, took part in the bond formation onto the solid surface. Moreover, the dense brushes of the silanes are available with the composite materials which traps the Cu(II) and forming the strong chemical bond on the surface which significantly enhances the sorptive removal of Cu(II) from aqueous solutions in a wide range of pH. Moreover, the further insights of Cu(II) by the BNMPTS is studied and demonstrated with Cd(II) sorption studies in later section 3.3.1.4. Further, based on the pH dependence studies an optimum pH (pH 4.0) was used for other experimentation in the removal of Cu(II).

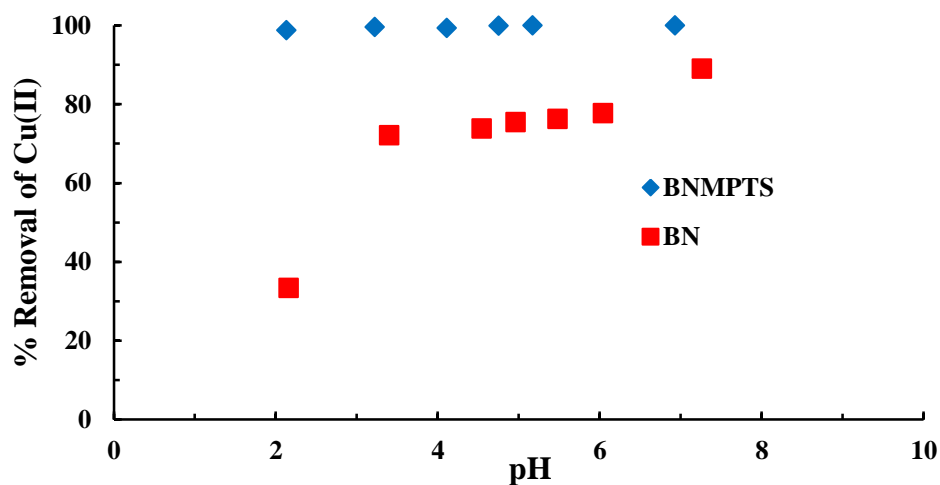


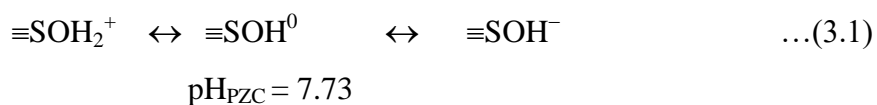
Figure 3.10: Effect of pH in the removal of Cu(II) by BNMPTS ([Cu(II)]: 10.0 mg/L; Solid dose: 2.0 g/L; Temperature: 25°C).

3.3.1.3. Removal of cadmium(II)

The removal of Cd(II) using pristine bentonite and BNMPTS materials was studied for a wide range of pH (2.0 to 10.0) using 5.0 mg/L Cd(II) solution at a solid dose of 2.0 g/L. The percentage removal of Cd(II) as a function of pH is shown in Figure. 3.11. It is noteworthy that the removal efficiency of pristine bentonite is significantly increased with the grafting of MPTS with bentonite network. Figure clearly evident that very high percentage (Ca 99 %) of Cd(II) was removed at wide pH range i.e., pH 3.0 to 10.0. The pH dependent study showed that BNMPTS exhibited reasonably high affinity towards Cd(II) within a wide pH range. This clearly indicated the potential of material towards the remediation of water contaminated with Cd(II).

The mechanism of the uptake of Cd(II) by the BNMPTS is proposed based on the surface and the solute properties in solutions at wide range of pH. Hence, the speciation studies of Cd(II) and the pH_{PZC} are the important parameters studied in detail for proposing plausible mechanism involved at solid/solution interface. The pH_{PZC} of the BNMPTS was found to be 7.73 which inferred that the surface of

BNMPTS possessed net positive charge at pH < 7.3 and net positive charge at pH < 7.3. The equilibrium is represented as equation 3.1.



On the other hand, the speciation of Cd(II) studied and results are shown in Figure 3.8 (d). It is evident from the Figure 3.8 (d) that the cadmium predominantly existed as cationic species Cd^{2+} up until pH 8.8. However, further increase in pH (pH>8.8), Cd(II) started forming the insoluble $\text{Cd}(\text{OH})_2(\text{s})$ species. In between *Ca* pH 8.7, about 5% of $\text{Cd}(\text{OH})^+$ species existed. Therefore, these results indicated that the Cd(II) is predominantly present as cationic species within wide range of pH (pH 2.0 ~ 9.0) (Tiwari *et al.*, 2007). It is notable that the high percentage of Cd(II) was removed even in the acidic conditions or below the pH_{pzc} of the BNMPTS. Therefore, it indicated that the BNMPTS is having strong affinity towards the solid surface. Cd(II) is forming stronger chemical bond on the surface of solid (also studied with background electrolyte concentrations studies.). The Cd(II) possibly forming the strong chemical bond with the available -OH or the -SH groups. Therefore, the insights of the sorption studies were conducted at pH 5.0. The Cd(II) sorbed on BNMPTS material was intended for XPS analysis which is given in later section 3.3.1.4. The XPS analysis could reveal the possible binding sites of Cd(II) onto the solid surface.

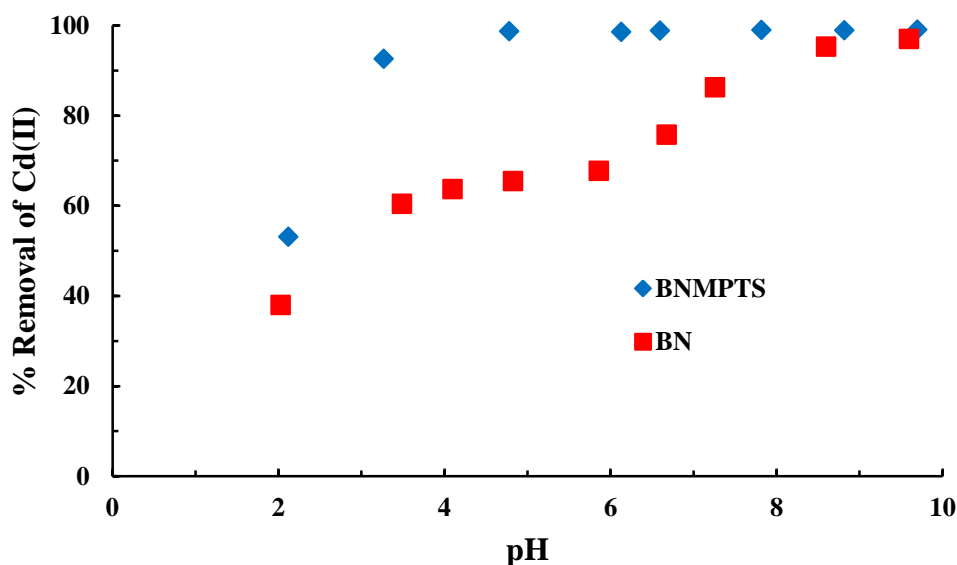


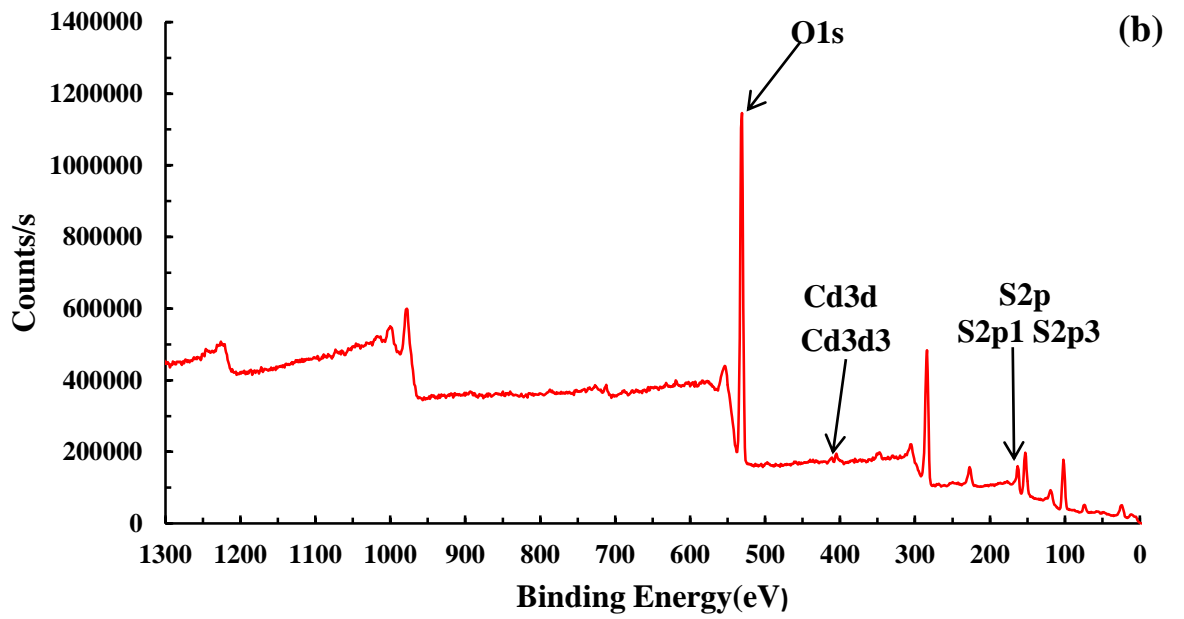
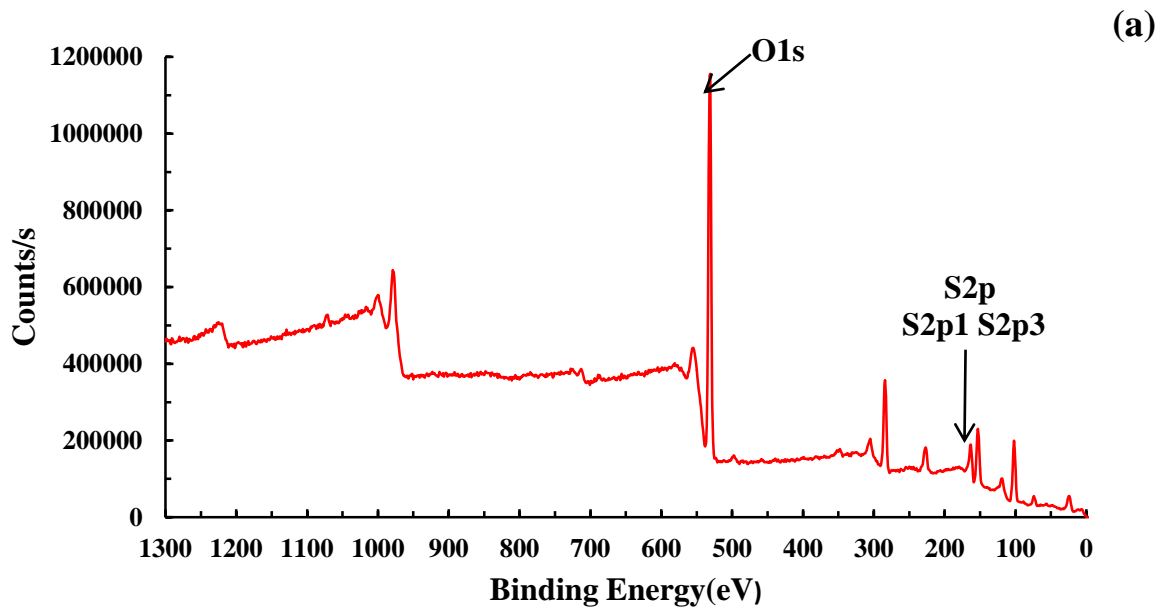
Figure 3.11: Effect of pH in the removal of Cd(II) by BNMPTS ([Cd(II): 10.0 mg/L; Solid dose: 2.0 g/L; Temperature: 25°C).

3.3.1.4. Mechanism of copper(II) and cadmium(II) sorption by BNMPTS

Previous reports have shown that an enhanced uptake of Cu(II) was achieved using mercapto functionalized silica aerogel (Štandeker *et al.*, 2011), Poly(vinyl alcohol)/silica (PVA/silica) membranes (Keshtkar *et al.*, 2013), electrospun CeO₂ nanofiber (Yari *et al.*, 2015) and palygorskite (Han *et al.*, 2015). Similarly, the removal of Cd(II) was obtained using the mercapto functionalized silica (Kosak *et al.*, 2015; Machida *et al.*, 2012), palygorskite (Liang *et al.*, 2013), attapulgite (Wang *et al.*, 2019), sepiolite (Liang *et al.*, 2011), zinc based metal organic framework (Zhang *et al.*, 2016) and coal gangue (Shang *et al.*, 2019). It was assumed that the metal ions (i.e., Cu(II)/Cd(II)) undergo with chemisorption on the surface of mercapto functionalized surface and consequently forming an ‘inner-sphere complexes’ at the surface. Further, several researchers have reported that the incorporated mercapto group play a key role in the removal of Cu(II)/Cd(II) (Shang *et al.*, 2019; Yari *et al.*, 2015; Zhang *et al.*, 2016); whereas few researchers reported that the removal of toxic metal ions using mercapto functionalized materials mainly

occurred through the adsorption on surface hydroxyl group (Han *et al.*, 2015; Wang *et al.*, 2019). In order to ascertain the mechanistic pathway of Cu(II) and Cd(II) adsorption onto the BNMPTS was analysed before and after the adsorption Cu(II) and Cd(II) by the X-ray photoelectron spectrometer (XPS) results. The wide scan spectra are shown in Figure 3.12 (a-c). The X-ray photoelectron spectra obtained after the adsorption of Cu(II) and Cd(II) evidently showed the Cu2p and Cd3d electrons peaks. The doublet at the binding energies of 933.3 and 957.3 eV peaks are obtained due to the Cu2p(1/2) and Cu2p(3/2) electrons. Similarly, the binding energy peaks at 405.7 and 412.4 eV are primarily due to the Cd3d(3/2) and Cd3d(5/2) electrons, respectively. These results clearly indicated that Cu(II) and Cd(II) is sorbed onto the BNMPTS surface.

Further, the change in binding energy of O1s before and after the adsorption of Cu(II) and Cd(II) are plotted and shown in Figure 3.13 (a). It is evident that the O1s peak was slightly shifted from 530.0 to 531.2 eV and 530 to 531.3 eV after the adsorption of Cu(II) and Cd(II), respectively. This inferred that the surface hydroxyl groups are predominantly involved in the adsorption of Cu(II) and Cd(II) onto BNMPTS (Jiang *et al.*, 2019; Shahrokhi-Shahraki *et al.*, 2021). Moreover, the binding energy of S2p electrons was obtained at 163.14 eV (Figure 3.13 (b)) and this peak is attributed to disulfide bond (Han *et al.*, 2015). This binding energy remain almost same after the adsorption of Cu(II)/or Cd(II) which suggested that the mercapto groups are not involved in the adsorption of these two toxic metal ions. Previously, Wang *et al.* studied the role of disulfide in the adsorption of Cd(II) by mercapto-functionalized attapulgite (MATP) using density functional theory (DFT) calculations and found that disulfide did not play significant role in Cd(II) adsorption (Wang *et al.*, 2019). Therefore, insight mechanisms study revealed that the adsorption of Cu(II)/or Cd(II) mainly occurred through the terminal hydroxyl groups present on the surface of BNMPTS material and consequently forming the ‘inner sphere complexes’ (Cf Figure 3.13(c)). Further, the XPS analytical results showed that substantial amount of Cu(II) and Cd(II) were adsorbed on the BNMPTS and the atomic percentage of Cu and Cd in the used BNMPTS solids were recorded as 0.87% and 0.45%, respectively.



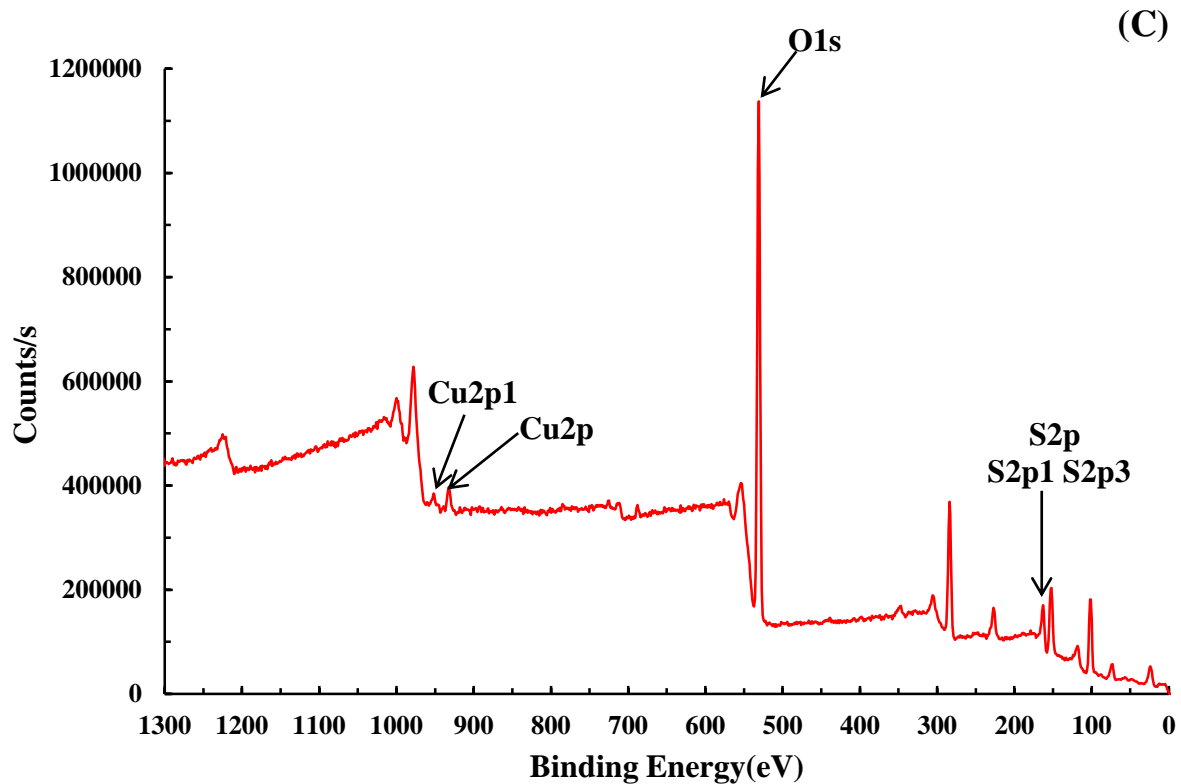
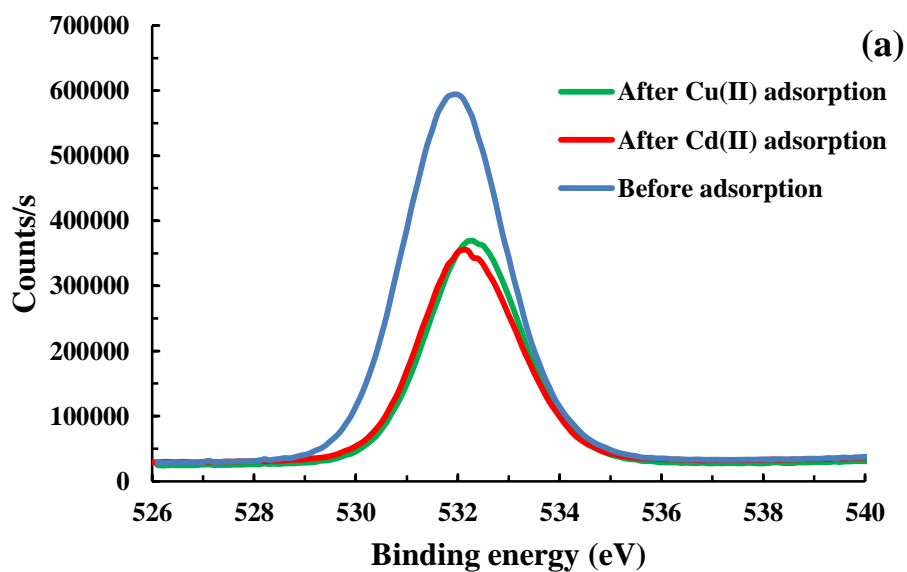


Figure 3.12: (a) XPS spectra of BNMPTS before adsorption of Cu(II) and Cd(II); (b) XPS spectra of BNMPTS after adsorption of Cd(II); and (c) XPS spectra of BNMPTS after adsorption of Cu(II).



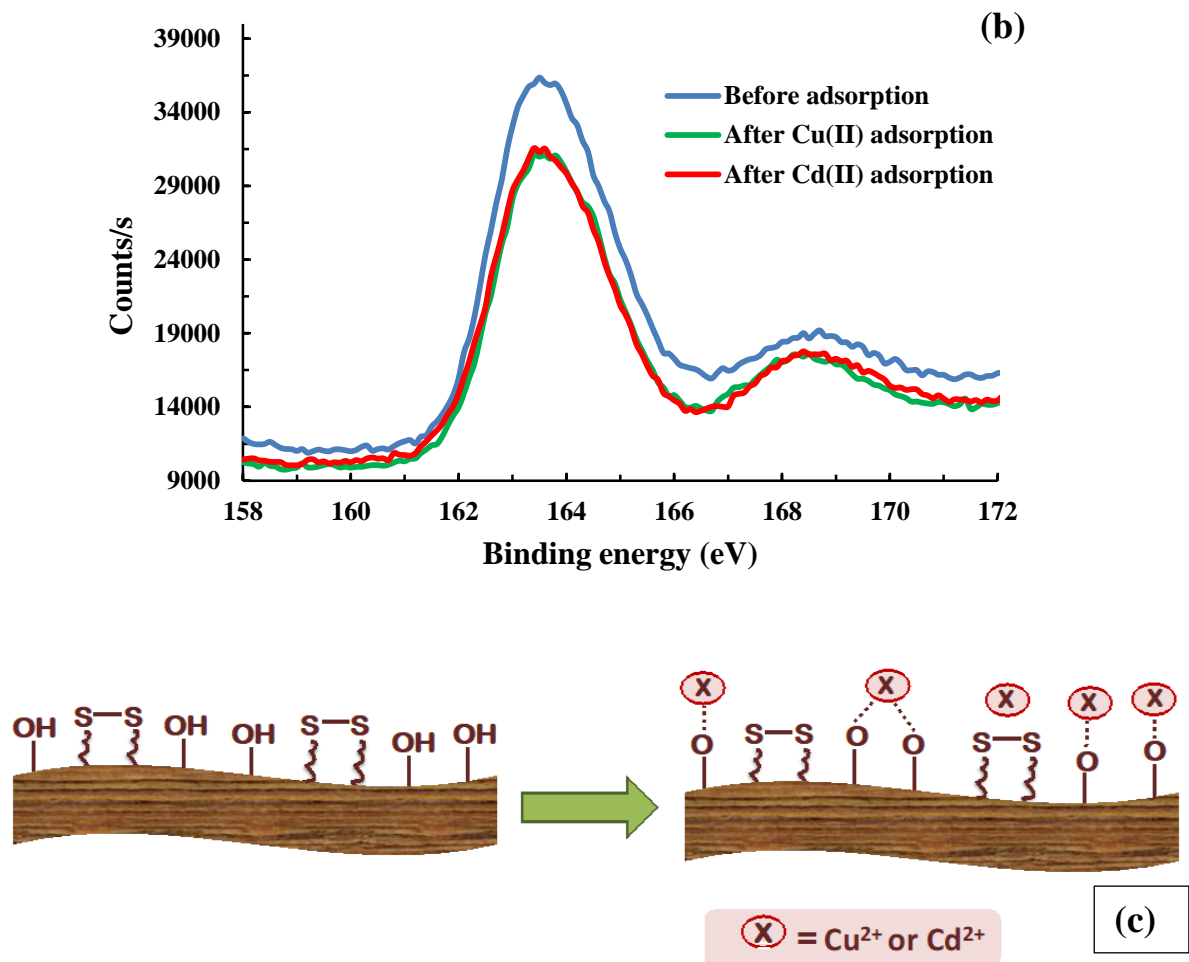


Figure 3.13: (a) O1s spectra before and after adsorption of Cu(II) and Cd(II) using BNMPTS; (b) S2p spectra before and after adsorption of Cu(II) and Cd(II) using BNMPTS; and (c) Schematic of sorption of Cu²⁺ and Cd²⁺ by the BNMPTS solid.

3.3.1.5. Tetracycline (TC)

The effect of pH on the removal of tetracycline using BNMPTS and BNAPTES along with pristine bentonite is performed at a wide pH range (pH 3.0 to 10.0) using the tetracycline concentration 10.0 mg/L. Results are presented as in Figure 3.14. It is notable that the percentage removal of tetracycline by BNMPTS and BNAPTES is significantly increased compared to the pristine bentonite. These results indicated that BNMPTS and BNAPTES materials possessed enhanced affinity towards the tetracycline. The tetracycline is having three acid dissociation constants

viz., pK_{a1} (3.31), pK_{a2} (7.72) and pK_{a3} (9.71) (Barbooti *et al.*, 2014; Gopal *et al.*, 2020). Therefore, using these pK_a values the distribution of these species at different pH values is obtained and the percentage distribution of each species of tetracycline as a function of pH is shown in Figure 3.15. It is evident that within the pH region 3.3–7.7, tetracycline mainly exists as zwitterion (TCH_2^0 or TCH_2^{0+}) structure due to the loss of a proton from phenolic di-ketone moiety. Further, the anionic species (TCH^- or TCH^{+-}) exists above the pH 7.7, by losing its proton leading to a net negative charge. And beyond pH 9.7, the di-anionic species of tetracycline is dominated which is due to the dissociation of third proton from the tri-carbonyl system and phenolic diketone moiety (Tiwari *et al.*, 2019).

The varied percentage elimination of tetracycline at various pH values are explained with the help of speciation studies of tetracycline as a function of pH as well the pH_{PZC} of the solids. Moreover, the results showed that the pristine bentonite possessed very high removal percentage for tetracycline at very low pH values i.e., *Ca* pH 3.7. However, the increase in pH has caused a sharp decrease in removal efficiency and only 10% of tetracycline was removed at pH *Ca* 10.0 using the pristine bentonite.

It is shown the very high percentage (*Ca* 98%) removal of tetracycline by BNMPTS was almost identical for a wide pH region i.e., pH 3.2 - 7.0, (*Cf* Figure 3.14). However, further increase in pH ($pH > 7.0$), the elimination of tetracycline is decreased sharply and reached to a value of 21% at pH ~10. As seen from the speciation studies, tetracycline is predominantly present in the anionic forms at $pH > 3.4$. On the other hand, the pH_{PZC} of pristine bentonite and BNMPTS is 7.81 and 7.73, respectively. Therefore, the surface is positively charged at $pH < 7.65$ (for BNMPTS) and $pH < 7.82$ (for BN). This showed that $pH < 7.0$, the anionic species of tetracycline is attracted by the positively charged surface of BNMPTS, hence, very high uptake of tetracycline is recorded in this region. The uptake of tetracycline by the BNMPTS is not only due to the electrostatic attraction, since almost similar pH_{PZC} was recorded for the bentonite solid but the uptake of tetracycline was sharply decreased at $pH > 3.6$ using the pristine bentonite. This implied that the grafting of silane within the bentonite network enabled the solid more hydrophobic with enhanced organophilic nature. This eventually, facilitated the sorption of tetracycline

by the BNMPTS solid. This caused for very high uptake of tetracycline by the BNMPTS solid at pH up until 7.0. However, further increase in pH i.e., $\text{pH} > 7.0$, a sharp decrease in percentage uptake of tetracycline was recorded. This is, perhaps, due to the fact that strong electrostatic repulsive forces are dominated and hindered the elimination of tetracycline by BNMPTS solid since both the sorbate and sorbent are possessed with net negative charges. Similar outcomes were reported on the adsorption of tetracycline onto Fe-Mt (Wu *et al.*, 2016) and illite (Chang *et al.*, 2012).

On the other hand, the high percentage removal of tetracycline (Ca 96%) by BNAPTES solid showed almost constant removal efficiency up until the pH 8 and further increase in pH had caused a slight decrease in percentage removal of tetracycline. The pH_{PZC} value of BNAPTES was found to be 7.81. This indicated that BNAPTES possessed a strong affinity towards the tetracycline molecules and caused for the high removal efficiency of removal. It is due to the fact that the BNAPTES provides fairly good hydrophobic environment having high organophilic nature which partitioned the tetracycline molecule at the solid surface and facilitated the removal of tetracycline. However, $\text{pH} > 8.0$, both the solid and sorbate species are possessed with net negative charges which hindered slightly the removal of tetracycline by BNAPTES. Hence, relatively lower uptake of tetracycline at very high pH values ($\text{pH} > 8.0$) was recorded. A similar decrease in the adsorption capacity of tetracycline on *Pinus taeda*-derived activated biochar at higher pH (> 7.0) was observed. This was due to a strong electrostatic repulsion between the negatively charged surfaces of *Pinus taeda*-derived activated and negative species of tetracycline with weak π - π electron donor acceptor (EDA) interaction (Jang *et al.*, 2018; Zhou *et al.*, 2017). On the other, hand the decrease in removal efficiency using the BNAPTES was not that significant for tetracycline even at $\text{pH} > 8$. This further, implied the potential applicability of functionalized material (BNAPTES) towards the removal of tetracycline from aqueous solutions.

The results obtained suggest that hydrophobic interaction is the main reason for the high uptake of tetracycline by BNAPTES compared to bentonite within the studied pH range (Thanhmingliana *et al.*, 2015)

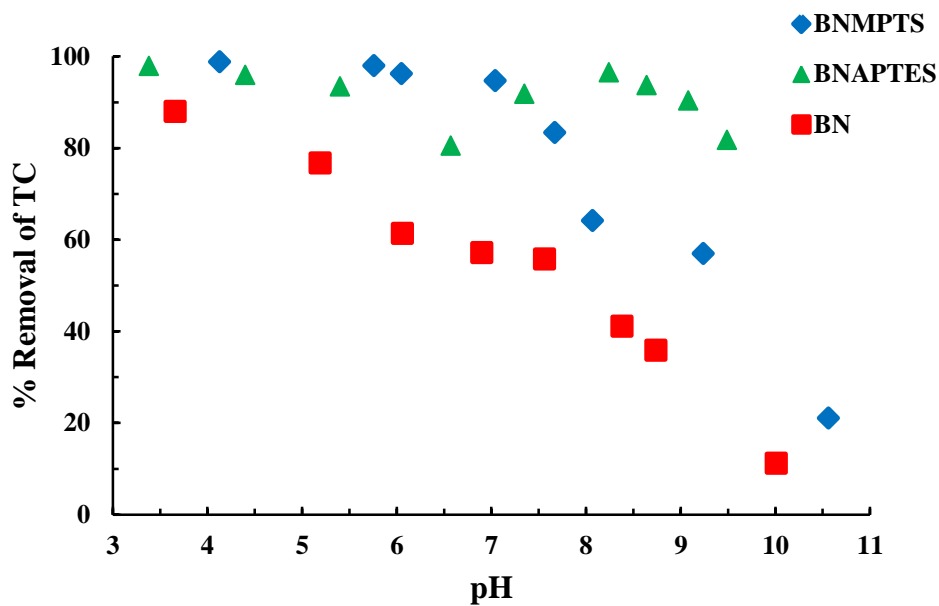


Figure 3.14: Percentage removal of tetracycline by pristine bentonite and functionalized bentonite (BNMPTS and BNAPTES) as a function of pH ([TC]: 10.0 mg/L; Solid dose: 2.0 g/L; Temperature: 25°C).

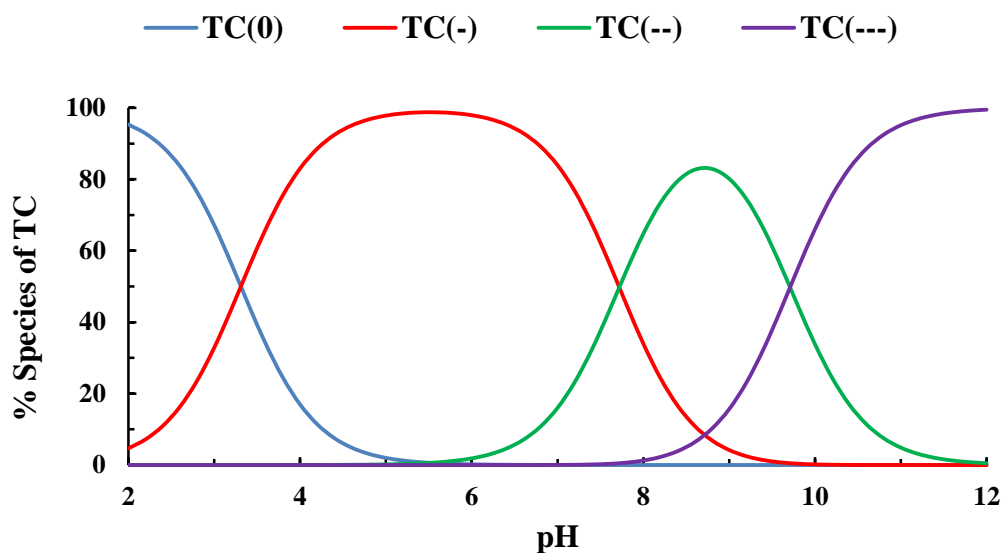


Figure 3.15: Percentage distribution of tetracycline (TC) as a function of pH ([TC]: 10.0 mg/L; Temperature: 25°C).

3.2.1.6. Triclosan (TCS)

The pH dependent removal of triclosan was conducted at wide range of pH 3.0 to 10.0. The percentage removal of triclosan using BNMPTS and BNAPTES along with the pristine bentonite is illustrated in Figure 3.16. The pristine clay bentonite showed relatively high uptake at lower pH~3.4, however, further increase in pH caused significant decrease in percentage uptake of triclosan and reached very low removal at neutral pH~7.0. Therefore, the pristine bentonite showed very limited implications in the elimination of triclosan from aqueous solution. However, the removal of triclosan is almost unaffected using BNMPTS and BNAPTES solid as the pH increased from *Ca.* pH 3.21 to 7.01. However, the removal of triclosan was decreased abruptly with further increase in pH (pH>7.0) and attained to low removal percentage at *Ca.* pH 10. The elimination of triclosan is almost constant within the pH<7.0. Triclosan is having the acid dissociation constant values as pK_{a1} : 7.90 and pK_{a2} : 8.1 (Solá-Gutiérrez *et al.*, 2020). Therefore, the speciation of triclosan is conducted and presented in Figure. 3.17 also reported previously (Tiwari *et al.*, 2020). It is evident from the speciation studies that triclosan is predominantly present as uncharged species at pH<7.0. However, pH>7.0, the dominant species are anionic species (i.e., TCS^- or TCS^{2-}). Therefore, very high uptake of triclosan at pH<7.0 is primarily due to the hydrophobic and organophilic nature of BNMPTS and BNAPTES towards the triclosan. The strong hydrophobic interactions between the triclosan molecules and organo-modified clay had enabled for enhanced elimination of triclosan (Styszko *et al.*, 2015). Similar, removal behaviour was reported previously in the removal of triclosan by kaolinite and montmorillonite (Behera *et al.*, 2010).

However, the increase in pH>7.0, a rapid decrease in percentage elimination of triclosan by the BNMPTS and BNAPTES is observed. This is due to the fact that the anionic species of triclosan and negatively charged solid surface caused strong repulsive forces which retarded significantly the sorption of triclosan by BNMPTS and BNAPTES. Generally, a high removal percentage of triclosan at neutral pH conditions is providing an optimum pH conditions indicating BNMPTS and BNAPTES in the treatment strategies for efficient removal of triclosan from water bodies at neutral pH conditions.

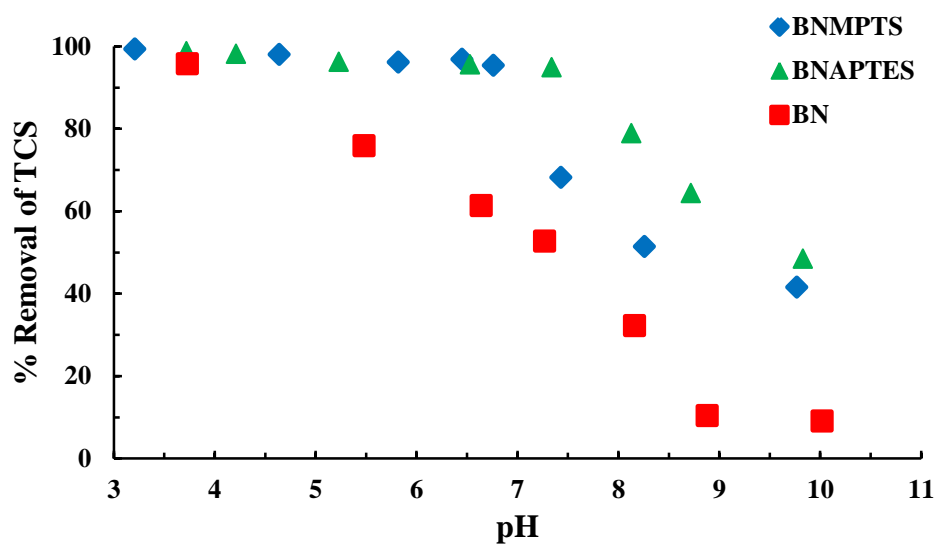


Figure 3.16: Percentage removal of triclosan (TCS) by pristine bentonite and functionalized materials (BNMPTS and BNAPTES) as a function of pH ([TCS]: 10.0 mg/L; Solid dose: 2.0 g/L; Temperature: 25°C).

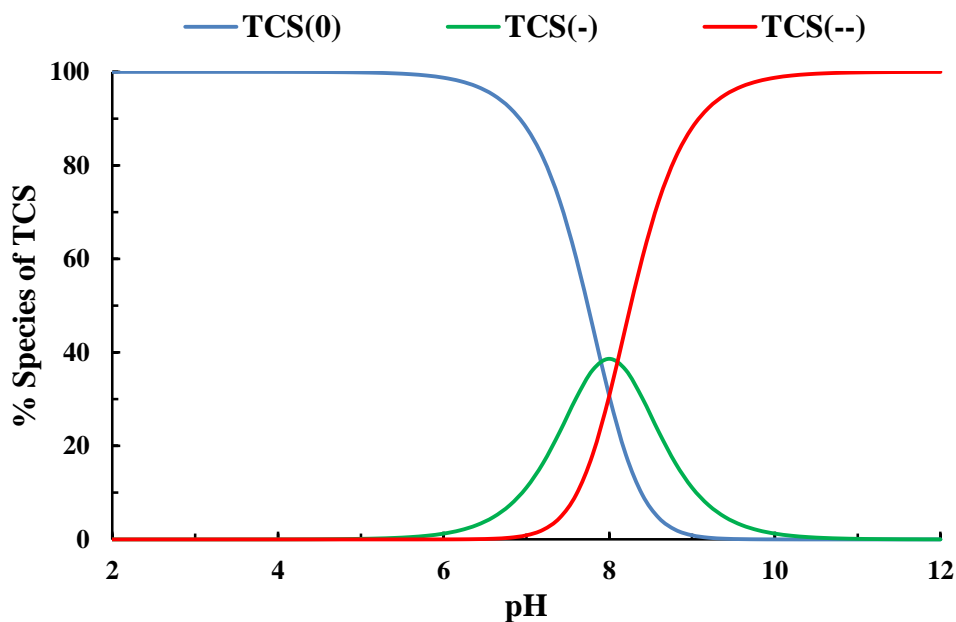


Figure 3.17: Percentage distribution of triclosan (TCS) as a function of pH ([TCS]: 10.0 mg/L; Temperature: 25°C).

3.2.1.7. 17 α -ethinylestradiol (EE2)

The pH dependence sorption of 17 α -ethinylestradiol (EE2) is illustrated in Figure 3.18. Figure reveals that the elimination of EE2 by the BN is quite low within the studied pH (pH 3.0 to 10.2). A maximum of *Ca* 43% of EE2 was recorded at pH 5.8. However, using the silane grafted bentonite solids i.e., BNMPTS and BNAPTES showed significantly enhanced elimination of EE2 within the studied pH (3.0 to 10.2). It is further noted that a maximum of *Ca* 85 and 74% of EE2 was eliminated using the BNMPTS and BNAPTES solids, respectively at around pH 6.0. The acid dissociation constant (pK_a) of EE2 was reported as 10.5 (Al-Khateeb *et al.*, 2014). Therefore, the EE2 exists as neutral species $pH \ll 10.5$ and carries net negative charge $pH \gg 10.5$ (*Cf* Figure 3.19). On the other hand, the pH_{PZC} (point of zero charge) of BN, BNMPTS and BNAPTES is obtained as 7.81, 7.73 and 7.63, respectively. Therefore, a high removal of EE2 by using the BNMPTS and BNAPTES solids at wide range of pH is demonstrated with the hydrophobic interaction between the EE2 and BNMPTS and BNAPTES solids. The organo-silanes introduced within the bentonite sheets provide enhanced hydrophobicity with the organophilic nature which intended to attract the EE2 molecules and enabled a high uptake of EE2. Moreover, the dense grafted structure of BNMPTS and BNAPTES has enabled significantly to trap the EE2 from aqueous solutions and enhanced the elimination of EE2. Further, it is noted that the removal of EE2 by the BNMPTS showed very high uptake which was almost unaffected within the pH region pH 4.0-10.0. This indicated that the EE2 showed very high affinity towards the denser composite solid (having specific surface area of 4.64 m²/g) and hence, the dense material traps efficiently the EE2. The similar results were reported for the removal of As(V) using the MPTS grafted chitosan where it was assumed that the introduced silanes provides sorbing sites along with the siloxane sites. Hence, the As(V) forms weaker bonds and caused for high percentage removal (Lalhmunsiana *et al.*, 2016a). On the other hand, the BNAPTES showed slightly less adsorption at lower pH values i.e., pH ~4.0. However, almost a constant removal of EE2 is obtained within the pH region i.e., pH~5.0-9.0. The low removal at pH 4.0 is possibly due to the competition between the H⁺ and EE2 towards the solid surface. Additionally, it is observed that BNAPTES showed relatively less percentage

removal compared to the BNMPTS. This is because of the reason that the BNAPTES is relatively less dense material compared to the BNMPTS since the specific surface area of BNAPTES is relatively high i.e., 12.5 m²/g. This restricted partly the uptake of EE2 by BNAPTES. A similar result in the removal of EE2 is reported using activated carbon powder (Zhang and Zhou, 2005) or even As(V) by APTS grafted chitosan (Lalhmunsiamma *et al.*, 2016b). Moreover, comparing to BNMPTS and BNAPTES, the BNMPTS showed relatively higher percentage removal of EE2 throughout the studied pH (3.0 to 10.0). This indicated the higher affinity of materials for EE2.

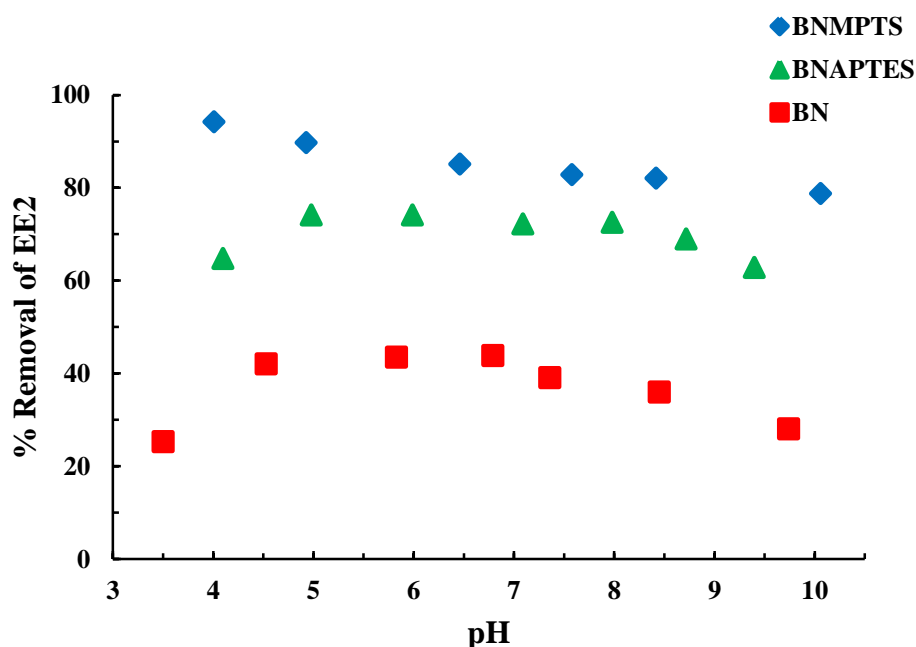


Figure 3.18: Percentage removal of EE2 by pristine bentonite and functionalized bentonite solids (BNMPTS and BNAPTES) as a function of pH ([EE2]: 10.0 mg/L; Solid dose: 2.0 g/L; Temperature: 25°C).

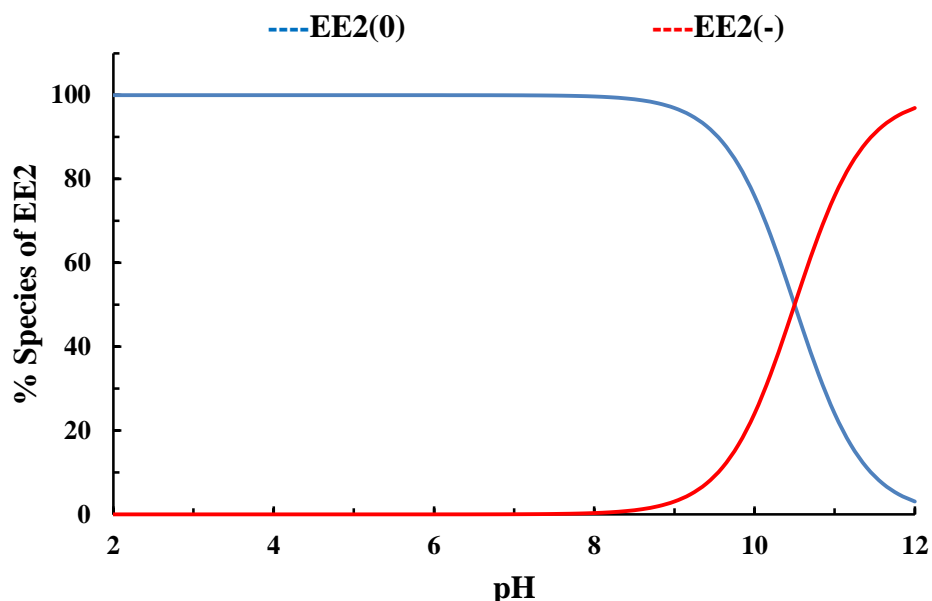


Figure 3.19: Percentage distribution of 17 α -ethinylestradiol (EE2) as a function of pH ([EE2]: 10.0 mg/L; Temperature: 25°C).

3.3.2. Effect of sorptive concentration

3.3.2.1. Arsenic(III) and arsenic(V)

The concentration dependence sorption of As(III) and As(V) using BNMPTS and BNAPTES, respectively was performed by varying the concentrations of arsenic from 1.0 to 25.0 mg/L; pH 3.5 for As(III) and As(V) and the results are shown in Figure 3.20. Increasing the concentration of As(III) and As(V) from 1.0 to 25.0 mg/L, the percentage removal was decreased from 90 to 70% for As(III) using BNMPTS and 89 to 67% for As(V) using BNAPTES. The high removal percentage of As(III) or As(V) even at high concentrations by the functionalized solids BNMPTS and BNAPTES inferred the high affinity of these pollutants towards the solids.

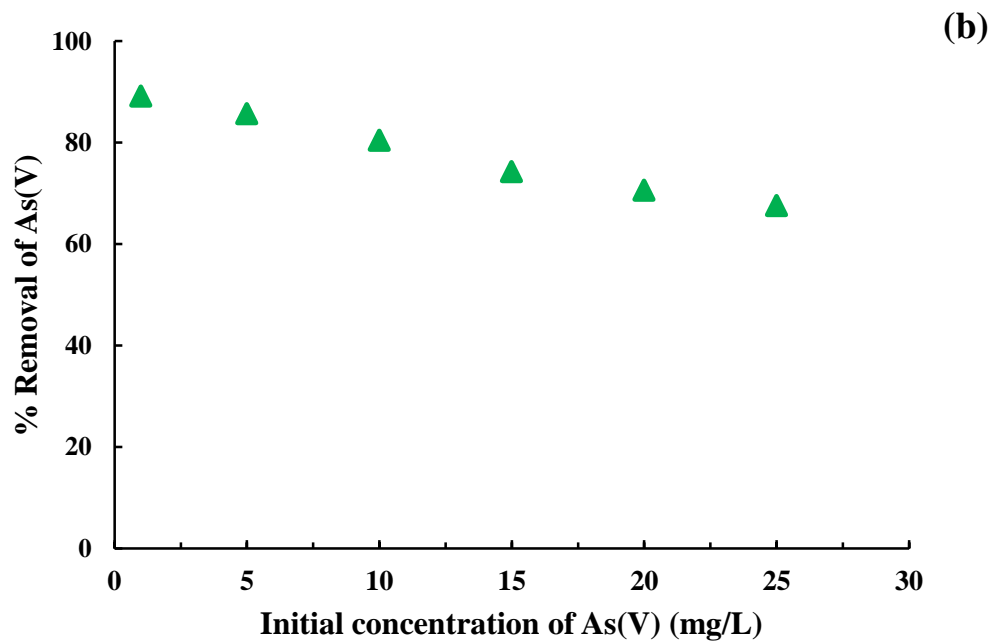
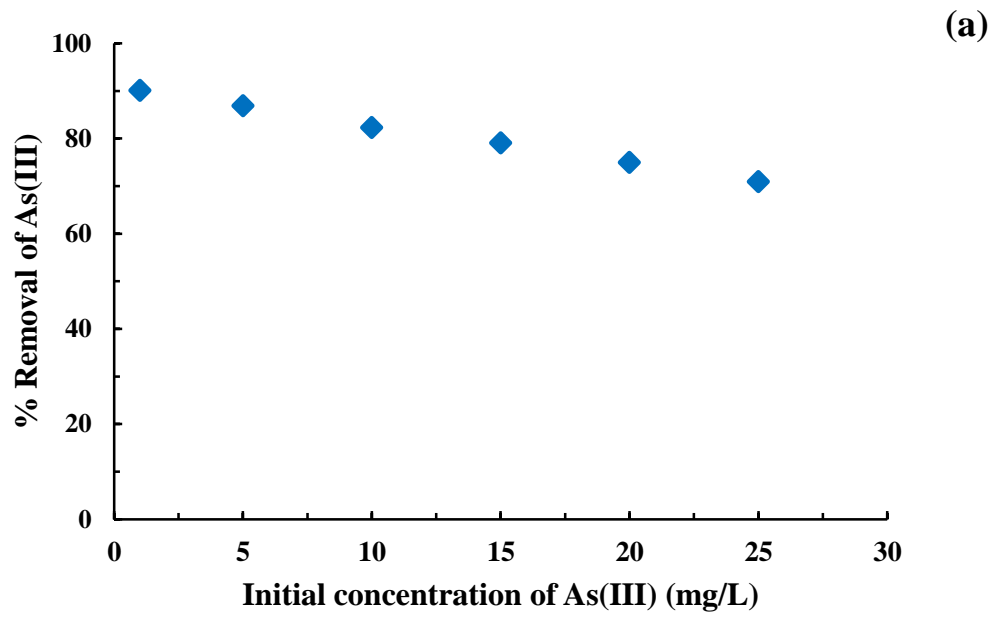


Figure 3.20: Effect of initial sorptive concentration in the removal of (a) As(III) by BNMPPTS; and (b) As(V) by BNAPTES (pH: 3.5; Solid dose: 2.0 g/L; Temperature: 25°C).

3.3.2.2. Copper(II)

Similarly, the concentration dependence removal of Cu(II) was conducted at pH 4.0 to estimate the efficiency and adsorption capacity of the modified material towards copper ions. The concentration dependence percentage removal of Cu(II) by the BNMPTS is illustrated in Figure 3.21. It is observed that BNMPTS is able to attain very high percentage removal of Cu(II) at varied concentrations of Cu(II). Increasing the initial Cu(II) concentrations from 1.0 to 25.0 mg/L did not affect very high percentage removal (almost 100%) of Cu(II). At the initial metal concentration of 25.0 mg/L, the BNMPTS is able to remove 96% Cu(II). These findings indicated that BNMPTS material is highly efficient for the removal of Cu(II) from aqueous solutions. The amount of Cu(II) removed from aqueous solutions is significantly increased while increasing the initial Cu(II) concentration from 1.0 to 25.0 mg/L, and the uptake amount of Cu(II) was increased from 0.493 to 11.955 mg/g.

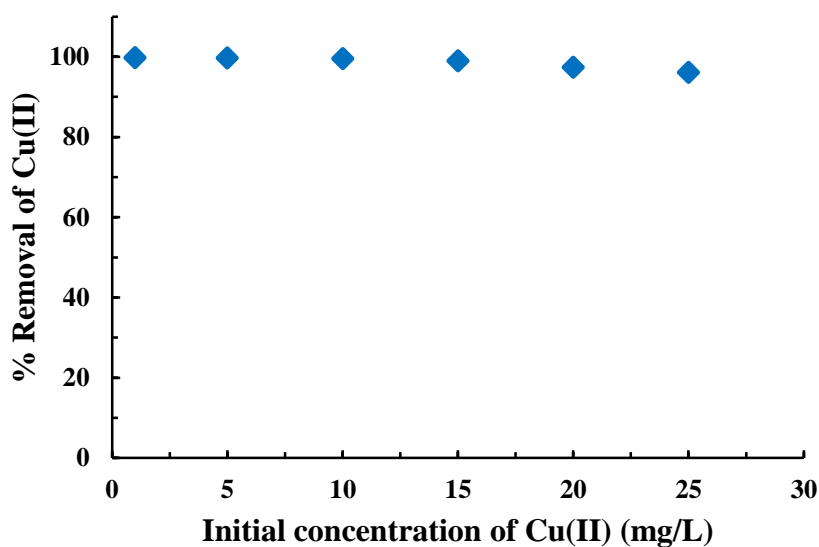


Figure 3.21: Effect of initial sorptive concentration in the removal of Cu(II) by BNMPTS (pH: 4.0; Solid dose: 2.0 g/L; Temperature: 25°C).

3.3.2.3. Cadmium(II)

The concentration dependence sorption of Cd(II) was conducted to estimate the efficiency and adsorption capacity of the silane grafted materials BNMPTS at wide range of initial cadmium(II) concentrations i.e., 1.0 to 25.0 mg/L at pH 5.0. Further, the percentage removal of Cd(II) by the BNMPTS at varied concentrations of Cd(II) is presented in Figure 3.22. A very high percentage removal at varied concentrations of Cd(II) is achieved using BNMPTS solid. Interesting to note that the percentage removal of Cd(II) was not affected by increasing the concentration of Cd(II) from 1.0 to 25.0 mg/L. BNMPTS was able to remove >93% of Cd(II) at the initial metal concentration of 25.0 mg/L. These outcomes reveal that BNMPTS material is highly efficient for the removal of Cd(II) from aqueous solutions. Moreover, increasing the initial concentrations of Cd(II), the amount of Cd(II) removed from aqueous solutions is significantly increased and the uptake amount of Cd(II) is increased from 0.418 to 11.592 mg/g while increasing the initial Cd(II) concentration from 1.0 to 25.0 mg/L, respectively.

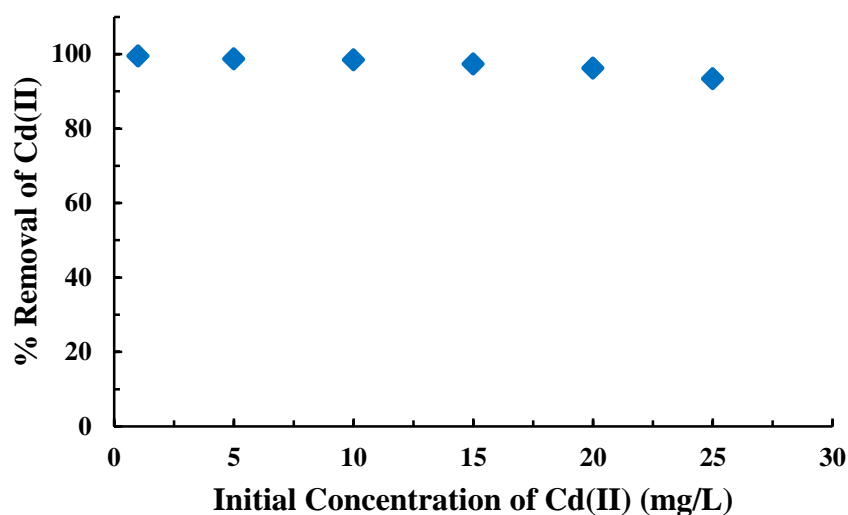


Figure 3.22: Effect of initial sorptive concentration in the removal of Cd(II) by BNMPTS solid (pH: 5.0; Solid dose: 2.0 g/L; Temperature: 25°C).

3.3.2.4. Tetracycline (TC)

The percentage removal of tetracycline using BNMPTS and BNAPTES at various initial concentrations is shown in Figure 3.23. It is noteworthy that very high percentage removal of tetracycline was obtained within the studied concentration range (1.0 to 25.0 mg/L) using the BNMPTS and BNAPTES solids. The percentage removal of tetracycline at the initial concentration of 1.0 mg/L is 97% for both the materials. Moreover, it is interesting to observe that the removal of tetracycline by BNMPTS and BNAPTES is very high even at the initial concentrations of 25.0 mg/L, i.e., 90% of tetracycline and 89% for BNMPTS and BNAPTES, respectively. In this sorption process, it is assumed that the initial concentration of the adsorbate act as a driving force to passed through the sorption barrier at the solid-solution interface; hence, the amount of tetracycline uptake was extensively enhanced from 0.6 to 11.5 mg/g and 0.5 to 11.33 mg/g and for BNMPTS and BNAPTES, respectively, while increasing the initial concentration of tetracycline from 1.0 to 25.0 mg/L. The higher uptake of tetracycline at fairly high initial concentrations reaffirmed the strong affinity of BNMPTS and BNAPTES solids towards the tetracycline.

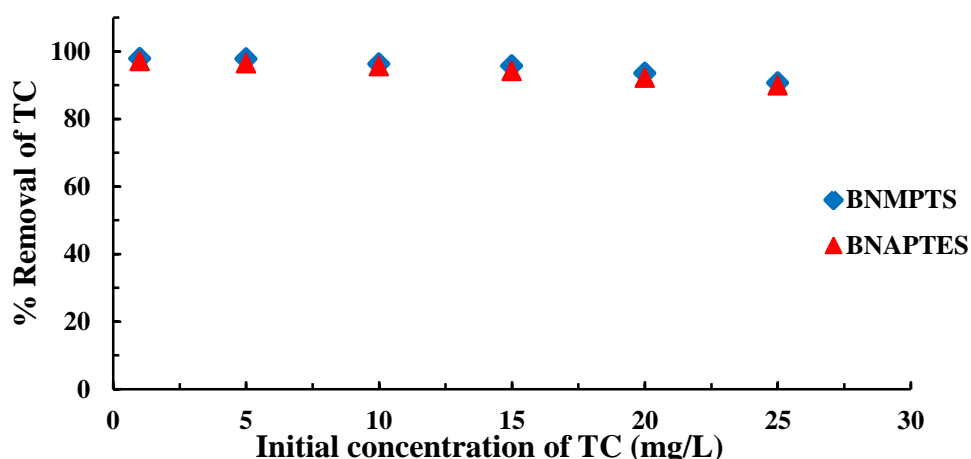


Figure 3.23: Percentage removal of tetracycline by the BNMPTS and BNAPTES materials as a function of initial tetracycline concentrations (pH: 4.0; Solid dose: 2.0 g/L; Temperature: 25°C).

3.3.2.5. Triclosan (TCS)

The sorption performance of BNMPTS and BNAPTES materials towards the triclosan is obtained by varying the triclosan concentrations from 1.0 to 25.0 mg/L (pH: 4.0) at solid dose of 2.0 g/L. Results are plotted with initial sorptive concentration against the percentage removal of triclosan and illustrated in Figure 3.24. Results inferred that the percentage elimination of triclosan is almost unaffected within the studied sorptive concentrations. This implied high affinity of BNMPTS and BNAPTES towards triclosan. Quantitatively, increasing the concentration of triclosan from 1.0 to 25.0 mg/L the removal efficiency is only decreased from 95.8 to 90.6% using BNMPTS and from 95.7 to 89% using BNAPTES solids.

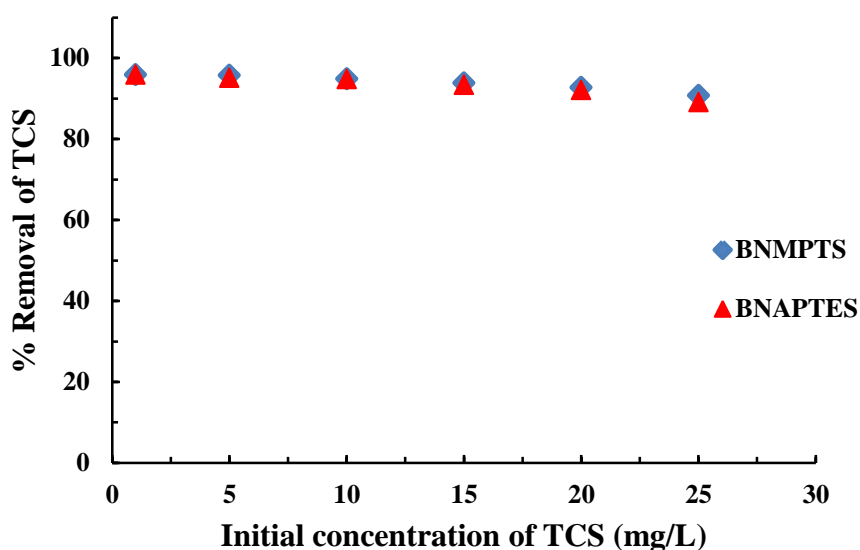


Figure 3.24: Percentage removal of triclosan by the BNMPTS and BNAPTES solids as a function of initial triclosan concentrations (pH: 4.0; Solid dose: 2.0 g/L; Temperature: 25°C).

3.3.2.6. 17 α -ethinylestradiol (EE2)

The relationship between the initial EE2 concentration (1.0 to 10.0 mg/L) and percentage removal of EE2 by the BNMPTS and BNAPTES materials is obtained at pH 4.0 and solid dose 2.0 g/L. The results are illustrated in Figure 3.25. Results indicated that increasing the concentration of EE2, the percentage elimination of EE2 is decreased slightly. Increasing concentration of EE2 from 1.0 to 10.0 mg/L the corresponding decrease in percentage elimination of EE2 is from 92.8 to 86.1% for BNMPTS and 93.3 to 74.4% for BNAPTES solids. Similar to other micro-pollutants, the high percentage uptake of EE2 even at high concentration of EE2 inferred the high affinity of BNMPTS and BNAPTES materials for EE2 and potential sorbing materials for decontamination of water contaminated with various micro-pollutants.

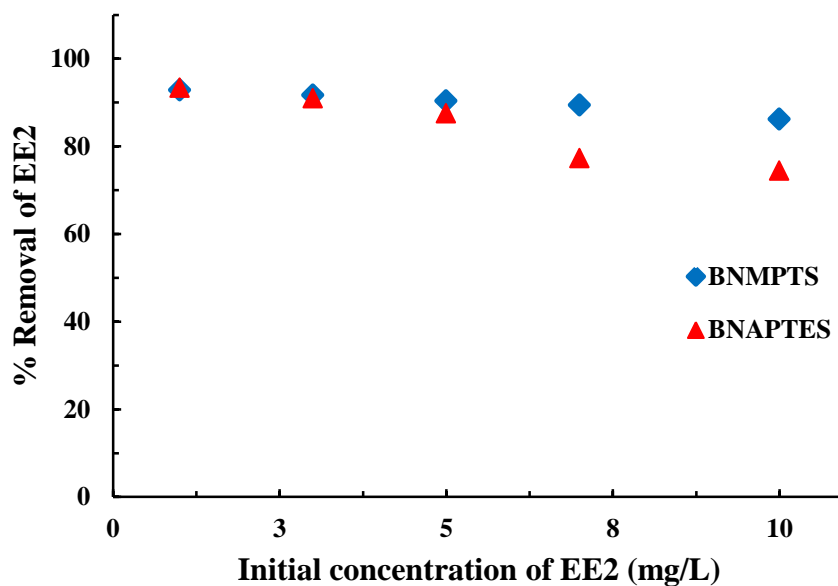


Figure 3.25: Percentage removal of EE2 by the BNMPTS and BNAPTES solids as a function of initial EE2 concentrations (pH: 4.0; Solid dose: 2.0 g/L; Temperature: 25°C).

3.3.3. Adsorption isotherm studies

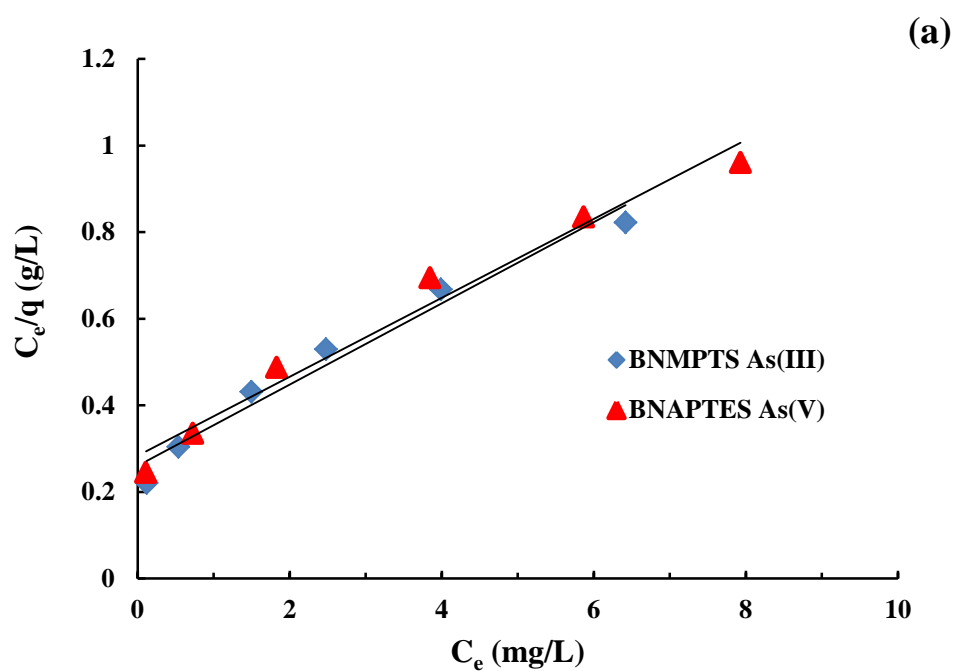
The equilibrium state sorption data acquired for varying sorptive concentrations at constant pH and temperature is further used to determine the adsorption isotherms especially the Langmuir and Freundlich adsorption isotherms.

3.3.3.1. Adsorption isotherm modelling for arsenic(III) and arsenic(V)

Langmuir and Freundlich adsorption isotherms are utilized to deduce the isotherm modelling obtained from the sorptive concentration dependent study (Tang *et al.*, 2017) and shown in Figure 3.26. The unknown constants i.e., Langmuir monolayer sorption capacity (q_o), Langmuir constant (b) and Freundlich constants (K_f and $1/n$) are estimated and presented as in Table. 3.4. Results showed that Langmuir adsorption isotherm is best fitted than the Freundlich isotherm at least for the adsorption of As(III) and As(V) by the functionalized materials since it showed reasonably high value of R^2 values. This result further suggested that monolayer sorption is the dominant mechanism in the sorption of As(III) and As(V) by functionalized materials (Montero *et al.*, 2018). Moreover, the Langmuir constant ' b ' is evaluated which reflects the strength and affinity of the solids towards the sorbing species (Gupta *et al.*, 2005). The sorption capacity obtained from Langmuir monolayer is found to be 10.50 mg/g for As(III) using BNMPTS and 11.93 mg/g for As(V) using BNAPTES. Table 3.3 show that comparatively high values of Langmuir constant (b) and Freundlich constant (K_f) reaffirms the strong attraction of the functionalized materials towards As(III) and As(V). Previous study reported that the maximum sorption capacity of As(III) on almond shell (ALS) and almond shell biochar (ASB) were found to be 4.6 and 4.86 mg/g, respectively. Similarly, for As(V), the maximum sorption capacities were 3.45 and 3.6 mg/g by almond shell (ALS) and almond shell biochar (ASB), respectively (Ali *et al.*, 2020).

Table 3.3. Langmuir and Freundlich constants estimated for the adsorption of As(III) and As(V) using functionalized materials.

Materials	Pollutants	Langmuir isotherm			Freundlich isotherm		
		q_o (mg/g)	b (L/g)	R^2	$1/n$	K_f (mg/g)	R^2
BNMPTS	As(III)	11.933	0.535	0.995	0.668	2.254	0.993
BNAPTES	As(V)	10.504	0.594	0.990	0.672	2.257	0.987



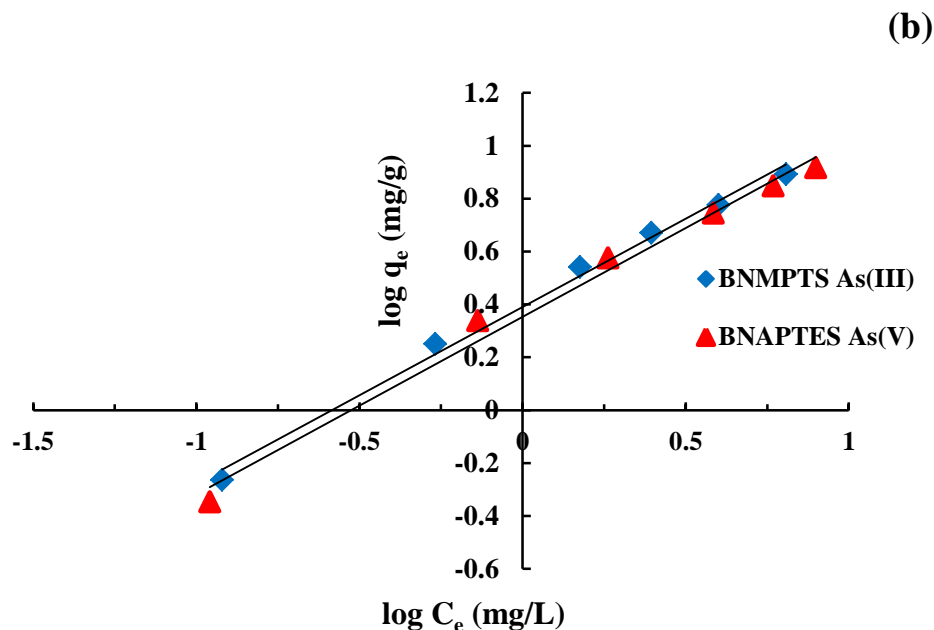


Figure 3.26: Fitting of (a) Langmuir adsorption isotherm for the adsorption of As(III) onto BNMPTS and As(V) onto the BNAPTES; and (b) Freundlich adsorption isotherms for As(III) onto BNMPTS and As(V) onto BNAPTES solids.

3.3.3.2. Adsorption isotherm modelling for copper(II) and cadmium(II)

The linear form of Langmuir and Freundlich adsorption isotherms were utilized for the adsorption of Cu(II) and Cd(II) onto the BNMPTS solid utilizing the concentration dependence data (Tiwari *et al.*, 2007). The results are illustrated in Figure 3.27. The unknown constants i.e., Langmuir monolayer sorption capacity (q_o) and Langmuir constant (b), Freundlich constants (K_f and $1/n$) are assessed and shown in Table 3.4. It is clear from the results that the sorption of Cu(II) and Cd(II) by BNMPTS material followed Langmuir adsorption isotherm model better than Freundlich adsorption isotherm since higher R^2 value was obtained for Langmuir adsorption isotherm. The high value of Langmuir monolayer sorption capacity (q_o) achieved for Cu(II) and Cd(II) by BNMPTS indicates the affinity of BNMPTS towards the Cu(II) and Cd(II). This result further shows the potential use of solid in the removal of these two heavy metal toxic ions from aqueous solutions. Furthermore, the applicability of Langmuir adsorption isotherm pointed that the

surface active sites are distributed evenly onto the surface of the solid (Gupta *et al.*, 2005). Similar results are reported in which the removal of Cd(II) by the dopamine-functionalized meso-structured silica (DMOS) and Cu(II) by mercapto functionalized palygorskite (MPAL) followed Langmuir adsorption isotherm (Chen *et al.*, 2016a; Han *et al.*, 2015). Furthermore, the affinity of BNMPTS towards Cu(II) and Cd(II) is shown by higher values of Langmuir constant (b). Moreover, the Freundlich constant ($1/n$); ($0 < 1/n < 1$) is having fractional values which further showed the heterogenous surface of the material and the available sites for adsorption is distributed exponentially (Raji *et al.*, 1998).

Table 3.4. Langmuir and Freundlich adsorption isotherm constants along with the R^2 values obtained for the adsorption of Cu(II) and Cd(II) using BNMPTS material.

Pollutants	Langmuir isotherm			Freundlich isotherm		
	q_o (mg/g)	b (L/g)	R^2	$1/n$	K_f (mg/g)	R^2
Cu(II)	12.594	10.447	0.988	0.521	3.317	0.928
Cd(II)	13.192	3.716	0.988	0.587	3.861	0.979

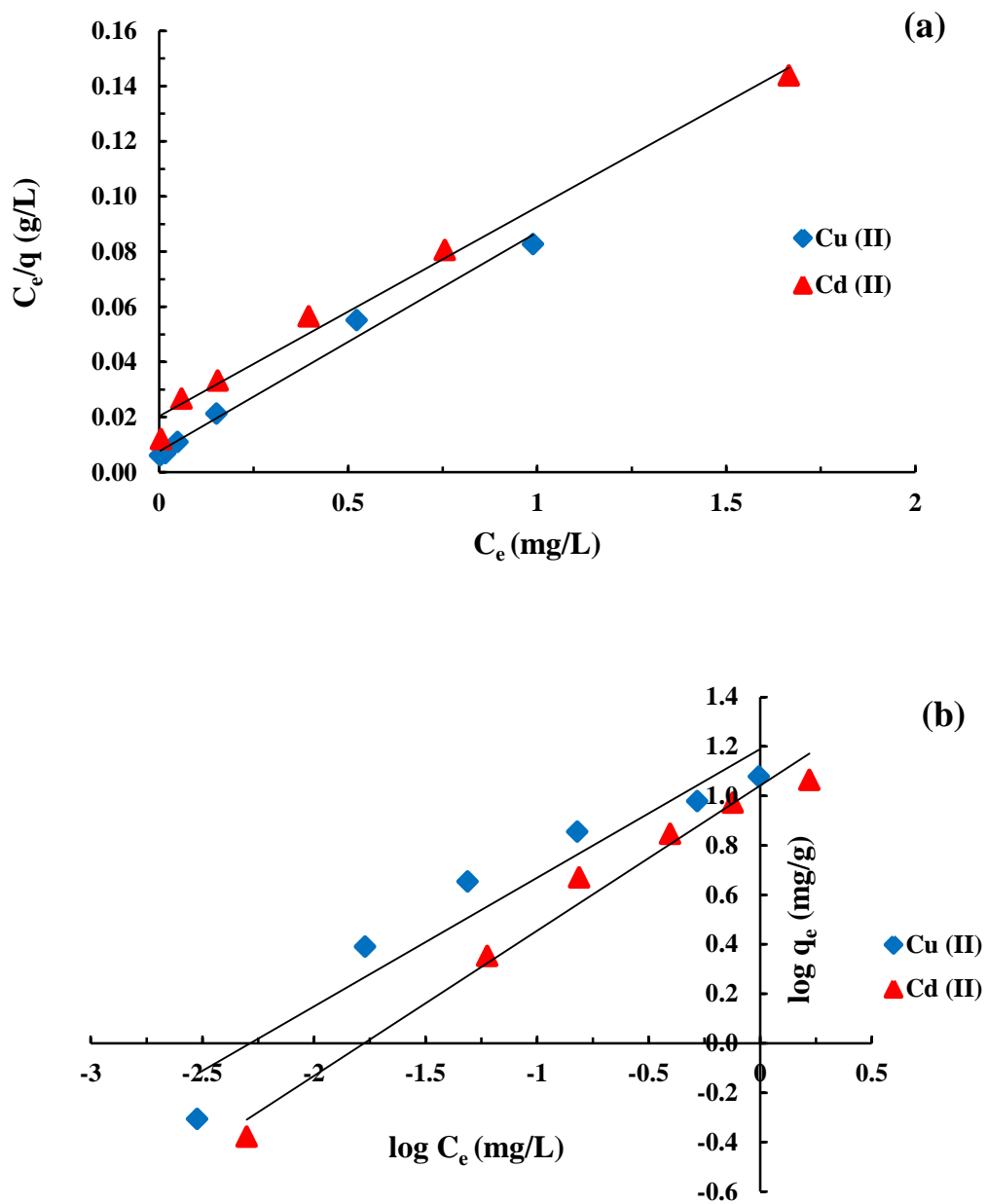


Figure 3.27: Fitting of (a) Langmuir adsorption; and (b) Freundlich adsorption isotherms in the sorption of Cu(II) and Cd(II) by BNMPTS material.

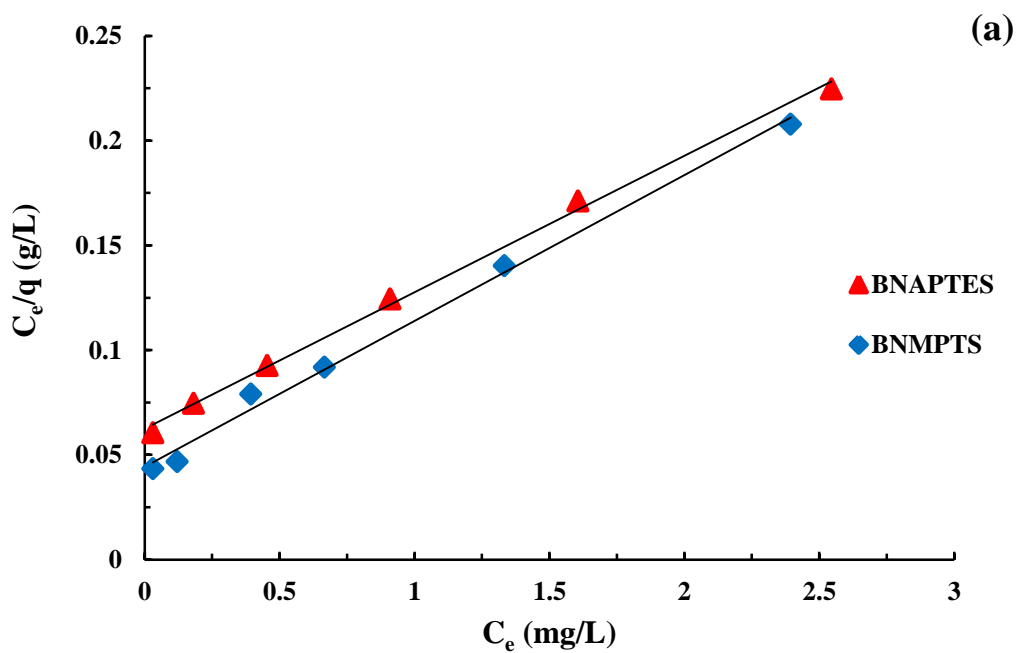
3.3.3.3. Adsorption isotherm modelling for tetracycline, triclosan and EE2

Result obtained from the concentration dependent study of tetracycline by the BNMPTS and BNAPTES is utilized to study the adsorption isotherm models *viz.*, Langmuir and Freundlich adsorption isotherms (Balarak *et al.*, 2016) and fitting results are presented graphically in Figure 3.28. The isotherm constants *i.e.*, Langmuir monolayer sorption capacity (q_o), Langmuir constant (b) and Freundlich constants (K_f and $1/n$) are hence, estimated and returned in Table 3.5. Since higher value of R^2 is obtained for Langmuir adsorption isotherm for tetracycline using BNMPTS and BNAPTES, which inferred the applicability of Langmuir adsorption isotherm in the adsorption of tetracycline by these solids. The applicability of the Langmuir isotherm specifies that monolayer coverage of the solid surfaces by tetracycline molecules and the active sites are homogeneously distributed on the surface (Zhang *et al.*, 2013). The Langmuir monolayer capacity (q_o) is relatively high, indicating the high chemical affinity of tetracycline towards the BNMPTS and BNAPTES solids (Rivera-Utrilla *et al.*, 2013).

The Langmuir monolayer capacity is found to be 16.64 and 15.36 mg/g respectively for BNMPTS and BNAPTES. Previously, it was reported that the sorption of tetracycline onto different montmorillonite SAz-1 (Ca-MMT containing 98% smectite), SWy-2 (Na-MMT containing 95% smectite), SHCa-1 (low-charge Li-bearing trioctahedral smectite) and SYn-1 (synthetic mica-MMT containing 95% mica-MMT) followed the Langmuir adsorption isotherm having removal capacity of 468, 404, and 243 mg/g, respectively (Chang *et al.*, 2014). Moreover, higher values of ($1/n$) and (b), Freundlich and Langmuir constants respectively indicated that the material has strong affinity towards tetracycline (Lee *et al.*, 2017).

Table 3.5. Langmuir and Freundlich constants estimated for sorption of tetracycline using BNMPTS and BNAPTES solids.

Materials	Langmuir			Freundlich		
	q_o (mg/g)	b (L/g)	R^2	$1/n$	K_f (mg/g)	R^2
BNMPTS	16.639	1.019	0.992	0.737	7.925	0.979
BNAPTES	15.361	1.042	0.997	0.709	7.101	0.978



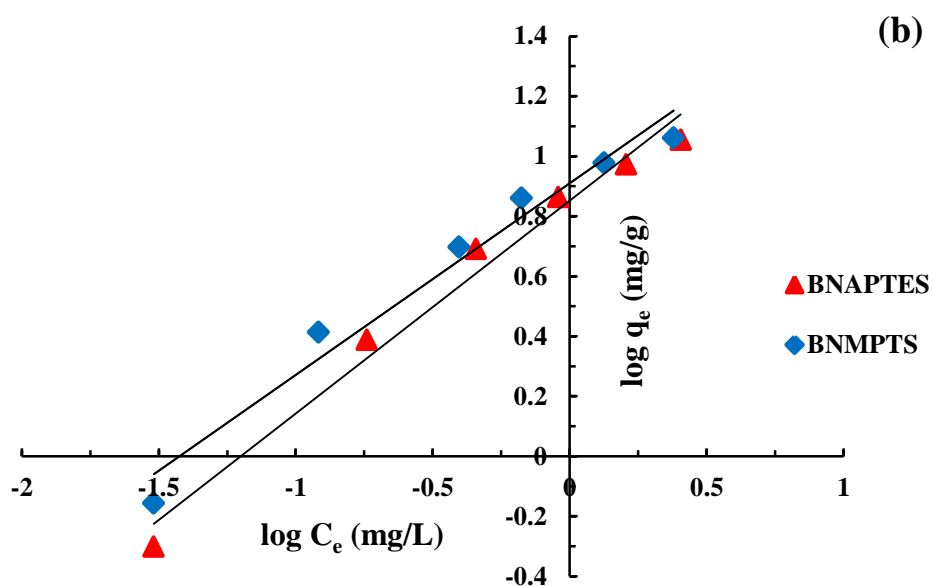


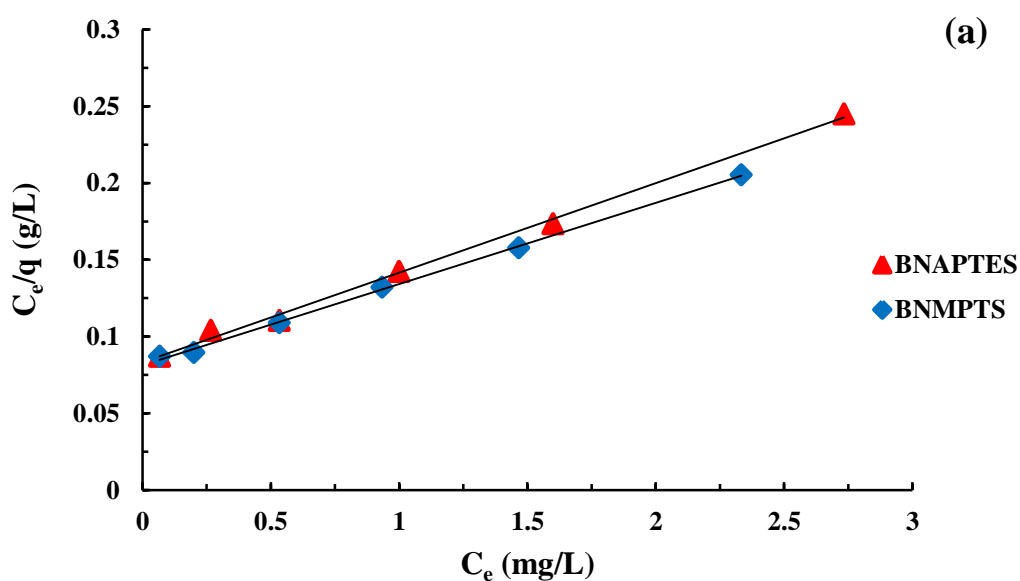
Figure 3.28: Fitting of concentration dependence data to (a) Langmuir adsorption; and (b) Freundlich adsorption isotherms in the sorption of tetracycline by BNMPTS and BNAPTES solids.

Furthermore, the equilibrium sorption data obtained for triclosan is utilized for plotting the sorption modelling studies i.e., the Langmuir and Freundlich adsorption isotherms (Lee *et al.*, 2012a; Ma *et al.*, 2019). The graphs were plotted for these two isotherms and shown in Figure 3.29. The unknown constants i.e., Langmuir monolayer adsorption capacity (q_o), Langmuir constant (b) along with the Freundlich constants (K_f and $1/n$) are estimated and given in Table 3.6. The isotherm studies showed that the removal of triclosan using BNMPTS and BNAPTES followed Langmuir adsorption isotherm better than Freundlich adsorption isotherm. Langmuir isotherm suggests that the adsorption sites of BNMPTS and BNAPTES solids have strong interactions with triclosan and the triclosan molecules are forming the monolayer onto the solid surfaces (Phuekphong *et al.*, 2020). The high value of Langmuir monolayer capacity (q_o) indicates the high affinity of triclosan towards BNMPTS and BNAPTES solids (Rivera-Utrilla *et al.*, 2013). The Langmuir

monolayer adsorption capacity (q_o) was found to be 18.87 and 17.15 mg/g for BNMPTS and BNAPTES, respectively. It is worth noted that a very high monolayer capacity was obtained for triclosan using the functionalized materials. Further, relatively high values obtained for Langmuir constant (b) and Freundlich constant (K) indicated the strong affinity of BNMPTS and BNAPTES towards triclosan in aqueous media (Lee *et al.*, 2012b; Lee *et al.*, 2017).

Table 3.6. Langmuir and Freundlich isotherm constants estimated for the sorption of triclosan using BNMPTS and BNAPTES solids.

Materials	Langmuir isotherm			Freundlich isotherm		
	q_o (mg/g)	b (L/g)	R^2	$1/n$	K_f (mg/g)	R^2
BNMPTS	18.87	0.652	0.998	0.764	6.95	0.985
BNAPTES	17.151	0.699	0.997	0.737	6.449	0.981



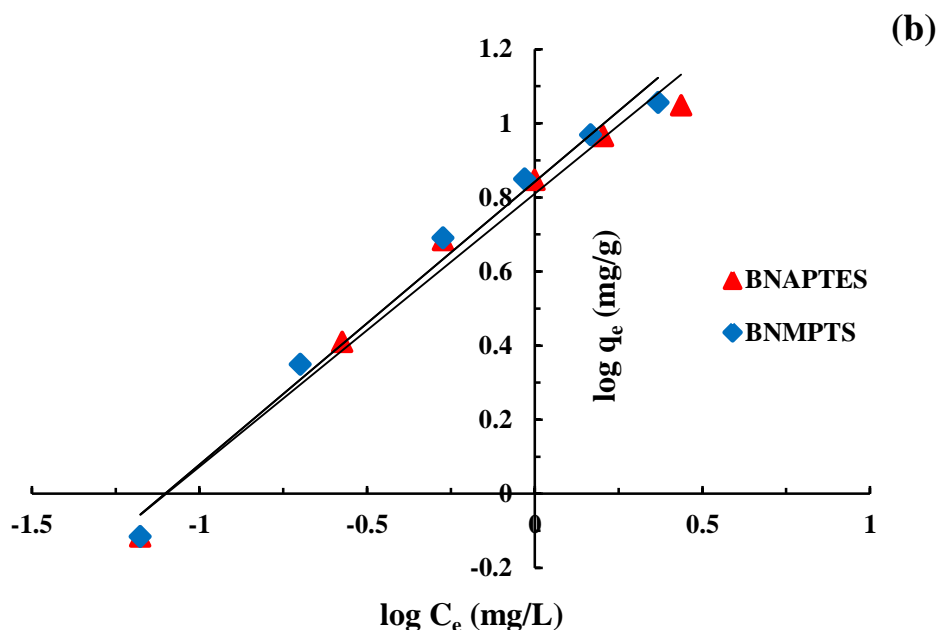


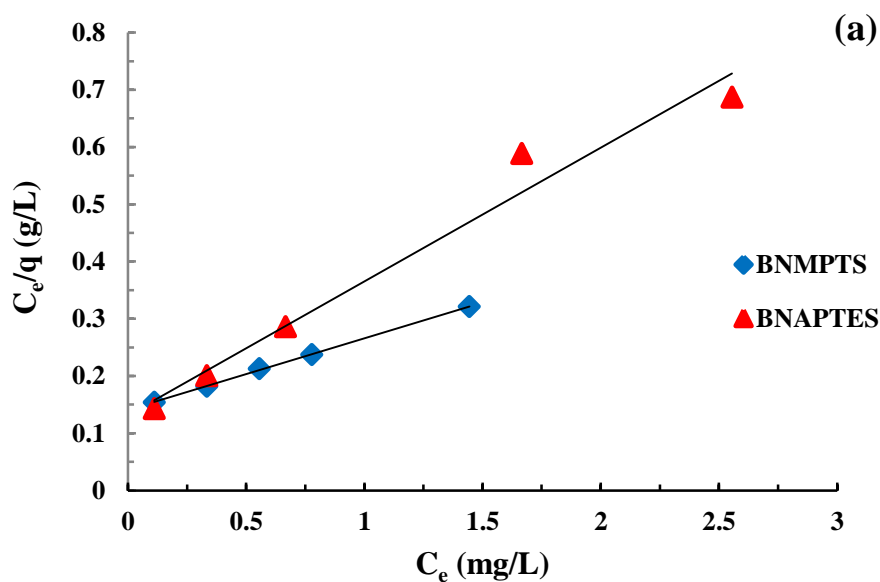
Figure 3.29: Fitting of concentration dependence data to the (a) Langmuir adsorption; and (b) Freundlich adsorption isotherms in the sorption of triclosan by the BNMPTS and BNAPTES solids.

Similarly, the linear form of Langmuir and Freundlich isotherms is utilized for isotherm modelling for the adsorption of EE2 by the BNMPTS and BNAPTES solids and the results are illustrated in Figure. 3.30. The unknown constants are estimated and presented in Table 3.7. The results showed that the equilibrium sorption data obtained for the removal of EE2 is reasonably fitted well to the Langmuir adsorption model compared with Freundlich isotherm model. This result further indicates the surface homogeneity of the BNMPTS and BNAPTES in the removal of the EE2 (Shin *et al.*, 2020). The high value of Langmuir monolayer sorption capacity (q_o) indicates the strong affinity of triclosan towards BNMPTS and BNAPTES (Rivera-Utrilla *et al.*, 2013). A high value of Langmuir monolayer capacity 8.1 and 4.283 mg/g is obtained for the EE2 using BNMPTS and BNAPTES materials, respectively. The sorption of 17 β -estradiol, 17 α -ethinylestradiol and bisphenol A on tea leaves (TL_H) and granular activated carbon (GAC) also followed Langmuir adsorption isotherm model. Moreover, the maximum adsorption capacities

of 3.46, 2.44 and 18.35 mg/g were achieved for TL_H compared to GAC capacities of 4.01, 2.97 and 16.26 mg/g for 17 β - estradiol, 17 α - ethinylestradiol and bisphenol A, respectively (Ifelebuegu *et al.*, 2015).

Table 3.7. Langmuir and Freundlich adsorption isotherm constants estimated for the sorption of EE2 by the BNMPTS and BNAPTES solids.

Materials	Langmuir isotherm			Freundlich isotherm		
	q_o (mg/g)	b (L/g)	R^2	$1/n$	K_f (mg/g)	R^2
BNMPTS	8.1	0.888	0.999	0.577	5.277	0.988
BNAPTES	4.283	1.774	0.972	0.392	2.935	0.959



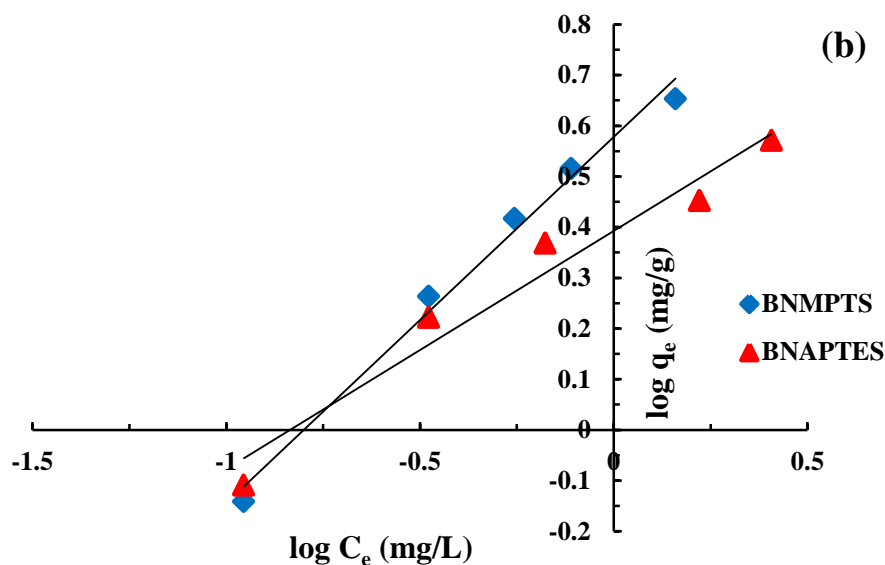


Figure 3.30: Fitting of concentration dependence data to the (a) Langmuir adsorption; and (b) Freundlich adsorption isotherms in the sorption of EE2 by the BNMPTS and BNAPTES materials.

3.3.4. Effect of contact time

3.3.4.1. Arsenic(III) and arsenic(V)

The amount of As(III) and As(V) adsorbed by BNMPTS and BNAPTES, respectively are obtained at different time intervals from 5 to 720 minutes which is useful to deduce the adsorption kinetics for these systems. Results are presented in Figure 3.31 ((a) and (b)). Initially, the uptake of arsenic by these materials is rapid and slowed down with the lapse of time. It is evident that more than 60% of arsenic was adsorbed within 60 minutes of contact. The high uptake of arsenic by the synthesized functionalized materials in the early contact time is due to the excess number of available active sites on the surface of the adsorbent which are occupied by the sorbate ions. Further, with the lapse of time, the uptake of arsenic is slowed down due to the lesser numbers of active sites are available for sorbate ions and it reaches to an apparent equilibrium with the time of 180 minutes of contact for As(III) using BNMPTS and As(V) using BNAPTES materials (Lee *et al.*, 2015). The result further infers that the uptake of arsenic is rapid by the BNMPTS and

BNAPTES hence, are found to be efficient in the removal of arsenic from aqueous solutions using these solids.

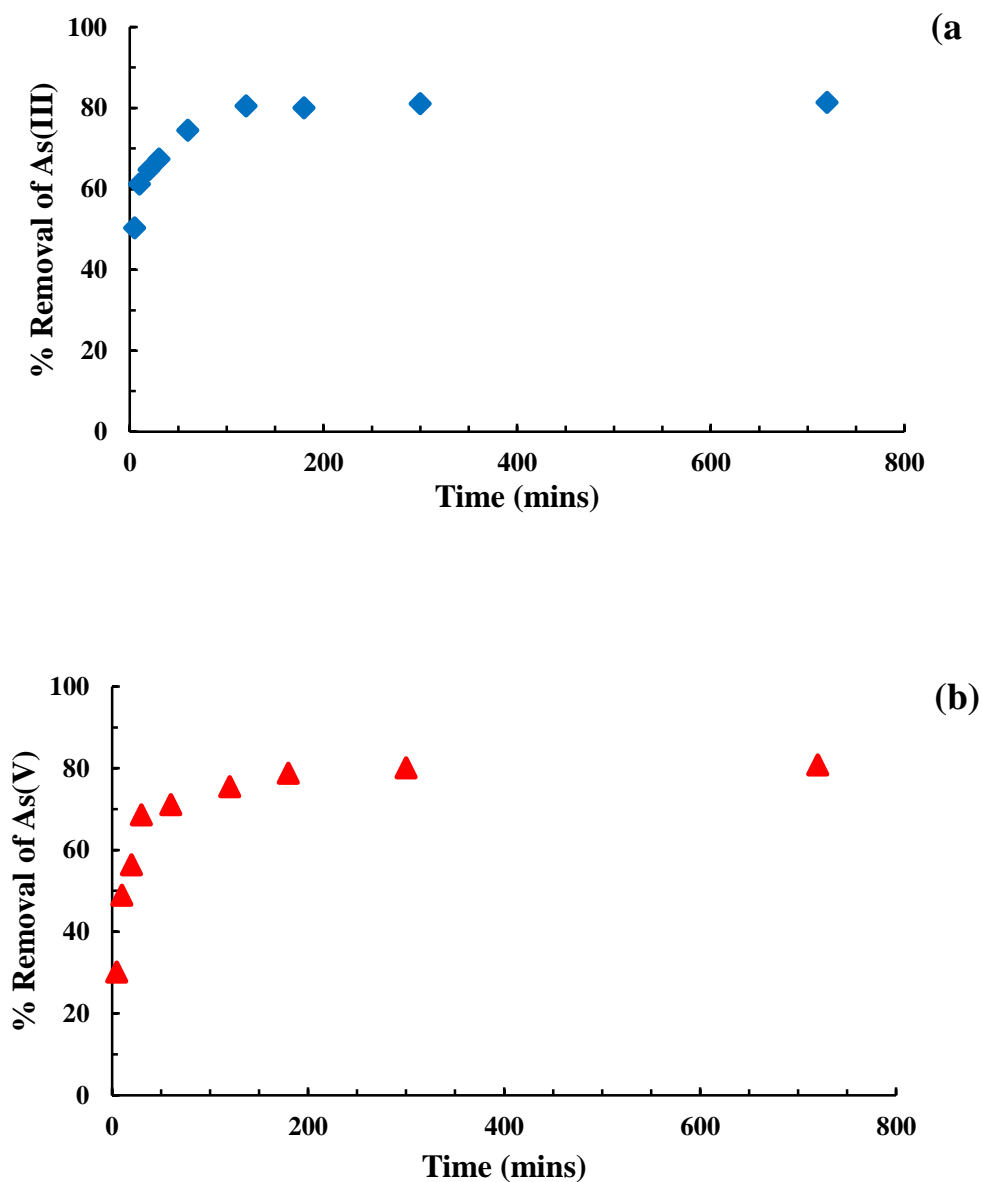


Figure 3.31: Effect of contact time in the removal of (a) As(III) by BNAPTES and; (b) As(V) by BNAPTES solids ([As(III)/or As(V)]: 10.0 mg/L; pH: 3.5; Solid dose: 2.0 g/L; Temperature: 25°C).

3.3.4.2. Copper(II)

The time dependent removal of Cu(II) using BNMPTS is obtained at a definite intervals up to a maximum of 360 minutes. Further, the time dependent percentage removal of Cu(II) by the BNMPTS is illustrated graphically in Figure 3.32. The uptake of Cu(II) by the BNMPTS solid is recorded very fast and within just 5 minutes of contact almost 95% of Cu(II) is removed. The percentage removal of Cu(II) is further increased gradually and an apparent sorption equilibrium is reached within 30 minutes of contact for Cu(II) using BNMPTS. The results inferred that the BNMPTS possessed very high affinity towards the Cu(II) and the active sites available on the surface of BNMPTS are readily available to capture Cu(II) toxic ions in aqueous solution (Liang *et al.*, 2014; Ouakouak *et al.*, 2020). This further reaffirms that the dense brushes of silanes available with BNMPTS material forming strong chemical bonds with the available cations and rapid removal of Cu(II) were observed using BNMPTS material. It was also reported that the removal of Cu(II) by rice husk treated with NaOH (TRH) reaches maximum uptake within 15 minutes of contact (Zafar *et al.*, 2020).

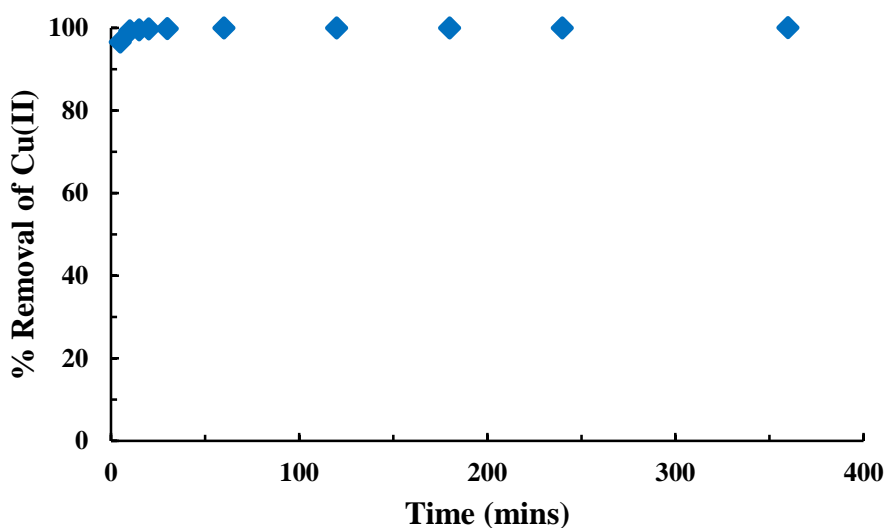


Figure 3.32: Effect of contact time in the removal of Cu(II) by the BNMPTS solid ([Cu(II)]: 10.0 mg/L; pH: 4.0; Solid dose: 2.0 g/L; Temperature: 25°C).

3.3.4.3. Cadmium(II)

Similarly, the time dependent percentage removal of Cd(II) by BNMPTS is obtained and shown in Figure 3.33. The Cd(II) is aggregated rapidly on the surface of BNMPTS which inferred a very affinity of Cd(II) towards the functionalized material. It is noted that about 94% of Cd(II) was adsorbed on to the surface of the BNMPTS within just 5 minutes of contact. However, an apparent equilibrium between the solid and solution was achieved within 30 minutes of contact. These results confirmed that the Cd(II) is forming strong chemical bonds onto the available surface functional groups. Similar result is also reported for the adsorption of Cu(II) and Cd(II) using natural clay in which the equilibrium contact time occurred within 30 minutes (El, 2018).

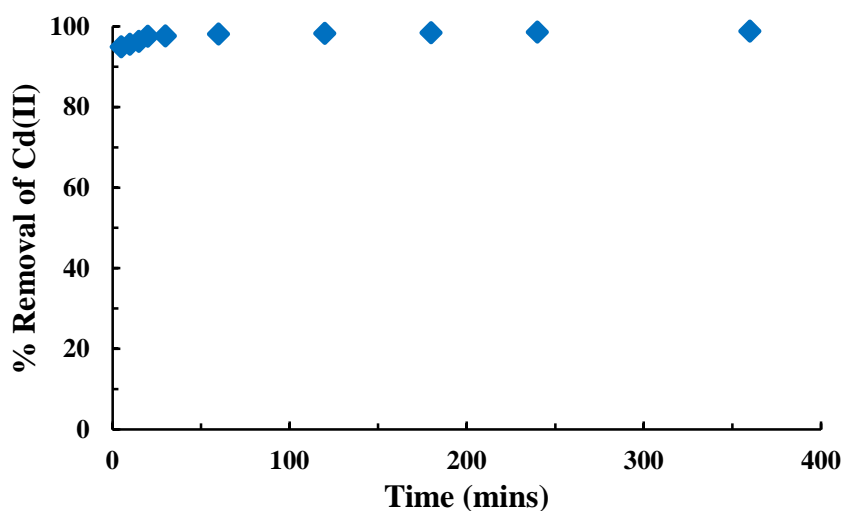


Figure 3.33: Effect of contact time in the removal of Cd(II) by the BNMPTS solid ([Cd(II)]: 5.0 mg/L; pH: 5.0; Solid dose: 2.0 g/L; Temperature: 25°C).

3.3.4.4. Tetracycline (TC)

The extent of tetracycline (TC) adsorbed by the BNMPTS and BNAPTES are obtained at different time intervals 5 to 720 minutes and the percentage removal of tetracycline by these solids are presented as a function of time in Figure 3.34. A fast uptake of tetracycline by these solids is observed during the initial period of contact and within 5 minutes of contact, *Ca* 72 and 78% of tetracycline are adsorbed using BNMPTS and BNAPTES, respectively. This inferred that the rate of adsorption of tetracycline by these solids is significantly high. This is primarily due to the fact that extent of active sites are relatively more at the functionalized materials surface during the initial period of time which enabled fast aggregation of tetracycline molecules onto the solid surface (Lalhmunsiana *et al.*, 2015). However, further increase in time, the rate of sorption slowed down and an apparent equilibrium is attained within 180 minutes of contact for tetracycline using BNMPTS and BNAPTES. This result signifies the materials are useful and efficient at least for the elimination of tetracycline from aqueous wastes.

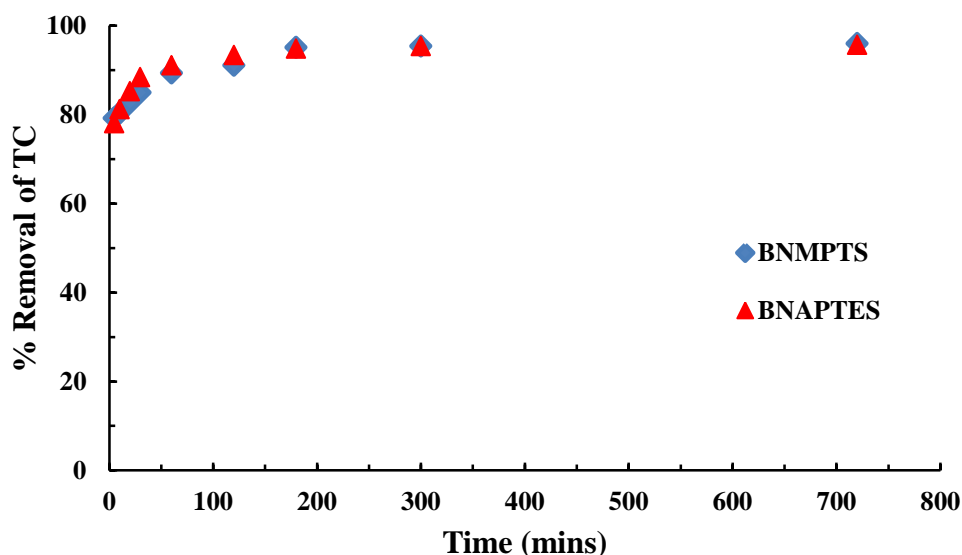


Figure 3.34: Effect of contact time in the removal of tetracycline by the BNMPTS and BNAPTES solids ([TC]: 10.0 mg/L; pH: 4.0; Solid dose: 2.0 g/L; Temperature: 25°C).

3.3.4.5. Triclosan (TCS)

The uptake of triclosan by BNMPTS and BNAPTES solids was studied at different interval of time between 5 to 720 minutes and the time dependent removal of these at various contact time are shown as in Figure 3.35. It is observed that during the initial period of contact, the uptake of triclosan by BNMPTS and BNAPTES was very fast and it was observed that *Ca* 71 and *Ca* 73% of triclosan were removed by the BNMPTS and BNAPTES, respectively within 5 minutes of contact. Further, increase in time caused for gradual increase in percentage removal of triclosan by these solids and apparent sorption equilibrium was achieved within 120 minutes of contact for triclosan using BNMPTS and BNAPTES. The fast uptake of triclosan suggested that the materials possessed greater affinity towards triclosan and is a potential solid to be employed in waste water treatment plants. Previously it was reported that the maximum time to reach the sorption equilibrium for the sorption of triclosan using biomass, *Phaeodactylum tricorutum* was 180 minutes (Santaeufemia *et al.*, 2019).

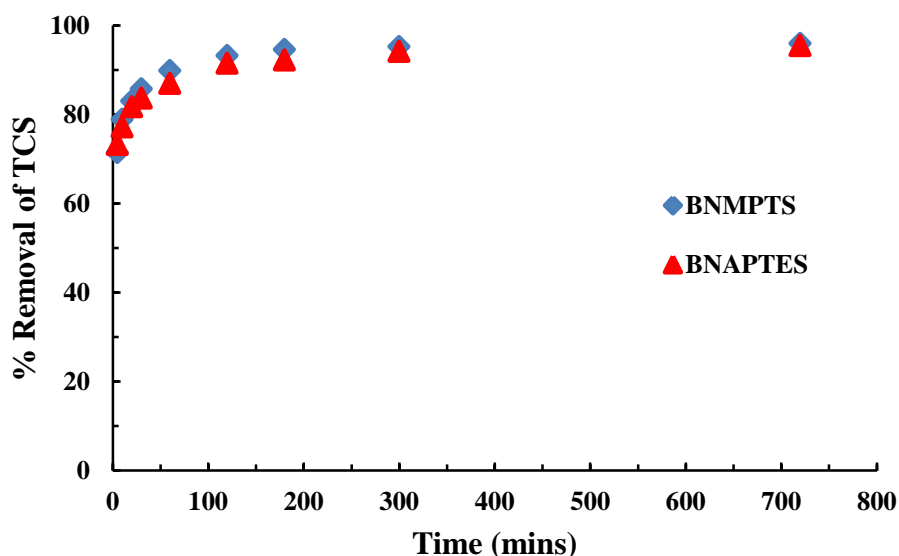


Figure 3.35: Effect of contact time in the removal of triclosan by the BNMPTS and BNAPTES solids ([TCS]: 10.0 mg/L; pH: 4.0; Solid dose: 2.0 g/L; Temperature: 25°C).

3.3.4.6. 17 α -ethinylestradiol (EE2)

The percentage elimination of EE2 by the BNMPTS and BNAPTES solids at different time intervals was obtained and returned in Figure 3.36. The percent removal of EE2 by both the materials was rapid during initial period of contact and *Ca* 57 and 42% of EE2 was removed within just 10 minutes of time by the BNMPTES and BNAPTES materials, respectively. Further, the sorption of EE2 onto these synthesized materials was saturated just within 120 minutes of contact. This indicated that the surface active sites of these two functionalized materials saturated within 120 minutes and no further removal of EE2 was obtained even after 720 minutes of contact (Hasan *et al.*, 2013). These results further inferred that both the materials possessed high affinity for the attenuation of EE2 and its applicability in treatment of wastewater.

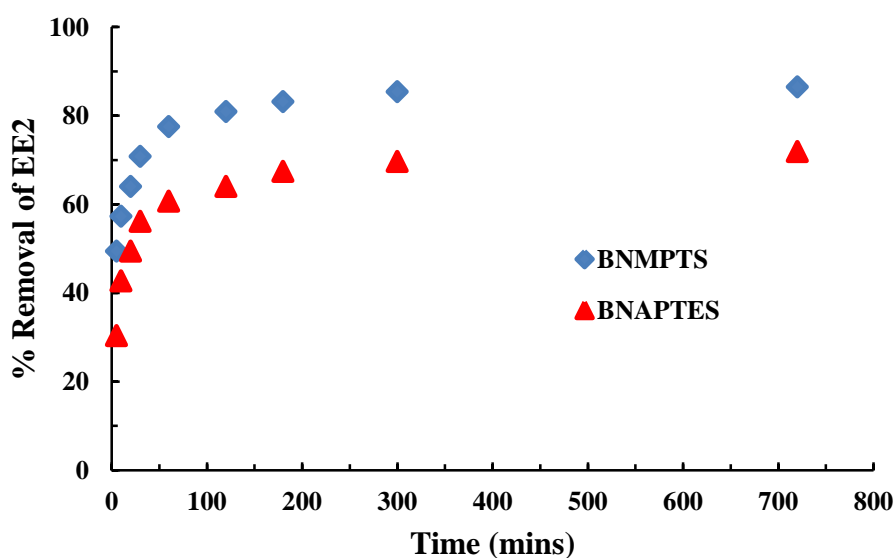


Figure 3.36: Effect of contact time in the removal of EE2 by the BNMPTS and BNAPTES solids ([EE2]: 10.0 mg/L; pH: 4.0; Solid dose: 2.0 g/L; Temperature: 25°C).

3.3.5. Kinetic modelling studies

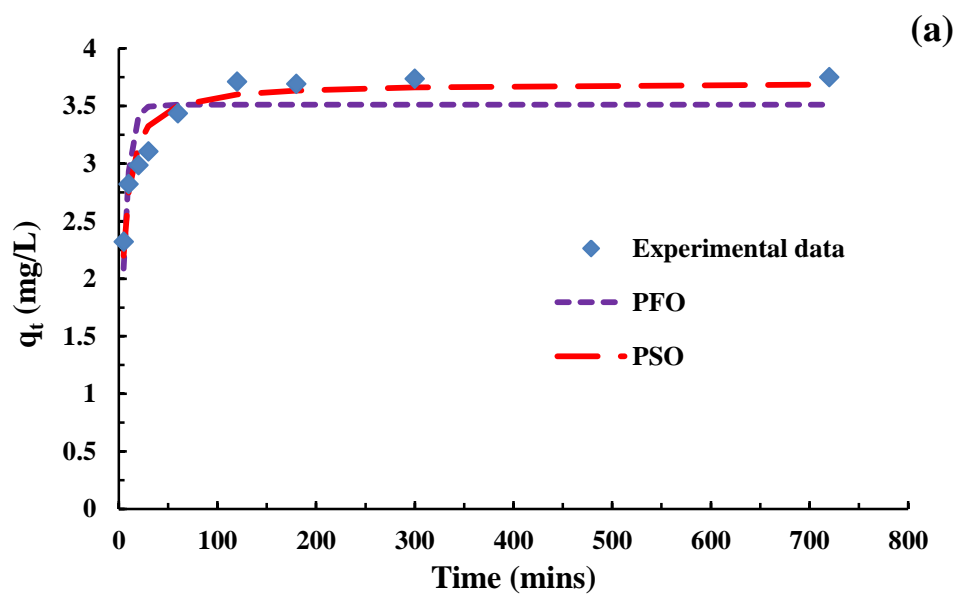
The time dependence data is further employed to deduce the sorption kinetics in the sorption of these pollutants using the solids. The two kinetic models *viz.*, pseudo-first order (PFO) (Azizian, 2004) and pseudo-second order (PSO) (Ho and McKay, 1999) equations were utilized for its non-linear fitting (equations 2.5 and 2.6). A non-linear least square fitting method is conducted for the estimation of unknown parameters along with the rate constant values. Further, the non-linear fitting enables to estimate the unknown constant involved in the basic equations i.e., the sorption capacity of solid for the specific pollutant.

3.3.5.1. Arsenic (III) and arsenic (V)

The adsorption kinetics of As(III) by BNMPTS and As(V) by BNAPTES is employed to perform the two non-linear kinetic models *viz.*, pseudo-first order (PFO) and pseudo-second order (PSO) models and the results are illustrated graphically in Figure 3.37. The calculated least square sum and unknown parameters were included in Table 3.8. These results clearly inferred that the kinetic data is well fitted to the PSO model compared to the PFO model since least square sum is reasonably low for the PSO model. These results further showed that As(III) and As(V) are bound to the materials with a strong chemical forces. Further, the sorption capacity estimated for the As(III) by BNMPTS and As(V) by the BNAPTES was found to be 3.703 and 4.074 mg/g, respectively. The results showed that the materials possessed very high sorption capacity for the As(III) and As(V). The sorption of As(III) and As(V) onto montmorillonite modified with Fe polycation and cetyltrimethylammonium bromide (CTMAB) also followed the pseudo-second order kinetics and found that the rate - limiting step was the ‘chemisorption’ (Ren *et al.*, 2014).

Table 3.8. Predicted kinetic parameters for pseudo-first order (PFO) and pseudo-second order (PSO) kinetic models in the sorption of As(III) by BNMPTS and As(V) by BNAPTES.

Materials	Pollutants	PFO Model			PSO Model		
		$q_e(\text{mg/g})$	$k_1(1/\text{min})$	s^2	$q_e(\text{mg/g})$	$k_2(\text{g/mg/min})$	s^2
BNMPTS	As (III)	3.511	0.18	0.59	3.703	0.078	0.127
BNAPTES	As (V)	3.821	0.086	0.355	4.074	0.161	0.088



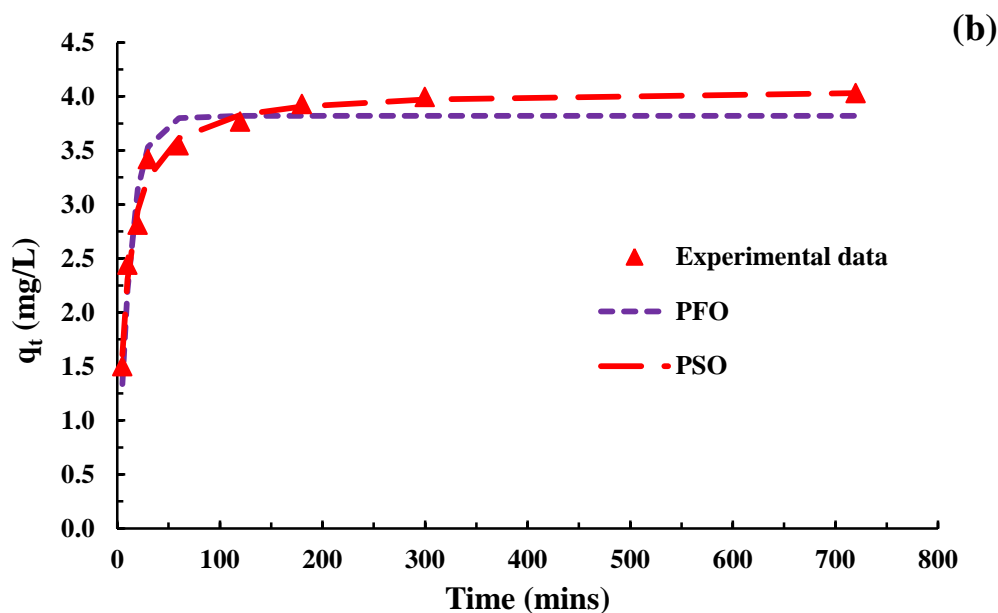


Figure 3.37: Plots of PFO and PSO kinetic models for the sorption of (a) As(III) by BNMPTS; and (b) As(V) by BNAPTES ([As(III)/ or As(V)]: 10.0 mg/L; pH: 3.5; Solid dose: 2.0 g/L; Temperature: 25°C).

3.3.5.2. Copper(II)

The time dependence data for the sorption of Cu(II) by the BNMPTS is employed for the kinetic modelling viz., PFO and PSO kinetic models. The least square fitting results are shown graphically in Figures 3.38. Further, the uptake capacity, rate constants and the least square sums were estimated and returned in Table 3.9. It is evident from the results that the PSO model is relatively better fitted to the sorption of Cu(II) by the BNMPTS since the least square sum is reasonably low for PSO model. The removal capacity thereby found to be 4.13 for Cu(II) using the BNMPTS solid. Further, the fitting of PSO model suggested that the chemical interactions are involved in the adsorption of Cu(II) using BNMPTS from aqueous solutions (Foo and Hameed, 2010). The removal of Cu(II) using bentonite coated with Fe₃O₄ magnetite nanoparticles and Cd(II) using 3-MPA@PMNPs were followed the PSO model (Ali *et al.*, 2019; Mohammed *et al.*, 2018). Saudi clay was employed for the removal of Cu(II) and Ag(I), the experimental data reveal that the uptake of these cations followed the pseudo-second-order model and suggested that

the ‘chemical sorption’ was the dominant and rate-controlling step (Alandis *et al.*, 2019).

Table 3.9. Predicted kinetic parameters for pseudo-first order (PFO) and pseudo-second order (PSO) kinetic models in the sorption of Cu(II) by the BNMPTS solid.

PFO Model			PSO Model		
q_e (mg/g)	k_1 (1/min)	s^2	q_e (mg/g)	k_2 (g/mg/min)	s^2
4.101	3.154	0.016	4.134	1.467	0.001

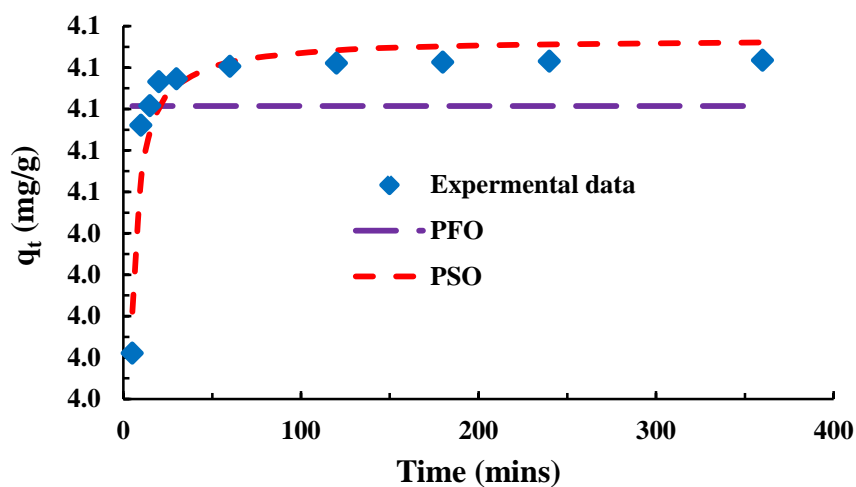


Figure 3.38: Plots of PFO and PSO kinetic models for the sorption of Cu(II) by the BNMPTS solid ([Cu(II)]: 10.0 mg/L; pH: 4.0; Solid dose: 2.0 g/L; Temperature: 25°C).

3.3.5.3. Cadmium(II)

Similarly, the kinetic modelling of Cd(II) was conducted for the known PFO and PSO modelling using the time dependence sorption data. The non-linear fitting results for the PFO and PSO models are shown in graphically in Figure 3.39. Moreover, the estimated unknown parameters i.e., the maximum removal capacity (q_e), rate constants and the least square sum are included in Table 3.10. It is clear from the results that the time dependence uptake of Cd(II) is relatively fitted well to the non-linear PSO model compared to the PFO model since least square sum is reasonably low for the PSO model. The applicability of PSO model indicated that the Cd(II) ions are accumulated onto the surface of BNMPTS with relatively stronger chemical forces (Ho and Mckay, 2000). Previously, it was also reported that the sorption of Pb(II) and Cd(II) using sawdust-kaolinite composite (SDKC) followed pseudo-second order model and inferred that the rate controlling step was 'chemisorption' (Ogbu *et al.*, 2019). Furthermore, the high value of sorption capacity obtained for Cd(II) by the BNMPTS solid showed the potential applicability of material towards the decontamination of water contaminated with Cd(II).

Table 3.10. Predicted kinetic parameters for the pseudo-first order (PFO) and pseudo-second order (PSO) kinetic models in the sorption of Cd(II) by BNMPTS.

PFO Model			PSO Model		
$q_e(\text{mg/g})$	$k_1(1/\text{min})$	s^2	$q_e(\text{mg/g})$	$k_2(\text{g/mg/min})$	s^2
2.016	0.703	0.004	2.031	2.252	0.0008

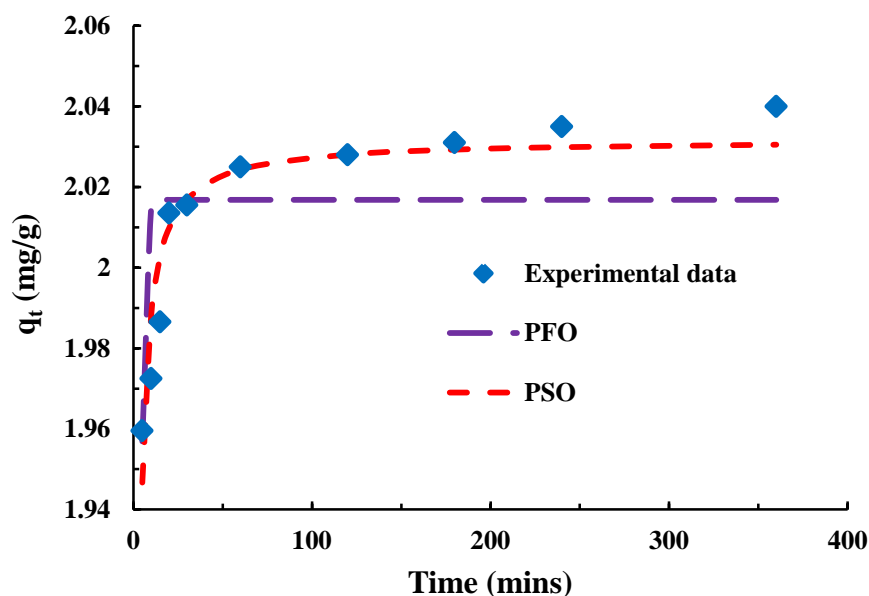


Figure 3.39: Plots of PFO and PSO kinetic models for the sorption of Cd(II) by the BNMPTS solid ([Cd(II)]: 5.0 mg/L; pH: 5.0; Solid dose: 2.0 g/L; Temperature: 25°C).

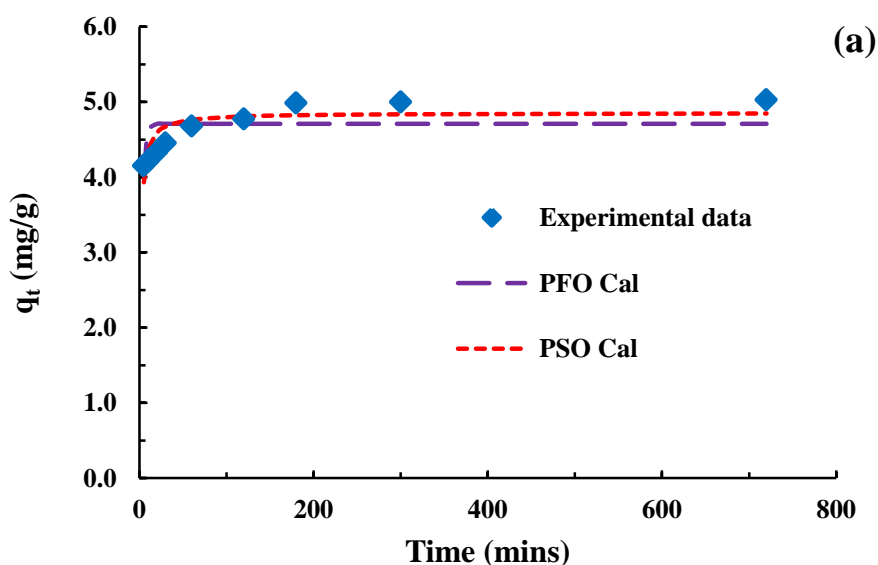
3.3.5.4. Tetracycline (TC)

The time dependence sorption data of tetracycline is utilized to study the kinetics of sorption by employing pseudo-first order (PFO) pseudo-second order (PSO) rate kinetics. The simulation results are illustrated graphically as in Figure 3.40. Moreover, the estimated parameters are returned in Table 3.12. Table 3.11 showed that the uptake of tetracycline by BNMPTS and BNAPTES followed the PSO kinetics model rather than PFO model since least square sum is significantly less for PSO kinetic model. The removal capacity of tetracycline is relatively high which pointed the potential applicability of the materials towards the removal of tetracycline from aqueous wastes. Further, the well-fitting of PSO with the sorption data indicated that tetracycline species were captured on the surface of the materials with the strong forces. Sorption of tetracycline onto Na-montmorillonite (Na-Mt) modified with carboxymethyl-chitosan is better fitted to the PSO kinetics (Ma *et al.*, 2019). Previously, the sorption of tetracycline and 17 α -ethynylestradiol using

various hybrid material at different contact time were best described by pseudo-second order (PSO) and fractal-like-pseudo-second order (FL-PSO) kinetic models, and it was suggested that these two micro-pollutants were bound to the adsorbent with relatively stronger forces (Thanhmingliana *et al.*, 2015). Moreover, the kinetic sorption of tetracycline using SBA15, N,N-SBA15 and Fe-N,N-SBA15 adsorbents were also well fitted to the pseudo-second order kinetic model where the tetracycline specifically sorbed by these adsorbents (Zhang *et al.*, 2018).

Table 3.11. Predicted kinetic parameters for pseudo-first order (PFO) and pseudo-second order (PSO) kinetic models in the sorption of tetracycline by the BNMPTS and BNAPTES solids.

Materials	PFO Model			PSO Model		
	$q_e(\text{mg/g})$	$k_1(1/\text{min})$	s^2	$q_e(\text{mg/g})$	$k_2(\text{g/mg/min})$	s^2
BNMPTS	4.71	0.387	0.647	4.855	0.175	0.271
BNAPTES	4.786	0.348	0.271	4.927	0.161	0.232



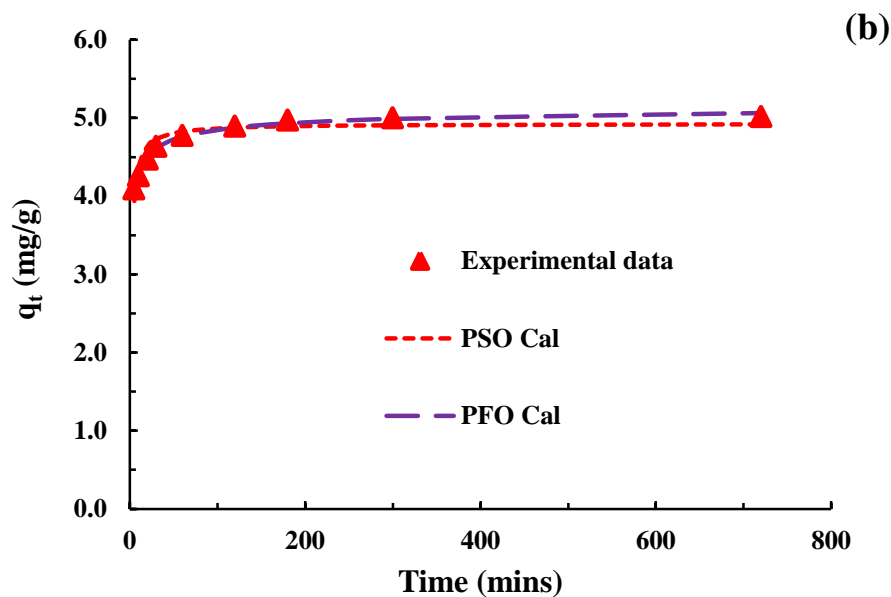


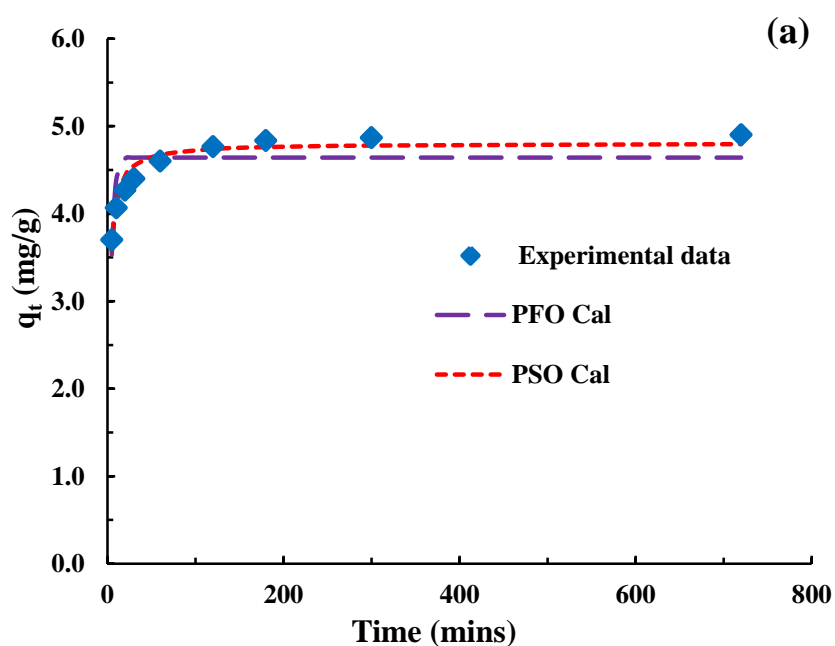
Figure 3.40: Plots of PFO and PSO kinetic models for the sorption of tetracycline by (a) BNMPTS and; (b) BNAPTES solids ([TC]: 10.0 mg/L; pH: 4.0; Solid dose: 2.0 g/L; Temperature: 25°C).

3.3.5.5. Triclosan(TCS)

The kinetic data of triclosan using BNMPTS and BNAPTES were modelled with the known pseudo-first order (PFO) and pseudo-second order (PSO) kinetic models. The non-fitting results for the PFO and PSO models are given in Figure 3.41. The rate constants and uptake capacity along with the least square sums were obtained and included in Table 3.12. The results indicated that sorption of triclosan by these solids followed better with the PSO model as compared to the PFO model since the least square sum is reasonably low for PSO model. The fitting of PSO model indicated that the triclosan species were sorbed by these solids with relatively stronger forces. It was reported previously that the removal of triclosan using *Phaeodactylum tricornutum* follows pseudo-second order kinetic model (Santaeufemia *et al.*, 2019). Chitosan/Poly composite membrane was employed for the sorption of triclosan and it was reported that the sorption kinetics fitted well to the pseudo-second order kinetics ($R^2 > 0.986$) as compared to the pseudo-first order kinetics (Liu and Xu, 2013).

Table 3.12. Predicted kinetic parameters for pseudo-first order (PFO) and pseudo-second order (PSO) kinetic models in the sorption of triclosan by BNMPTS and BNAPTES solids.

Materials	PFO Model			PSO Model		
	$q_e(\text{mg/g})$	$k_1(1/\text{min})$	s^2	$q_e(\text{mg/g})$	$k_2(\text{g/mg/min})$	s^2
BNMPTS	4.641	0.286	0.483	4.806	0.121	0.093
BNAPTES	4.555	0.3	0.549	4.713	0.131	0.147



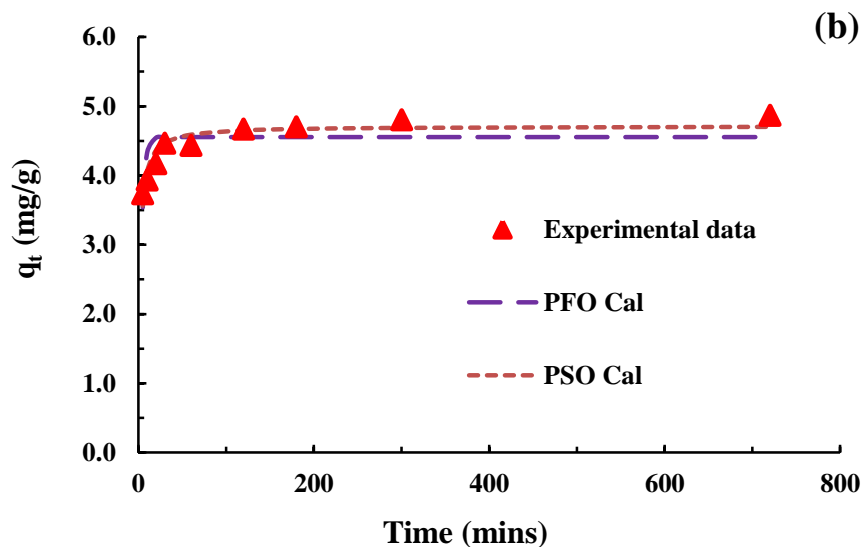


Figure 3.41: Plots of PFO and PSO kinetic models for the sorption of triclosan by (a) BNMPTS; and (b) BNAPTES solids ([TCS]: 10.0 mg/L; pH: 4.0; Solid dose: 2.0 g/L; Temperature: 25°C).

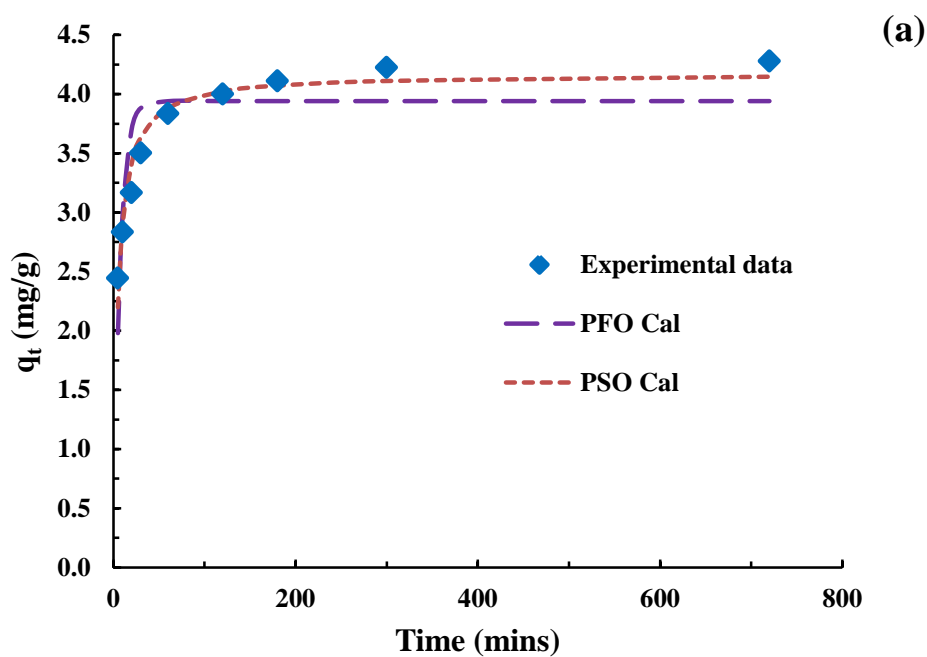
3.3.5.6. 17 α -ethynylestradiol (EE2)

The sorption kinetics of EE2 using BNMPTS and BNAPTES solids employing pseudo-first order (PFO) and pseudo-second order (PSO) kinetic models and the non-linear simulation results are presented in Figure 3.42. Further, the optimized results are shown in Table 3.13. The results showed that PSO model is fitted well since the least square sum is significantly low compared to the PFO model. The sorption of EDCs (trimethoprim (TMP), estrone (E1), 17 β -estradiol (E2) and 17 α -ethynylestradiol (EE2)) using -SnO₂ pillared montmorillonite also followed PSO kinetic model (Vidal *et al.*, 2014). Electrospun poly (butylenedipate-co-terephthalate) (PBAT) fibers was employed for the sorption of estrone (E1), 17 β -estradiol (E2), and 17 α -ethynylestradiol (EE2). The experimental kinetic data is well described by PSO model compared to the PFO model. Further, the difference between calculated and experimental sorption capacities indicated that PSO model is more favourable. Hence, the sorption of E1, E2 and EE2 onto the PBAT microfiber surfaces occurred predominantly through the ‘chemical interactions’ (Westrup *et al.*, 2021). Further, it is observed that the BNMPTS and BNAPTES materials possessed

relatively high removal capacity for EE2 which affirms the greater applicability of the materials in the remediation of aqueous waste contaminated with EE2.

Table 3.13. Predicted kinetic parameters for the pseudo-first order (PFO) and pseudo-second order (PSO) kinetic models in the sorption of EE2 by BNMPTS and BNAPTES solids.

Materials	PFO Model			PSO Model		
	q_e (mg/g)	k_1 (1/min)	s^2	q_e (mg/g)	k_2 (g/mg/min)	s^2
BNMPTS	3.94	0.139	0.898	4.172	0.053	0.171
BNAPTES	3.24	0.093	0.47	3.457	0.041	0.064



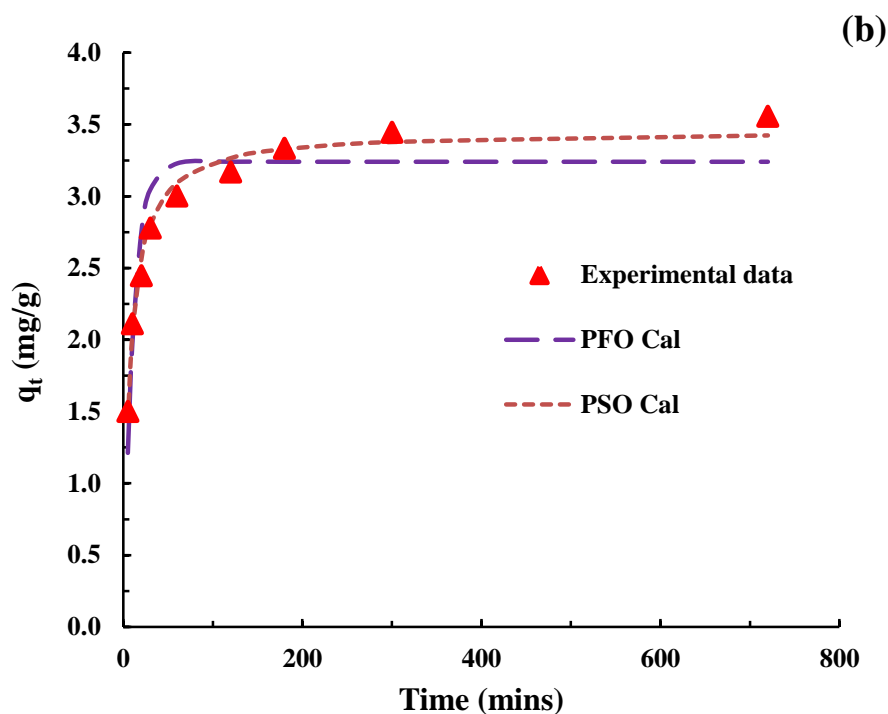


Figure 3.42: Plots of the PFO and PSO kinetic models for the sorption of EE2 by (a) BNMPTS; and (b) BNAPTES solids ([EE2]: 10.0 mg/L; pH: 4.0; Solid dose: 2.0 g/L; Temperature: 25°C).

3.3.6. Effect of background electrolyte concentrations

The effect of background electrolyte concentration is an important factor to study the binding nature of sorbate species onto the solid materials (Tiwari and Lee, 2012). The specific and non-specific sorption of As(III), As(V), Cu(II), Cd(II), tetracycline, triclosan and EE2 onto these functionalized materials is studied by collecting the sorption data at different background electrolyte concentrations. It is reported that the sorption through the outer-sphere complexation is sensitive to the change in background electrolyte concentrations whereas the inner sphere complexes are not altered with the change in background electrolyte concentrations since the adsorbed ions are residing at the plane which is closer to surface where usually background electrolyte ions are not located (Lee *et al.*, 2015; Lalhmunsiamma *et al.*,

2016c). Therefore, the studies were extended to vary the background electrolyte concentrations in the removal of these pollutants by the functionalized materials.

3.3.6.1. Arsenic(III) and arsenic(V)

The effect background electrolyte concentrations on the sorption of As(III) and As(V) on the functionalized materials was studied by increasing the NaCl concentrations from 0.0001 to 0.1 mol/L having the initial concentration of As(III) or As(V) 10.0 mg/L, pH 3.5. The results are shown as percentage removal of As(III) or As(V) as a function of background electrolyte concentrations (*Cf* Figure 3.43 ((a) and (b)). Figure clearly showed that 1000 times increase in NaCl concentration could not cause to affect significantly the percentage removal of As(III) and As(V) by these materials. The result indicated that the As(III) or As(V) are bound with strong chemical forces and forming the ‘inner sphere complex’ at the surface. The outer sphere complex formation is greatly influenced by the increase in ionic strength (Li *et al.*, 2019c). The uptake of As(III) and As(V) by manganese pillared clay (MnPILC) and iron pillared clay (FePILC) was studied in presence of Cl^- and Fe^{3+} ions. Results show that the presence of Cl^- and Fe^{3+} decreased the percentage removal by 2 to 4% only (Mishra and Mahato, 2016). The sorption of As(III) and As(V) onto molybdate impregnated chitosan beads is not affected by the presence of Ca^{2+} , Mg^{2+} , Cl^- , SO_4^{2-} and CO_3^{2-} (Chen *et al.*, 2008).

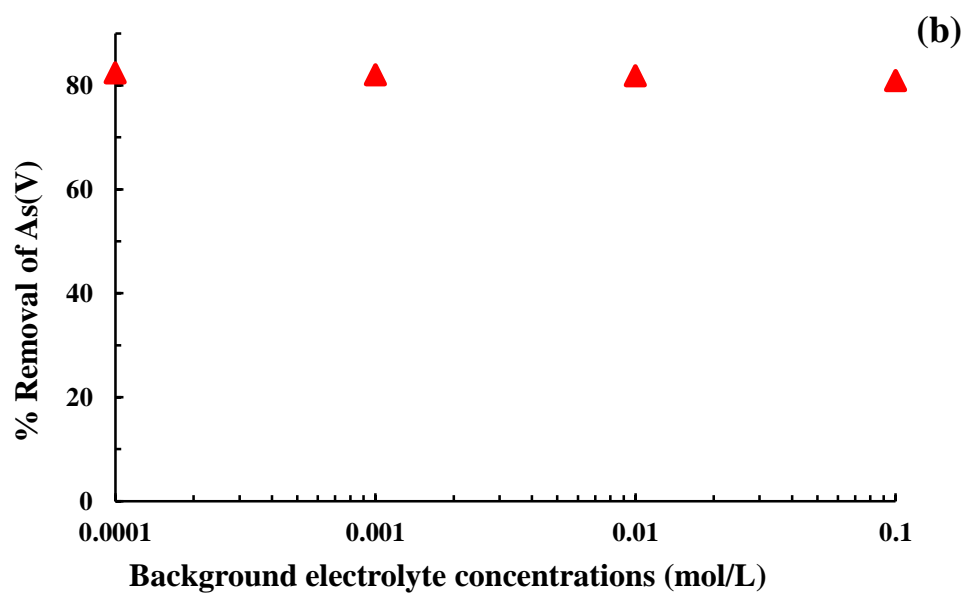
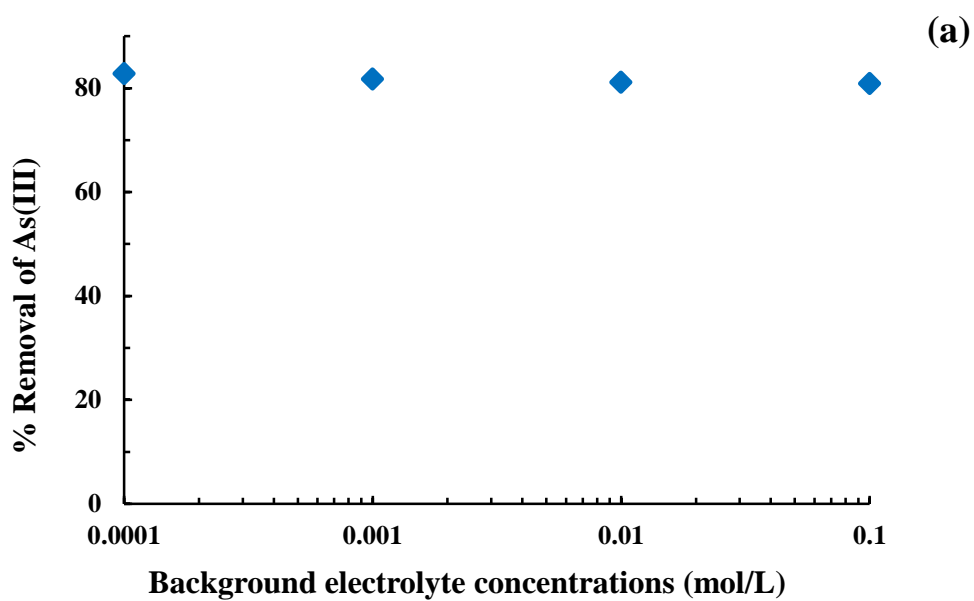


Figure 3.43: Effect of background electrolyte concentrations in the removal of (a) As(III) by the BNMPTS solid and; (b) As(V) by the BNAPTES solid ([As(III)/ or As(V)]: 10.0 mg/L; pH: 3.5; Solid dose: 2.0 g/L; Temperature: 25°C).

3.3.6.2. Copper(II)

The sorption of Cu(II) is conducted by varying background electrolyte (NaCl) concentrations from 0.0001 to 0.1 mol/L at a constant pH of 4.0 and initial concentration of Cu(II) 10.0 mg/L. The results are shown in Figure 3.44. It is evident from the figure that increasing the concentration of background electrolyte from 0.0001 to 0.1 mol/L (i.e., 1000 times), the percentage uptake of Cu(II) by BNMPTS was not affected. The findings again inferred that the functionalized bentonite has a strong affinity towards Cu(II) and the Cu(II) ions are aggregated onto BNMPTS solid through the strong chemical bonds. Possibly, the terminal -OH group leads the formation of 'inner-sphere' complexes at the solid surface (Lalchhingpuii *et al.*, 2017). The percentage removal of Cu(II) by walnut (WNS) (*Juglans regia*), hazelnut (HNS) (*Corylus avellana*), and almond (AS) (*Prunus dulcis*) is negligible when the concentration of KNO₃ was increased from 0.01 to 0.1 mol/L (Altun and Pehlivan, 2007).

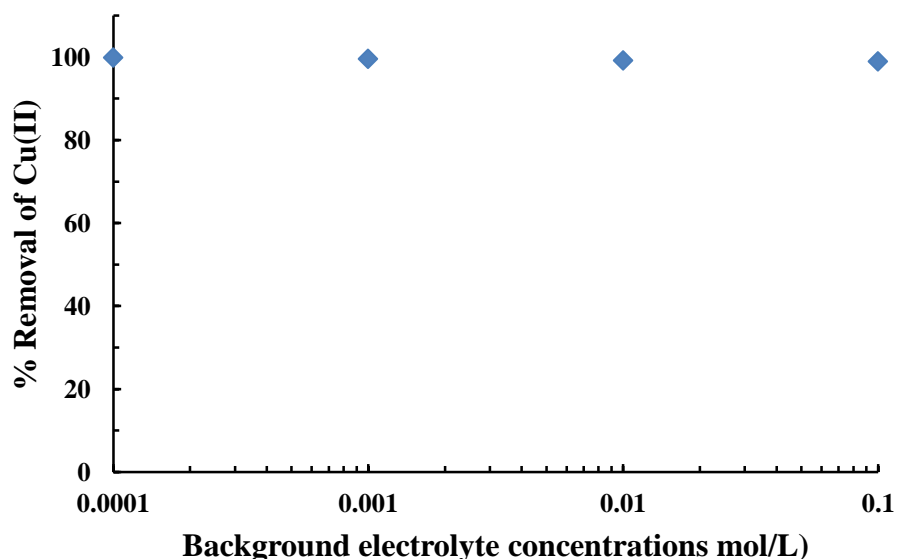


Figure 3.44: Effect of background electrolyte concentrations (NaCl) in the removal of Cu(II) by the BNMPTS solid ([Cu(II)]: 10.0 mg/L; pH: 4.0; Solid dose: 2.0 g/L; Temperature: 25°C).

3.3.6.3. Cadmium(II)

The background electrolyte concentration dependence adsorption of Cd(II) is obtained by increasing the NaCl concentrations from 0.0001 to 0.1 mol/L. The initial concentration of Cd(II) was taken as 5.0 mg/L and pH 5.0. The percentage of Cd(II) eliminated as a function of background electrolyte concentrations is presented in Figure 3.45. It is clear from the figure that increasing the background electrolyte concentration (0.0001 to 0.1 mol/L, NaCl), the percentage removal of Cd(II) remained unaffected. This inferred that the Cd(II) is forming a strong chemical bond between the Cd(II) and the surface of BNMPTS. Hence, the ‘inner sphere complexes’ formation is likely to occur between adsorbate ions and the available functional groups onto the solid surface (Lalhmunsiana *et al.*, 2014). The removal of Cd(II) in the presence of NaClO₄, NaCl and NaNO₃ by magnetic graphene oxide–supported sulfanilic acid (MGO-SA) was significantly affected at different pH value in the following order: NaCl < NaNO₃ < NaClO₄ (Hu *et al.*, 2014).

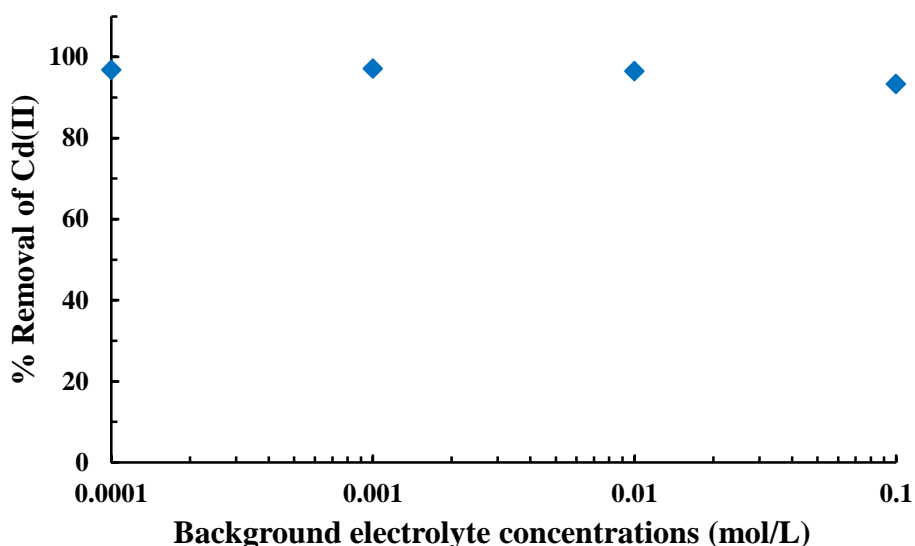


Figure 3.45: Effect of background electrolyte concentrations (NaCl) in the removal of Cd(II) by the BNMPTS solids ([Cd(II)]: 5.0 mg/L; pH: 5.0; Solid dose: 2.0 g/L; Temperature: 25°C).

3.3.6.4. Tetracycline (TC)

The concentration of background electrolyte (NaCl) concentrations was studied in the removal of tetracycline by the BNMPTS and BNAPTES solids. The background electrolyte concentration was increased from 0.0001 to 0.1 mol/L having the initial tetracycline concentration of 10.0 mg/L and the pH were adjusted to pH 4.0. The results are shown as in Figure 3.46. It is evident from the figure that 1000 times increase in NaCl concentration did not affect significantly the removal of tetracycline by the BNMPTS or BNAPTES solids. Quantitatively, the percentage removal of tetracycline was decreased from 90.24 to 88.35% for BNAPTES while the percentage removal of tetracycline by BNMPTS remained constant while increasing the NaCl concentrations from 0.0001 to 0.1 mol/L. This concludes that the tetracycline is aggregated onto the surface of solid with relatively stronger forces. The partitioning the tetracycline is occurred at the solid surface. These results are in conformity with the pH studies in which concluded that the hydrophobic nature of BNMPTS attracted tetracycline having stronger forces. However, increasing the concentration of NaCl (0.0 to 0.5 mol/L), the extent of tetracycline removal was increased from 132.4 to 172.7 mg/g using activated carbon produced from tomato waste (TAC) which was due to the inability of big tetracycline molecules aggregated at high ionic strength to enter adsorption sites in the pores of TAC in which electrostatic interaction has overcome by the hydrophobic interaction of tetracycline (Saygili and Guzel, 2016). Similarly, an increase in the concentrations of NaCl did not significantly affect the removal of tetracycline using Cu-immobilized alginate beads (Zhang *et al.*, 2019), HDTMA modified bentonite and local clay and Al pillared HDTMA modified bentonite and local clay (Thanhmingliana *et al.*, 2015) and MOF/graphite oxide pellets (Yu *et al.*, 2018).

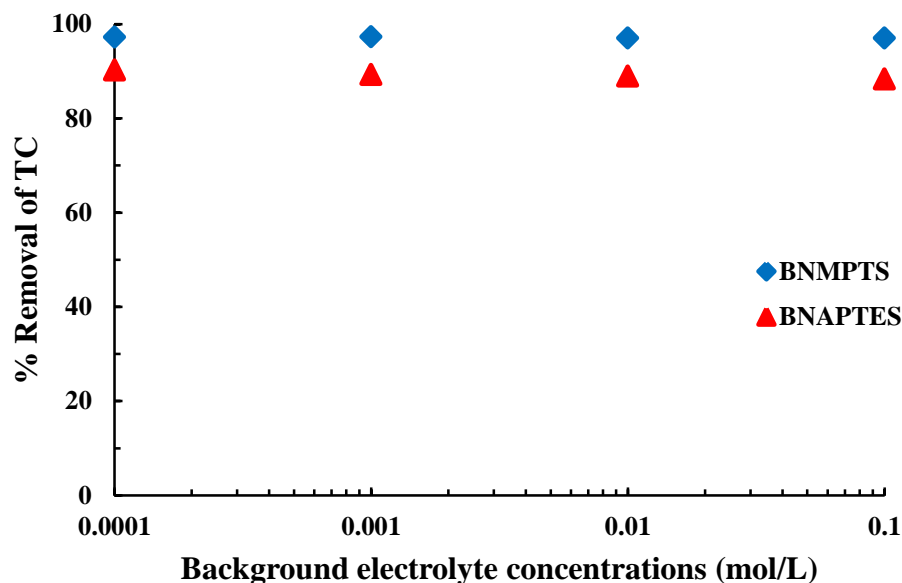


Figure 3.46: Effect of background electrolyte concentrations (NaCl) in the removal of tetracycline by the BNMPTS and BNAPTES solids ([TC]: 10.0 mg/L; pH: 4.0; Solid dose: 2.0 g/L; Temperature: 25°C).

3.3.6.5. Triclosan (TCS)

Similarly, the effect of background electrolyte (NaCl) concentrations on the removal of triclosan by BNMPTS and BNAPTES was performed and the background electrolyte (NaCl) concentration was increased from 0.0001 to 0.1 mol/L. The percentage removal efficiency of triclosan by BNMPTS and BNAPTES as a function of background electrolyte concentrations is shown in Figure 3.47. Figure 3.47 showed that the percentage uptake of triclosan was remained, almost, constant while the background electrolyte concentration was increased from 0.0001 to 0.1 mol/L. In brief, the percentage removal of triclosan was decreased from 96.05 to 94.03% using BNMPTS and 94.73 to 91.27% using BNAPTES, increasing the NaCl concentrations from 0.0001 to 0.1 mol/L, respectively. These results indicated that triclosan are adsorbed by the stronger forces, perhaps van der Waals, at the surface of functionalized materials. These results are in a line to the pH dependence studies concluded that the strong interactions occurred between the BNMPTS/or BNAPTES solids and the triclosan sorbate species. Previously, it was reported that the sorption

of triclosan by polystyrene microplastic was not affected by increasing the concentration of background electrolyte (NaCl) from 0.0 to 0.1 M (Li *et al.*, 2019a).

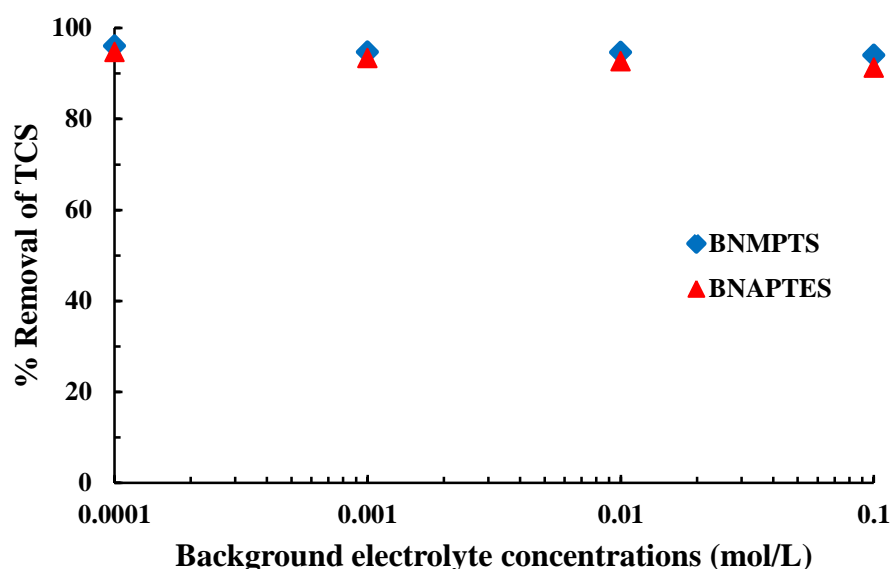


Figure 3.47: Effect of background electrolyte concentrations (NaCl) in the removal of triclosan by the BNMPTS and BNAPTES solids ([TCS]: 10.0 mg/L; pH: 4.0; Solid dose: 2.0 g/L; Temperature: 25°C).

3.3.6.6. 17 α -ethinylestradiol (EE2)

The impact of background electrolyte (0.0001 to 0.1 mol/L, NaCl), concentrations on the adsorption of EE2 by BNMPTS and BNAPTES materials are conducted as this enables to deduce the type of interactions involved between the sorbate species and the sorbent. Percentage elimination of EE2 using the BNMPTS and BNAPTES materials is unaffected by increasing the background electrolyte (NaCl) concentrations from 0.0001 to 0.1 mol/L (1000 times) (*Cf* Figure 3.48). These results inferred that 1000 times increase in background electrolyte concentration has unaffected the percentage sorption of EE2 by BNMPTS or BNAPTES solids. This confirms that sorbate species EE2 enters into the Stern layer at the surface and bonded with relatively stronger forces. This entails that the EE2 is interacted at the

surface of solids with hydrophobic interactions and proceed through organophilic attractions. Earlier, it was mentioned that presence of background electrolyte (NaCl) has unaffected the percent elimination of EE2 by advanced materials (Thanhmingliana *et al.*, 2015). Increasing ionic strength of NaCl from 0 to 320 mM in leachate solutions has not affected sorption of bisphenol A and EE2 by single-walled carbon nanotubes (SWCNTs) (Joseph *et al.*, 2011b). Sorption of estrone (E1), 17 β -estradiol (E2) and 17 α -ethinyl estradiol (EE2) using n-propyl functionalized mesoporous material (30% Pr-MCM-41) on increasing the concentration of NaCl from 0.001 to 0.1 M did not significantly affect the elimination of E1, E2 and EE2. The result is due to the same contribution produced by salting effect for estrogens and squeezing-out effect for 30%Pr-MCM-41 in presence of co-existed ions. The high removal of estrogens was due to the π - π and hydrophobic interaction between a 30%Pr-MCM-41 and estrogens (Gao *et al.*, 2019).

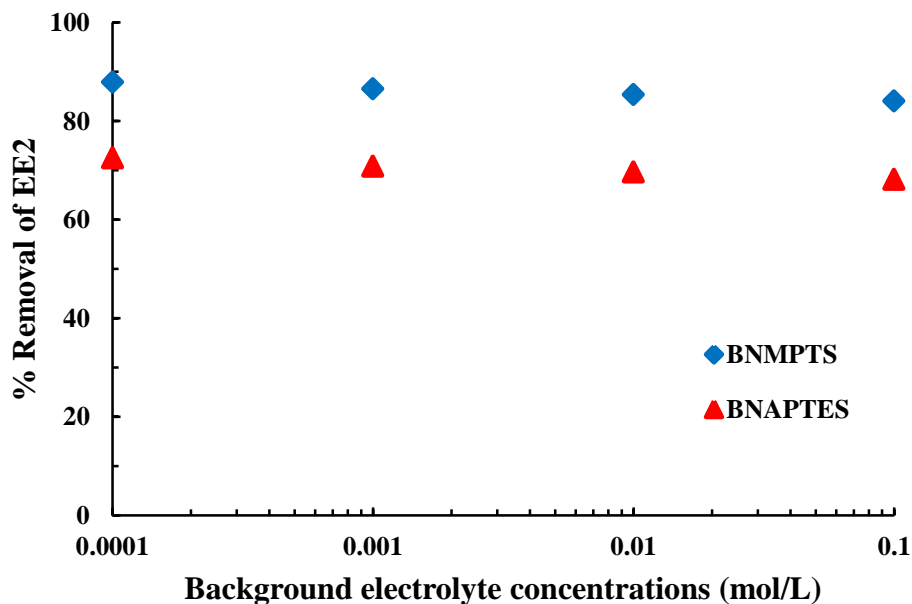


Figure 3.48: Effect of background electrolyte concentrations in the removal of EE2 by the BNMPTS and BNAPTES solids ([EE2]: 10.0 mg/L; pH: 4.0; Solid dose: 2.0 g/L; Temperature: 25°C).

3.3.7. Effect of co-existing ions in the removal of arsenic(III) and arsenic(V)

The presence of several co-existing ions in the removal of As(III) and As(V) by the BNMPTS and BNAPTES solids, respectively was conducted by keeping the initial concentration of As(III) and As(V) 10.0 mg/L, co-existing ions concentration 50.0 mg/L at constant pH 3.5. The cations chosen are Mn(II), Mg(II), Ca(II) and Ni(II) whereas the anions are ethylenediaminetetraacetic acid (EDTA), glycine, phosphate and oxalic acid. Results are shown in Figure 3.50 and 3.51 for As(III) and As(V), respectively. Figure 3.49 and 3.50 clearly show that the presence of Mn(II), Mg(II), Ca(II), Ni(II), glycine, phosphate and oxalic acid did not affect the percentage removal of As(III) and As(V) by these materials. Hence, this indicated the greater applicability of these materials in the effective and selective removal of As(III) and As(V) from aqueous solutions. However, the presence of EDTA and phosphate reduced the removal efficiency of As(V) by BNAPTES from 80% to 78 and 76%, respectively. While in case of As(III) removal by BNMPTS, the removal efficiency was decreased from 82% to 74 and 73% for EDTA and phosphate, respectively. Previous studies showed EDTA was effectively employed in the immobilization and elimination of arsenic, lead, chromium, iron, copper, cadmium, and mercury from heavy metal contaminated soils (Kartal, 2003). Similarly, the presence of excess metal ions (Cu(II), Cd(II), Pb(II) and Mn (II)) did not affect the adsorption of As(V) and phosphate by Fe-sericite composite beads. Results showed that these metal ions were sorbed by the functional group present in alginate while As(V)/phosphate species were specifically sorbed through a strong bond and formed surface complexes with the iron oxide present with the beads. Phosphate and arsenic (As(III) and As(V)) are having identical chemical behaviours in solutions since phosphorus and arsenic are present in the same group elements in the periodic table of elements and therefore, can compete with As(III) and As(V) for adsorption sites (Dong *et al.*, 2019; Yang *et al.*, 2017b). It was also reported that the presence of phosphate decreases the removal of arsenic by ferrous based red mud sludge, but, the presence of carbonate showed no effect in the removal arsenic (Li *et al.*, 2010).

The adsorption of arsenic by laterite soil in presence of varied concentrations of EDTA (0 to 25 mg/L) was significantly affected and the removal efficiency was decreased in presence of EDTA. This was demonstrated due to the complex

formation of EDTA with iron and aluminium on the surface of adsorbent. Additionally, the competition of arsenate and EDTA affected the removal efficiency of As(V) (Maji *et al.*, 2007). The presence of anions, HCO_3^- and SO_4^{2-} did not significantly affect the percent removal of As(V) by Fe-modified charred granulated attapulgite. Only a slight decrease i.e., 4.6 and 1.1% for HCO_3^- and SO_4^{2-} , respectively was observed. However, the presence of PO_4^{3-} in the sorptive solution greatly affected the percent removal of As(V). On the other hand, the presence of these anions significantly affected the removal of As(III) with PO_4^{3-} producing maximum effect. Since phosphate and arsenic are having identical chemical structure and thus PO_4^{3-} compete with arsenic for the binding sites at the surface of Fe-modified charred granulated attapulgite (Yin *et al.*, 2017). Similar results are reported in the previous literatures (Gong *et al.*, 2015; Ocinski *et al.*, 2015; Te *et al.*, 2017). It was also reported that the presence of Ca^{2+} and Fe^{2+} could not affect significantly the removal of arsenic by laterite soil (Maji *et al.*, 2007).

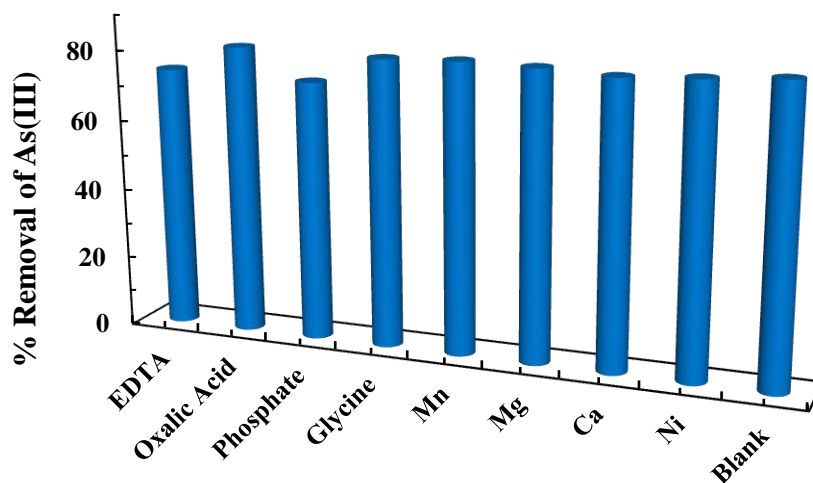


Figure 3.49: Effect of co-existing cations in the removal of As(III) by the BNMPST solid ([As(III)]: 10.0 mg/L; [Cations]: 50.0 mg/L; pH: 3.5; Solid dose: 2.0 g/L; Temperature: 25°C).

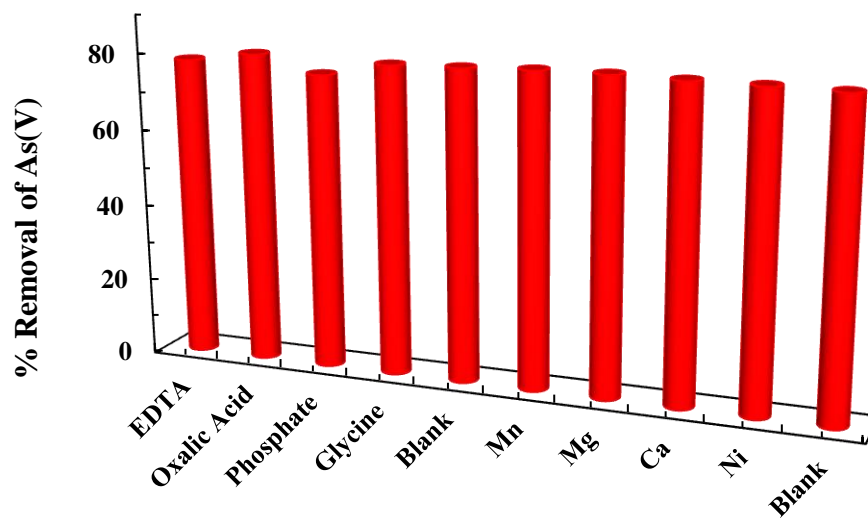


Figure 3.50: Effect of co-existing anions in the removal of As(V) by the BNAPTES solid ([As(V)]: 10.0 mg/L; [Anions]: 50.0 mg/L; pH: 3.5; Solid dose: 2.0 g/L; Temperature: 25°C).

3.3.8. Effect of co-existing ions in the removal copper(II) and cadmium(II)

The removal of Cu(II) using BNMPST is studied in presence of several co-existing cations (Mg(II), Mn(II), Ca(II) and Ni(II)) and anions (Ethylenediaminetetraacetic acid (EDTA), oxalic acid, glycine and phosphate). The co-existing ions concentration was taken 50.0 mg/L and Cu(II) concentration 10.0 mg/L at pH 4.0 and the results are shown in Figure 3.51 and 3.52 for cations and anions, respectively. The presence of EDTA significantly suppressed the removal of Cu(II) which is due to the formation of stable complexes of EDTA and Cu(II) and the complexed species are feebly bound on the solid surface (Chen *et al.*, 2019). On the other hand, it is observed that the presence of other cations or anions did not affect the removal of Cu(II) from aqueous solutions. Therefore, the findings further showed the selectivity and the efficiency of BNMPST towards Cu(II) in presence of several cations/anions. It was also reported that the presence of Na⁺, K⁺ and Ca²⁺, or Mg²⁺ had no significant effect on the binding of copper and lead using Fe₃O₄.

However, a slight decrease in the removal of Cu(II) was observed in presence of Mg^{2+} at 3000 mg/L (Tamez *et al.*, 2016). Similarly, the presence of anions in the removal of copper (II) and lead (II) by nonliving green algae (*Cladophora fascicularis*) was almost negligible. However, the presence of 1.0 mmol/L EDTA caused to suppress the removal of copper (II) and lead (II) (Deng *et al.*, 2006).

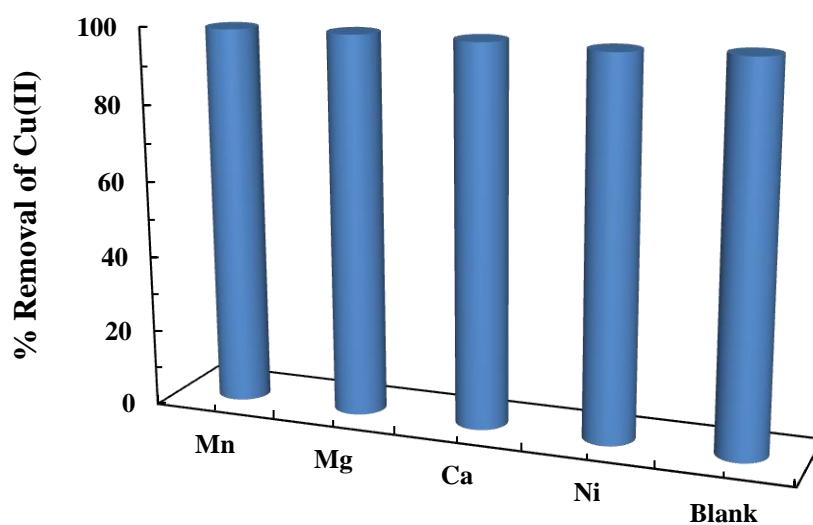


Figure 3.51: Effect of co-existing cations in the removal of Cu(II) by the BNMPTS solid ([Cu(II)]: 10.0 mg/L; [Cations]: 50.0 mg/L; pH: 4.0; Solid dose: 2.0 g/L; Temperature: 25°C).

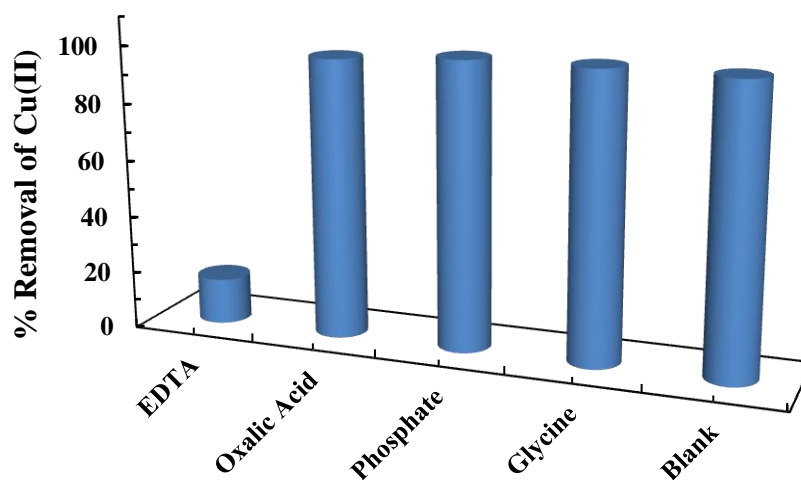


Figure 3.52: Effect of co-existing anions in the removal of Cu(II) by the BNMPTS solid ([Cu(II)]: 10.0 mg/L; [Anions]: 50.0 mg/L; pH: 4.0; Solid dose: 2.0 g/L; Temperature: 25°C).

Similarly, the sorption of Cd(II) by the BNMPTS was performed in simultaneous presence of these cations and anions separately, maintaining the concentration of Cd(II) 5.0 mg/L at pH 5.0 having solid dose of 2.0 g/L. The co-existing ion concentration was taken as 50.0 mg/L. The results are illustrated graphically in Figures 3.53 and 3.54. It is clear from Figure 3.55 that the percentage removal of Cd(II) was significantly reduced in presence of EDTA. This is due to the formation of stable complexes between EDTA and Cd(II) and the complexed species are not adsorbed at the surface of material (Ezzeddine *et al.*, 2015). However, the presence of other cations or anions could not hamper the removal percentage of Cd(II) by BNMPTS. This further reveals the greater applicability and selectivity of BNMPTS towards the removal of Cd(II). Previously, it was observed that the removal of Cd(II), Cu(II), Pb(II) and Hg(II) by ZnS and FeS nanomaterials is 99% in mixed metal cation solutions in presence of 60 fold concentrations of Ca^{2+} and Mg^{2+} . Therefore, the presence cations showed a negligible effect in the removal efficiency of metal-sulfide nanomaterials at least for Cd(II) removal (Wang *et al.*, 2020a). In

other study, the removal of Cd(II) using MnO₂ loaded D301 resin in presence of interfering cations (Na⁺, K⁺ and Ca²⁺, or Mg²⁺) and anions (Cl⁻, NO₃⁻, SO₄²⁻ and PO₄³⁻) showed no significant affect except of PO₄³⁻ (Zhu et al., 2007). The presence of EDTA on the sorption of Cd(II) and Zn(II) by apatite showed a decrease in the uptake of Cd(II) and Zn(II) due to the formation of [CdEDTA]²⁻ and [ZnEDTA]²⁻ complex species and solubility of apatite is increased due to [CaEDTA]²⁻ complex formation (Viipsi *et al.*, 2013). Further, the removal of Cd(II) by brown, green, and red seaweeds was not much affected in presence of nitrate salts of sodium, potassium and magnesium. However, the uptake of cadmium was suppressed. The initial calcium concentration of 1.62 mmol/L had caused to reduce the percentage removal of Cd(II) to 80% and further increase in calcium concentration to 3.24 mmol/L had caused to decrease the removal percentage of Cd(II) to 65% (Hashim *et al.*, 2004).

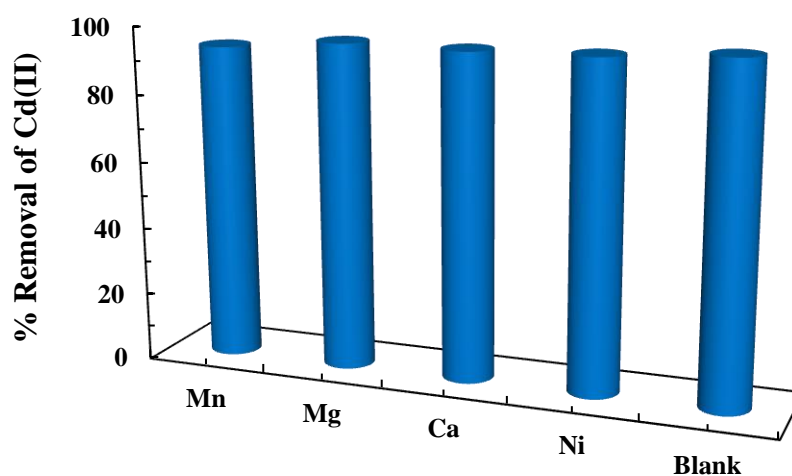


Figure 3.53: Effect of co-existing cations in the removal of Cd(II) by BNMPSTs solid ([Cd(II)]: 5.0 mg/L; [Cations]: 50.0 mg/L; pH: 5.0; Solid dose: 2.0 g/L; Temperature: 25°C).

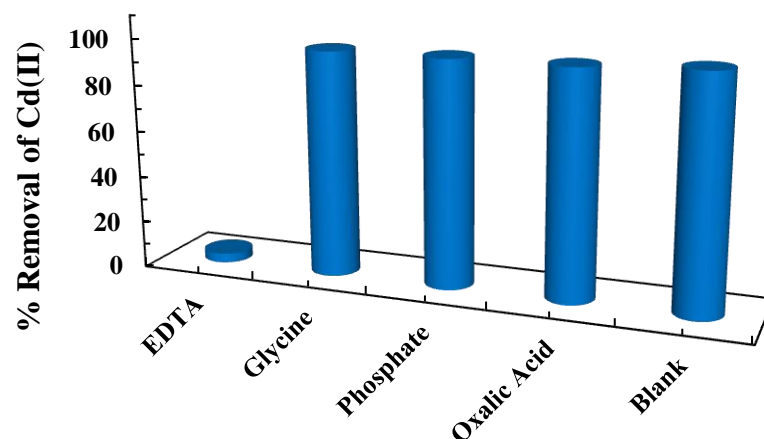


Figure 3.54: Effect of co-existing anions in the removal of Cd(II) by BNMPTS solid ([Cd(II)]: 5.0 mg/L; [Anions]: 50.0 mg/L; pH: 5.0; Solid dose: 2.0 g/L; Temperature: 25°C).

3.3.9. Effect of co-existing ions in the removal of tetracycline, triclosan and EE2

The presence of co-existing ions (cations and anions) in the removal of tetracycline by the BNMPTS and BNAPTES composite solids was studied with initial tetracycline and co-ions concentrations 10.0 mg/L and 50.0 mg/L, respectively at pH 4.0. The results are shown in Figure 3.55 and 3.56. The cations chosen were Mn(II), Mg(II), Ca(II), and Ni(II); whereas the anions were taken as ethylenediaminetetraacetate (EDTA), oxalic acid, phosphate and glycine. Figure 3.55 and 3.56 showed that the removal efficiency of tetracycline by both the functionalized solids was almost unaffected in presence of these co-existing cations *viz.*, Mn(II), Mg(II), Ca(II), and Ni(II). However, a slight decrease in percentage uptake of tetracycline was observed in presence of anions *viz.*, glycine, phosphate and oxalic using the BNAPTES solid (*Cf* Figure 3.56). Similarly, the presence of EDTA effected significantly the percentage removal of tetracycline by the BNMPTS and BNAPTES solids. The results apparently indicated therefore, that the presence of EDTA considerably suppressed the uptake and the percentage removal of tetracycline was decreased from 95 to 80% for BNAPTES and from 96 to 80% for

BNMPTS. The effect of Cl^- , NO_3^- , SO_4^{2-} anions in the sorption of tetracycline by modified biochar was studied in real water samples and it was observed that these anions could not affect the removal percentage of tetracycline, however, the presence of PO_4^{2-} showed a considerable influence in the removal percentage of tetracycline by modified biochar (Dai *et al.*, 2020a). On the other hand, the cations such as Mg^{2+} and Ca^{2+} caused a slight decrease in the adsorption capacity of tetracycline while the K^+ and Na^+ did not affect the sorption of tetracycline by NiFe_2O_4 -COF-chitosan-terephthalaldehyde nanocomposite films (Li *et al.*, 2020). Moreover, it was also reported that the presence of 0.01M (Mg^{2+} , Ca^{2+} , K^+ and Na^+) had a little effect on the percentage removal of tetracycline by $\text{Fe}_3\text{O}_4@\text{SiO}_2$ -Chitosan/Graphene oxide nanocomposite (MSCG) material (Huang *et al.*, 2017).

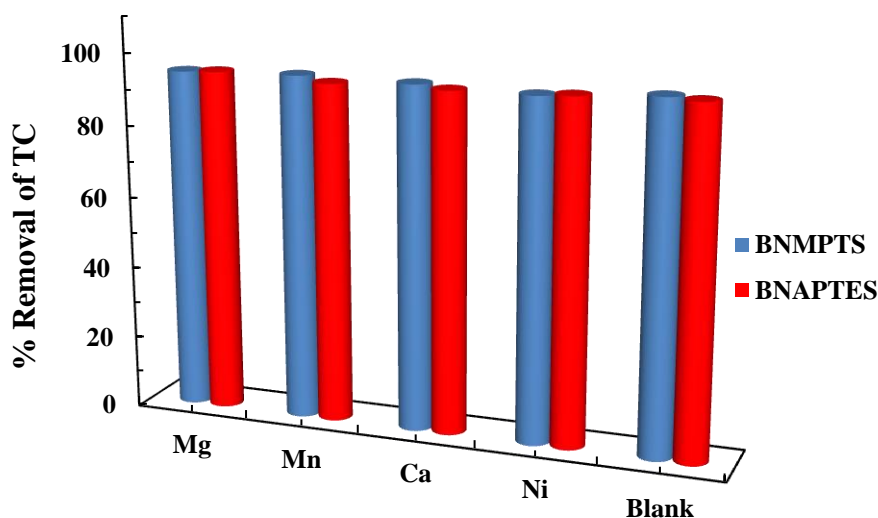


Figure 3.55: Effect of co-existing cations in the removal of tetracycline by BNMPTS and BNAPTES solids ([TC]: 10.0 mg/L; [Cations]: 50.0 mg/L; pH: 4.0; Solid dose: 2.0 g/L; Temperature: 25°C).

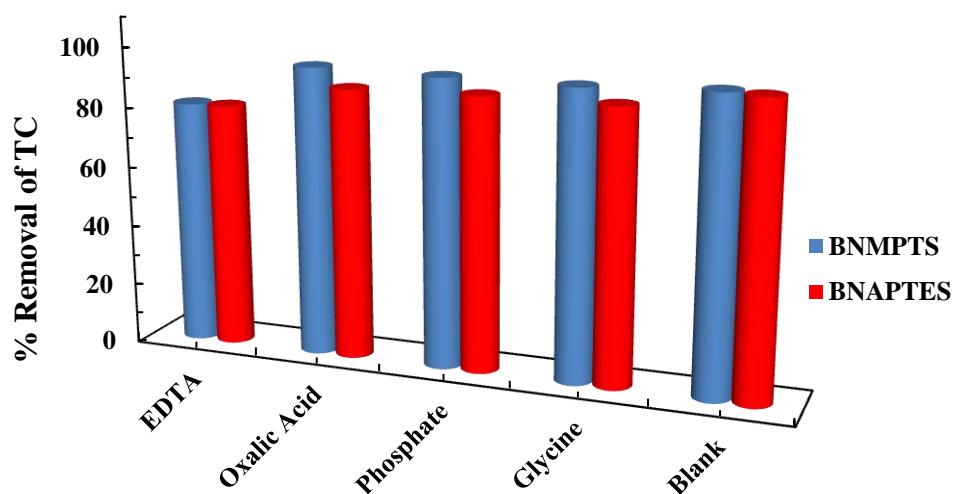


Figure 3.56: Effect of co-existing anions in the removal of tetracycline by BNMPTS and BNAPTES solids ([TC]: 10.0 mg/L; [Anions]: 50.0 mg/L; pH: 4.0; Solid dose: 2.0 g/L; Temperature: 25°C).

Similarly, the sorption of triclosan by BNMPTS and BNAPTES was conducted in simultaneous presence of several coexisting ions. The initial concentration of triclosan was taken 10.0 mg/L at pH 4.0. The cations are included as Mn(II), Mg(II), Ca(II) and Ni(II) whereas the anions are chosen as ethylenediaminetetraacetic acid (EDTA), glycine, phosphate and oxalic acid. The concentration of co-ions was maintained as 50.0 mg/L. Further, the results are presented in Figure 3.57 and 3.58. Results showed that these co-existing ions showed no effect in the sorption efficiency of BNMPTS and BNAPTES for triclosan except the presence of EDTA. The presence of EDTA had suppressed the removal efficiency of triclosan from 95 to 74% using BNMPTS and 95 to 73% using BNAPTES. Previously, it was reported that the sorption of triclosan using MIL-53(Al) and MIL-53(Al)-1 was not affected in presence of several co-existing ions. However, the presence of humic acid (HA) affected the sorption of triclosan by the solid since the percent removal of triclosan was decreased in presence of HA (Dou *et al.*, 2017).

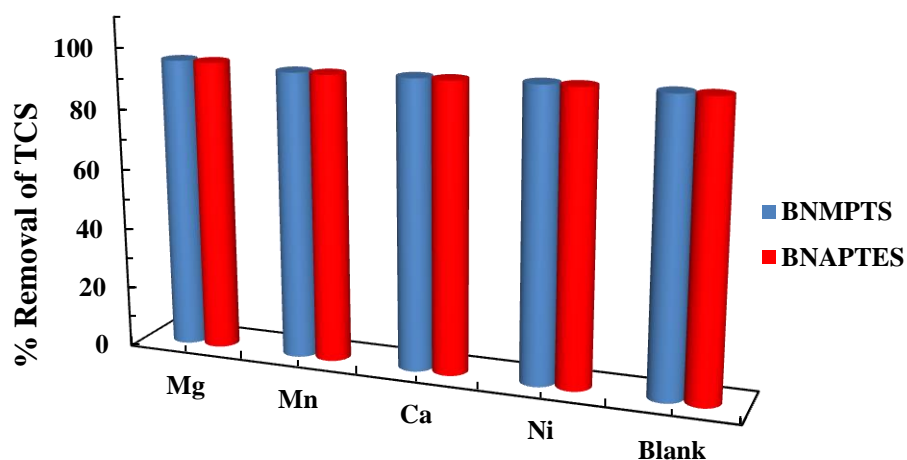


Figure 3.57: Effect of co-existing cations in the removal of triclosan by BNMPTS and BNAPTES solids ([TCS]: 10.0 mg/L; [Cations]: 50.0 mg/L; pH: 4.0; Solid dose: 2.0 g/L; Temperature: 25°C).

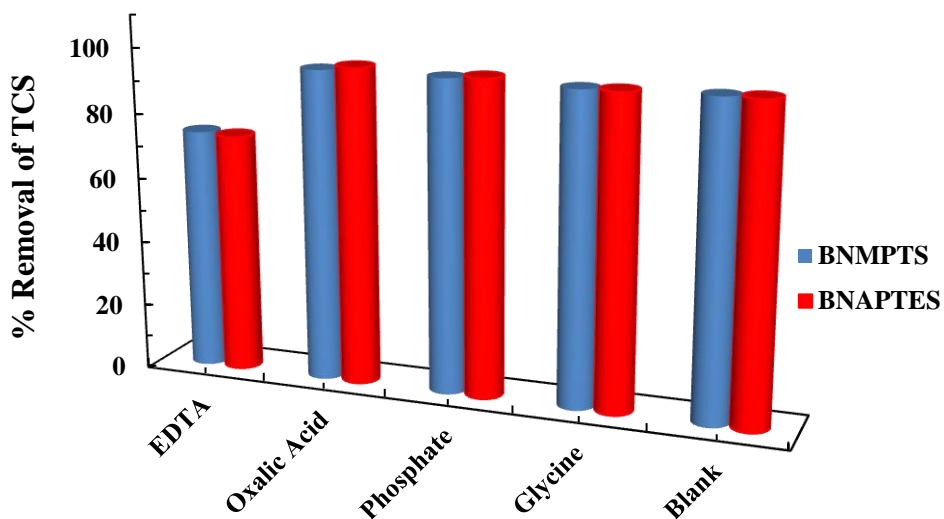


Figure 3.58: Effect of co-existing anions in the removal of triclosan by BNMPTS and BNAPTES solids ([TCS]: 10.0 mg/L; [Anions]: 50.0 mg/L; pH: 4.0; Solid dose: 2.0 g/L; Temperature: 25°C).

Co-ions (cations: Mn(II), Mg(II), Ca(II) and Ni(II) or anions: ethylenediaminetetraacetic acid (EDTA), oxalic acid, glycine and phosphate) effect in the elimination of EE2 by BNMPTS and BNAPTES was extensively studied. The concentration of EE2 and co-ions are taken as 10.0 mg/L and 50.0 mg/L, respectively at pH 4.0. Results are shown as percentage elimination of EE2 in presence these co-existing ions and presented in Figure 3.59 and 3.60. The percentage removal of EE2 was not changed in presence of these co-ions except EDTA which significantly affected the removal of EE2 from 86 to 18% using BNMPTS and 75 to 29% using BNAPTES. This is, perhaps, due to the competitive sorption of EDTA towards solid surface. It was previously reported that the sorption of EE2 using PA612 was unaffected in presence of cations (0.1 mol/L) viz., Zn(II), K(I) or Ca(II) however, only a slight reduction in sorption was recorded in presence of Mg(II) (Han *et al.*, 2013).

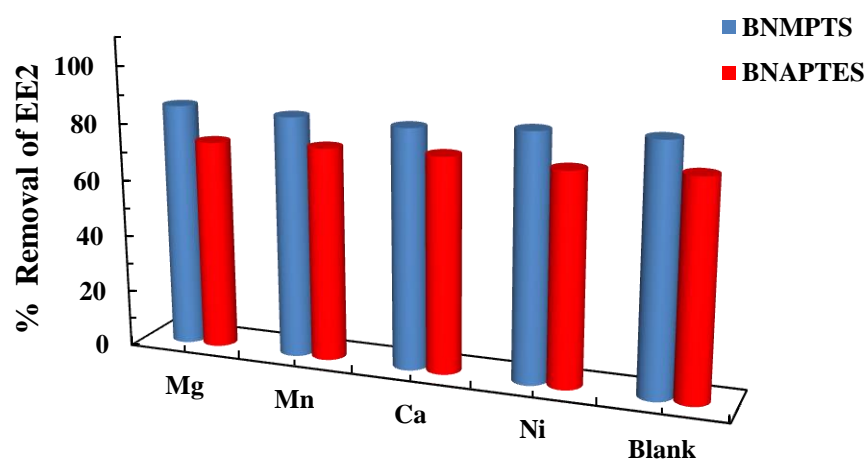


Figure 3.59: Effect of co-existing cations in the removal of EE2 by BNMPTS and BNAPTES solids ([EE2]: 10.0 mg/L; [Cations]: 50.0 mg/L; pH: 4.0; Solid dose: 2.0 g/L; Temperature: 25°C).

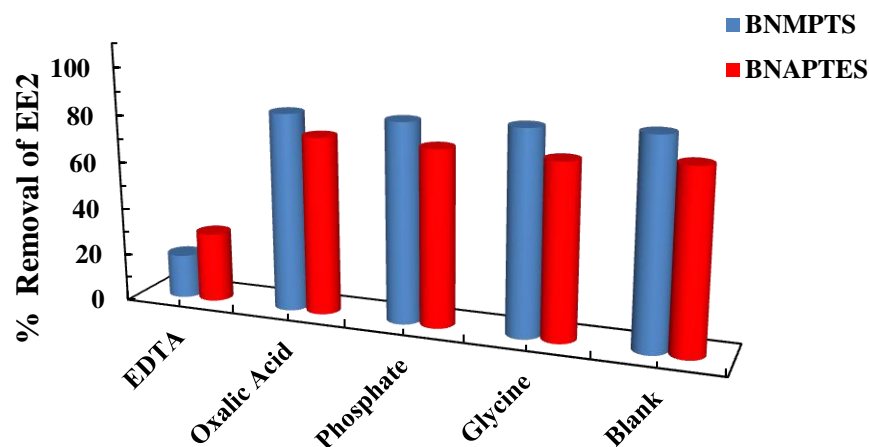


Figure 3.60: Effect of co-existing anions in the removal of EE2 by BNMPTS and BNAPTES solids ([EE2]: 10.0 mg/L; [Anions]: 50.0 mg/L; pH: 4.0; Solid dose: 2.0 g/L; Temperature: 25°C).

3.4. COLUMN REACTOR STUDIES

To determine the removal/loading capacity and the applicability of BNMPTS and BNAPTES in real water treatment, fixed bed column experiment was conducted under dynamic conditions. Therefore, column studies was conducted for the removal of Cu(II), Cd(II), tetracycline, triclosan and EE2 from aqueous solutions. The detailed experimental procedures are followed as described previously (Chapter 2.3.7).

3.4.1. Copper(II)

The removal/loading capacity of BNMPTS for Cu(II) under the dynamic conditions was conducted using fixed-bed column reactor operations. The concentration of Cu(II) was maintained at 10.0 mg/L; pH 4.0. The breakthrough curve for the removal of Cu(II) using the BNMPTS for different loadings of solids is shown in Figure 3.61. It is evident from the breakthrough curves that relatively high breakthrough volume was obtained for the Cu(II). Quantitatively, a complete breakthrough volume was obtained with the throughput volume of 1.40 L and 3.69 L

using the BNMPTS loading of 0.25 g and 0.50 g, respectively for Cu(II). Furthermore, the Thomas equation is utilized to obtain the non-linear least square fitting using the breakthrough column data. The two unknown parameters, Thomas constant (K_T) and loading capacity (q_0) are optimized using the least square fitting method. The Thomas constants along with the least square sum is included in Table 3.14. Additionally, the fitting curves are shown in Figure 3.61. The data evidently showed that the material possessed a high loading capacity for Cu(II) under the dynamic conditions. This might be due to the fact that a fixed-bed process has an extra advantage of the continuous interaction of sorbing species with the surface of solid which results in enhanced exhaustion of the solids than the batch reactor operations. These results are consistent with other reports in which the Thomas equation was employed to determine the loading capacity of pollutants using different sorbents (Lee *et al.*, 2014). This result further showed the potential applicability of BNMPTS solid in the remediation of aqueous solutions contaminated with Cu(II) (Lalchhingpuii *et al.*, 2016). Chitosan immobilized on bentonite (CHB) was used for the removal of Cu(II) from aqueous solutions in a column system where the dynamics of the adsorption method were estimated by using bed depth service time (BDST) model and Thomas model. The adsorption capacity of 14.92 mg copper(II)/g CHB with 24 hours breakthrough was attained at 500 mg/L of initial concentration, bed height of 4.3 cm, and flow rate was 0.20 mL/min (Futalan *et al.*, 2011).

Table 3.14. Thomas constants estimated for the removal of Cu(II) by BNMPTS material. ([Cu(II)]: 10.0 mg/L; Flow rate: 1.0 mL/min; pH: 4.0; Amount of solid loaded: 0.25/or 0.50 g; Temperature: 25°C).

Amount of BNMPTS taken in column (g)	Thomas constants		Least square sum (s^2)
	q_0 (mg/g)	K_T (L/min/mg)	
0.25	28.87	8.14×10^{-4}	1.0×10^{-2}
0.50	32.03	3.60×10^{-4}	9.2×10^{-3}

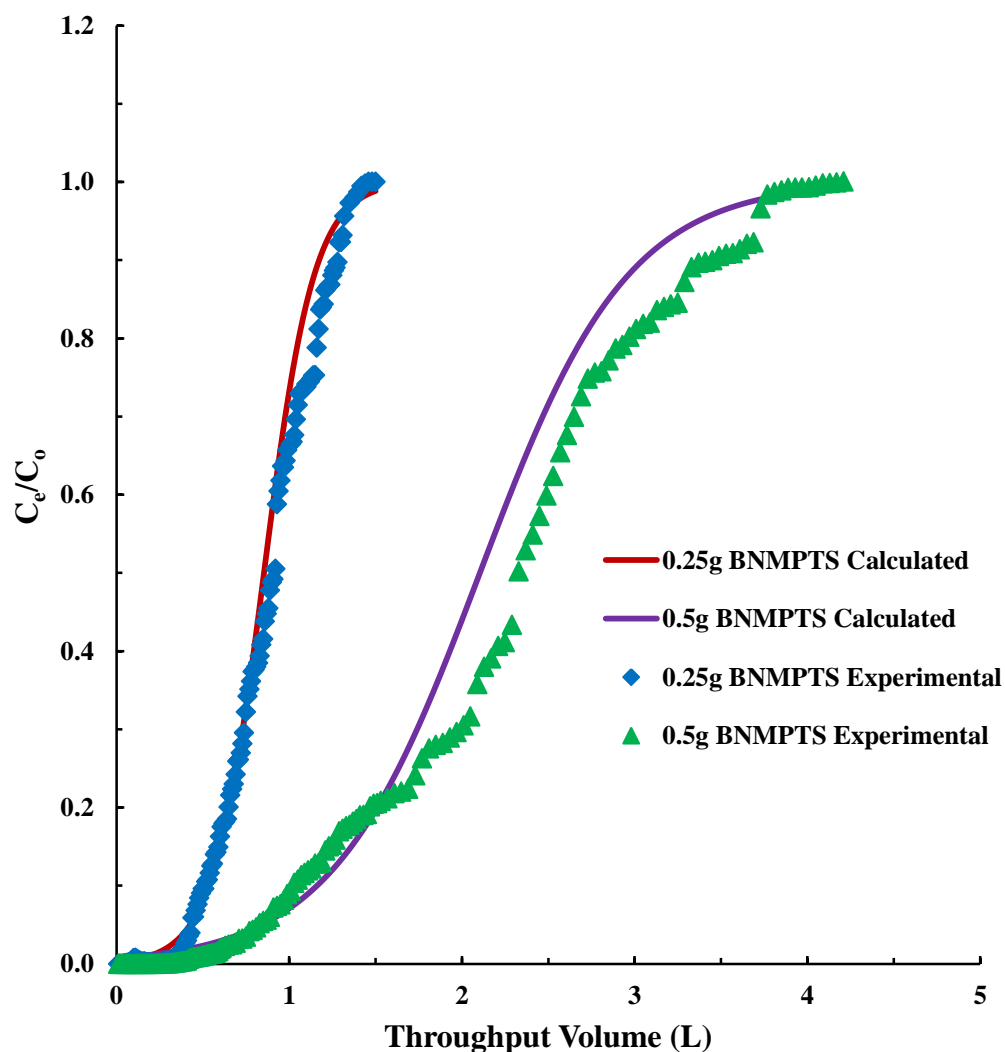


Figure 3.61: Breakthrough curves obtained for the removal of Cu(II) by BNMPTS ([Cu(II)]: 10.0 mg/L; Flow rate: 1.0 mL/min; pH: 4.0; Amount of solid loaded: 0.25/or 0.50 g; Temperature: 25°C).

3.4.2. Cadmium(II)

Similarly, the fixed bed column studies were performed for the removal of Cd(II) 5.0 mg/L; pH 5.0 for different loadings of BNMPTS i.e., 0.25 g and 0.50 g. The breakthrough curves are obtained and shown in Figure 3.62. It is evident from the figure that the high breakthrough volume was achieved for Cd(II) using the composite material. Quantitatively, a complete breakthrough volume for Cd(II) was

obtained as 2.60 L and 6.64 L respectively for the column loading of 0.25 g and 0.50 g of BNMPTS. These results indicated that a small loading of BNMPTS enabled to obtain very breakthrough volume. Further, the breakthrough results are utilized for the fitting to Thomas equation to optimize the Thomas constants i.e., Thomas constants (K_T) and loading capacity (q_0) of Cd(II). The fitting results are therefore included in Table 3.15. Quantitatively, the loading capacities of Cd(II) was found to be 19.71 and 35.09 mg/g of Cd(II) using the BNMPTS loading of 0.25 and 0.50 g, respectively in the column. The results further clarified the applicability of BNMPTS for the elimination of Cd(II) in waste water under continuous flow system. Previously, it was reported that relatively high breakthrough volume is achieved for Cd(II) employing mesoporous materials (TMS and AMS) under fixed bed column reactor operation. The loading capacity of TMS and AMS solids were found to be 11.65 and 6.68 mg/g, respectively. Furthermore, it was found that the removal of Cd(II) under fixed-bed study is higher compared to batch study. This is maybe due to the fact that the sorbing species had received prolong and continuous contact with the solid surface which resulted a complete exhaustion of solid and giving out an enhanced removal capacity (Lalchhingpuii *et al.*, 2017). In other study, the removal capacity of biomass *Macrophthalmusrouxii* at the flow rate of 2.28 mL/min for Pb(II) was found to be 4.06 mg/g and for Cd(II), the removal capacity at the flow rate 2.60 mL/min was found to be 1.25 mg/g (Yan and Viraraghavan, 2011).

Table 3.15. Thomas constants estimated for the removal of Cd(II) by BNMPTS material ([Cd(II)]: 5.0 mg/L; Flow rate: 1.0 mL/min; pH: 5.0; Amount of solid loaded: 0.25/or 0.50 g; Temperature: 25°C).

Amount of BNMPTS taken in column (g)	Thomas constants		Least square sum (s ²)
	q ₀ (mg/g)	K _T (L/min/mg)	
0.25	19.71	1.0X 10 ⁻⁴	1.9 X 10 ⁻²
0.50	35.09	2.8 X 10 ⁻⁴	2.0 X 10 ⁻¹

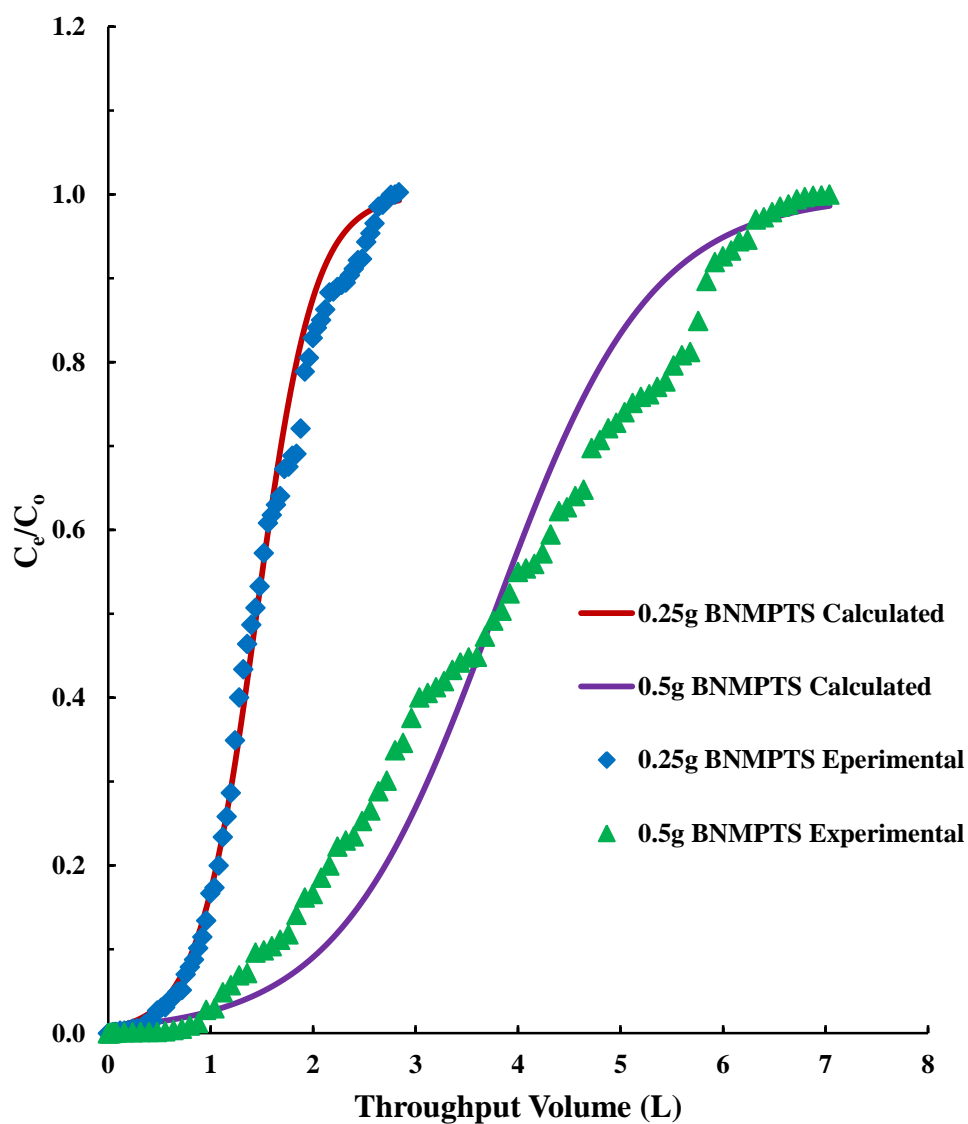


Figure 3.62. Breakthrough curves obtained for the removal of Cd(II) by BNMPTS solid ([Cd(II)]: 5.0 mg/L; Flow rate: 1.0 mL/min; pH: 5.0; Amount of solid loaded: 0.25/or 0.50 g; Temperature: 25°C).

3.4.3. Tetracycline, triclosan and EE2

Further, the micro-pollutants removal was obtained under the fixed-bed column operations and the removal capacity of BNMPTS and BNAPTES was assessed for the tetracycline, triclosan and EE2 under the dynamic conditions. The micro-pollutant concentration was taken as 10.0 mg/L at pH 4.0 and the column was packed with the 0.25 and 0.50 g of solids i.e., BNMPTS and BNAPTES. The breakthrough curves obtained for the tetracycline is shown in Figure 3.63. It is noted that a high breakthrough volume was achieved using these materials. The column packed with 0.25 g and 0.50 g of BNMPTS material showed a complete breakthrough volume at throughput volume of 3.01 L and 6.06 L for tetracycline, respectively. Similarly, a complete breakthrough volume of 1.98 L and 4.02 L for tetracycline was obtained for a loading of 0.25 g and 0.50 g of BNAPTES, respectively. Further, breakthrough results are fitted to the Thomas equation and the unknown parameters i.e., the Thomas constant (K_T), loading capacity (q_0) was optimized. The fitting results are shown in Table 3.16. The column results indicated that very high loading capacity was achieved using the BNMPTS or BNAPTES solids for the removal of tetracycline under the continuous flow system as well. These results further pointed the potential of these solids for practical implacability in the decontamination of tetracycline from aqueous wastes. It was reported earlier that increasing the bed height of modified silica from 3 to 10 cm for the sorption of tetracycline in column experiments leads to enhance the removal capacity from 388.5 to 412.7 mg/g (Liu *et al.*, 2013). Moreover, bentonite modified with hexadecyltrimethylammonium bromide (BH), aluminium pillared bentonite modified with hexadecyltrimethylammonium bromide (BAH), local clay modified with hexadecyltrimethylammonium bromide (LCH) and aluminium pillaring local clay modified with hexadecyltrimethylammonium bromide (LCAH) show high removal capacity 111.979, 97.987, 86.965, 64.996 mg/g for tetracycline under fixed bed column operations (Thanhmingliana *et al.*, 2015).

Table 3.16. Thomas constants estimated for the removal of tetracycline by BNMPTS and BNAPTES ([TC]: 10.0 mg/L; Flow rate: 1.0 mL/min; pH: 4.0; Amount of solid loaded: 0.25/or 0.50 g; Temperature: 25°C).

Amount of materials taken in column (g)	Thomas constants		Least square sum (s ²)
	q _o (mg/g)	K _T (L/min/mg)	
0.25 BNMPTS	60.86	3.82x10 ⁻⁴	1.2
0.50 BNMPTS	75.58	1.69 X 10 ⁻⁴	1.3
0.25 BNAPTES	40.78	4.4 x10 ⁻⁴	1.1
0.50 BNAPTES	55.97	2.2 X 10 ⁻⁴	1.3

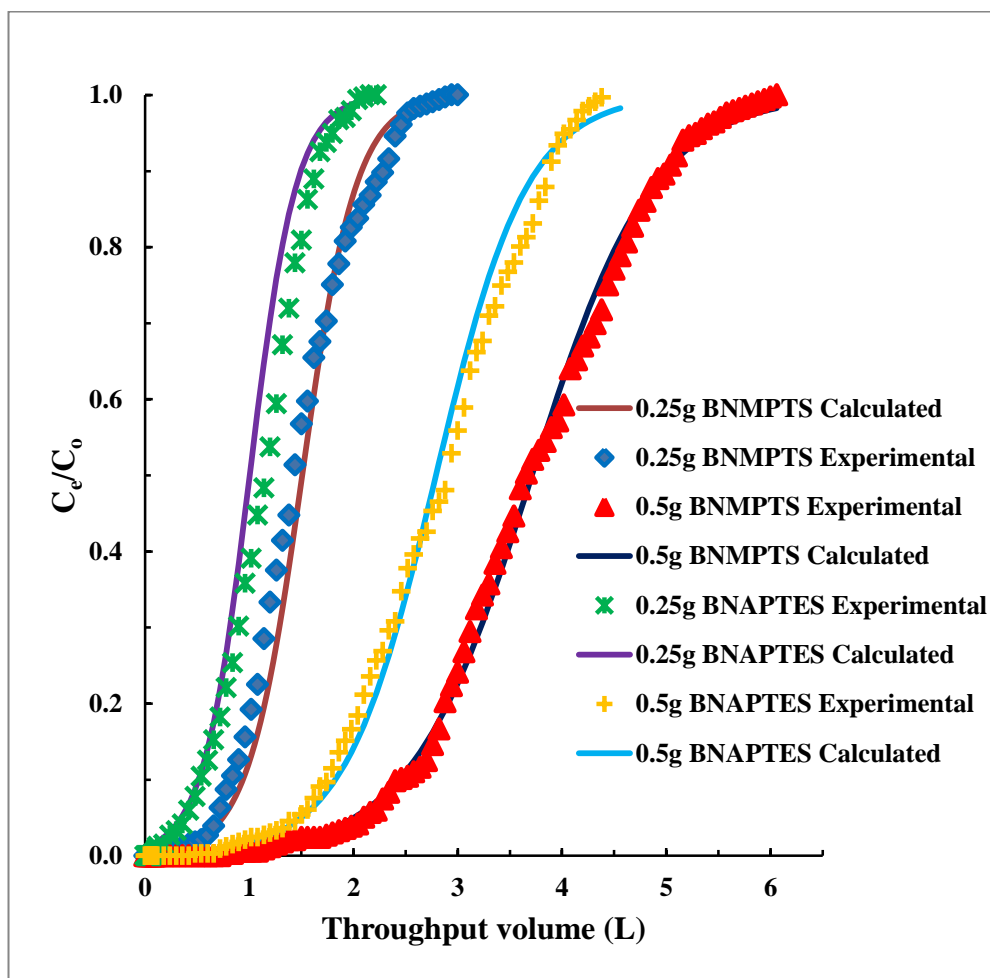


Figure 3.63: Breakthrough curves obtained for the removal of tetracycline by BNMPTS and BNAPTES solids ([TC]: 10.0 mg/L; Flow rate: 1.0 mL/min; pH: 4.0; Amount of solid loaded: 0.25/0.50 g; Temperature: 25°C).

The breakthrough results for the removal of triclosan by the BNMPTS and BNAPTES materials packed columns are shown in Figure 3.65. It is evident from the figure that fairly high breakthrough volumes were obtained for the loading of triclosan using these solids. As shown in Figure 3.64, a complete breakthrough volume was obtained at the throughput volume of 2.34 L and 4.56 L using 0.25 g and 0.50 g of BNMPTS, respectively for triclosan. On the other hand, a complete breakthrough volume was obtained at the throughput volume of 1.5 L and 3.3 L using 0.25 g and 0.50 g of BNAPTES for the removal of triclosan. Further, a non-linear least square fitting were conducted for the Thomas equation and the unknown

parameters such as Thomas constant (K_T) and the loading capacity (q_0) were obtained. The loading capacity of the column and Thomas constants along with the least square sum are given in Table 3.17. The high loading capacity obtained for the removal of triclosan by BNMPTS and BNAPTES materials again suggested the promising of these materials for the efficient removal of triclosan in aqueous solutions and possessed potential application in the remediation of aqueous waste contaminated with micro-pollutants (Ahmed and Hameed, 2018; Lee *et al.*, 2017). Magnetic porous reduced graphene oxide (MPrGO) was employed for the removal of triclosan in column system. Results showed that, 50 days of the breakthrough time was observed for the bed depth of 2.3 mm at the inlet triclosan concentration of 100 $\mu\text{g/L}$, and the breakthrough time increased with the increased bed depth at lower triclosan concentration. The Thomas and Yoon-Nelson models showed better fitting curves than that by Adams-Bohart model. Moreover, MPrGO exhibited a higher affinity toward triclosan than powder activated carbon (PAC) and, the breakthrough time for MPrGO was 6.5 times greater than that of PAC (Li *et al.*, 2019b). Chitosan was used for the removal of triclosan from an aqueous medium in fixed-down-flow column bed. The column-bed with physically entrapped chitosan showed removal efficiency up to 99% at a significantly high concentration of triclosan (90 ppm). Lower initial concentration of triclosan (10 ppm), lower flow rate and higher adsorbent dose are most favourable for higher removal efficiency of triclosan in the column bed operations. Further, Yoon-Nelson model showed the best agreement between the experimental and calculated values (Matolia *et al.*, 2019).

Table 3.17. Thomas constants estimated for the removal of triclosan by BNMPTS and BNAPTES ([TCS]: 10.0 mg/L; Flow rate: 1.0 mL/min; pH: 4.0; Amount of solid loaded: 0.25/0.50 g; Temperature: 25°C).

Amount of materials taken in column (g)	Thomas constants		Least square sum (s ²)
	q ₀ (mg/g)	K _T (L/min/mg)	
0.25 BNMPTS	49.494	3.6 X 10 ⁻⁴	1.1
0.50 BNMPTS	60.167	2.16 X 10 ⁻⁴	1.3
0.25 BNAPTES	31.494	5.0 X 10 ⁻⁴	1.1
0.50 BNAPTES	44.425	3.02 X 10 ⁻⁴	1.3

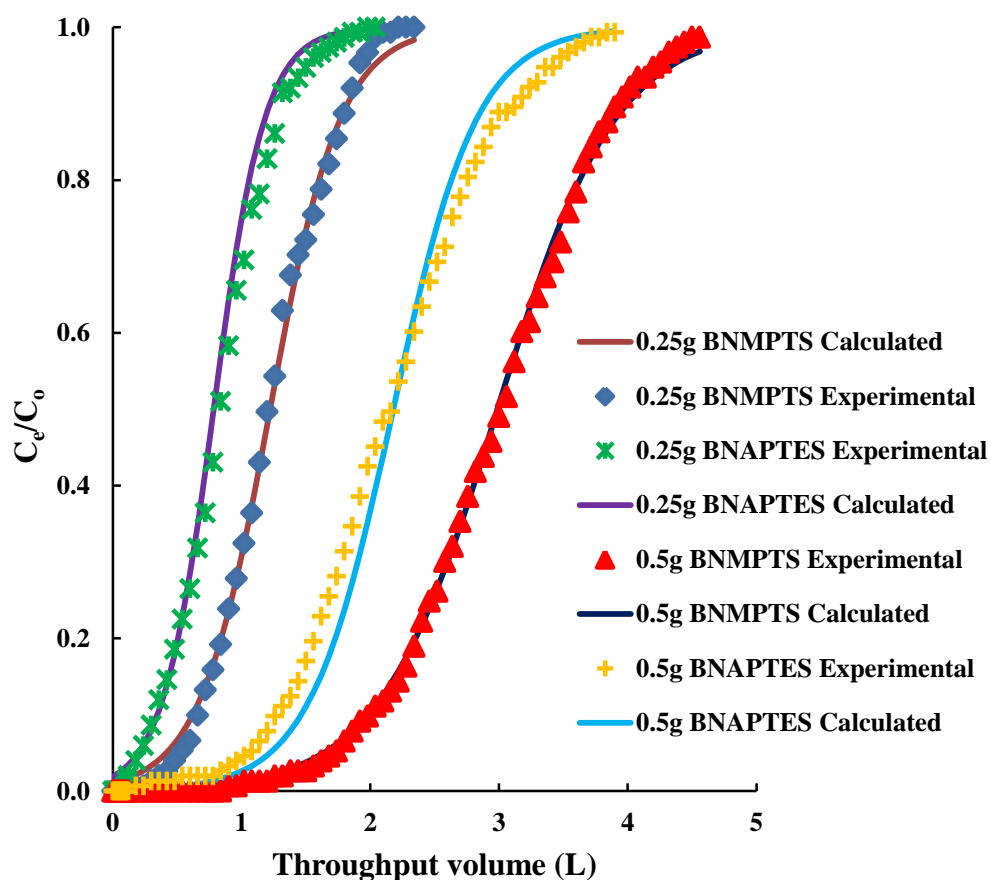


Figure 3.64: Breakthrough curves obtained for the removal of triclosan by BNMPTS and BNAPTES solids ([TCS]: 10.0 mg/L; Flow rate: 1.0 mL/min; pH: 4.0; Amount of solid loaded: 0.25/or 0.50 g; Temperature: 25°C).

Finally, the loading capacity of BNMPTS and BNAPTES materials for EE2 was obtained under the fixed-bed column reactor operations. The breakthrough results are shown in Figure 3.65. It is evident from the breakthrough curves that these materials possessed relatively high breakthrough volumes for EE2. Further, it is observed that increasing the amount of solids in the column has enabled to increase the breakthrough volume of EE2. A complete breakthrough for EE2 was achieved having throughput volume of 0.84 L and 1.50 L using 0.25 g and 0.50 g BNAPTES, respectively. Similarly, a complete breakthrough is attained at the volume of 0.96 L and 1.80 L using 0.25 g and 0.50 g of BNMPTS, respectively. Breakthrough data is

intended to utilize for a non-linear least square fitting using Thomas equation. The fitting results are illustrated in Figure 3.66. Moreover, optimized constants are returned in Table 3.18. Results showed that under the dynamic conditions, the BNMPTS and BNAPTES possessed very high loading capacity for EE2. This again reaffirmed that BNMPTS and BNAPTES are having potential in the elimination of EE2 from aqueous wastes. The removal of EE2 by rabbit food (RF) in aqueous and solid phases was demonstrated using column experiments. Results showed that flow rate strongly influenced the behaviour of breakthrough curves and RF adsorption capacity. Further, breakthrough curves obtained using Thomas and Yoon–Nelson models agreed with the experimental data. Moreover, the absolute error analysis proved that Thomas model produced the most accurate predictive results (Zayyat and Suidan, 2018). It was also reported that aliphatic polyamides612 (PA612) fixed-bed adsorption column could remove EE2 from 10,700 bed volumes (24.1 L) of EE2 concentration (30 µg/L) to non-detectable levels by the HPLC analysis prior to column breakthrough. On increasing the concentration of EE2 by 10- and 100-fold, the treatment capacity reduced to 6600 bed volumes (14.9 L) and 3800 bed volumes (8.6 L), respectively before the column breakthrough. The results further reveal the efficiency and large treatment capacities of fixed-bed PA612 particles for the removal of EE2 from water on a continuous flow basis (Han *et al.*, 2012).

Table 3.18. Thomas constants for EE2 using BNMPTS and BNAPTES materials ([EE2]: 10.0 mg/L; Flow rate: 1.0 mL/min; pH: 4.0; Amount of solid loaded: 0.25/ or 0.50 g; Temperature: 25°C).

Amount of materials taken in column (g)	Thomas constants		Least square sum (s ²)
	q ₀ (mg/g)	K _T (L/min/mg)	
0.25g BNMPTS	17.07	8.32 X 10 ⁻⁴	3.1 X 10 ⁻²
0.50g BNMPTS	20.75	6.27 X 10 ⁻⁴	5.1 X 10 ⁻³
0.25g BNAPTES	11.23	1.23 X 10 ⁻³	1.1 X 10 ⁻²
0.50g BNAPTES	16.57	7.03 X 10 ⁻⁴	3.8 X 10 ⁻³

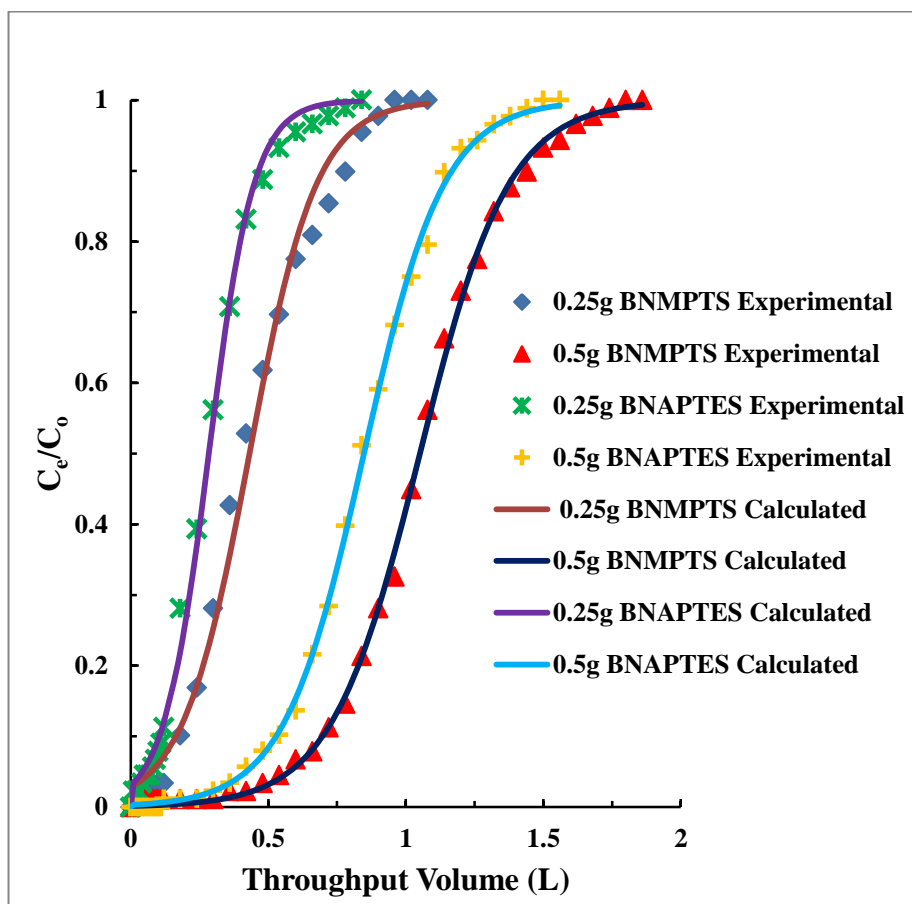


Figure 3.65: Breakthrough curves obtained for the removal of EE2 by BNMPTS and BNAPTES materials ([EE2]: 10.0 mg/L; Flow rate: 1.0 mL/min; pH: 4.0; Amount of solid loaded: 0.25/or 0.50 g; Temperature: 25°C).

3.5. Applications of BNMPTS and BNAPTES materials in real water sample

The removal of tetracycline, triclosan and EE2 using real matrix samples were conducted at different pH values. The physico-chemical analysis of river water was conducted and the results are shown in Table 3.19. Analytical results showed that river water contained with low levels of Fe, Mn, Ca, and Zn. But, the concentration of Ca is relatively high and found to be 0.51 mg/L. The concentration of Pb and Cu are negligible. The river water is also subjected to TOC analysis and the data showed that high value of non-purgeable organic carbon (NPOC) and remarkable quantity of inorganic carbon is present. Moreover, the sulphate (1.10 mg) and nitrates (2.0 mg/ L) are present in this water sample. River water sample was spiked with the tetracycline, triclosan and EE2 separately having the concentration of 10.0 mg/L. The pH of these solutions were adjusted and subjected for the removal of these pollutants employing these composite materials. The pH dependent removal efficiency of BNMPTS and BNAPTES is obtained and shown in Figure 3.66, 3.67 and 3.68, respectively for the tetracycline, triclosan and EE2. The percentage removal of these pollutants in purified water is also included in the figures for useful comparison. The results indicated that the removal efficiency of tetracycline, triclosan and EE2 using BNMPTS and BNAPTES in real water sample is not substantially affected compared to the purified water. Hence, the BNMPTS and BNAPTES show high selectivity and applicability for attenuation of tetracycline, triclosan and EE2 in real water sample. Therefore, materials show potential in its possible implications in the real water sample treatment at least for the elimination of these micro-pollutants (Awad *et al.*, 2019; Liu *et al.*, 2021; Shakerian *et al.*, 2020).

Table 3.19. Different parameters result obtained from real water sample.

Elements studied	mg/L
Fe	0.021
Zn	0.1
Mn	0.07
Ca	0.51
Pb	ND
Cu	ND
TOC analysis	mg/L
IC	1.45
NPOC	8.95
Anions studied	mg/L
Sulfate	1.10
Phosphate	0.08
Fluoride	ND
Nitrate	1.98

ND = NOT DETECTED

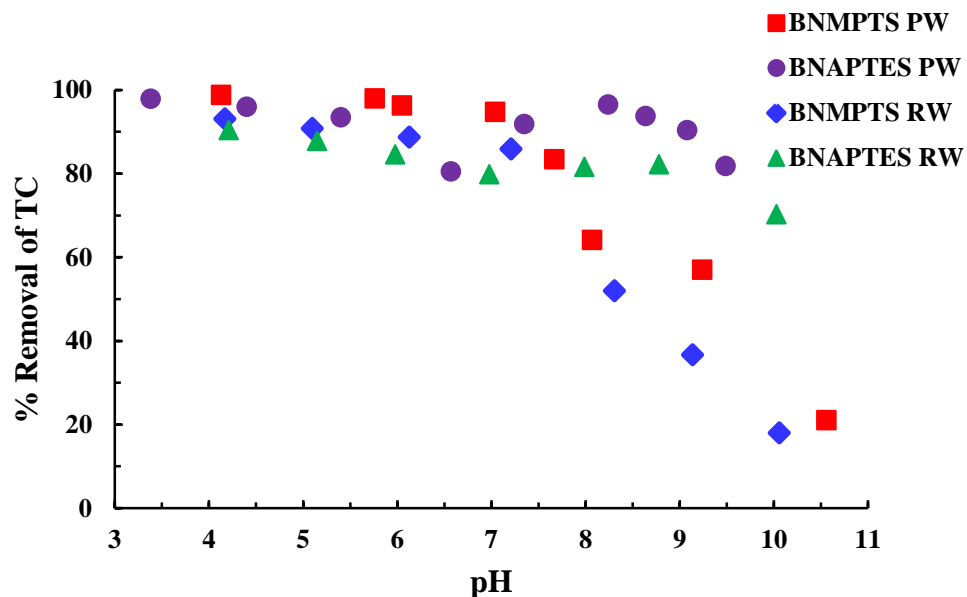


Figure 3.66: Removal of tetracycline in purified water (PW) and real water (RW) using BNMPTS and BNAPTES materials as a function of pH ([TC]: 10.0 mg/L; Solid dose: 2.0 g/L; Temperature: 25°C).

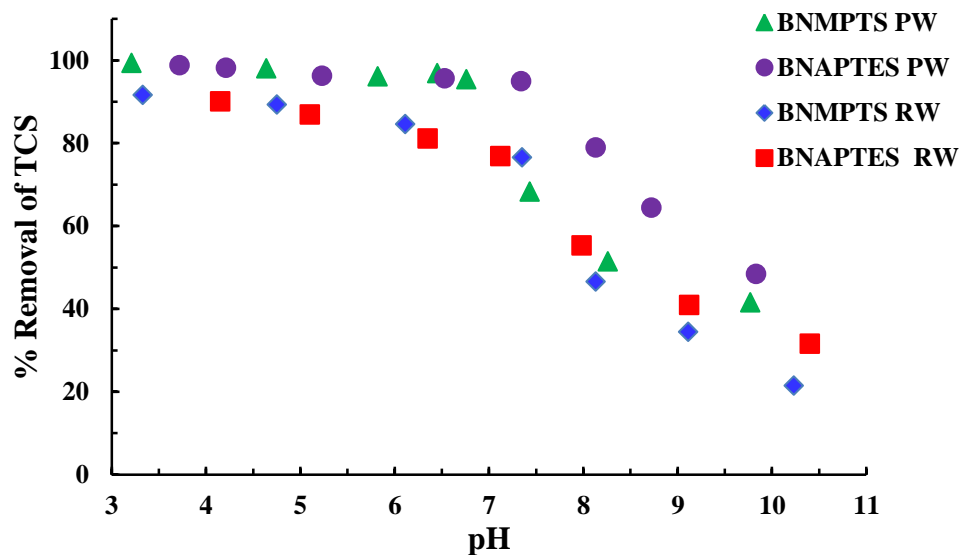


Figure 3.67: Removal of triclosan in purified water (PW) and real water (RW) using BNMPTS and BNAPTES materials as a function of pH ([TCS]: 10.0 mg/L; Solid dose: 2.0 g/L; Temperature: 25°C).

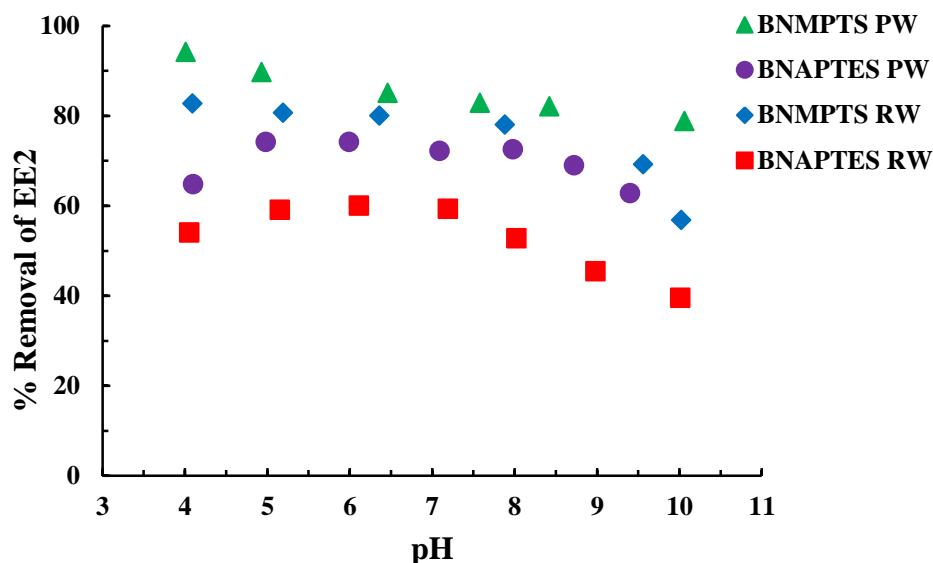


Figure 3.68: Removal of EE2 in purified water (PW) and real water (RW) using BNMPTS and BNAPTES materials as a function of pH ([EE2]: 10.0 mg/L; Solid dose: 2.0 g/L; Temperature: 25°C).

3.6. Desorption and reusability of the solids

It is important to find out the suitable eluent for desorption with appropriate concentrations which allow reusability of the adsorbent. It was found that 0.01 mol/L HCl is a suitable eluent to desorb the pre-adsorbed Cu(II) from BNMPTS, tetracycline, triclosan and EE2 from BNMPTS and BNAPTES solids. The percentage desorption of Cu(II) using 0.01 mol/L HCl from BNMPTS was found to be 98% within 60 minutes of contact. The reusability of BNMPTS for the removal of Cu(II) is graphically shown in Figure 3.69. It was found that the percentage removal of Cu(II) was found to decrease from 97.8 to 88.9% using BNMPTS while the material undergoes six replicates adsorption-desorption cycles. The decreased in the adsorption percentage might be due to the acid employed for desorption which may destruct the active sites of the solids (Unuabonah *et al.*, 2008). In other studies, the reusability of sodium alginate composite gel (SACL) was conducted with 0.05 mol/L HNO₃. The percentage removal of Cu(II) and Cd(II) by SACL were found to decreased from 96 to 85% and 73.9 to 60%, respectively after four adsorption-desorption cycles. These results further showed the strong reusability of SCAL for the removal of Cu(II) and Cd(II). On the other hand, the removal rates of metal ions

was decreased which may be due to the weight loss of SACL after four desorption cycles (Zhao *et al.*, 2020).

The percentage desorption of tetracycline using 0.01 mol/L HCl from BNMPTS and BNAPTES was found to be 96 and 97%, respectively within 60 minutes. The reusability of BNMPTS and BNAPTES for the removal of tetracycline is graphically shown in Figure 3.70. The percentage removal of tetracycline was decreased from 85.3 to 75.1% using BNMPTS and 82.4 to 73.1% using BNAPTES for six adsorption-desorption cycles. On the other hand, tetracycline ions were irreversibly bound to some adsorption sites on the surface of BNMPTS and BNAPTES. It resulted in certain adsorption sites being unavailable for tetracycline adsorption, as well as a reduction in adsorption percentage upon regeneration (Liu *et al.*, 2013). Previously, the reusability of activated carbon (TAC) for tetracycline was conducted using 0.05 mol/L NaOH eluent. The adsorption-desorption experiments showed that adsorption capacity of TAC was decreased from 98.57 mg/g to 53.80 mg/g at the end of five cycles of operations (Saygili and Guzel, 2016).

The percentage desorption of triclosan using 0.01 mol/L HCl from BNMPTS and BNAPTES was found to be 97 and 98%, respectively within 60 minutes. The reusability of BNMPTS and BNAPTES for the removal of triclosan is shown in Figure 3.71. Results showed that percentage removal of triclosan was decreased from 96.4 to 84.3% using BNMPTS and 96.1 to 84.2% using BNAPTES while the material was utilized for six cycles of adsorption-desorption. This might be because some active adsorption sites were lost when BNMPTS and BNAPTES were desorbed with 0.01 mol/L HCl (Maged *et al.*, 2020). The reusability of bentonite modified with dioctadecyldimethylammonium (2C18-BT) was performed using n-hexane as desorbing agent for five adsorption/desorption cycles for triclosan. It was found that more than 98% of triclosan was desorbed from 2C18-BT after washing with n-hexane. Triclosan was fully adsorbed and desorbed from 2C18-BT for the first cycle. The amount of triclosan adsorbed slightly decreased after subsequent adsorption/desorption cycles, however, the removal percentage was 98.7% after the fifth cycles. The quantity of residual triclosan increased slightly upon repeating the adsorption/washing cycles (Phuekphong *et al.*, 2020). In other study, it was reported that, the removal percentage of triclosan using chitosan/poly (vinyl alcohol)

(CS/PVA) composite nanofibrous membranes was above 67% after five regeneration cycles when treated with 95% ethyl alcohol for 240 minutes which revealed the good reusability of nanofibrous membranes (Liu and Xu, 2013).

Similarly, the percentage desorption of EE2 using 0.01 mol/L HCl from BNMPTS and BNAPTES were found to be 87 and 79%, respectively within 60 minutes of contact. The reusability of BNMPTS and BNAPTES for the removal of EE2 is shown in Figure 3.72. It was observed that percentage removal of EE2 was decreased from 82.8 to 60.7% using BNMPTS and 72.1 to 54.8% using BNAPTES while the materials were employed for six adsorption-desorption cycles. The reduction of removal rate might be due to the loss of irreversible occupation of partial-adsorption sites on the surface of BNMPTS and BNAPTES (Wang *et al.*, 2020b). Previously, it was also reported that, acetonitrile was used to desorb the pre-adsorbed 17 α -ethinylestradiol (EE2) onto montmorillonite intercalated with cetyltrimethylammonium cation (CTA⁺). Results showed that this material is favourably regenerated using acetonitrile and is reused without substantial loss of adsorption capacity even after five reuses. This was indicated that, perhaps, the cetyltrimethylammonium cation (CTA⁺) firmly attached to the clay structure and was not solubilized by the acetonitrile (Burgos *et al.*, 2016).

Therefore, these results indicated that BNMPTS and BNAPTES are suitable to reuse for removal of Cu(II), tetracycline, triclosan and EE2 without substantial loss in adsorption efficiency.

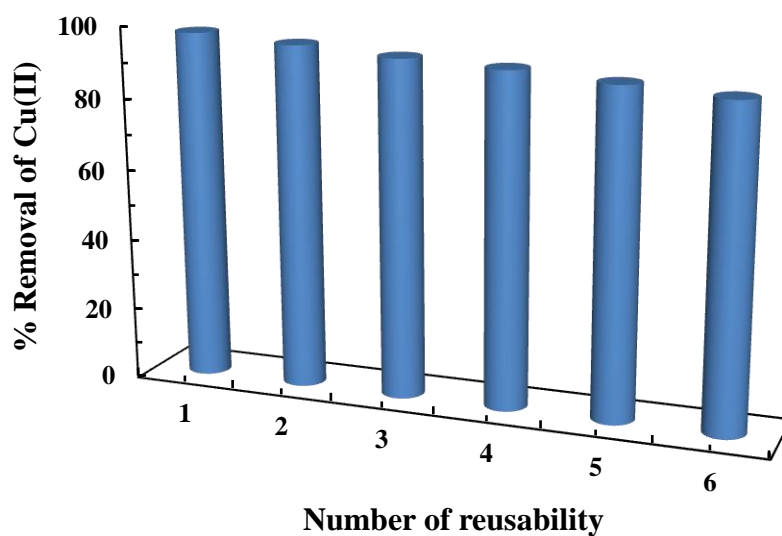


Figure 3.69: Reusability of BNMPTS for the removal of Cu(II) ([Cu(II)]:10.0 mg/L; Solid dose: 2.0 g/L; [HCL]: 0.01 mol/L; pH: 4.0).

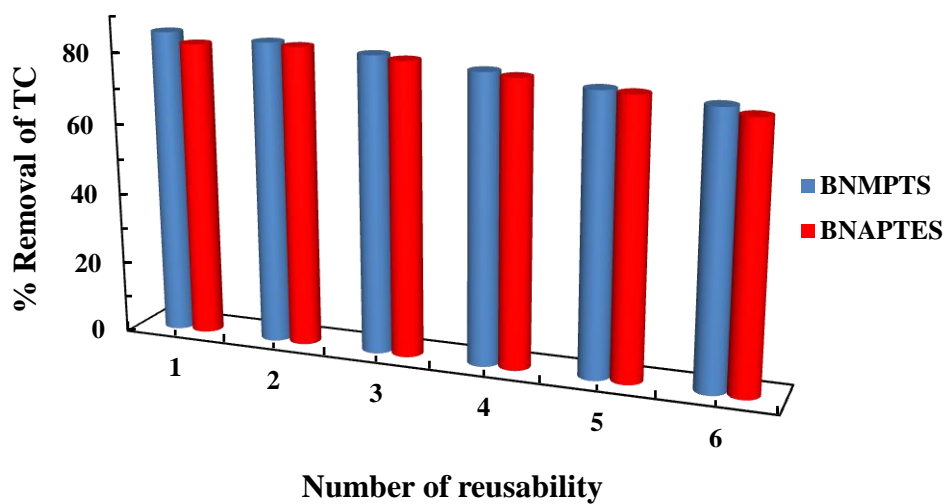


Figure 3.70: Reusability of BNMPTS and BNAPTES for the removal of tetracycline ([TC]:10.0 mg/L; Solid dose: 2.0 g/L; [HCL]: 0.01 mol/L; pH: 6.0).

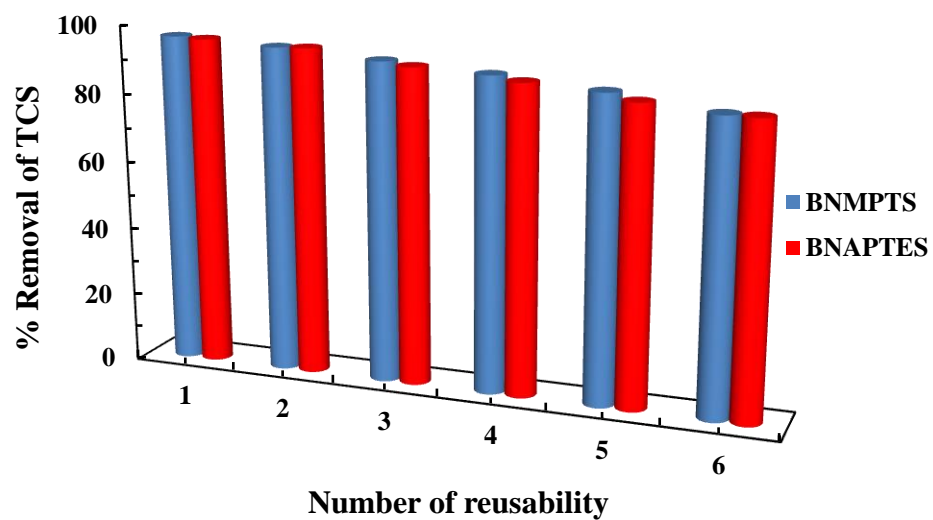


Figure 3.71: Reusability of BNMPTS and BNAPTES for the removal of triclosan ([TCS]:10.0 mg/L; Solid dose: 2.0 g/L; [HCL]: 0.01 mol/L; pH: 4.0).

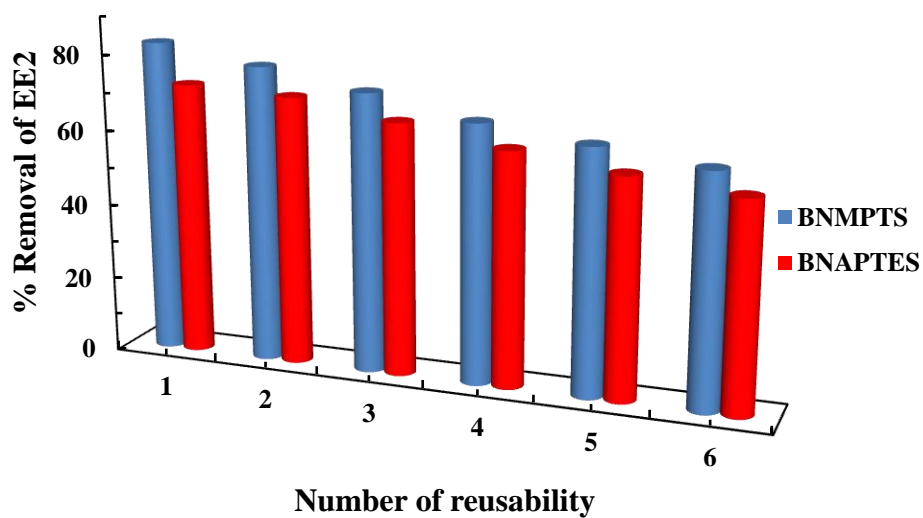


Figure 3.72: Reusability of BNMPTS and BNAPTES for the removal of EE2 ([EE2]:10.0 mg/L; Solid dose: 2.0 g/L; [HCL]: 0.01 mol/L; pH: 4.0).

CHAPTER - 4

CONCLUSIONS

4. CONCLUSIONS

The bentonite clay (BN) was grafted with the 3-mercaptopropyl trimethoxysilane (MPTS), and 3-aminopropyltriethoxysilane (APTES) to obtain the novel composite materials (BNMPTS and BNAPTES). The composite materials were obtained in a facile and single pot synthetic route conducted under the nitrogen atmosphere. Further these materials were employed in the removal of several heavy metal toxic ions along with some micro-pollutants from aqueous solutions under the batch and column reactor studies.

The BNMPTS and BNAPTES along with the pristine bentonite were characterized by the FT-IR (Fourier Transform Infrared) spectroscopy, FE-SEM (Field-Emission Scanning Electron Microscopic), TEM (Transmission Electron Spectroscopy) and XRD (X-ray Diffraction) analytical tools. The FT-IR results showed that the organosilane (3-mercaptopropyl trimethoxysilane and 3-aminopropyltriethoxysilane) were well incorporated within the clay network. The XRD data showed that the main mineral phase was montmorillonite since the characteristics diffraction peaks of montmorillonite were identified at 2θ value of 6.03° , 19.85° , 36.62° and 50° . Additionally, the XRD pattern also confirmed the existence of the smectite phase in all the solid samples. The TEM images showed a straight lattice fringe without defection for pristine bentonite and functionalized solids. Further, the basal spacing obtained for pristine clay and functionalized clay using TEM analyses were identical as that obtained by XRD analysis. The SEM images of raw bentonite and modified materials (BNMPTS and BNAPTES) showed heterogeneous and disordered surface structure. Furthermore, the porosity is significantly decreased in the modified samples compared to the raw bentonite which inferred that BNMPTS and BNAPTES molecules are incorporated within the pores of bentonite surface. This result is in a line with the textural properties obtained by BET surface area analyzer. Moreover, the composition of BN, BNMPTS and BNAPTES were obtained using energy-dispersive X-ray spectroscopy (EDX). Results showed that the sulphur and nitrogen peaks, which was not present in the EDX image of BN, were observed in the BNMPTS and BNAPTES EDX images, respectively. Therefore, this confirmed the grafting of MPTS and APTES molecules with the bentonite network.

The specific surface area, pore volume, and pore size of raw bentonite and composite solids were obtained using the Brunauer Emmett and Teller (BET) method. The BET result revealed that pristine bentonite and silane grafted bentonite samples exhibited type IV isotherm with H3 hysteresis loop which further confirmed that the solid materials possessed mesoporous surface structure. Moreover, the N₂ adsorption-desorption isotherm showed that a larger hysteresis loop with the pore size of 68.42 Å and pore volumes of 0.07 cm³/g was obtained for the pristine bentonite. On the other hand, the pore size and pore volume of BNMPTS and BNAPTES were found to be 237.91 Å, 0.03 cm³/g and 165.12 Å, 0.05 cm³/g, respectively. The BET specific surface area of BN, BNMPTS and BNAPTES were found to be 41.14, 4.64 and 12.50 m²/g, respectively. It is noteworthy that the modified samples exhibited significant reduction in the specific surface area after the functionalized with organo silanes. This result further confirmed that the pores on the surface of bentonite were occupied by the MPTS/or APTES molecules.

The functionalized materials along with the pristine bentonite clay were utilized in the removal of As(III) and As(V) under batch study. Similarly, the potential water pollutants viz., Cu(II), Cd(II), tetracycline (TC), triclosan (TCS) and 17 α -ethinylestradiol (EE2) were studied under the batch and column reactor operations extensively using these novel materials in the removal processes. The p*H*_{PZC} of the pristine bentonite (BN), BNMPTS and BNAPTES were found to be 7.81, 7.73 and 7.63, respectively. The sorption of As(III) using BNMPTS and As(V) using BNAPTES were conducted from pH 2.0 to 10.0. Higher percentage removal of As(III) and As(V) was achieved within pH range of 4.0 to 6.0 using the composite materials. The composite materials possessed significantly higher removal efficiency as compared to the pristine bentonite in the removal of As(III) and As(V). Increasing the sorptive concentration of As(III) and As(V), the percentage removal of these pollutants was decreased from 90 to 70% for As (III) by BNMPTS and 89 to 67% for As(V) BNAPTES. Increasing the background electrolyte concentrations from 0.0001 to 0.1 mol/L NaCl did not affect the percentage removal of As(III) and As(V) by these composite materials. The results indicated that As(III) and As(V) were aggregated with relatively stronger chemical forces and possibly forming an ‘inner sphere complexes’. The presence of co-existing ions (anions and cations) except

EDTA and phosphate did not affect the percentage removal of As(III) and As(V) using the functionalized materials. The uptake of As(III) and As(V) by the functionalized materials was rapid and an apparent sorption equilibrium was achieved at 120 and 180 minutes of contact for As(III) using BNMPTS and As(V) using BNAPTES materials, respectively. Further, the kinetic data were well fitted to the pseudo-second-order rate kinetics rather pseudo-first-order rate kinetics. The equilibrium state sorption data is reasonably fitted well to the Langmuir adsorption isotherms for As(III) and As(V). The high value of sorption capacity obtained for the As(III) and As(V) using the composite materials indicated high affinity of these pollutants towards the functionalized materials.

Similarly, the BNMPTS was successfully employed in the remediation of aqueous solutions contaminated with Cu(II) and Cd(II) under the batch and column reactor operations. The pH dependence sorption of Cu(II) and Cd(II) by BNMPTS was conducted in the pH range from 2.0 to 7.0 and 2.0 to 10.0, respectively. The result indicated that very high percentage uptake of Cu(II) and Cd(II) were achieved for BNMPTS and it is interesting to note that very high percentage uptake of Cu(II) and Cd(II) was almost unaffected with change in solution pH. Similarly, the increase in Cu(II) and Cd(II) concentrations (1.0 to 25.0 mg/L) could not affect the percentage removal of these two cations using the BNMPTS solid. Further, the equilibrium state sorption of Cu(II) and Cd(II) by the BNMPTS material was found to follow Langmuir adsorption isotherm model. The time dependent data showed that the uptake of Cu(II) and Cd(II) by the BNMPTS was fast and rapid and an apparent solid/solution equilibrium was achieved within 30 minutes of contact. The kinetic data is fitted well to the pseudo-second order kinetic model for both the pollutants using BNMPTS material. Increasing the concentration of background electrolyte (NaCl, 0.0001 to 0.1 mol/L), the percentage removal of Cu(II) and Cd(II) was not affected indicated that the composite material possessed a strong affinity towards Cu(II) and Cd(II) using BNMPTS. Similarly, the presence of several cations (Mg(II), Mn(II), Ca(II) and Ni(II)) and anions (oxalic acid, glycine and phosphate) did not affect the percentage removal of Cu(II) and Cd(II) using BNMPTS. This inferred that these co-existing ions did not interfere the sorption of Cu(II) and Cd(II) by BNMPTS. However, the percentage removal of Cu(II) and Cd(II) using the

BNMPTS was significantly affected in presence of EDTA. This was explicable due to the formation of strong complexes of Cu(II)/or Cd(II) with EDTA which were not sorbed strongly onto the surface of BNMPTS solid. The column reactor experiments result showed that very high breakthrough volume were obtained for the attenuation of Cu(II) and Cd(II) using 0.2 g and 0.5 g of the BNMPTS material. Moreover, the non-linear least square fitting were conducted using the Thomas equation and results indicated that very high loading capacity of Cu(II) and Cd(II) was achieved by the BNMPTS solid under the dynamic conditions; which further reaffirmed the affinity of BNMPTS towards the Cu(II) and Cd(II).

Furthermore, the BNMPTS and BNAPTES solids were effectively and efficiently employed in the elimination of micro-pollutants *viz.*, tetracycline, triclosan and EE2 from aqueous solutions under the batch and column reactor operations. The pH dependent studies for these micro-pollutants using the BNMPTS and BNAPTES materials were conducted at a wide range of pH ~3.0 to 10.0. The percentage uptake of tetracycline by BNMPTS was very high in the pH range 3.2 to 7.0 and decreased sharply and reached to a very low removal at pH 10. On the other hand, the percentage uptake of tetracycline by BNAPTES showed almost a constant removal efficiency up until the pH 7-8 and then a noticeably decrease was observed. However, the decrease in efficiency using the BNAPTES was not that significant for tetracycline even at pH>7.3. This further inferred the potential applicability of BNMPTS and BNAPTES towards the attenuation of tetracycline from aqueous solutions using these materials. The effect of pH in the removal of triclosan by raw bentonite showed very limited implications in the elimination of triclosan from aqueous solution. However, the uptake of triclosan by BNMPTS and BNAPTES was remained almost constant from pH 3.21 to 7.01 but further increase in pH (pH>7.0), caused significant decrease in the uptake of triclosan by these two composite materials. The removal of triclosan was almost unaffected using BNMPTS and BNAPTES as the pH was increased from *Ca.* pH 3.21 to 7.01. However, the removal of triclosan was decreased abruptly at pH>7.0 and attained to a very low removal percentage at pH ~10. Therefore, a high uptake of triclosan around neutral pH conditions is providing an optimum pH conditions indicating BNMPTS and BNAPTES in the treatment processes for efficient removal of triclosan from aqueous

at neutral pH conditions. The pH dependent study of EE2 showed that the uptake of EE2 by the BNMPTS and BNAPTES was increased significantly with an increase in pH from 3.0 to 10.0. The high uptake of micro-pollutants by the BNMPTS and BNAPTES materials at wide range of pH was demonstrated due to the hydrophobic interaction between the micro-pollutant molecules and BNMPTS/or BNAPTES solids. Moreover, the dense grafted structure of BNMPTS and BNAPTES has enabled to trap significantly the micro-pollutants from the aqueous solutions and enhanced the elimination of micro-pollutants. On the other hand, it was observed that the pristine bentonite showed significantly low sorption efficiency as compared to the composite solids viz., BNMPTS or BNAPTES. This further inferred the greater applicability of these novel solids in the removal of micro-pollutants from aqueous solutions.

The initial sorptive concentration dependent study of tetracycline, triclosan and EE2 showed that BNMPTS and BNAPTES exhibited strong affinity towards the removal of these micro-pollutants. Further, the sorption isotherm of these micro-pollutants was obtained from the concentration dependence data showed that the sorption equilibrium of these micro-pollutants followed Langmuir adsorption isotherm. The effect of contact time in the removal of these micro-pollutants showed that rapid uptake of these pollutants was achieved and apparent equilibrium between the solid/solution phase was obtained within 120 minutes of contact for triclosan and EE2 and 180 minutes for tetracycline using these two solids. The kinetic modelling was conducted for these pollutants and results showed that the uptake of these micro-pollutants by the BNMPTS or BNAPTES fitted well to the PSO model compared to the PFO model. The applicability of PSO model showed that the tetracycline, triclosan and EE2 were bound onto the surface of the BNMPTS and BNAPTES materials by relatively stronger forces. Increasing the background electrolyte concentrations of NaCl (1000 times) had unaffected the removal percentage of these micro-pollutants by the BNMPTS and BNAPTES solids. This further inferred that the tetracycline, triclosan and EE2 were forming 'inner-sphere-complexes' at surface of solids having relatively stronger forces. Similarly, the presence of diverse co-existing cations viz., Mg(II), Mn(II), Ca(II) and Ni(II) and anions viz., ethylenediaminetetraacetate (EDTA), oxalic acid, phosphate and glycine did not

affect the percentage uptake of these micro-pollutants except the presence of EDTA. The presence of EDTA significantly affected the removal of tetracycline, triclosan and EE2 using BNMPTS and BNAPTES.

The column reactor operations showed that very high breakthrough volumes were obtained for the elimination of these micro-pollutants using 0.25 g and 0.5 g of the BNMPTS or BNAPTES materials. Moreover, the break through data was utilized to the Thomas equation and the Thomas constants were estimated using the least square non-linear fitting of column data. Result showed that on increasing the amount of the modified solids in the column, an increased in the loading capacity of these pollutants was obtained by BNMPTS and BNAPTES under the continuous flow systems. This again reaffirmed greater affinity of these solids towards the tetracycline, triclosan and EE2.

Additionally, applicability of these novel materials in the removal of micro-pollutants viz., tetracycline, triclosan and EE2 in real matrix sample (River water samples) was conducted under varied pH values. Results showed that the removal of these micro-pollutants was not affected as compared to the results obtained with purified water. These results showed the selectivity of solids towards these micro-pollutants and possible implacability in real matrix treatment.

Furthermore, the reusability of BNMPTS in the removal of Cu(II) showed that the percentage removal of Cu(II) was decreased from 97.8 to 88.9% after six replicates of adsorption-desorption cycles. Moreover, the reusability of BNMPTS and BNAPTES for the removal of tetracycline, triclosan and EE2 showed that the percentage removal of tetracycline decreased from 85.3 to 75.1% using BNMPTS and 82.4 to 73.1% using BNAPTES. Similarly, the percentage removal of triclosan was decreased from 96.4 to 85.3% using BNMPTS and from 96.5 to 84.2% using BNAPTES. The percentage removal of EE2 was decreased from 82.8 to 60.7.3% using BNMPTS and from 72.1 to 54.8% using BNAPTES while the materials were intended for six replicates adsorption-desorption cycles. Therefore, the studies indicated that BNMPTS and BNAPTES possessed greater stability and could be reutilized for successive operations in the removal of Cu(II), tetracycline, triclosan and EE2 from aqueous solutions. The studies showed that the novel and, possibly cost-effective functionalized solids possessed reasonably good suitability and

selectively in the removal of several heavy metal toxic ions along with several micro-pollutants from aqueous solutions. The materials could be further employed in the large-scale treatment of wastewaters contaminated with these pollutants at least at the 'Pilot Scale' treatment and the treatment process would be, possibly, sustainable and extended applicability.

REFERENCES

- Abbas, S.H., Ismail, I.M., Mostafa, T.M., Sulaymon, A.H., (2014). Biosorption of heavy metals: A review. *J. Chem. Sci. Technol.*, **3**: 74-102.
- Abbasi, B., (2017). Removal of Dye by Biological Methods Using Fungi. *Int. J. Med. Rev.*, **4(4)**: 112-118.
- Abeywardena, S.B.Y., Parera, S., de Silva, K.M.N., Tissera, N.P., (2017). A facile method to modify bentonite nanoclay with silane. *Int. Nano. Lett.*, **7** : 237-241.
- Ahamad, T., Naushad, M., Al-Shahrani, T., Al-hokbany, N., Alshehri, S.M., (2020). Preparation of chitosan based magnetic nanocomposite for tetracycline adsorption: Kinetic and thermodynamic studies. *Int. J. Biol. Macromol.*, **147**: 258–267.
- Ahmed, M. J., Hameed, B. H., Hummadi, E. H., (2020). Review on recent progress in chitosan/chitin-carbonaceous material composites for the adsorption of water pollutants,” *Carbohydr. Polym.*, **247**:116690.
- Ahmed, M.J. (2016). Application of agricultural based activated carbons by microwave and conventional activations for basic dye adsorption: Review. *J. Environ. Chem. Eng.*, **4**: 89–99.
- Ahmed, M.J., Hameed, B.H., (2018). Removal of emerging pharmaceutical contaminants by adsorption in a fixed-bed column: A review. *Ecotoxicol. Environ. Saf.*, **149**: 257–266.
- Ainger, C., Butler, D., Caffor, I., Crawford–Brown, D., Helm, D., Stephenson, T., (2009). *A Low Carbon Water Industry in 2050 – Report: SC070010/R3*, Environment Agency, Bristol

- Akl, M.A.A., Dawy, M.B., Serage, A.A., (2014). Efficient removal of phenol from water samples using sugarcane bagasse based activated carbon. *J. Anal. Bioanal. Tech.*, **5**: 189.
- Alandis, N.M., Mekhamer, W., Aldayel, O., Hefne, J.A.A., Alam, M., (2019). Adsorptive applications of montmorillonite clay for the removal of Ag(I) and Cu(II) from aqueous medium. *J. Chem.*, **1-4**: 1–7.
- Ali, I., Asim, M., Khan, T.A., (2012). Low cost adsorbents for the removal of organic pollutants from wastewater, *J. Environ. Manage.*, **113**:170-183.
- Ali, I., Peng, C., Naz, I., (2019). Removal of lead and cadmium ions by single and binary systems using phytogenic magnetic nanoparticles functionalized by 3-mercaptopropanoic acid. *Chin. J. Chem. Eng.*, **27**: 949–964.
- Ali, M.E.M., Abd El-Aty, A.M., Badawy, M.I., Ali, R.K., (2018). Removal of pharmaceutical pollutants from synthetic wastewater using chemically modified biomass of green alga *Scenedesmus obliquus*. *Ecotoxicol. Environ. Saf.*, **151**: 144–152.
- Ali, S., Rizwan, M., Shakoor, M.B., Jilani, A., Anjum, R., (2020). High sorption efficiency for As(III) and As(V) from aqueous solutions using novel almond shell biochar. *Chemosphere*, **243**: 125330.
- Alimohammadi, M., Saeedi, Z., Akbarpour, B., Rasoulzadeh, H., Yetilmezsoy, K., Al-Ghouti, M.A., Khraisheh, M., McKay, G., (2017). Adsorptive Removal of Arsenic and Mercury from Aqueous Solutions by Eucalyptus Leaves. *Water. Air. Soil Pollut.*, **228**: 429.
- Alkaram, U.F., Mukhlis, A.A., Al-Dujaili, A.H., (2009). The removal of phenol from aqueous solutions by adsorption using surfactant–modified bentonite and kaolinite. *J. Hazard. Mater.*, **169**: 324–332.
- Al-Khaldi, F.A., Abu-Sharkh, B., Abulkibash, A.M., Qureshi, M.I., Laoui, T., Atieh, M.A. (2015). Effect of acid modification on adsorption of hexavalent chromium (Cr (VI)) from aqueous solution by activated carbon and carbon nanotubes. *Desalin. Water Treat.*, **57**: 7232–7244.

- Al-Khateeb, L.A., Obaid, A.Y., Asiri, N.A., Abdel Salam, M., (2014). Adsorption behavior of estrogenic compounds on carbon nanotubes from aqueous solutions: Kinetic and thermodynamic studies. *J. Ind. Eng. Chem.*, **20**: 916–924.
- Al-Lagtah, N., Saud, A.A., Albadarin, A., Salameh, Y., Walker, G., Allen, S., Ahmad, M., (2011). The Removal of Heavy Metals from Aqueous Solutions by Commercial Activated Carbon, in: *World Environmental and Water Resources Congress: Bearing Knowledge for Sustainability*. pp. 3402–3411.
- Altun, T., Pehlivan, E., (2007). Removal of Copper(II) Ions from Aqueous Solutions by Walnut-, Hazelnut- and Almond-Shells. *Clean (Weinh)*, **35**: 601–606.
- Altundoğan, H.S., Altundoğan, S., Tümen, F., Bildik, M., (2002). Arsenic adsorption from aqueous solutions by activated red mud. *Waste Manage.*, **22**: 357–363.
- Amari, T., Ghnaya, T., Abdelly, C., (2017). Nickel, cadmium and lead phytotoxicity and potential of halophytic plants in heavy metal extraction. *S. Afr. J. Bot.*, **111**:99–110.
- Ameh, T., Sayes, C.M., (2019). The potential exposure and hazards of copper nanoparticles: A review. *Environ. Toxicol., Pharmacol.*, **71**: 103220.
- Amen, R., Yaseen, M., Mukhtar, A., Klemeš, J.J., Saqib, S., Ullah, S., Al-Sehemi, A.G., Rafiq, S., Babar, M., Fatt, C.L., Ibrahim, M., Asif, S., Qureshi, K.S., Akbar, M.M., Bokhari, A., (2020). Lead and cadmium removal from wastewater using eco-friendly biochar adsorbent derived from rice husk, wheat straw, and corncob. *Clean. Eng. Technol.*, **1**: 100006.
- Anastopoulos, I., Bhatnagar, A., Hameed, B.H., Yong, S.O., Omirou, M., (2017). A review on waste-derived adsorbents from sugar industry for pollutant removal in water and wastewater. *J. Mol. Liq.*, **240**: 179–188.
- Anastopoulos, I., Kyzas, G.Z., (2014). Agricultural peels for dye adsorption: A review of recent literature. *J. Mol. Liq.*, **200**: 381–389.
- Anayurt, R. A.; Sari, A.; Tuzen, M., (2009). Equilibrium, thermodynamic and kinetic studies on biosorption of Pb (II) and Cd (II) from aqueous solution by

- macrofungus (*Lactarius scrobiculatus*) biomass. *Chem. Eng. J.*, **151**: 255–261.
- Anjum, H., Johari, K., Gnanasundaram, N., Ganesapillai, M., Arunagiri, A., Regupathi, I., Thanabalan, M., (2019). A review on adsorptive removal of oil pollutants (BTEX) from wastewater using carbon nanotubes. *J. Mol. Liq.*, **277**: 1005–1025.
- Antonini, L.G., Luder, H.U., (2011) Discoloration of teeth from tetracyclines – even today? *Schweiz Monatsschr Zahnmed.*, **121(5)**: 414–431.
- Aprile, A., and De Bellis, L., (2020). Editorial for Special Issue “Heavy Metals Accumulation, Toxicity, and Detoxification in Plants”. *Int. J. Mol. Sci.*, **21(11)**: 4103.
- Aragaw, T. A., (2020). Functions of various bacteria for specific pollutants degradation and their application in wastewater treatment: a review. *Int. J. Environ. Sci. Technol.*, **18**: 2063–2076.
- Aranami, K., Readman, J.W., (2007). Photolytic degradation of triclosan in freshwater and seawater, *Chemosphere*, **66**: 1052–1056.u
- Arbabi, M., Golshani, N., (2016). Removal of copper ions Cu (II) from industrial wastewater: A review of removal methods. *Int. J. Epidemiol.*, **3**: 283-293.
- Aroke, U.O., El-Nafaty, U., (2014). XRF, XRD and FTIR properties and characterization of HDTMA-Br surface modified organokaolinite clay, *Inter. J. Emerg. Technol. Adv. Eng.*, **4**: 817–825.
- Asgari, M., Sundararaj, U., (2017). Silane functionalization of sodium montmorillonite nanoclay: The effect of dispersing media on intercalation and chemical grafting. *Appl. Clay Sci.*, **153** : 228–238.
- Asha, K.K., Sankar, T.V., Viswanathan Nair, P.G., (2007). Effect of tetracycline on pancreas and liver function of adult male albino rats. *J. Pharm. Pharmacol.*, **59**: 1241–1248.
- Assis, S., Warri, A., Cruz, M.I., Laja, O., Tian, Y., Zhang, B., Wang, Y., Huang, T.H-M., Hilakivi-Clarke, L., (2012). High-fat or ethinyl-oestradiol intake

- during pregnancy increases mammary cancer risk in several generations of offspring. *Nat. Commun.*, **3**: 1053.
- Atkinson, S.K., Marlatt, V.L., Kimpe, L.E., Lean, D.R.S., Trudeau, V.L., Blais, J.M., (2012). The occurrence of steroidal estrogens in south–eastern Ontario wastewater treatment plants. *Sci. Total Environ.*, **430**: 119–125.
- Awad, A.M., Shaikh, S.M.R., Jalab, R., Gulied, M.H., Nasser, M.S., Benamor, A., Adham, S., (2019). Adsorption of organic pollutants by natural and modified clays: A comprehensive review. *Sep. Purif. Technol.*, **228**: 115719.
- Azizian, S., (2004). Kinetic models of sorption: a theoretical analysis. *J. Colloid Interf. Sci.*, **276**: 47–52.
- Balarak, D., Mahdavi, Y., Mostafapour, F., (2016). Application of Alumina-coated Carbon Nanotubes in Removal of Tetracycline from Aqueous Solution. *Br. J. Pharm. Res.*, **12**: 1–11.
- Balouch, A., Kolachi, M., Talpur, F.N., Khan, H., Bhanger, M.I., (2013). Sorption Kinetics, Isotherm and Thermodynamic Modeling of Defluoridation of Ground Water Using Natural Adsorbents. *Am. J. Anal. Chem.*, **04**: 221–228.
- Banerjee, S., Chattopadhyaya, M.C., (2017). Adsorption characteristics for the removal of a toxic dye, tartrazine from aqueous solutions by a low cost agricultural by-product. *Arab. J. Chem.*, **10**: S1629-S1638.
- Barakat, M.A., Schmidt, E., (2010). Polymer-enhanced ultrafiltration process for heavy metals removal from industrial wastewater. *Desalination*, **256**: 90–93.
- Barbooti, M.M., Su, H., Punamiya, P., Sarkar, D., (2014). Oxytetracycline sorption onto Iraqi montmorillonite. *Int. J. Environ. Sci. Technol.*, **11**: 69–76.
- Barkat, M., Chegrouche, S., Mellah, A., Bensmain, B., Nibou, D., Boufatit, M., (2014). Application of Algerian Bentonite in the Removal of Cadmium (II) and Chromium (VI) from Aqueous Solutions. *J. Surf. Eng. Mater. Adv. Technol.*, **04**: 210–226.
- Bashir, A., Malik, L.A., Ahad, S., Manzoor, T., Bhat, M.A., Dar, G. N., Pandith, A.H., (2019). Removal of heavy metal ions from aqueous system by ion-exchange and biosorption methods. *Environ. Chem. Lett.*, **17**: 729–754.

- Bazrafshan, E., Mostafapour, F.K., Hosseini, A.R., Khorshid, A.R., Mahvi, A.H., (2013). Decolorisation of reactive red 120 dye by using single-walled carbon nanotubes in aqueous solutions. *J. Chem.*, p. 8. ISSN: 2090-9063.
- Behera, S.K., Oh, S.-Y., Park, H.-S., (2010). Sorption of triclosan onto activated carbon, kaolinite and montmorillonite: Effects of pH, ionic strength, and humic acid. *J. Hazard. Mater.*, **179**: 684–691.
- Behilil, A., Lancene, D., Zahraoui, B., Belhachemi, M., Benmehdi, H., Choukchou-Braham, A., (2020). Natural and Modified Clays for the Removal of Cationic Dye from Water. *Environ. Clim. Technol.*, **24**: 562–579.
- Belhadri, M., Sassi, M., Bengueddach, A., (2019). Preparation of Economical and Environmentally Friendly Modified Clay and Its Application for Copper Removal. *J. Water. Chem. Technol.*, **41**: 357–362.
- Bendezu, Y., Fuentes, W.S., (2019). Use of nanoclay as an adsorbent to remove Cu(II) from Acid Mine Drainage (AMD). *Chem. Eng. Trans.*, **73**: 241-246.
- Benhamou, A., Basly, J.P., Baudu, M., Derriche, Z., Hamacha, R., (2013). Amino-functionalized MCM-41 and MCM-48 for the removal of chromate and arsenate. *J. Colloid Interface Sci.*, **404**: 135-139.
- Bergaya F., Theng B.K.G., Lagaly G., (2006). **Handbook of Clay Science**, (First Edition).
- Bernal, V., Giraldo, L., Moreno-Piraján, J.C., (2018). Physicochemical properties of activated carbon: their effect on the adsorption of pharmaceutical compounds and adsorbate–adsorbent interactions. *C—Journal Carbon Res.*, **4**: 62.
- Bertuoli, P.T., Piazza, D., Scienza, L.C., Zattera, A.J., (2014). Preparation and characterization of montmorillonite modified with 3-aminopropyltriethoxysilane. *Appl. Clay Sci.*, **87**: 46–51.

- Bhatnagar, A., Sillanpää, M., (2010). Utilization of agro-industrial and municipal waste materials as potential adsorbents for water treatment— A review. *Chem. Eng. J.*, **157**: 277–296.
- Bhatnagar, A., Sillanpää, M., Witek-Krowiak, A., (2015). Agricultural waste peels as versatile biomass for water purification—A review. *Chem. Eng. J.*, **270**: 244–271.
- Bhattacharyya, K.G., Gupta, S.S., (2008). Adsorption of a few heavy metals on natural and modified kaolinite and montmorillonite: A review. *Adv. Colloid Interf. Sci.*, **140**: 114–131.
- Bilal, M., Shah, J.A., Ashfaq, T., Gardazi, S.M.H., Tahir, A.A., Pervez, A., Haroon, H., Mahmood, Q., (2013). Waste biomass adsorbents for copper removal from industrial wastewater- A review. *J. Hazard. Mater.*, **263**: 322–333.
- Bodzek, M., (2015). Membrane technologies for the removal of micropollutants in water treatment, in: *Advances in Membrane Technologies for Water Treatment*. Elsevier, pp. 465–517.
- Bost, M., Houdart, S., Oberli, M., Kalonji, E., Huneau, J-F., Margaritis, I., (2016). Dietary copper and human health: Current evidence and unresolved issues. *J. Trace. Elem. Med. Biol.*, **35**:107-115.
- Bourliva, A., Michailidis, K., Sikalidis, C., Filippidis A., Betsiou, M., (2015). Adsorption of Cd(II), Cu(II), Ni(II) and Pb(II) onto natural bentonite: study in mono- and multi-metal systems. *Environ. Earth. Sci.*, **73**: 5435-5444.
- Boyacı, E., Çağır, A., Shahwan, T., Eroğlu, A.E., (2011). Synthesis, characterization and application of a novel mercapto- and amine-bifunctionalized silica for speciation/sorption of inorganic arsenic prior to inductively coupled plasma mass spectrometric determination. *Talanta*, **85**: 1517–1525.
- Briffa, J., Sinagra, E., Blundell, R., (2020). Heavy metal pollution in the environment and their toxicological effects on humans. *Heliyon*, **9(6)**: e04691
- Brinzila, C.I., Pacheco, M.J., Ciriaco, L., Ciobanu, R.C., Lopes, A., (2011) Electro degradation of tetracycline on BDD anode. *Chem. Eng. J.*, **209**: 54–61.
- Bui, T.X., Kang, S.Y., Lee, S.H., Choi, H., (2011). Organically functionalized mesoporous SBA-15 as sorbents for removal of selected pharmaceuticals from water. *J. Hazard. Mater.*, **193**: 156-163.

- Burgos, A.E., Ribeiro-Santos, T.A., Rochel M. Lago, R.M., (2016). Adsorption of the harmful hormone ethinyl estradiol inside hydrophobic cavities of CTA+ intercalated montmorillonite. *Water Sci.Technol.*, **74(3)**: 663–671.
- Burham, N., Sayed, M., (2016). Adsorption behavior of Cd²⁺ and Zn²⁺ onto natural egyptian bentonitic clay. *Minerals*, **6(4)**: 129.
- Butt, H.J., Graf, K., Kappl, M., (2013). Physics and chemistry of interfaces. John Wiley & Sons. DOI:10.1002/3527602313.
- Cargouet, M., Perdiz, D., Mouatassim–Souali, A., Tamisier–Karolak, S., Levi, Y., (2004). Assessment of river contamination by estrogenic compounds in Paris area (France). *Sci. Total Environ.*, **324**: 55–66.
- Carvalho, W.A., Carolina Vignado, C., Fontana, J., (2008). Ni(II) removal from aqueous effluents by silylated clays. *J. Hazard. Mater.*, **153**: 1240–1247.
- Chang, P.H., Li, Z., Jean, J.S., Jiang, W.T., Wang, C.J., Lin, K.H., (2012). Adsorption of tetracycline on 2:1 layered non-swelling clay mineral illite. *Appl.Clay.Sci.*, **67–68**: 158–163.
- Chang, P.H., Li, Z., Jiang, W.H., Kuo, C.Y., Jean, J.S., (2014). Adsorption of tetracycline on montmorillonite: influence of solution pH, temperature, and ionic strength. *Desalination Water Treat.*, **55(5)**: 1380-1392.
- Chen, B., Zhao, H., Chen, S., Long, F., Huang, B., Yang, B., Pan, X., (2019). A magnetically recyclable chitosan composite adsorbent functionalized with EDTA for simultaneous capture of anionic dye and heavy metals in complex wastewater. *Chem. Eng. J.*, **356**: 69–80.
- Chen, C.Y., Chang, T.H., Kuo, J.T., Chen, Y.F., Chung, Y.C., (2008). Characteristics of molybdate-impregnated chitosan beads (MICB) in terms of arsenic removal from water and the application of a MICB-packed column to remove arsenic from wastewater. *Bioresour. Technol.*, **99**: 7487–7494.
- Chen, H., Zhao, J., Zhong, A., Jin, Y., (2011). Removal capacity and adsorption mechanism of heat-treated palygorskite clay for methylene blue. *Chem. Eng. J.*, **174** :143- 150.

- Chen, Y., Gao, J., Wen, X., Wu, W., (2016a). Efficient removal of cadmium using facile functionalized of mesoporous silica via a biomimetic coating. *RSC Adv.*, **6**: 18340–18347.
- Chen, Y., Wang, F., Duan, L., Yang, H., Gao, J., (2016b). Tetracycline adsorption onto rice husk ash, an agricultural waste: Its kinetic and thermodynamic studies. *J. Mol. Liq.*, **222**: 487–494.
- Chon, K., Kyong Shon, H., Cho, J., (2012). Membrane bioreactor and nanofiltration hybrid system for reclamation of municipal wastewater: Removal of nutrients, organic matter and micro-pollutants. *Bioresour. Technol.*, **122**: 181–188.
- Cui, H., Q, Yan., Li, Q., Wei. Z., (2013). Fast removal of Hg(II) ions from aqueous solution by amine-modified attapulgite. *Appl. Clay Sci.*, **72**: 84-90.
- Dai, C.M., Zhang, J., Zhang, Y.L., Zhou, X.F., Duan, Y.P., Liu, S.G., (2012). Selective removal of acidic pharmaceuticals from contaminated lake water using multi-templates molecularly imprinted polymer. *Chem. Eng. J.*, **211–212**: 302.
- Dai, J., Meng, X., Zhang, Y., Huang, Y., (2020a). Effects of modification and magnetization of rice straw derived biochar on adsorption of tetracycline from water. *Bioresour. Technol.*, **311**: 123455.
- Dai, Y., Liu, M., Li, J., Yang, S., Sun, Y., Wang, W., Lu, L., Zhang, K., Xu, J., Zheng, W., Hu, Y., Tang, Y., Gao, Y., Liu, Z., (2020b). A review on pollution situation and treatment methods of tetracycline in groundwater. *Sep. Sci. Technol.*, **55**: 1005-1021.
- D'Amico, D.A., Ollier, R.P., Alvarez, V.A., Schroeder, W.F., Cyras, V.P., (2014). Modification of bentonite by combination of reactions of acid-activation, silylation and ionic exchange. *Appl. Clay Sci.*, **99** : 254-260.
- Daniel, L.M., Frost, R.L., Zhu, H.Y., (2008). Edge-modification of laponite with dimethyloctylmethoxysilane. *J. Colloid Interf. Sci .*, **321**: 302–309.

- Danouche, M., El Arroussi, H., Bahafid, W., El Ghachtouli, N., (2021). An overview of the biosorption mechanism for the bioremediation of synthetic dyes using yeast cells. *Environ. Technol. Rev.*, **10**: 58–76.
- Dawodu, F.A., Akpomie, K.G., (2014). Kinetic, equilibrium, and thermodynamic studies on the adsorption of cadmium (II) ions using “Aloji kaolinite” mineral. *The Pacific J. Sci. Technol.*, **15**: 268–276.
- De Gisi, S., Lofrano, G., Grassi, M., Notarnicola, M., (2016). Characteristics and adsorption capacities of low-cost sorbents for wastewater treatment: A review. *Sustain. Mater. Technol.*, **9**: 10–40.
- de Romana, D.L., Olivares, M., Uauy, R., Araya, M., (2011). Risks and benefits of copper in light of new insights of copper homeostasis. *J. Trace Elem. Med. Biol.*, **25**: 3–13.
- De Wit, M., Keil, D., van der Ven, K., Vandamme, S., Witters, E. and De Coen, W. (2010). An integrated transcriptomic and proteomic approach characterizing estrogenic and metabolic effects of 17 α -ethinylestradiol in zebrafish (*Danio rerio*). *Gen. Comp. Endocrinol.*, **167**: 190-201.
- Demirbas, A., (2008). Heavy metal adsorption onto agro-based waste materials: a review. *J. Hazard. Mater.*, **157**: 220–229.
- Deng, L., Su, Y., Su, H., Wang, X., Zhu, X., (2006). Biosorption of copper (II) and lead (II) from aqueous solutions by nonliving green algae *Cladophora fascicularis*: Equilibrium, kinetics and environmental effects. *Adsorption*, **12**: 267–277.
- Dhillon, G.S., Kaur, S., Pulicharla, R., Brar, S.K., Cledon, M., Verma, M., Surampalli, R.Y., (2015). Triclosan: Current Status, Occurrence, Environmental Risks and Bioaccumulation Potential. *Int. J. Environ. Res. Public Health.*, **12**: 5657-5684.
- Dogan, M., Turhan, Y., Alkan, M., Namli, H., Turan, P., Demibraz, O., (2008). Functionalized sepiolite for heavy metal ions adsorption. *Desalination*, **230**: 248–268.

- Dogan, M., Türkyilmaz, A., Alkan, M., Demyrbaş, O., (2009). Adsorption of copper (II) ions onto sepiolite and electrokinetic properties. *Desalination*, **238**: 257–270.
- Dong, Y., M., Song, Z., Qiu, W., (2019). Adsorption mechanism of As(III) on polytetrafluoroethylene particles of different size. *Environ. Pollut.*, **254**: 112950.
- Dou, R., Zhang, J., Chen, Y., Feng, S., (2017). High efficiency removal of triclosan by structure-directing agent modified mesoporous MIL-53(Al). *Environ. Sci. Pollut. Res.*, **24**: 8778–8789.
- Duan, J., Lu, D., Chen, R., D, Y., Wang, L., Gao, L., Pan, S., (2010). Synthesis of a novel flocculant on the basis of crosslinked Konjac glucomannan-graft-polyacrylamide-co-sodium xanthate and its application in removal of Cu^{2+} ion. *Carbohydr. Polym.*, **80(2)**: 436-441.
- Durán-Álvarez. J.C., Prado-Pano, B., Jiménez-Cisneros, B., (2012). Sorption and desorption of carbamazepine, naproxen and triclosan in a soil irrigated with raw wastewater: Estimation of the sorption parameters by considering the initial mass of the compounds in the soil. *Chemosphere*. **88**: 84.
- Dwivedi, A.K., (2017). Researches in water pollution: A review. *Int. Res. J. Nat. Sci.*, **4(1)**: ISSN: (2349-4077).
- Eckenfelder, W.W., Cleary, J.G., (2013). Activated sludge technologies for treating industrial wastewaters: Design and troubleshooting: DEStech Publications, Inc.
- Edelstein, M., Ben-Hur, M., (2018). Heavy metals and metalloids: Sources, risks and strategies to reduce their accumulation in horticultural crops. *Sci. Hortic.*, **234**: 431-444.
- El, A.K., (2018). Adsorption of cadmium and copper onto natural clay: Isotherm, kinetic and thermodynamic studies. *Glob. Nest. J.*, **20(2)**: 198-207.

- El-Bindary, A.A., El-Sonbati, A.Z., Shoair, A.F., Mohamed, A.S., (2015). Adsorptive removal of hazardous azorhodanine dye from an aqueous solution using rice straw fly ash. *J. Mater. Environ. Sci.*, **6 (6)**: 1723–1732.
- El-Ghonemy, A.M.K., (2012). Fresh water production from/by atmospheric air for arid regions, using solar energy :Review. *Renew. Sustain. Energy Rev.*, **16**: 6384–6422.
- Engwa, G.A., Ferdinand, P.U., Nwalo, F.N., Unachukwu, M.N., (2019). Mechanism and Health Effects of Heavy Metal Toxicity in Humans. *Poisoning in the modern world-new tricks for an old dog*, **10**: 1-23.
- Escudero-Oñate, C., Martínez-Francés, E., (2018). A Review of Chitosan-Based Materials for the Removal of Organic Pollution from Water and Bioaugmentation, in: Dongre, R.S. (Ed.), *Chitin-Chitosan - Myriad Functionalities in Science and Technology*. InTech. DOI: [10.5772/intechopen.76540](https://doi.org/10.5772/intechopen.76540).
- Ezzeddine, Z., Batonneau-Gener, I., Pouilloux, Y., Hamad, H., Saad, Z., Kazpard, V., (2015). Divalent heavy metals adsorption onto different types of EDTA-modified mesoporous materials: Effectiveness and complexation rate. *Microporous and Mesoporous Mater.*, **212**: 125–136.
- Feng, Y., Zhang, Z., Gao, P., Su, H., Yu, Y., Ren, N., (2010). Adsorption behavior of EE2 (17 α -ethinylestradiol) onto the inactivated sewage sludge: Kinetics, thermodynamics and influence factors. *J. Hazard. Mater.*, **175**: 970–976.
- Ferdous, A., Maisha, N., Sultana, N., Ahmed, S., (2016). Removal of heavy metal from industrial effluents using Baker's yeast. International conference on mechanical engineering: Proceedings of the 11th international conference on mechanical engineering (ICME 2015), Dhaka, Bangladesh, p. 060011.
- Fernandez, Y., Maranon, E., Castrillon, L., Vazquez, I., (2005). Removal of Cd and Zn from inorganic industrial waste leachate by ion exchange. *J. Hazard. Mater.*, **126**: 169-75.

- Fiss, E.M., Rule, K.L., Vikesland, P.J., (2007). Formation of chloroform and other chlorinated byproducts by chlorination of triclosan-containing antibacterial products. *Environ. Sci. Technol.*, **41**: 2387–2394.
- Foo, K.Y., Hameed, B.H., (2010). Insights into the modeling of adsorption isotherm systems. *Chem. Eng. J.*, **156**: 2–10.
- Fosshage, M., (2014). A new wastewater treatment technology for developing countries. *Filtr. Sep.*, **51**: 14–17.
- Fu, F., Wang, Q., (2011). Removal of heavy metal ions from wastewaters: a review. *J. Environ. Manage.*, **92**: 407–418.
- Futalan, C.M., Kan, C.C., Dalida, M.L., Pascua, C., Wan M.W., (2011). Fixed-bed column studies on the removal of copper using chitosan immobilized on bentonite. *Carbohydr. Polym.*, **83**: 697–704.
- Gao, H., Song, Z., Zhang, W., Yang, X., Wang, X., Wang, D., (2016). Synthesis of highly effective adsorbents with waste quenching blast furnace slag to remove methyl orange from aqueous solution. *J. Environ. Sci.*, **53**: 68–77.
- Gao, P., Yang, C., Liang, Z., Wang, W., Zhao, Z., Hu, B., Cui, F., (2019). N-propyl functionalized spherical mesoporous silica as a rapid and efficient adsorbent for steroid estrogen removal: Adsorption behaviour and effects of water chemistry. *Chemosphere*, **214**: 361–370.
- Genchi, G., Sinicropi, M.S., Lauria, G., Carocci, A., Catalano, A., (2020). The effects of cadmium toxicity. *Int. J. Environ. Res.*, **17(11)**: 3782.
- Ghasemi, Z., Sourinejad, I., Kazemian, H., Rohani, S., (2016). Application of zeolites in aquaculture industry: a review. *Rev. Aquac.*, **10**: 75–95.
- Ghosh, S.K., Bandyopadhyay, A., (2016). Characterizing acidic fly ash with and without biomass combustion residue for adsorptive removal of crystal violet with optimization of mixed adsorbent by response surface modeling. *Environ. Earth Sci.*, **75**: 820.
- Gilberto, T.J., Marçal, L., Silva, J.M., Rocha, L.A., Ciuffi, K.J., Faria, E.H., Nassar, E.J., (2016). Hybrid materials based on bentonite functionalized with amine groups via the hydrolytic sol-gel method. *J. Braz. Chem. Soc.*, **27**: 933–940.

- Gleick, P.H., (1993). *Water in Crisis: A Guide to the World's Freshwater Resources*. Oxford University Press Inc., 198 Madison Avenue, New York.
- Gong, X.J., Li, W.G., Zhang, D.Y., Fan, W.B., Zhang, X.R., (2015). Adsorption of arsenic from micro-polluted water by an innovative coal-based mesoporous activated carbon in the presence of co-existing ions. *Int. Biodeterior. Biodegrad.*, **102**: 256–264.
- Gopal, G., Alex, S.A., Chandrasekaran, N., Mukherjee, A., (2020). A review on tetracycline removal from aqueous systems by advanced treatment techniques. *RSC Adv.*, **10**: 27081.
- Greenlee, L.F., Lawler, D.F., Freeman, B.D., Marrot, B., Moulin, P., (2009). Reverse osmosis desalination: Water sources, technology, and today's challenges. *Water Res.*, **43**: 2317–2348.
- Guerra, D.L., Santos, M.R.M.C., Airoidi, C., (2009). Mercury adsorption on natural and organofunctionalized smectites - Thermodynamics of cation removal. *J. Braz. Chem. Soc.*, 20(4): 594-603.
- Guimaraes, A.M.F., Cimineli, V.S.T., Vasconcelos, W.L., (2009). Smectite organofunctionalized with thiol groups for adsorption of heavy metal ions. *Appl. Clay Sci.*, **42** : 410–414.
- Gundersen, P., Steinnes, E., (2003). Influence of pH and TOC concentration on Cu, Zn, Cd and Al speciation in rivers, *Water Res.*, **37**: 307–318.
- Gupta, A., Balomajumder, C., (2015). Removal of Cr(VI) and phenol from binary solution using *Bacillus sp.* immobilized onto tea waste biomass. *J. Water Process Eng.*, **6**: 1–10.
- Gupta, A., Yunus, M., Sankararamakrishnan, N., (2012). Zerovalent iron encapsulated chitosan nanospheres – A novel adsorbent for the removal of total inorganic Arsenic from aqueous systems. *Chemosphere*, **86**: 150–155.
- Gupta, V.K., Saini, V.K., Jain, N., (2005). Adsorption of As(III) from aqueous solutions by iron oxide-coated sand, *J. Colloid Interf. Sci.*, **288**:55–60.

- Han, H., Rafiq, M.K., Zhou, T., Xu, R., Mašek, O., Li, X., (2019). A critical review of clay-based composites with enhanced adsorption performance for metal and organic pollutants. *J. Hazard. Mater.*, **369**: 780–796.
- Han, J., Liang, X., Xu, Yingming, Xu, Yuanjian, (2015). Removal of Cu^{2+} from aqueous solution by adsorption onto mercapto functionalized palygorskite. *J. Ind. Eng Chem.*, **23**: 307–315.
- Han, J., Qiu, W., Cao, Z., Hu, J., Gao, W., (2013). Adsorption of ethinylestradiol (EE2) on polyamide 612: Molecular modeling and effects of water chemistry. *Water Res.*, **47**: 2273-2284.
- Han, J., Qiu, W., Meng, S., Gao, W., (2012). Removal of ethinylestradiol (EE2) from water via adsorption on aliphatic polyamides. *Water Res.*, **46(17)**: 5715-5724.
- Hao, J., Han, M.-J., Wang, C., Meng, X., (2009). Enhanced removal of arsenite from water by a mesoporous hybrid material – Thiol-functionalized silica coated activated alumina. *Microporous Mesoporous Mater.*, **124**: 1–7.
- Hasan, Z., Choi, E.-J., Jhung, S.H., (2013). Adsorption of naproxen and clofibric acid over a metal–organic framework MIL-101 functionalized with acidic and basic groups. *Chem. Eng. J.*, **219**: 537–544.
- Hasfalina, C.M., Maryam, R. Z., Luqman C.A., Rashid, M., (2012). Adsorption of copper (II) from aqueous medium in fixed-bed column by kenaf fibres. *APCBEE Procedia*, **3**: 255 – 263.
- Hashim, M.A., Chu, K.H., (2004). Biosorption of cadmium by brown, green, and red seaweeds. *Chem. Eng. J.*, **97**: 249–255.
- Hashim, M.A., Mukhopadhyay, S., Sahu, J.N., Sengupta, B., (2011). Remediation technologies for heavy metal contaminated groundwater. *J. Environ. Manage.*, **92**: 2355-2388.
- Hassard, F., Biddle, J., Cartmell, E., Jefferson, B., Tyrrel, S., Stephenson. T., (2015). Rotating biological contactors for wastewater treatment—A review. *Proc. Saf. Environ. Protect.*, **94**: 285-306.
- Hayat, M.T., Nauman, M., Nazir, N., Ali, S., Bangash, N., (2019). Environmental Hazards of Cadmium: Past, Present, and Future. Cadmium Toxicity and

Tolerance in Plants: From Physiology to Remediation. Elsevier, 163-183.
DOI: <https://doi.org/10.1016/B978-0-12-814864-8.00007-3>

- He, H.P., Guo, J.G., Xie, X.D., Lin, H.F., Li, L.Y., (2002). A microstructural study of acid-activated montmorillonite from Choushan, China. *Clay. Miner.*, **37** : 337-334.
- He, H., Duchet, J., Galy, J., Gerard, J.-F., (2005). Grafting of swelling clay materials with 3-aminopropyltriethoxysilane. *J. Colloid Interface Sci.*, **288** : 171-176.
- Herrera, N.N., Letoffe, J.-M., Reymond, J.-P., Bourgeat-Lami, E.,(2005). Silylation of laponite clay particles with monofunctional and trifunctional vinyl alkoxy silanes. *J. Mater. Chem.*, **15**: 863.
- Hlihor, R.M., Figueiredo, H., Tavares, T., Gavrilescu, M., (2016). Biosorption potential of dead and living *Arthrobacter viscosus* biomass in the removal of Cr(VI): Batch and column studies. *Process Saf. Environ. Prot.*, **108**: 44-56.
- Ho, Y.S., (2006). Review of second-order models for adsorption systems. *J. Hazard. Mater.*, **136**: 681–689.
- Ho, Y.S., McKay, G., (1998). A comparison of chemisorption kinetic models applied to pollutant removal on various sorbents. *Process Saf. Environ. Protect.*, **76**: 332–340.
- Ho, Y.S., McKay, G., (1999). Pseudo-second order model for sorption processes. *Process Biochem.*, **34**: 451–465.
- Ho, Y.S., McKay, G., (2000). The kinetics of sorption of divalent metal ions onto *sphagnum* moss peat. *Water Res.*, **34**: 735–742.
- Hoang, P., Yoon, K. B., Kim, D. P., (2012). Synthesis of hierarchically porous zeolite A crystals with uniform particle size in a droplet microreactor. *RSC Advances*, **2(12)**: 5323-5328.
- Hollas, J.M., (2005). *Modern Spectroscopy*. 4th Edition, John Wiley and Sons Ltd., USA, p. 262.
- Hu, X., Li, Y., Wang, Y., Li, X., Li, H., Liu, X., Zhang, P., (2010). Adsorption kinetics, thermodynamics and isotherm of thiacalix[4]arene-loaded resin to heavy metal ions, *Desalination*, **259**: 76–83.

- Hu, X.J., Liu, Y.G., Zeng, G.M., You, S.H., Wang, H., Xi, H., Guo, Y.M., Tan, X.F., Guo, F.Y., (2014). Effects of background electrolytes and ionic strength on enrichment of Cd(II) ions with magnetic graphene oxide-supported sulfanilic acid., *J. Colloid Interf. Sci.*, **435**: 138–144.
- Huang, B., Liu, Y., Li, B., Liu, S., Zeng, G., Zeng, Z., Wang, X., Ning, Q., Zheng, B., Yang, C., (2017). Effect of Cu(II) ions on the enhancement of tetracycline adsorption by Fe₃O₄@SiO₂-Chitosan/graphene oxide nanocomposite. *Carbohydr. Polym.*, **157**: 576–585.
- Huggett, J.M., (2021). Clay Minerals, in: Encyclopedia of Geology. Elsevier, pp. 341–349. DOI: <https://doi.org/10.1016/B978-0-12-409548-9.11855-X>.
- Huisman, J.L., Schouten, G., Schultz, C., (2006). Biologically produced sulphide for purification of process streams, effluent treatment and recovery of metals in the metal and mining industry. *Hydrometallurgy*. **83(1)**:106-113.
- IARC (International Agency for Research on Cancer), 2016. IARC monographs on the evaluation of carcinogenic risks to humans. Volumes 1–115. Available at: http://monographs.iarc.fr/ENG/Classification/latest_classif.php (accessed on Jan 16, 2017).
- Ibrahim, W.M., Hassan, A.F., Azab, Y.A., (2016). Biosorption of toxic heavy metals from aqueous solution by *Ulva lactuca* activated carbon, Egypt. *J. Basic Appl. Sci.*, **3**: 241–249.
- Ifelebuegu, A.O., Ukpebor, J.E., Obidiegwu, C.C., Kwofi, B.C., (2015). Comparative potential of black tea leaves waste to granular activated carbon in adsorption of endocrine disrupting compounds from aqueous solution. *Glob. J. Environ. Sci. Manag.*, **1**: 205–214.
- Iijima, S., (1991). Helical microtubules of graphitic carbon. *Nature*, **354**: 56-58.
- Iyer, A.P., Xue, J., Honda, M., Robinson, M., Kumosani, T.A., Abulnaja, K., Kannan, K., (2018). Urinary levels of triclosan and triclocarban in several Asian countries, Greece and the USA: Association with oxidative stress. *Environ. Res.*, **160**: 91–96.

- Jaafarzadeh, N., Mengelizadeh, N., Jalil, M., Takdastan, A., NadAli Alavi, N., Niknam, N., (2016). Removal of zinc and nickel from aqueous solution by chitosan and polyaluminum chloride. *Int. J. Env. Health Eng.*, **5**:16.
- Jadhav, S.V., Gadipelly, C.R., Marathe, K.V., Rathod, V.K., (2014). Treatment of fluoride concentrates from membrane unit using salt solutions. *J. Water Process Eng.*, **2**: 31–36.
- Jang, H.M., Yoo, S., Choi, Y.K., Park, S., Kan, E., (2018). Adsorption isotherm, kinetic modeling and mechanism of tetracycline on Pinus taeda-derived activated biochar. *Bioresour. Technol.*, **259**: 24-31.
- Jiang, D., Yang, Y., Huang, C., Huang, M., Chen, J., Rao, T., Ran, X., (2019). Removal of the heavy metal ion nickel (II) via an adsorption method using flower globular magnesium hydroxide. *J. Hazard. Mater.*, **373**: 131–140.
- Jiang, N., Shang, R., Heijman, S.G.J., Rietveld, L.C., (2020). Adsorption of triclosan, trichlorophenol and phenol by high-silica zeolites: Adsorption efficiencies and mechanisms. *Sep. Purif. Technol.*, **235**: 116152.
- Jiang, M.Q., Jin, X.Y., Lu, X.Q., Chen, Z.-L., (2010). Adsorption of Pb(II), Cd(II), Ni(II) and Cu(II) onto natural kaolinite clay. *Desalination*, **252**: 33–39.
- Joseph, L., Heo, J., Park, Y.G., Flora, J.R.V., Yoon, Y., (2011a). Adsorption of bisphenol A and 17 alpha ethinyl estradiol on single walled carbon nanotubes from seawater and brackish water. *Desalination*, **281**: 68–74.
- Joseph, L., Zaib, Q., Khan, I. A., Berge, N.D., Park, Y.G., Saleh, N.B., Yoon, Y., (2011b) Removal of bisphenol A and 17 alpha-ethinyl estradiol from landfill leachate using single-walled carbon nanotubes. *Water Res.*, **45**: 4056–68.
- Jovic-Jovicic, N., Milutinovic-Nikolic, A., Bankovic, P., Dojctnovic, B., Vasiljevic, B., Grzetic, I., Jovanovic, D., (2010). Synthesis, Characterization and Adsorptive Properties of Organobentonites. *Acta Physica Polonica A.*, **117**: 849–854.
- Kanaujiya, D.K., Paul, T., Sinharoy, A., Pakshirajan, K., (2019). Biological treatment processes for the removal of organic micropollutants from wastewater: A review. *Curr. Poll. Rep.*, **5**:112–128.

- Kannan, N., Veemaraj, T., (2010). Dynamics and equilibrium studies for the removal of Cd^{2+} and Cd^{2+} EDTA onto lemon peel carbon. *Indian J. Environ. Prot.*, **30**: 26–33.
- Karim, M.M., (2000). Arsenic in groundwater and health problems in Bangladesh. *Water Res.*, **34**(1): 304-310.
- Kartal, S.N., (2003). Removal of copper, chromium, and arsenic from CCA-C treated wood by EDTA extraction. *Waste Manage.*, **23**: 537–546.
- Kausar, A., Bhatti, H.N., (2013). Adsorptive removal of uranium from wastewater: a review. *J. Chem. Soc. Pak.*, **35**: 1041–1052.
- Keshtkar, A.R., Irani, M., Moosavian, M.A., (2013). Comparative study on PVA/silica membrane functionalized with mercapto and amine groups for adsorption of Cu(II) from aqueous solutions. *J. Taiwan Inst. Chem. Eng.*, **44**: 279–286.
- Khormaei, M., Nasernejad, B., Edrisi, M., Eslamzadeh, T., (2007). Copper biosorption from aqueous solutions by sour orange residue. *J. Hazard. Mater.*, **149**: 269–274.
- Kidd, K.A., Blanchfield, P.J., Mills, K.H., Palace, V.P., Evans, R.E., Lazorchak, J.M., Flick, R.W., (2007). Collapse of a fish population after exposure to a synthetic estrogen. *Proc. Natl. Acad. Sci., USA* **104**: 8897–8901.
- Kim, H.Y., Jeon, J., Hollender, J., Yu, S., Kim, S.D., (2014). Aqueous and dietary bioaccumulation of antibiotic tetracycline in *D. magna* and its multigenerational transfer. *J. Hazard. Mater.*, **279**: 428–435.
- Kiran, K.A., Venkata, M.S, (2012). Removal of natural and synthetic endocrine disrupting estrogens by multi-walled carbon nanotubes (MWCNT) as adsorbent: Kinetic and mechanistic evaluation. *Sep. Purif. Technol.*, **87**: 22.
- Komesli, O.T., Muz, M, Ak, M.S., Bakirdere, S., Gokcay, C.F., (2015). Occurrence, fate and removal of endocrine disrupting compounds (EDCs) in Turkish wastewater treatment plants. *Chem. Eng. J.*, **277**: 202–208.

- Konsowa, A.H., (2010). Intensification of the rate of heavy metal removal from wastewater by cementation in a jet reactor. *Desalination*, **254**: 29–34.
- Košak, A., Lobnik, A., Bauman, M., (2015). Adsorption of mercury (II), lead (II), cadmium (II) and zinc (II) from aqueous solutions using mercapto-modified silica particles. *Int. J. Appl. Ceram. Technol.*, **12**: 461–472.
- Kosek, K., Luczkiewicz, A., Fudala –Książek, S., Jankowska, K., Szopińska, M., Svahn, O., Tränckner, J., Kaiser, A., Langas, V., Björklund, E., (2020). Implementation of advanced micropollutants removal technologies in wastewater treatment plants (WWTPs) - Examples and challenges based on selected EU countries. *Environ. Sci. Policy*, **112**: 213–226.
- Kotal, M., Bhowmick, A.K., (2015). Polymer nanocomposites from modified clays: Recent advances and challenges. *Prog. Polym. Sci.*, **51**: 127–187.
- Kragović, M., Stojmenović, M., Petrović, J., Loredo, J., Pašalić, S., Nedeljković, A., Ristović, I., (2019). Influence of Alginate Encapsulation on Point of Zero Charge (pHpzc) and Thermodynamic Properties of the Natural and Fe(III) - Modified Zeolite. *Procedia. Manuf.*, **32**: 286–293.
- Kumar, M., Deka, J.P., Kumari, O., (2020). Development of Water Resilience Strategies in the context of climate change, and rapid urbanization: a discussion on vulnerability mitigation. *Groundw. Sustain. Dev.*, **10**:100308.
- Kumar, P.S., Ramalingam, S., Sathyaselvabala, V., Kirupha, S.D., Sivanesan, S., (2011). Removal of copper(II) ions from aqueous solution by adsorption using cashew nut shell. *Desalination*, **266**: 63–71.
- Kumar, S., (2008). *Spectroscopy of Organic Compounds*. Guru Nanak Dev University, Amritsar. <http://nsdl.niscair.res.in/jspui/handle/123456789/793>.
- Kumar, V., Singh, K., Shah, M.P., (2021). Advanced oxidation processes for complex wastewater treatment, in: *Advanced Oxidation Processes for Effluent Treatment Plants*. Elsevier, pp. 1–31.
- Kundu, S., Gupta, K.A., (2006). Investigation on the adsorption efficiency of iron

oxide coated cement (IOCC) towards As(V)– kinetics, equilibrium and thermodynamics studies. *Colloids Surf. A: Physicochem. Eng. Aspects*, **273**: 121–128.

Kunduru, K.R., Nazarkovsky, M., Farah, S., Pawar, R.P., Basu, A., Domb, A.J., (2017). Nanotechnology for water purification: applications of nanotechnology methods in wastewater treatment. *Water Purif.*, 33-74: ISBN 9780128043004.

Lalchhingpuii, Lee, S.M., Tiwari, D., (2016). Synthesis and Characterization of Chitosan templated Mesoporous Silica: Efficient use of mesoporous silica in the removal of Cu(II) from aqueous solutions. *S.T.J.*, Vol. **4** Issue: II ISSN: 2321-3388.

Lalchhingpuii, Tiwari, D., Lalhmunsiam, Lee, S.M., (2017). Chitosan templated synthesis of mesoporous silica and its application in the treatment of aqueous solutions contaminated with cadmium(II) and lead(II). *Chem. Eng. J.*, **328**: 434-444.

Lalhmunsiam, Lalchhingpuii, Nautiyal, B.P., Tiwari, D., Choi, S.I., Kong, S.H., Lee, S.M., (2016a). Silane grafted chitosan for the efficient remediation of aquatic environment contaminated with arsenic(V). *J. Colloid Interface Sci.*, **467**: 203–212.

Lalhmunsiam, Lee, S.M., Lalchhingpuii, Tiwari, D., (2016b). Functionalized hybrid material precursor to chitosan in the efficient remediation of aqueous solutions contaminated with As(V). *J. Environ. Chem. Eng.*, **4**: 1537–1544.

Lalhmunsiam, Lee, S.M., Tiwari, D., (2013). Manganese oxide immobilized activated carbons in the remediation of aqueous wastes contaminated with copper(II) and lead(II). *Chem. Eng. J.*, **225**: 128–137.

Lalhmunsiam, Tiwari, D., Lee, S.M., (2012). Activated Carbon and Manganese Coated Activated Carbon Precursor to Dead Biomass in the Remediation of Arsenic Contaminated Water. *Environ. Eng. Res.*, **17**: 41–48.

- Lalhmunsiamia, Tiwari, D., Lee, S.M., (2015). Physico-chemical studies in the removal of Sr(II) from aqueous solutions using activated sericite. *J. Environ. Radioact.*, **147**: 76–84.
- Lalhmunsiamia, Tiwari, D., Lee, S.M., (2016c). Surface-functionalized activated sericite for the simultaneous removal of cadmium and phenol from aqueous solutions: Mechanistic insights. *Chem. Eng. J.*, **283**: 1414–1423.
- Lalhmunsiamia., Lalhriatpuia, C., Tiwari, D., Lee, S.M., (2014). Immobilized nickel hexacyanoferrate on activated carbons for efficient attenuation of radio toxic Cs(I) from aqueous solutions. *Appl. Surf. Sci.* **321**: 275–282.
- Larcher, S., Delbes, G., Robaire, B., Yargeau, V., (2012). Degradation of 17 α ethinylestradiol by ozonation – identification of the by-products and assessment of their estrogenicity and toxicity. *Environ. Int.*, **39**: 66–72.
- Lazaratou, C.V., Vayenas, D.V., Papoulis, D., (2020). The role of clays, clay minerals and clay-based materials for nitrate removal from water systems: A review. *Appl. Clay Sci.*, **185**: 105377.
- Lee, C., Jung, J., Pawar, R.R., Kim, M., Lalhmunsiamia, Lee, S.M., (2017). Arsenate and phosphate removal from water using Fe-sericite composite beads in batch and fixed-bed systems. *J. Ind. Eng. Chem.*, **47**: 375–383.
- Lee, D.G., Zhao, F., Rezenom, Y.H., Russell, D.H., Chu, K.H., (2012a). Biodegradation of triclosan by a wastewater microorganism. *Water Res.*, **46**: 4226–4234.
- Lee, S. M., Lalhmunsiamia, Tiwari, D., (2014). Sericite in the remediation of Cd(II) and Mn(II)-contaminated waters: batch and column studies. *Environ. Sci. Pollut. Res. Int.*, **21**: 3686–3696.
- Lee, S.M., Laldawngliana, C., Tiwari, D., (2012b). Iron oxide nano-particles-immobilized-sand material in the treatment of Cu(II), Cd(II) and Pb(II) contaminated waste waters. *Chem. Eng. J.*, **195–196**: 103–111.
- Lee, S.M., Lalhmunsiamia, Thanhmingliana, Tiwari, D., (2015). Porous hybrid materials in the remediation of water contaminated with As(III) and As(V). *Chem. Eng. J.*, **270**: 496–507.

- Lee, S.M., Tiwari, D., (2012). Organo and inorgano–organo–modified clays in the remediation of aqueous solutions: an overview. *Appl. Clay Sci.*, **59–60**: 84–102.
- Levy, S.B., (2002). Factors impacting on the problem of antibiotic resistance. *J. Antimicrob. Chemotherapy*, **49**: 25–30.
- Lewis, A.E., (2010). Review of metal sulphide precipitation. *Hydrometallurgy*, **104**: 222–234.
- Li, P., Zhang, X., Chen, Y., Bai, T., Lian, H., Hu, X., (2014). One-pot synthesis of thiol- and amine-bifunctionalized mesoporous silica and applications in uptake and speciation of arsenic. *RSC Adv.*, **4**: 49421–49428.
- Li, Y., Li, M., Li, Z., Yang, L., Liu, X., (2019a). Effects of particle size and solution chemistry on triclosan sorption on polystyrene microplastic. *Chemosphere*, **231**: 308–314.
- Li, Y., Liu, S., Wang, C., Ying, Z., Huo, M., Yang, W., (2019b). Effective column adsorption of triclosan from pure water and wastewater treatment plant effluent by using magnetic porous reduced graphene oxide. *J. Hazard Mater.*, **386**:121942.
- Li, Z., Liu, X., Jin, W., Hu, Q., Zhao, Y., (2019c). Adsorption behavior of arsenicals on MIL-101(Fe): The role of arsenic chemical structures. *J. Colloid Interface Sci.* 554, 692–704.
- Li, Z., Liu, Y., Zou, S., Lu, C., Bai, H., Mu, H., Duan, J., (2020). Removal and adsorption mechanism of tetracycline and cefotaxime contaminants in water by NiFe₂O₄-COF-chitosan-terephthalaldehyde nanocomposites film. *Chem. Eng. J.*, **382**: 123008.
- Liang, X., Han, J., Xu, Y., Wang, L., Sun, Y., Tan, X., (2014). Sorption of Cd²⁺ on mercapto and amino functionalized palygorskite. *Appl. Surf. Sci.*, **322**: 194–201.
- Liang, X., Xu, Y., Sun, G., Wang, L., Sun, Yuebing, Sun, Yang, Qin, X., (2011). Preparation and characterization of mercapto functionalized sepiolite and their application for sorption of lead and cadmium. *Chem. Eng. J.*, **174**: 436–444.

- Liang, X., Xu, Y., Tan, X., Wang, L., Sun, Yuebing, Lin, D., Sun, Yang, Qin, X., Wang, Q., (2013). Heavy metal adsorbents mercapto and amino functionalized palygorskite: Preparation and characterization. *Colloids Surf. A Physicochem. Eng. Asp.*, **426**: 98–105.
- Lindsey, M.E., Meyer, M., Thurman, E.M., (2001). Analysis of trace levels of sulfonamide and tetracycline antimicrobials, in groundwater and surface water using solid-phase extraction and liquid chromatography/mass spectrometry. *Anal. Chem.*, **73**: 4640–4646.
- Liu, A.M., Hidajat, K., Kawi, S., Zhao, D.Y., (2000). A new class of hybrid mesoporous materials with functionalized organic monolayers for selective adsorption of heavy metal ions. *Chem. Commun.*, **230(13)**: 1145–1146.
- Liu, M., Hou, L., Yu, S., Xi, B., Zhao, Y., Xia, X., (2013). MCM-41 impregnated with A zeolite precursor: Synthesis, characterization and tetracycline antibiotics removal from aqueous solution. *Chem. Eng. J.*, **223**: 678–687.
- Liu, R., Li, S., Tu, Y., Hao, X., (2021). Capabilities and mechanisms of microalgae on removing micropollutants from wastewater: A review. *J. Environ. Manage.*, **285**: 112149.
- Liu, S., Xu, R., (2013). Adsorption characteristics of triclosan on chitosan/poly(vinyl alcohol) composite nanofibrous membranes. *Appl. Mech. Mater.*, **448–453**: 134–138.
- Loganathan, P., Vigneswaran, S., Kandasamy, J., (2013). Enhanced removal of nitrate from water using surface modification of adsorbents – a review. *J. Environ. Manage.*, **131**: 363-374.
- Luo, X., Wang, C., Luo, S., Dong, R., Tu, X., Zeng, G., (2012). Adsorption of As (III) and As (V) from water using magnetite Fe₃O₄-reduced graphite oxide–MnO₂ nanocomposites. *Chem. Eng. J.*, **187**: 45–52.
- Lye, J.W.P., Saman, N., Sharuddin, S.S.N., Othman, N.S., Mohtar, S.S., Md Noor, A.M., Buhari, J., Cheu, S.C., Kong, H., Mat, H., (2017). Removal Performance of Tetracycline and Oxytetracycline From Aqueous Solution

- Via Natural Zeolites: An Equilibrium and Kinetic Study: Water. *CLEAN - Soil Air Water*, **45**: 1600260.
- Ma, J., Lei, Y., Khan, M.A., Wang, F., Chu, Y., Lei, W., Xia, M., Zhu, S., (2019). Adsorption properties, kinetics & thermodynamics of tetracycline on carboxymethyl-chitosan reformed montmorillonite. *Int. J. Biol. Macromol.*, **124**: 557–567.
- Ma, X.M., Tsige, M., Uddin, S., Talapatra, S., (2011). Application of carbon nanotubes for removing organic contaminants from water. *Mater Express.*, **1**:183–200.
- Machida, M., Fotoohi, B., Amamo, Y., Ohba, T., Kanoh, H., Mercier, L., (2012). Cadmium(II) adsorption using functional mesoporous silica and activated carbon. *J. Hazard. Mater.*, **221–222**: 220–227.
- Madsen, E., Gitlin, J.D., (2007). Copper and iron disorders of the brain. *Annu. Rev. Neurosci.*, **30**:317–37.
- Maeng, S. K., Choi, B. G., Lee, K.T., Song, K. G., (2013). Influences of solid retention time, nitrification and microbial activity on the attenuation of pharmaceuticals and estrogens in membrane bioreactors. *Water Res.*, **47(9)**: 3151–62.
- Maged, A., Iqbal, J., Kharbish, S., Ismael, I.S., Bhatnagar, A., (2020). Tuning tetracycline removal from aqueous solution onto activated 2:1 layered clay mineral: characterization, sorption and mechanistic studies. *J. Hazard Mater.*, **384**: 121320.
- Mahouachi, L., Rastogi, T., Palm, W-U., Ghorbel-Abid, I., Chehimi, D.B.H., Kummerer, K., (2020). Natural clay as a sorbent to remove pharmaceutical micropollutants from wastewater. *Chemosphere*, **258**: 127213.
- Maji, S., Ghosh, Ayan, Gupta, K., Ghosh, Abir, Ghorai, U., Santra, A., Sasikumar, P., Ghosh, U.C., (2018). Efficiency evaluation of arsenic(III) adsorption of novel graphene oxide@iron-aluminium oxide composite for the contaminated water purification. *Sep. Purif. Technol.*, **197**: 388–400.
- Maji, S.K., Pal, A., Pal, T., (2007). Arsenic removal from aqueous solution by adsorption on laterite soil. *J. Environ. Sci. Health A.*, **42(4)**:453-62.

- Malek, A., Farooq, S., (1996). Comparison of isotherm models for hydrocarbon adsorption on activated carbon, *AIChE J.*, **42**: 3191–3201.
- Marjanovi, V., Lazarevi, V.S., Castvan, I.J., Potkonjak, B., Janackovi, D., Petrovi, R., (2011). Chromium (VI) removal from aqueous solutions using mercaptosilane functionalized sepiolites. *Chem. Eng. J.*, **166** : 198-206.
- Martín-Lara, M.A., Calero, M., Ronda, A., Iáñez-Rodríguez, I., Escudero, C., (2020). Adsorptive behavior of an activated carbon for bisphenol A removal in single and binary (bisphenol A-heavy metal) solutions. *Water*, **12**: 2150.
- Matolia, J., Shukla, S. P., Kumar, S., Kumar, K., Singh, A. R., (2019). Physical entrapment of chitosan in fixed-down-flow column bed enhances triclosan removal from water. *Water Sci. Technol.*, **80(7)**: 1374–1383.
- McMurry, L.M., Oethinger, M., Levy, S.B., (1998). Triclosan targets lipid synthesis. *Nature*, **394**: 531–532.
- Medda, N., De, S.K., Maiti, S., (2021). Different mechanisms of arsenic related signaling in cellular proliferation, apoptosis and neo-plastic transformation. *Ecotoxicol. Environ. Saf.*, **208**: 111752.
- Mehrizad, A., Aghaie, M., Gharbani, P., Dastmalchi, S., Monajjemi, M., Zare, K., (2012). Comparison of 4-chloro-2-nitrophenol adsorption on single-walled and multi-walled carbon nanotubes. *J. Environ. Heal. Sci. Eng.*, **9**: 2–7.
- Mekatel, E.H., Amokrane, S., Aid, A., Nibou, D., Trari, M., (2015). Adsorption of methyl orange on nanoparticles of a synthetic zeolite NaA/CuO. *C. R. Chim.*, **18**: 336–344.
- Meseldzija, S., Jelena Petrovic, J., Onjia, A., Volkov-Husovic, T., Nestic, A., Vukelic, N., (2019). Utilization of agro-industrial waste for removal of copper ions from aqueous solutions and mining-wastewater. *J. Ind. Eng. Chem.*, **75**: 246-252.
- Mezohegyi, G., van der Zee, F.P., Font, J., Fortuny, A., Fabregat, A., (2012). Towards advanced aqueous dye removal processes: A short review on the versatile role of activated carbon. *J. Environ. Manage.*, **102**: 148–164.

- Miranda, K., Pereira-Filho, E.R., (2009). Potentialities of thermospray flame furnace atomic absorption spectrometry (TS–FF–AAS) in the fast sequential determination of Cd,Cu, Pb and Zn. *Anal. Methods.*, **1**: 215–219.
- Mishra, T., Mahato, D.K., (2016). A comparative study on enhanced arsenic(V) and arsenic(III) removal by iron oxide and manganese oxide pillared clays from ground water. *J. Environ. Chem. Eng.*, **4**: 1224–1230.
- Mnasri-Ghnnimi, S., Frini-Srasra, N., (2019). Removal of heavy metals from aqueous solutions by adsorption using single and mixed pillared clays. *Appl. Clay Sci.*, **179**: 105151.
- Mohamad, N., Abustan, I., Mohamad, M., Samuding, K., (2018). Metal removal from municipal landfill leachate using mixture of laterite soil, peat soil and rice husk. *Mater. Today Proc.*, **5**: 21832–21840.
- Montalvo, S., Cahn, I., Borja, R., Huilnir, C., Guerrero, L., (2017). Use of solid residue from thermal power plant (fly ash) for enhancing sewage sludge anaerobic digestion: Influence of fly ash particle size. *Bioresour. Technol.*, **244**: 416–422.
- Montero, J.I.Z., Monteiro, A.S.C., Gontijo, E.S.J., C. Bueno, C.C., de Moraes, M.A., Rosa, A.H., (2018). High efficiency removal of As(III) from waters using a new and friendly adsorbent based on sugarcane bagasse and corncob husk Fe-coated biochars. *Ecotoxicol. Environ. Saf.*, **162**: 616-624.
- Mook, W.T., Aroua, M.K., Issabayeva, G., (2014). Prospective applications of renewable energy based electrochemical systems in wastewater treatment: A review. *Renew. Sust. Ener. Rev.*, **38**: 36–46.
- Mora, B.P., Bellú, S., Mangiameli, M.F., Frascaroli, M.I., González, J.C., (2019). Response surface methodology and optimization of arsenic continuous sorption process from contaminated water using chitosan. *J. Water Process Eng.*, **32**: 100913.
- Moritz, M., Geszke-Moritz, M., (2014). Application of nanoporous silicas as adsorbents for chlorinated aromatic compounds. A comparative study. *Mater. Sci. Eng.*, **41**: 42-51.

- Mukhopadhyay, R., Bhaduri, D., Sarkar, B., Rusmin, R., Hou, D., Khanam, R., Sarkar, S., Kumar Biswas, J., Vithanage, M., Bhatnagar, A., Ok, Y.S., (2020). Clay–polymer nanocomposites: Progress and challenges for use in sustainable water treatment. *J. Hazard. Mater.*, 383: 121125.
- Mustaqeem, M., Bagwan, M.S., Patil, P.R., (2013). Evaluation of removal efficiency of Ni(II) from aqueous solution by natural leaves. *Rasayan J. Chem.*, **6**: 307 – 314.
- Mwewa , B., Stopic, S., Ndlovu, S., Simate, G.S., Xakalashé, B., Friedrich, B., (2019). Synthesis of poly-alumino-ferric sulphate coagulant from acid mine drainage by precipitation. *Metals*, **9(11)**: 1166.
- N'diaye, A.D.; Bollahi, M.A.; Kankou, M.S.A., (2019). Sorption of paracetamol from aqueous solution using groundnut shell as a low cost sorbent. *J. Mater. Environ. Sci.*, **10**: 553–562.
- Nada, S.A., Mahmoud S.A., (2004). Protective effect of panax ginseng against tetracycline toxicity in rats. *J. Jinseng Res.*, **24(2)**: 93-98.
- Nagpal, G., Bhattacharya, A., Singh, N.B., (2016). Removal of chromium(VI) from aqueous solutions by carbon waste from thermal power plant. *Desalin. Water Treat.*, **57**: 9765–9775.
- Naiya, T.K., Bhattacharya, A.K., Das, S.K., (2009). Clarified sludge (basic oxygen furnace sludge) – an adsorbent for removal of Pb(II) from aqueous solutions – kinetics, thermodynamics and desorption studies. *J. Hazard. Mater.*, **170**: 252–262.
- Nassef, E., El-Taweel, Y.A., (2015), Removal of copper from wastewater by cementation from simulated leach liquors. *J. Chem Eng. Process Technol.*, **6**: 1-4.
- Nath, K., (2008). Membrane Separation Processes. PHI Learning Pvt. Ltd., New Delhi.
- Navarro, P., Alguacil, F.J., (2002). Adsorption of antimony and arsenic from a copper electrorefining solution onto activated carbon. *Hydrometallurgy*, **66**: 101–105.

- Nebagha, K.C., Ziat, K., Rghioui, L., Khayet, M., Saidi, M., Aboumaria, K., El Hourch, A., Sebti, S., (2015). Adsorptive removal of copper (II) from aqueous solutions using low cost Moroccan adsorbent. Part I: Parameters influencing Cu(II) adsorption. *J. Mater. Environ. Sci.*, **6 (11)** : 3022-3033.
- Nechita, Petronela. (2017). Applications of Chitosan in Wastewater Treatment. 10.5772/65289.
- Nfodzo, P., Hu, Qinhong., Choi, Hyeok., (2012). Impacts of pH-dependent metal speciation on the decomposition of triclosan by sulfate radicals. *Water Supply.*, **12 (6)**: 837–843.
- Niu, J., Ding, S., Zhang, L., Zhao, J., Feng, C., (2013). Visible-light-mediated Sr-Bi₂O₃ photocatalysis of tetracycline: kinetics, mechanisms and toxicity assessment. *Chemosphere*, **93**: 1–8.
- Noubactep, C., (2010). Elemental metals for environmental remediation: learning from cementation process. *J. Hazard Mater.*, **181**: 1170 – 1174.
- Ociński, D., Jacukowicz-Sobala, I., Mazur, P., Raczyk, J., Kociołek-Balawejder, E., (2016). Water treatment residuals containing iron and manganese oxides for arsenic removal from water – Characterization of physicochemical properties and adsorption studies. *Chem. Eng. J.*, **294**: 210–221.
- Odabasi, S.U., Buyukgungor, H., (2016). Removal of Micropollutants in Water with Advanced Treatment Processes. 1st International Black Sea Congress On Environmental Sciences (IBCESS).
- Ogbu, I., Akpomie, K., Osunkunle, A., Eze, S., (2019). Sawdust-kaolinite composite as efficient sorbent for heavy metal ions. *Bangladesh J. Sci. Ind. Res.*, **54**: 99–110.
- Ojedokun, A.T., Bello, O.S., (2016). Sequestering heavy metals from wastewater using cow dung. *Water Res. Ind.*, **13**: 7-13.
- Oliveira, H. G., Ferreira, L. H., Bertazzoli, R., Longo, C. (2015). Remediation of 17- α -ethinylestradiol aqueous solution by photocatalysis and electrochemically-assisted photocatalysis using TiO₂ and TiO₂/WO₃ electrodes irradiated by a solar simulator. *Water Res.*, **72**: 305–314.

- Ouakouak, A., Rihani, K., Youcef, L., Hamdi, N., Guergazi, S., (2020). Adsorption characteristics of Cu (II) onto CaCl₂ pretreated algerian bentonite. *Mater. Res. Express.*, **7**: 025045.
- Paiva, L.B., Morales, A.R., Valenzuela Diaz, F.R., (2008). Organoclays: properties, preparation and applications. *Appl. Clay Sci.*, **42**: 8–24.
- Park, Y., Ayoko, G.A., Frost, R.L., (2011). Application of organoclays for the adsorption of recalcitrant organic molecules from aqueous media. *J. Colloid Interf. Sci.*, **354**: 292–305.
- Patil, D.S., Chavan, S.M., Oubagaranadin, J.U.K., (2016). A review of technologies for manganese removal from wastewaters. *J. Environ. Chem. Eng.*, **4**: 468–487.
- Paul, B., Martens, W.N., Fros, R.L., (2011). Organosilane grafted acid-activated beidellite clay for the removal of non-ionic alachlor and anionic imazaquin. *Appl. Surf. Sci.*, **257**: 5552-5558.
- Pauwels, B., Wille, K., Noppe, H., De Brabandar, H., de Wiele, T.V., Verstraete, W., Boon, N., (2008). 17 α -ethinylestradiol cometabolism by bacteria degrading estrone, 17 β -estradiol and estriol. *Biodegradation*, **19**: 683–693.
- Pérez-Botella E., Palomino M., Valencia S., Rey F. (2019). Zeolites and Other Adsorbents. In: Kaneko K., Rodríguez-Reinoso F. (eds) Nanoporous Materials for Gas Storage. Green Energy and Technology. Springer, Singapore. https://doi.org/10.1007/978-981-13-3504-4_7.
- Petit, S., Madejova, J., (2013). Fourier Transform Infrared Spectroscopy, in: F. Bergaya, G. Lagaly (Eds.), *Developments in Clay Science*, Elsevier, pp. 213–231.
- Phuekphong, A.F., Imwiset, K.J., Makoto Ogawa, M., (2020). Organically modified bentonite as an efficient and reusable adsorbent for triclosan removal from water. *Langmuir*, **36(31)**: 9025–9034.
- Piscitelli, F., Posocco, P., Toth, R., Fermeglia, M., Pricl, S., Mensitieri, G., Lavorgna, M., (2010). Sodium montmorillonite silylation: unexpected effect of the aminosilane chain length. *J. Colloid Interf. Sci.*, **351** : 108–115.

- Plappally, A.K., Lienhard V, J.H., (2012). Energy requirements for water production, treatment, end use, reclamation, and disposal. *Renew. Sust. Ener. Rev.*, **16**: 4818–4848.
- Potgieter, J.H., Potgieter-Vermaak, S.S., Kalibantonga, P.D., (2006). Heavy metals removal from solution by palygorskite clay. *Minerals Eng.*, **19 (5)**: 463–470.
- Prabhu, P.P., Prabhu, B., (2018). A review on removal of heavy metal ions from waste water using natural/ modified bentonite. *MATEC Web Conf.*, **144** : 02021.
- Prokić, D., Vukčević, M., Kalijadis, A., Maletić, M., Babić, B., Đurkić, T., (2020). Removal of Estrone, 17 β Estradiol, and 17 α -Ethinylestradiol from water by adsorption onto chemically modified activated carbon cloths. *Fibers Polym.*, **21**: 2263–2274.
- Qin, Z., Yuan, P., Yang, S., Liu, D., He, H., Zhu, J., (2014). Silylation of Al13-intercalated montmorillonite with trimethylchlorosilane and their adsorption for Orange II. *Appl. Clay Sci.*, **99**: 229–236.
- Queiroga, L.N.F., Pereira, M.B.B., Silva, L.S., Silva Filho, E.C., Santos, I.M.G., Fonseca, M.G., Georgelin, T., Jaber, M., (2019). Microwave bentonite silylation for dye removal: Influence of the solvent. *Appl. Clay Sci.*, **168**: 478–487.
- Raji, C., Anirudhan, T.S., (1998). Batch Cr(VI) removal by polyacrylamide-grafted sawdust: Kinetics and thermodynamics. *Water Res.*, **32**: 3772–3780.
- Rayaroth, M.P., Escobedo, E., Chang, Y.-S., (2020). Degradation studies of halogenated flame retardants. *Compr. Anal. Chem.*, **88**: 303–339.
- Ren, X., Zhang, Z., Luo, H., Hu, B., Dang, Z., Yang, C., Li, L., (2014). Adsorption of arsenic on modified montmorillonite. *Appl. Clay Sci.*, **97**: 17–23.
- Renault, F., Sancey, B., Badot, P.M., Crini, G., (2009). Chitosan for coagulation/flocculation processes –An eco-friendly approach. *Eur. Polym. J.*, **45**: 1337–1348.

- Renu, K., Madhyastha, H., Madhyastha, R., Maruyama, M., Vinayagam, S., Valsala Gopalakrishnan, A., (2018). Review on molecular and biochemical insights of arsenic-mediated male reproductive toxicity. *Life Sci.*, **212**: 37–58.
- Ribeiro, A.R.L., Moreira, N.F.F., Li Puma, G., Silva, A.M.T., (2019). Impact of water matrix on the removal of micropollutants by advanced oxidation technologies. *Chem. Eng. J.*, **363**: 155–173.
- Rivera-Utrilla, J., Gomez-Pacheco, C.V., Sanchez-Polo, M., Lopez-Penalver, J.J., Ocampo-Perez, R., (2013). Tetracycline removal from water by adsorption/bioadsorption on activated carbons and sludge-derived adsorbents. *J. Environ. Manage.*, **131**: 16-24.
- Rubin, E., Rodriguez, P., Herrero, R., Sastre de Vicente, M.E., (2010). Adsorption of methylene blue on chemically modified algal biomass: equilibrium, dynamic, and surface data. *J. Chem. Eng.*, **55**: 5707–5714.
- Şahan, T., Erol, F., Yılmaz, S., (2018). Mercury(II) adsorption by a novel adsorbent mercapto-modified bentonite using ICP-OES and use of response surface methodology for optimization. *Microchem. J.*, **138**: 360–368.
- Salam, M.A., Burk, R.C., (2010). Thermodynamics and kinetics studies of pentachlorophenol adsorption from aqueous solutions by multi-walled carbon nanotubes. *Water Air Soil Pollut.*, **210**: 101–111
- Salazar-Rabago, J.J., Leyva-Ramos, R., Rivera-Utrilla, J., Ocampo-Perez, R., Cerino-Cordova, F.J., (2017). Biosorption mechanism of Methylene Blue from aqueous solution onto White Pine (*Pinus durangensis*) sawdust: Effect of operating conditions. *Sustain. Environ. Res.*, **27**: 32–40.
- Sankararamkrishnan, N., Gupta, A., Vidyarthi, S.R., (2014). Enhanced arsenic removal at neutral pH using functionalized multiwalled carbon nanotubes. *J. Environ. Chem. Eng.*, **2**: 802–810.
- Santaefemia, S., Abalde, Enrique Torres, E., (2019). Eco-friendly rapid removal of triclosan from seawater using biomass of a microalgal species: Kinetic and equilibrium studies. *J. Hazard. Mater.*, **369**: 674-683.

- Saravanan, D., Gomathi, T., Sudha, P.N., (2013). Sorption studies on heavy metal removal using chitin/bentonite biocomposite. *Int. J. Biol. Macromol.*, **53**: 67–71.
- Sarmah, A.K., Meyer, M.T., Boxall, A.B.A., (2006). A global perspective on the use, sales, exposure pathways, occurrence, fate and effects of veterinary antibiotics (VAs) in the environment. *Chemosphere*, **65**: 725–759.
- Sassman, S.A., Lee, L.S., (2005). Sorption of three tetracyclines by several soils: assessing the role of pH and cation exchange. *Environ. Sci. Technol.*, **39**: 7452–7459.
- Saygılı, H., Güzel, F., (2016). Effective removal of tetracycline from aqueous solution using activated carbon prepared from tomato (*Lycopersicon esculentum* Mill.) industrial processing waste. *Ecotoxicol. Environ. Saf.*, **131**: 22–29.
- Scala-Benuzzi, M.L., Takara, E.A., Alderete, M., Soler-Illia, G.J.A.A., Schneider, R.J., Rabaa, J., Messina, G.A., (2018). Ethinylestradiol quantification in drinking water sources using a fluorescent paper based immunosensor. *Microchem. J.*, **141**: 287-293.
- Schell, L.M., Knutson, K.L., Bailey, S., (2012). Environmental Effects on Growth. *In Human Growth and Development*, Elsevier Inc, 245–286.
- Sdiri, A., Khairy, M., Bouaziz, S., El-Safy, S., (2016). A natural clayey adsorbent for selective removal of lead from aqueous solutions. *Appl. Clay Sci.*, **126**: 89–97.
- Sen, T.K., (2013). Review on Dye Removal from Its Aqueous Solution into Alternative Cost Effective and Non-Conventional Adsorbents. *J. Chem. Process Eng.*, DOI: [10.17303/jce.2014.105](https://doi.org/10.17303/jce.2014.105).
- Shahrokhi-Shahraki, R., Benally, C., El-Din, M.G., Park, J., (2021). High efficiency removal of heavy metals using tire-derived activated carbon vs commercial activated carbon: Insights into the adsorption mechanisms. *Chemosphere*, **264**: 128455.

- Shakerian, F., Zhao, J., Li, S.P., (2020). Recent development in the application of immobilized oxidative enzymes for bioremediation of hazardous micropollutants – A review. *Chemosphere*, **239**: 124716.
- Shaligram, S., Campbell, A., (2013). Toxicity of copper salts is dependent on solubility profile and cell type tested. *Toxicol. In.Vitro.*, **27**: 844–851.
- Shang, Z., Zhang, L., Zhao, X., Liu, S., Li, D., (2019). Removal of Pb(II), Cd(II) and Hg(II) from aqueous solution by mercapto-modified coal gangue. *J. Environ. Manage.*, **231**: 391–396.
- Shanmugam, G., Jawahar, G. S., Ravindran, S., (2004). Review on the Uses of Appropriate Techniques for Arid Environment, *International Conf. on Water Resources & Arid Environment*.
- Shanmugharaj, A.M., Rhee, K.Y., Ryu, S.H., (2006). Influence of dispersing medium on grafting of aminopropyltriethoxysilane on swelling clay minerals. *J. Colloid Interf. Sci.*, **298**: 854–859.
- Shen, W., He, H.P., Zhu, J.X., Yuan, P., Ma, Y.H., Liang, X.L., (2009). Preparation and characterization of 3-aminopropyltriethoxysilane grafted montmorillonite and acid activated montmorillonite. *Sci. Bull.*, **54** : 265–271.
- Shin, J., Lee, Y.G., Lee, S.H., Kim, S., Ochir, D., Park, Y., Kim, J., Chon, K., (2020). Single and competitive adsorptions of micropollutants using pristine and alkalimodified biochars from spent coffee grounds. *J. Hazard. Mater.*, **400**: 123102.
- Silva, C.P., Otero, M., Esteves, V., (2012). Processes for the elimination of estrogenic steroid hormones from water: A review. *Environ. Poll.*, **165**: 38–58.
- Silva, L.L.S., Moreira, C.G., Curzio, B.A., da Fonseca, F.V., (2017). Micro-pollutant removal from water by membrane and advanced oxidation processes—A review. *J. Water Resour. Prot.*, **9**: 411-431.
- Silva, M.A.L., Haberbeck, B.A.A., de Oliveira, M.C.M., (2003). Influence of tetracycline in the hepatic and renal development of rat's offspring. *Braz. Arch. Biol. Technol.*, **46(1)**: 47–51.

- Singh, S., Garg, A., (2021). Advanced oxidation processes for industrial effluent treatment, in: *Advanced Oxidation Processes for Effluent Treatment Plants*. Elsevier, pp. 255–272.
- Sipma, J., Osuna, B., Collado, N., Monclús, H., Ferrero, G., Comas, J., Rodriguez-Roda, I., (2010). Comparison of removal of pharmaceuticals in MBR and activated sludge systems. *Desalination*. **250**: 653.
- Skoog, D.A., Crouch, S.R., Holler, F.J., (2007). *Principles of Instrumental Analysis*. 6th ed. Belmont, CA: Thomson Brooks/Cole, p.169–173.
- Solá-Gutiérrez, C., Schröder, S., San-Román, M.F., Ortiz, I., (2020). Critical review on the mechanistic photolytic and photocatalytic degradation of triclosan. *J. Environ. Manage.*, **260**: 110101.
- Sophia, A.C., Lima, E.C., (2018). Removal of emerging contaminants from the environment by adsorption. *Ecotoxicol. Environ. Saf.*, **150**: 1–17.
- Štandeker, S., Veronovski, A., Novak, Z., Knez, Ž., (2011). Silica aerogels modified with mercapto functional groups used for Cu(II) and Hg(II) removal from aqueous solutions. *Desalination*, **269**: 223–230.
- Styszko, K., Nosek, K., Motak, M., Bester, K., (2015). Preliminary selection of clay minerals for the removal of pharmaceuticals, bisphenol A and triclosan in acidic and neutral aqueous solutions. *Comptes Rendus Chim.*, **18**: 1134–1142.
- Su, L., Tao, Q., He, H., Zhu, J., Yuan, P., Zhu, R., (2013). Silylation of montmorillonite surfaces: Dependence on solvent nature. *J. Colloid Interf. Sci.*, **391**: 16–20.
- Sui, Q., Huang, J., Deng, S., Yu, G., Fan, Q., (2010). Occurrence and removal of pharmaceuticals, caffeine and DEET in wastewater treatment plants of Beijing, China. *Water Res.*, **44**: 417-426.
- Sun, H.J., Rathinasabapathi, B., Wu, B., Luo, J., Pu, L.P., Ma, L.Q., (2014). Arsenic and selenium toxicity and their interactive effects in humans –Review. *Environ. Inter.*, **69**: 148–158.
- Suryan, S., Ahluwalia, S.S., (2012). Biosorption of heavy metals by paper mill waste from aqueous solution. *Int. J. Env. Sci.*, **2 (3)**: 1331–1343.

- Svenningsen, H., Henriksen, T., Priemé, A., Johnsen, A.R., (2011). Triclosan affects the microbial community in simulated sewage-drain-field soil and slows down xenobiotic degradation. *Environ. Pollut.*, **159**:1599–1605.
- Szalowska, E., van der Burg, B., Man H.Y., (2014). Model Steatogenic Compounds (Amiodarone, Valproic Acid, and Tetracycline) Alter Lipid Metabolism by Different Mechanisms in Mouse Liver Slices. *PLoS One.*, **9(1)**: 86795.
- Taha, A.A., Shreadah, M.A., Heiba, H.F., Ahmed, A.M., (2017). Validity of Egyptian Na-montmorillonite for adsorption of Pb^{2+} , Cd^{2+} and Ni^{2+} under acidic conditions: characterization, isotherm, kinetics, thermodynamics and application study. *Asia-Pac. J. Chem. Eng.*, **12**: 292–306.
- Tamez, C., Hernandez, R., Parsons, J.G., (2016). Removal of Cu (II) and Pb (II) from aqueous solution using engineered iron oxide nanoparticles. *Microchem. J.*, **125**: 97–104.
- Tang, L., Feng, H., Tang, J., Zeng, G., Deng, Y., Wang, J., Liu, Y., Zhou, Y., (2017). Treatment of arsenic in acid wastewater and river sediment by Fe@Fe₂O₃ nanobunches: The effect of environmental conditions and reaction mechanism. *Water Res.*, **117**: 175–186.
- Tanis, E., Hanna, K., Emmanuel, E., (2008). Experimental and modeling studies of sorption of tetracycline onto iron oxides-coated quartz. *Colloids Surf A Physicochem Eng Asp.*, **327**: 57–63.
- Tao, Q., Fang, Y., Li, T., Zhang, D., Chen, M., Ji, S., He, H., Komarneni, S., Zhang, H., Dong, Y., Noh, Y.D., (2016). Silylation of saponite with 3-aminopropyltriethoxysilane. *Appl. Clay Sci.*, **132–133**: 133–139.
- Tcheumi, H.L., Tonle, I.K., Ngameni, E., Walcarius, A., (2010). Electrochemical analysis of methylparathion pesticide by a gemini surfactant-intercalated clay-modified electrode. *Talanta*, **81**: 972–979.
- Te, B., Wichitsathian, B., Yossapol, C., (2017). Adsorptive behavior of low-cost modified natural clay adsorbents for arsenate removal from water. *Int. J. Geomate.*, **12(33)**: 1-7.
- Teh, C.Y., Budiman, P.M., Shak, K.P.Y., Wu, T.Y., (2016). Recent advancement of coagulation–flocculation and its application in wastewater treatment. *Ind. Eng. Chem. Res.*, **55**: 4363–4389.

- Terzic, A., Pezo, L., Andric, L., Pavlović, V.B., Mitic, V.V., (2016). Optimization of bentonite clay mechano-chemical activation using artificial neural network modelling. *Ceram. Int.*, **43(2)**: 2549-2562.
- Thanhmingliana, Lee, S.M., Tiwari, D., Prasad, S.K., (2015). Efficient attenuation of 17 α -ethynylestradiol (EE2) and tetracycline using novel hybrid materials: batch and column reactor studies. *RSC Adv.*, **5**: 46834–46842.
- Thanhmingliana, Tiwari, D., (2015). Efficient use of hybrid materials in the remediation of aquatic environment contaminated with micro-pollutant diclofenac sodium. *Chem. Eng. J.*, **263**: 364–373.
- Thue, P.S., Sophia, A.C., Lima, E.C., Wamba, A.G.N., de Alencar, W.S., dos Reis, G.S., Rodembusch, F.S., Dias, S.L.P., (2018). Synthesis and characterization of a novel organic-inorganic hybrid clay adsorbent for the removal of acid red 1 and acid green 25 from aqueous solutions. *J. Clean. Prod.*, **171**: 30–44.
- Tinkov, A.A., Filippini, T., Ajsuvakova, O.P., Aaseth, J., Gluhcheva, Y.G., Ivanova, J.M., Bjorklund, G., Skalnaya, M.G., Gatiatulina, E.R., Popova, E.V., Nemereshina, O.N., Vinceti, M., Skalny, M.A., (2017). The role of cadmium in obesity and diabetes. *Sci. Total. Environ.*, **601-602**: 741-755.
- Tiwari, A., Shukla, A., Lalliansanga, Tiwari, D., Lee, S.-M., (2019). Au-nanoparticle/nanopillars TiO₂ meso-porous thin films in the degradation of tetracycline using UV-A light. *J. Ind. Eng. Chem.*, **69**: 141–152.
- Tiwari, A., Shukla, A., Lalliansanga, Tiwari, D., Lee, S.M., (2020). Synthesis and characterization of Ag⁰ (NPs)/TiO₂ nanocomposite: insight studies of triclosan removal from aqueous solutions. *Environ. Technol.*, **41**: 3500–3514.
- Tiwari, D., Kim, H.U., Lee, S.M., (2007). Removal behavior of sericite for Cu(II) and Pb(II) from aqueous solutions: Batch and column studies. *Sep. Purif. Methods.*, **57**: 11–16.
- Tiwari, D., Lee, S.M., (2012). Novel hybrid materials in the remediation of ground waters contaminated with As (III) and As (V). *Chem. Eng. J.*, **204**: 23–31.
- Tonle, I.K., Ngameni, E. Njopwouo, D., Carteret, C., Walcarius, A., (2003). Functionalization of natural smectite-type clays by grafting with

- organosilanes: Physico-chemical characterization and application to mercury(II) uptake. *Phys. Chem. Chem. Phys.*, **5(21)**: 4951-4961.
- Tounsadi, H., Khalidi, A., Machrouhi, A., Farnane, M., Elmoubarki, R., Elhalil, A., Sadiq, M., Barka, N., (2016). Highly efficient activated carbon from *Glebionis coronaria* L. biomass: Optimization of preparation conditions and heavy metals removal using experimental design approach. *J. Environ. Chem. Eng.*, **4**: 4549–4564.
- Trinelli, M.A., Areco, M.M., Afonso Mdos, S., (2013). Co-biosorption of copper and glyphosate by *ulva lactuca*. *Colloids Surf. B.*, **105**: 251–258.
- Uddin, M.K., (2017). A review on the adsorption of heavy metals by clay minerals, with special focus on the past decade. *Chem. Eng. J.*, **308**: 438-462.
- Undabeytia, T., Madrid, F., Vázquez, J., Pérez-Martínez, J.I., (2019). Grafted sepiolites for the removal of pharmaceuticals in water treatment. *Clays Clay Miner.*, **67**: 173–182.
- United Nations., (2006). The 2nd UN World Water Development Report: Water, A shared responsibility.
- Unuabonah, E.I., Olu-Owolabi, B.I., Adebowale, K.O., Yang, L.Z., (2008). Removal of lead and cadmium ions from aqueous solution by polyvinyl alcohol-modified kaolinite clay: A novel nano-clay adsorbent. *Adsorp. Sci. Technol.*, **26(6)**:383-405.
- Unuabonah, E.I., Taubert, A., (2014). Clay–polymer nanocomposites (CPNs): Adsorbents of the future for water treatment–Review. *Appl. Clay Sci.*, **99**: 83–92.
- Valdés, O., Marican, A., Mirabal-Gallardo, Y., Santos, L.S., (2018). Selective and efficient arsenic recovery from water through quaternary amino-functionalized silica. *Polymers*, **10**: 626.
- Vandenberg, L.N., Colborn, T., Hayes, T.B., Heindel, J.J., Jacobs, D.R., Lee, D-H., Myers, J.P., Shioda, T., Saal, F.S., Welshons, W.V., Zoeller, R.T., (2013). Regulatory decisions on endocrine disrupting chemicals should be based on the principles of endocrinology. *Reprod. Toxicol.*, **38**: 1-15

- Vardhan, K.H., Kumar, P.S., Panda, R.C., (2019). A review on heavy metal pollution, toxicity and remedial measures: Current trends and future perspectives. *J. Mol. Liq.*, **290**: 111197.
- Verma, R., Kundu, L.M., Pandey, L.M., (2021). Decontamination of distillery spent wash through advanced oxidation methods, in: *Advanced Oxidation Processes for Effluent Treatment Plants*. Elsevier, pp. 103–117.
- Vidal, C.B., Oliveira, J.T., Raulino, G.S.C., Melo, D. de Q., Pessoa, G.P., Santos, A.B. dos, Nascimento, R.F. do, (2014). Removal of endocrine disruptors from wastewater with adsorption onto tin pillared montmorillonite. XX Congresso Brasileiro de Engenharia Química.
- Vidal, R.R.L., Moraes, J.S., (2019). Removal of organic pollutants from wastewater using chitosan: a literature review. *Int. J. Environ. Sci. Technol.*, **16**: 1741–1754.
- Viipsi, K., Sjöberg, S., Tõnsuaadu, K., Shchukarev, A., (2013). Cd²⁺ and Zn²⁺ sorption on apatite in the presence of EDTA and humic substance. *E3S Web Conf.*, **1(1)**: 01008.
- Vijayalakshmi, K., Gomathi, T., Latha, S., Hajeeth, T., Sudha, P.N., (2016). Removal of copper(II) from aqueous solution using nanochitosan/sodium alginate/microcrystalline cellulose beads. *Int. J. Biol. Macromol.*, **82**: 440–452.
- Visa, M., (2016). Synthesis and Characterization of New Zeolite Materials Obtained from Fly Ash for Heavy Metals Removal in Advanced Wastewater Treatment. *Powder Technol.*, **294**: 338-347.
- Vithanage, M., Herath, I., Joseph, S., Bundschuh, J., Bolan, N., Ok, Y.S., Kirkham, M.B., Rinklebe, J., (2017). Interaction of arsenic with biochar in soil and water: A critical review. *Carbon*, **113**: 219–230.
- Wahab, N., Saeed, M., Ibrahim, M., Munir, A., Saleem, M., Zahra, M., Waseem, A., (2019). Synthesis, characterization, and applications of Silk/Bentonite clay

- composite for heavy metal removal from aqueous solution. *Front. Chem.*, **7**: 654.
- Walcarius, A., Etienne, M., Bessière, J., (2002). Rate of access to the binding sites in organically modified silicates. 1. Amorphous silica gels grafted with amine or thiol groups. *Chem. Mater.*, **14**: 2757–2766.
- Walsh, A., (1955). The application of atomic absorption spectra to chemical analysis. *Spectrochim. Acta.*, **7**: 108 – 117.
- Wamba A.G.N., Kofa, G.P., Koungou, S.N., Thue, P.S., Lima, E.C., dos Reis, G.S., Kayem, J.G., (2018). Grafting of Amine functional group on silicate based material as adsorbent for water purification: A short review. *J. Environ. Chem. Eng.*, **6(2)**: 3192-3203.
- Wang, C., Yin, H., Bi, L., Su, J., Zhang, M., Lyu, T., Cooper, M., Pan, G., (2020a). Highly efficient and irreversible removal of cadmium through the formation of a solid solution, *J. Hazard. Mater.*, **384**: 121461.
- Wang, L., Liu, Y., Wang, C., Zhao, X., Mahadeva, G.D., Wu, Y., Ma, J., Zhao, F., (2018). Anoxic biodegradation of triclosan and the removal of its antimicrobial effect in microbial fuel cells. *J. Hazard. Mater.*, **344**: 669–678.
- Wang, L., Shi, Y., Yao, D., Pan, H., Hou, H., Chen, J., Crittenden, J.C., (2019). Cd complexation with mercapto-functionalized attapulgite (MATP): Adsorption and DFT study. *Chem. Eng. J.*, **366**: 569–576.
- Wang, S., Peng, Y., (2010). Natural zeolites as effective adsorbents in water and wastewater treatment. *Chem. Eng. J.*, **156**: 11–24.
- Wang, Y., Gong, S., Yazhuo Li, Y., Li, Z., Fu, J., (2020b). Adsorptive removal of tetracycline by sustainable ceramsite substrate from bentonite/red mud/pine sawdust. *Sci. Rep.*, **10**: 2960.

- Wasewar, K.L., Singh, S., Kansal, S.K., (2020). Process intensification of treatment of inorganic water pollutants. *Inorganic pollutants in water*. Elsevier, 245-271.
- Westerhoff, P., Yoon, Y., Snyder, S., Wert, E., (2005). Fate of endocrine-disruptor, pharmaceutical, and personal care product chemicals during simulated drinking water treatment processes. *Environ. Sci. Technol.*, **39**: 6649–6663.
- Westrup, J.L., Bertoldi, C., Cercena, R., Dal-Bó, A.G., Soares, R.M.D., Fernandes, A.N., (2021). Adsorption of endocrine disrupting compounds from aqueous solution in poly(butyleneadipate-co-terephthalate) electrospun microfibers. *Colloids Surf. A Physicochem. Eng. Asp.*, **611**: 125800.
- WHO, 3rd ed., (2008). *Guidelines for Drinking Water Quality: Recommendations*, vol. 1, World Health Organisation, Geneva.
- Wołowiec, M., Komorowska-Kaufman, M., Pruss, A., Rzepa, G., Bajda, T., (2019). Removal of Heavy Metals and Metalloids from Water Using Drinking Water Treatment Residuals as Adsorbents: A Review. *Minerals*, **9**: 487.
- Wu, H., Xie, H., He, G., Guan, Y., Zhang, Y., (2016). Effects of the pH and anions on the adsorption of tetracycline on iron-montmorillonite. *Appl. Clay Sci.*, **119**: 161–169.
- Wu, J., Ling, L., Xie, J., Mab, G., Wang, B., (2014). Surface modification of nanosilica with 3-mercaptopropyl trimethoxysilane: Experimental and theoretical study on the surface interaction. *Chem. Phy. Lett.*, **591** : 227–232.
- Xi, J., Duan, Q., Luo, Y., Xie, Z., Liu, Z., Mo, X., (2017). Climate change and water resources: Case study of eastern monsoon region of China. *Adv. Clim. Change Res.*, **8 (2)**: 63-67.
- Xiong, W., Zeng, Z., Li, X., Zeng, G., Xio, R., Yang, Z., Zhou, Y., Zhang, C., Cheng, M., Hu, L., Zhou, C., Qin, L., Xu, R., Zhang, Y., (2018). Multi-walled carbon nanotube/amino functionalized MIL-53(Fe) composites: Remarkable adsorptive removal of antibiotics from aqueous solutions. *Chemosphere*, **210**: 1061-1069.

- Xu, M., McKay, G., (2017). Removal of Heavy Metals, Lead, Cadmium, and Zinc, Using Adsorption Processes by Cost-Effective Adsorbents. in: Bonilla-Petriciolet, A., Mendoza-Castillo, D.I., Reynel-Ávila, H.E. (Eds.), Adsorption Processes for Water Treatment and Purification. Springer International Publishing, Cham, pp. 109–138.
- Xu, Y.H., Nakajima, T., Ohki, A., (2002). Adsorption and removal of arsenic(V) from drinking water by aluminum-loaded shirasu-zeolite. *J. Hazard. Mater.*, **92(3)**:275-87.
- Yadav, V.B., Gadi, R., Kalra, S., (2019). Clay based nanocomposites for removal of heavy metals from water: A review. *J. Environ. Manage.*, **232**: 803–817.
- Yan, G., Viraraghavan, T., (2011). Heavy metal removal in a biosorption column by immobilized *M. Rouxii* biomass. *Bioresour. Technol.*, **78**: 243 – 249.
- Yang, X., Xia, L., Song, S., (2017). Arsenic adsorption from water using graphene-based materials as adsorbents: A critical review. *Surf. Rev. Lett.*, **24(1)**: 1730001.
- Yari, S., Abbasizadeh, S., Mousavi, S.E., Moghaddam, M.S., Moghaddam, A.Z., (2015). Adsorption of Pb(II) and Cu(II) ions from aqueous solution by an electrospun CeO₂ nanofiber adsorbent functionalized with mercapto groups. *Process Saf. Environ.*, **94**: 159–171.
- Yi, L., Zuo, L., Wei, C., Fu, H., Qu, X., Zheng, S., Xu, Z., Guo, Y., Li, H., Zhu, D., (2020). Enhanced adsorption of bisphenol A, tylosin, and tetracycline from aqueous solution to nitrogen-doped multiwall carbon nanotubes via cation- π and π - π electron-donor-acceptor (EDA) interactions. *Sci. Total Environ.*, **719**: 137389
- Yılmaz, S., Sahan, T., Karabakan, A., (2017). Response surface approach for optimization of Hg(II) adsorption by 3-mercaptopropyl trimethoxysilane-modified kaolin minerals from aqueous solution . *Korean J. Chem. Eng.*, **34(8)**: 2225-2235.

- Yin, H., Kong, M., Gu, X., Chen, H., (2017). Removal of arsenic from water by porous charred granulated attapulgite-supported hydrated iron oxide in bath and column modes. *J. Clean. Prod.*, **166**: 88–97.
- Youssef, Y.M., Moukhtar, N., Hassan, I., Abdel-Aziz, M. H., (2020). Recovery of heavy metals from liquid effluent by galvanic cementation. *Mining Metal. Explor.*, **38**: 177–186.
- Yu, L., Cao, W., Wu, S., Yang, C., Cheng, J., (2018). Removal of tetracycline from aqueous solution by MOF/graphite oxide pellets: Preparation, characteristic, adsorption performance and mechanism. *Ecotoxicol. Environ. Saf.*, **164**: 289–296.
- Yu, W., Deng, L., Yuan, P., Liu, D., Yuan, W., Liu, P., He, H., Li, Z., Chen, F., (2015). Surface silylation of natural mesoporous/macroporous diatomite for adsorption of benzene. *J. Colloid Interface Sci.*, **448**: 545-552.
- Yu, Y., Addai-Mensah, J., Losic, D., (2012). Functionalized diatom silica microparticles for removal of mercury ions. *Sci. Technol. Adv. Mater.*, **13**: 015008.
- Zafar, S., Khan, M.I., Lashari, M.H., Khraisheh, M., Almomani, F., Mirza, M.L., Khalid, N., (2020). Removal of copper ions from aqueous solution using NaOH-treated rice husk. *Emergent Mater.*, **3**: 857–870.
- Zanin, E., Scapinello, J., de Oliveira, M., Rambo, C.L., Franscescon, F., Freitas, L., de Mello, J.M.M., Fiori, M.A., Oliveira, J.V., Dal Magro, J., (2017). Adsorption of heavy metals from wastewater graphic industry using clinoptilolite zeolite as adsorbent. *Process Saf. Environ. Prot.*, **105**: 194–200.
- Zayyat, R. M., Suidan, M.T., (2018). Attenuation of 17 α -ethynylestradiol onto model vegetable waste. *Clean Technol. Environ. Policy*, **20**:2275–2286
- Zermane, F., Bouras, O., Baudu, M., Basly, J.-P., (2010). Cooperative coadsorption of 4-nitrophenol and basic yellow 28 dye onto an iron organo–inorgano pillared montmorillonite clay. *J. Colloid Interface Sci.*, **350**: 315–319.
- Zhang, J., Ding, T., Zhang, Z., Xu, L., Zhang, C., (2015). Enhanced adsorption of trivalent arsenic from water by functionalized diatom silica shells. *PLoS One*, **10(4)**: e0123395.

- Zhang, J., Xiong, Z., Li, C., Wu, C., (2016). Exploring a thiol-functionalized MOF for elimination of lead and cadmium from aqueous solution. *J. Mol. Liq.*, **221**: 43–50.vv
- Zhang, X., Lin, X., He, Y., Chen, Y., Luo, X., Shang, R., (2019). Study on adsorption of tetracycline by Cu-immobilized alginate adsorbent from water environment. *Int. J. Biol. Macromol.*, **124**: 418–428.
- Zhang, Y., Zhou, J.L., (2005). Removal of estrone and 17 β -estradiol from water by adsorption. *Water Res.*, **39**: 3991–4003.
- Zhang, Z., Li, H., Liu, H., (2018). Insight into the adsorption of tetracycline onto amino and amino-Fe³⁺ functionalized mesoporous silica: Effect of functionalized groups. *J. Environ. Sci.*, **65**: 171–178.
- Zhao, Y., Gao, Q., Tang, T., Xu, Y., Wu, Dong., (2011). Effective NH₂-grafting on mesoporous SBA-15 surface for adsorption of heavy metal ions. *Mater. Letters.*, **65** : 1045-1047.
- Zhao, Y., Zhan, L., Xue, Z., Yusef, K.K., Hu, H., Wu, M., (2020). Adsorption of Cu(II) and Cd(II) from wastewater by sodium alginate modified materials. *Materials. J. Chem.*, **2020**:1–13.
- Zhou, Y., Liu, X., Xiang, Y., Wang, P., Zhang, J., Zhang, F., Wei, J., Luo, L., Lei, M., Tang, L., (2017). Modification of biochar derived from sawdust and its application in removal of tetracycline and copper from aqueous solution: Adsorption mechanism and modelling. *Bioresour. Technol.*, **245**: 266-273.
- Zhu, L., Tian, S., Zhu, J., Shi, Y., (2007a). Silylated pillared clay (SPILC): A novel bentonite-based inorgano-organocomposite sorbent synthesized by integration of pillaring and silylation. *J. Colloid Interface Sci.*, **315**: 191–199.
- Zhu, R., Chen, Q., Zhou, Q., Xi, Y., Zhu, J., He, H., (2016). Adsorbents based on montmorillonite for contaminant removal from water: a review. *Appl. Clay Sci.*, **123**: 239–258.
- Zhu, Z., Ma, H., Zhang, R., Ge, Y., Zhao, J., (2007b). Removal of cadmium using MnO₂ loaded D301 resin. *J. Environ. Sci.*, **19**: 652–656.

Zorrilla, L. M., Gibson, E. K., Jeffay, S. C., Crofton, K. M., Setzer, W. R., Cooper, R. L. & Stoker, T. E. (2009). The effects of triclosan on puberty and thyroid hormones in male *Wistar rats*. *Toxicol. Sci.*, **107** (1): 56.

BIO-DATA

1. **NAME** : R. Malsawmdawngzela
2. **DATE OF BIRTH** : 16th October, 1988.
3. **FATHER'S NAME** : R. Liankhuma
4. **PERMANENT ADDRESS** : 30, Vengthar, Kawnpui, 796070.
5. **EDUCATIONAL QUALIFICATIONS :**

Qualification	Year of Passing	Board/University	Subjects	% of Marks	Division
HSLC	2005	Mizoram Board of School Education	English, Mizo, Science, Social Sciences, Mathematics	78.4	Distinction
HSSLC	2007	Mizoram Board of School Education	English, Mizo, Chemistry, Physics, Mathematics	45.6	Third
B.Sc (Chemistry)	2012	Mizoram University	Chemistry, Physics, Mathematics	53.25	Second
M.Sc (Chemistry)	2014	Mizoram University	Physical Chemistry(specialization), Analytical Chemistry, Organic Chemistry, Inorganic Chemistry	69.9	First

PARTILCULARS OF THE CANDIDATE

NAME OF CANDIDATE : R.Malsawmdawngzela
DEGREE : Doctor of Philosophy (Ph.D.)
DEPARTMENT : Chemistry
TITLE OF THESIS : Silane functionalized composite materials in the remediation of aquatic environment contaminated with some micro-pollutants and heavy metal toxic ions.

DATE OF ADMISSION : 17th August, 2015

APPROVAL OF RESEARCH PROPOSAL

1. **B.O.S** : 13th April 2016
2. **SCHOOL BOARD** : 21st April 2016
3. **MZU REGN. NO.** : 882 of 2007-08
4. **Ph.D. REGISTRATION NO.**
& **DATE** : MZU/Ph.D/848 of 21.04.2016
5. **EXTENSION** : Extension period 21.04.2016
to 21.04.2022
(No.16-2/MZU(Acad)20/391-393)

Head

Department of Chemistry

LIST OF PUBLICATIONS

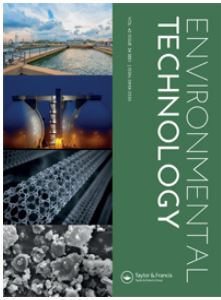
(A) Journals:

1. **Malsawmdawngzela, R.,** Tiwari, D., (2021). 17α -ethinylestradiol elimination using synthesized and dense nanocomposite materials: Mechanism and real matrix treatment. *Korean Journal of Chemical Engineerin*, Paper Online: DOI: 10.1007/s11814-021-0958-2
2. **Malsawmdawngzela, R.,** Siama, L., Tiwari, D., Lee, S.M., Kim, D.J., (2021). Efficient and selective use of functionalized material in the decontamination of water: Removal of emerging micro-pollutants from aqueous wastes. *Environmental Technology*, 31: 1-15. Paper Online: <https://doi.org/10.1080/09593330.2021.1994654>
3. **Malsawmdawngzela, R.,** Diwakar Tiwari. Facile synthesis and implications of novel hydrophobic materials: Newer insights of pharmaceuticals removal. *Indian Journal of Biochemistry and Biophysics*, 58: 520-531.
4. **Malsawmdawngzela, R.,** Lalhmunsiana, Tiwari, D., (2021). Novel and Highly Efficient Functionalized Bentonite for Elimination of Cu^{2+} and Cd^{2+} from Aqueous Wastes. *Environmental Engineering Research*, 27(6): 210355.
5. **Malsawmdawngzela, R.,** Sarikokba, Thanhmingliana, Tiwari, D., Lee, S.M., (2021). Hybrid materials precursor to natural bentonite in the decontamination of Alizarin Yellow from aqueous solutions. *Environmental Engineering Research*, 27(6): 210104.
6. **Malsawmdawngzela, R.,** Thanhmingliana, Tiwari, D., (2021). Sorption of rhodamine B dye onto bentonite clay-silane composite materials. *Science and Technology Journal*, 9(2): ISSN: 2321-3388.
7. **Ralte Malsawmdawngzela,** Lalhmunsiana, Diwakar Tiwari, Seung-Mok Lee and Dong-Jin Kim. (2021). Synthesis of novel clay-based nanocomposite and its application in the remediation of arsenic contaminated water. *Journal of Environmental Science and Technology*, (Communicated).

(B) Conferences/Seminar:

1. **R.Malsawmdawngzela**, Ngainunsiami, Seung-Mok Lee and Diwakar Tiwari. Silane Grafted Bentonite Clay In The Remediation of Copper From Aquatic Environment. The International Conference on Chemistry and Environmental Sustainability (ICCES-2019), from 19th – 22nd February 2019. Organized by Department of Chemistry, School of Physical Sciences, Mizoram University, Aizawl, Mizoram, India.
2. **R.Malsawmdawngzela** and Diwakar Tiwari. Efficient use of hybrid material in the remediation aqueous solutions contaminated with antibiotic tetracycline. National Conference on Emerging Trends In Environmental Research (NACETER 2019), organized by Department of Environmental Science, Pachhunga University College, Aizawl in collaboration with Environment, Forest and Climate Change Department, Government of Mizoram, during 31 October – 2 November 2019.
3. **R.Malsawmdawngzela** and Diwakar Tiwari. “Efficient Use of Silane Grafted Bentonite in the Remediation of Aqueous Solutions Contaminated with Rhodamine B” in the 2nd Annual Convention of North East (India) Academy of Science and Technology (NEAST) & International Seminar on Recent Advances in Science and Technology (IRSRAST) during 16th – 18th November 2020 (Virtual) organized by NEAST, Mizoram University, Aizawl- 796004, Mizoram (India).
4. **R.Malsawmdawngzela** and **Diwakar Tiwari**. Surface Functionalized Bentonite Clay in the Decontamination of Water: Removal of Cadmium (II) from Aqueous Solutions. National Conference on Functional Materials and Applications – 2019 (NCFMA-2019), organized by Department of BS&HSS (Physics), N.I.T. Mizoram during November 22nd – 23rd, 2019.
5. Lalchhingpuii, **R.Malsawmdawngzela**, Lalhmunsiamia and Diwakar Tiwari. Synthesis of functionalized biomaterials and its application in the effective remediation of aquatic environment contaminated with Cr(VI). 13th- 14th October, 2016, Mizoram Science Congress, Mizoram University, Aizawl, Mizoram.

6. Lalchhingpuii, **R.Malsawmdawngzela** and Diwakar Tiwari. Synthesis and application of mesoporous silica materials for the efficient removal of Cd(II) from aqueous solutions, National Symposium on advances in Chemical Sciences.(NSACS-2017), 11th to 12th January, 2017, Assam University, Silchar, Assam, India.





Efficient and selective use of functionalized material in the decontamination of water: removal of emerging micro-pollutants from aqueous wastes

Ralte Malsawmdawngzela, Lalhmunsiam Siam, Diwakar Tiwari, Seung-Mok Lee & Dong-Jin Kim

To cite this article: Ralte Malsawmdawngzela, Lalhmunsiam Siam, Diwakar Tiwari, Seung-Mok Lee & Dong-Jin Kim (2021): Efficient and selective use of functionalized material in the decontamination of water: removal of emerging micro-pollutants from aqueous wastes, Environmental Technology, DOI: [10.1080/09593330.2021.1994654](https://doi.org/10.1080/09593330.2021.1994654)


To link to this article: <https://doi.org/10.1080/09593330.2021.1994654>

 View supplementary material [↗](#)

 Published online: 31 Oct 2021.

 Submit your article to this journal [↗](#)

 Article views: 2

 View related articles [↗](#)

 View Crossmark data [↗](#)



Facile synthesis and implications of novel hydrophobic materials: Newer insights of pharmaceuticals removal

Ralte Malsawmdawngzela¹, Lalhmunsiam² & Diwakar Tiwari^{1*}

¹Department of Chemistry; & ²Department of Industrial Chemistry, Mizoram University, Aizawl-796 004, India

Received 15 December 2020; revised 18 March 2021

The residual escape of pharmaceuticals from wastewater treatment plants (WWTP) is a serious environmental concern due to the adverse effects towards living organisms. Therefore, it is important to devise the newer technologies for safe and efficient elimination of emerging micro-pollutants from effluents of existing water treatment plants. Bentonite is grafted with 3-mercaptopropyletrimethoxy silane by facile one-pot method to obtain dense composite material (MPTS/BENT). The materials are characterized by the FT-IR, XRD, BET and SEM/EDX analytical tools. Various parametric experiments conducted for the removal of tetracycline hydrochloride (TCH) and triclosan (TCS) using MPTS/BENT under batch experimentations. Further, column adsorption experiments have been performed. The incorporation of organosilane with bentonite is confirmed by FT-IR and EDX analyses. BET surface area analysis showed that the surface area of MPTS/BENT is significantly small compared with pristine clay. pH dependent sorption of TCH and TCS is almost unaffected within the pH 3.0 to 7.0. Rapid uptake of TCH and TCS by MPTS/BENT followed PSO kinetics. High percentage removal was achieved at wide concentration range of pollutants. The uptake of TCH and TCS is unaffected on increasing the background electrolyte concentrations for 1000 times. Column experiment confirmed the high efficiency of MPTS/BENT towards these pollutants. Moreover, the removal of TCH/or TCS from real water sample at varied pH values showed that the synthesized composite is selective and efficient towards these micro-pollutants. This study showed that the synthesized material, *i.e.*, MPTS/BENT could be efficiently employed for the additional purification of WWTP effluents.

Keywords: Fixed bed reactors, Hydrophobic materials, Mechanism of removal, Newer insights, Pharmaceuticals, Real matrix treatment

Pharmaceuticals and personal care products (PPCPs) received greater attention in recent times because of its uncertainty imposed to human beings for prolonged exposure at lower concentrations¹. The drug compounds administered to human or live-stocks is only partially metabolized in the biological systems and in bulk *Ca.* 60-70% is excreted through the urine or feces and enhancing the pollutants load on the water bodies². Moreover, the existing wastewater treatment (WWT) plants are not efficient or designed to eliminate these calcitrant pollutants efficiently hence, these compounds can easily go through the WWT plants at lower concentration levels and entered into the water bodies. Consequently, these micro-pollutants detected even in the drinking water systems^{3,4}. This imposes greater risks to human and even impact adversely the microbiological ecology and the ecological functions as well^{5,6}. Therefore,

these compounds are known to be emerging pollutants and needs greater attention for its effective and efficient removal from water bodies.

Tetracycline (TC) is one of the widely prescribed antibiotic to human and live stocks to prevent infectious diseases⁷. Animal manure considerably enhanced the tetracycline load in soil since soil readily adsorbs the tetracycline⁸. It is known fact that the bioaccumulation of tetracycline through the food chain showed antibiotic-resistance in microorganisms and having several chronic and acute diseases to human⁹. Further, gastrointestinal distress and skin lesions are the major side effects of tetracyclines¹⁰. Additionally, a prolonged exposure of tetracycline in human affects liver and kidney^{11,12} or cause an acute hepato-nephrotoxicity¹³. TC with four rings fused together has tricarbonylamide, phenolic diketone and dimethylamino functional groups and it is slightly soluble in water¹⁴. The amino and enone groups are lack of electron whereas phenolic group is rich with electron. Tetracycline possessed three different pK_a values *viz.*, 3.30, 7.7 and 9.7¹⁵⁻¹⁷.

*Correspondence

Phone: +91-9862323015 (Mob)

E-mail: diw_tiwari@yahoo.com

Suppl. Data available on respective page of NOPR

17 α -Ethinylestradiol elimination using synthesized and dense nanocomposite materials: Mechanism and real matrix treatment

Ralte Malsawmdawngzela and Diwakar Tiwari[†]

Department of Chemistry, Mizoram University, Aizawl-796004, India
(Received 14 July 2021 • Revised 12 September 2021 • Accepted 14 September 2021)

Abstract—Endocrine disrupting chemicals (EDCs) are emerging water contaminants and efficient elimination is a greater challenge for environmental engineers. The present communication is intended to synthesize the novel dense nanocomposite materials precursors to the bentonite and 3-mercaptopropyletrimethoxy silane/or 3-aminopropyltriethoxy silane. The materials are highly dense, hence the surface area is significantly reduced compared to the pristine bentonite. Further, the materials are intended to be utilized in the elimination of one of the important EDC 17 α -ethinylestradiol (EE2). The sorption mechanism is greatly demonstrated based on various parametric studies. It is shown that grafted silane with bentonite network provides enhanced hydrophobicity with organophilic nature and greatly favors the uptake of EE2 at a wide range of pH (5.0-10.0). Relatively rapid uptake of EE2 by the nanocomposite solids followed by a pseudo-second-order kinetic model indicated that the materials are highly efficient for elimination of EE2. Increasing the concentration of EE2 (1.0 to 10.0 mgL⁻¹) favored the extent of removal of EE2 and followed the Langmuir adsorption isotherm. Further, the increase in background electrolytes by 1,000 times did not affect the removal of EE2 by these nanocomposites, indicating the sorbing species are attracted with relatively stronger forces. Moreover, the simultaneous presence of several co-ions did not affect the percentage elimination of EE2; this, perhaps, shows an enhanced selectivity of materials towards the 17 α -ethinylestradiol. A high loading capacity of EE2 is achieved under column reactor operation using these nanocomposites. Additionally, the materials are promising in the real matrix treatment.

Keywords: 17 α -Ethinylestradiol Elimination, Real Matrix Treatment, Nanocomposites, Silane Grafted Bentonite, Fixed-bed Treatment, Hydrophobic Interactions

INTRODUCTION

An enhanced level of emerging micro-pollutants, including pharmaceuticals or personal care products, in water bodies has received global attention and it poses greater challenges to maintaining water quality. The diverse chemical compositions and potential of micro-pollutants, as well as the intricate network of exposure pathways, create innumerable problems to researchers or regulatory bodies for possible solutions [1,2]. These pollutants are increasingly entering into the terrestrial environment as toxic chemicals, and due to their persistence in nature are partly eliminated from biological treatment plants. It is pointed out that even at low concentrations, these micro-pollutants are active and stable in the water bodies, which shows a long exposure to aquatic life [3]. Similarly, the endocrine disrupting chemicals (EDC) are posing serious concern due to the negative impact on human beings [4]. The Environmental Protection Agency (EPA) has described endocrine disruptors (EDCs) as, “exogenous compounds which intervene the production, emission, binding and movement of natural hormones which are essential for the growth and function of living organisms” [5]. EDCs are classified as natural and synthetic estrogens, which affect the biological systems of aquatic organisms even at very low concentra-

tions, i.e., 0.1 ngL⁻¹ [6]. The most harmful endocrine disruptor is known to be ethinyl estradiol (EE2), the major primary substance used in contraceptive pills and postmenopausal hormone supplements [4,7,8]. EE2 is commonly detected in domestic sewage systems and some industrial wastewaters [9,10]. Human urine is regarded as the primary source of estrogens in wastewater [11]. Previous study reported that a significant amount of free EE2 is detected in wastewaters and having the concentration of 7-42 ngL⁻¹ from the effluents of wastewater treatment plants [12]. It was also reported that treated water for drinking in Germany contained a significant amount of EE2 at 0.5 ngL⁻¹ [13]. According to several reports, human health is significantly affected by EE2 and causes diseases such as disorders of the reproductive system, cancer and impotence [14-16]. Compared to natural estrogens, the half-life of EE2 is longer and is more harmful [17]. EE2 is readily gathered in silt and ecosystems [18] and hence, the concentrations of EE2 ranged from 0.1-10 ngL⁻¹ which affected the life of fish and other organisms in water [19]. Research conducted by spiking a lake in Canada with EE2 concentration 5-6 ngL⁻¹, resulted in the deaths of the entire fish population [20].

Several methods, including adsorption [21], advanced oxidation process [22], membrane filtration [23], biological treatment [24] are often demonstrated for efficient removal of EE2. Among these methods, adsorption using advanced and efficient materials has attracted greater interest in elimination or retaining contaminants [25,26]. The method is versatile and sorption properties can

[†]To whom correspondence should be addressed.

E-mail: diw_tiwari@yahoo.com

Copyright by The Korean Institute of Chemical Engineers.

Sorption of Rhodamine B Dye onto Bentonite Clay-silane Composite Materials

Ralte Malsawmdawngzela¹, Thanhmingliana² and Diwakar Tiwari*

¹Department of Chemistry, School of Physical Sciences, Mizoram University, Aizawl, Mizoram, India

²Department of Chemistry, Pachhunga University College, Mizoram University, Aizawl, Mizoram, India

*Email: diw_tiwari@yahoo.com

Abstract—The aim of this communication is to assess the sorption behavior of silanes grafted bentonite composite materials for Rhodamine B (RhB) from aqueous solution. The nanocomposites were synthesized by functionalization of the bentonite with 3-mercaptopropyltrimethoxysilane and 3-aminopropyltriethoxysilane under inert atmosphere. The batch experimental data indicated that the composite materials showed high percentage removal of RhB over a wide pH range, i.e., pH ~4.0 to 10.0. A high percentage removal of RhB was achieved within the concentrations studied from 1.0 to 25.0 mgL⁻¹. Langmuir and Freundlich adsorption isotherm were obtained using equilibrium state sorption data. The equilibrium sorption was attained within 180 min of contact and the kinetic model best fitted the pseudo-second-order model. Further, the change in background electrolyte (NaCl) concentrations from 0.0001 to 0.1 molL⁻¹ NaCl and the presence of co-existing ions do not significantly affect the sorption of RhB by the composite sorbents except for EDTA.

Keywords: Bentonite, Silanes, Composite Material, Rhodamine B, Sorption

INTRODUCTION

Surplus amount of dyes have been discharged into the environment over the last decades due to the rapid development of printing and dyeing industries. Dyes are common chemical compounds that are extensively used to color a variety of items including textiles, paper, rubber, leather and printing (Rocha *et al.* 2016; Sharma *et al.* 2021; Zhou *et al.* 2019). And several nations are basically depending on this industry (Holkar *et al.* 2016; Mani *et al.* 2019). Despite the fact that the textile industry is one of the largest industries in the world; however, it discharges massive quantity of dyes, toxic heavy metals and other chemicals in the effluent. Therefore, the main environmental impact in the textile industry is manifested by the discharge of large amounts of chemical dyes into the receiving environment (Toprak and Anis 2017; Muthu 2017). Dyes are classified into two categories *viz.*, natural and synthetic dyes. Synthetic dyes are both ionic and non-ionic. Non-ionic dyes are further classified into anionic and cationic dyes whereas non-ionic dyes are vat and dispersion dyes (Ngulube *et al.* 2017; Zhou *et al.* 2015). Over ten thousand dyes and pigments are estimated to be utilized in industry

and around 0.7 million tonnes of dyes are produced annually (Azari *et al.* 2020; Munagapati and Kim 2017; Ougubue and Sawidis 2011).

Dyes are chemical compounds in which electrons can delocalize due to the presence of aryl rings and can form bond with substances thereby producing color (Carmen and Daniela 2012). According to a research, approximately 200,000 tons of dye generated is wasted each year through the textile treatment process and finishing stages (Tara *et al.* 2019). Dyes can produce coloration in water with less than 1 mgL⁻¹ (Gupta *et al.* 2003; Rafatullah *et al.* 2010) and thus the effluent containing high colored dyes can alter the solubility of gas, pH and temperature on water bodies (Verma *et al.* 2012). Dyes such as direct, reactive, acids and basic dyes are highly soluble in water and are inconvenient to eliminate using conventional techniques (Mahapatra 2016). Furthermore, these colored dyes blocked the light penetration through water thereby decreasing the rate of photosynthesis of autotrophic organisms. As a result, the food web and their population are significantly affected (Albadarin *et al.* 2014; Lellis *et al.* 2019). Decomposition of certain dyestuff produced toxic products and metal complex dyes released toxic heavy metals into water bodies. Because of their high solubility in

ABSTRACT

**SILANE FUNCTIONALIZED COMPOSITE MATERIALS IN
THE REMEDIATION OF AQUATIC ENVIRONMENT
CONTAMINATED WITH SOME MICRO-POLLUTANTS AND
HEAVY METAL TOXIC IONS**

**A THESIS SUBMITTED IN PARTIAL FULFILLMENT OF THE
REQUIREMENTS FOR THE DEGREE OF DOCTOR OF
PHILOSOPHY**

R.MALSAWMDAWNGZELA

MZU REGISTRATION NUMBER: 882 OF 2007-08

PH.D REGISTRATION NUMBER: MZU/PH.D/848 OF 21.4.2016



**DEPARTMENT OF CHEMISTRY
SCHOOL OF PHYSICAL SCIENCES**

NOVEMBER, 2021

ABSTRACT

**SILANE FUNCTIONALIZED COMPOSITE MATERIALS IN THE
REMEDICATION OF AQUATIC ENVIRONMENT CONTAMINATED WITH
SOME MICRO-POLLUTANTS AND HEAVY METAL TOXIC IONS**

BY

R.MALSAWMDAWNGZELA

Department of Chemistry

Under the supervision of

Prof. Diwakar Tiwari

Submitted

**In partial fulfillment of the requirement of the Degree of Doctor of Philosophy
in Chemistry of Mizoram University, Aizawl.**

ABSTRACT

Water is a basic need of living organisms and the supply of clean water is important for healthy life; however, the shortage of clean water has become a serious concern around the globe. The scarcity of fresh water is one of the main public health concerns in developing countries, which may even more severe in the developing nations or in under developed nations. Therefore, the availability/supply of clean and safe water is a greater concern and also due to the scarcity of fresh water a proper management of water is even more important. The discharge of untreated or partially treated sewage or industrial wastewaters is greatly contaminating the fresh water. The two major chemicals that are polluting water on the surface and ground waters are organic and inorganic contaminants. Various water pollutants are present at concentrations exceeding the permissible levels and posing serious threat to living organisms including human.

Wastewater treatment technologies are intended to remove/eliminate variety of toxic pollutants and provide clean water which is demanded by the government body regulations. However, a large number of pollutants such as arsenic, toxic heavy metals and micro-pollutants are reported to escape from the existing wastewater treatment plants since the existing treatment plants are not efficient enough to remove these pollutants at required low levels. The escaped pollutants through the effluent of treated wastewaters thereby enter into the water bodies and contaminating the water resources to a greater extent. Therefore, there is an urgent need to develop the efficient advanced treatment technologies which could be annexed with the existing wastewater treatment plants to remove/eliminate efficiently the micro-pollutants along with the heavy metal toxic ions from the effluent of wastewaters.

A wide range of materials are utilized as sorbent materials for the treatment of polluted waters. Among these materials, clay minerals and its modified forms are found to be suitable materials for wastewater treatment technologies due to their large abundance and comparatively low cost. The presence of exchangeable cations, micro-porosity, surface functional groups as well as the net charge possessed by clay minerals make it a potential natural adsorbent to be employed for decontamination of polluted waters. However, clay materials have a low sorption capacity and selectivity

for a variety of organic contaminants as well as anionic contaminants. Therefore, the incorporation of an appropriate organic molecule within clay structure makes it suitable for the attenuation of a variety of organic and inorganic contaminants.

Clay minerals are functionalized using a suitable organic molecule in order to increase its selectivity and applicability. Recent study is an attempt to graft efficiently the variety of silane within the bentonite network. The applicability of silylated clay is manifold as it possessed strong bond formation between clay and organic moieties hence, restricted the leaching of organic moieties into the water bodies and preventing the secondary contamination. Moreover, the functionalized materials are having greater mechanical strength and showed selectivity towards the variety of organic and inorganic pollutants. However, grafting of silane molecules within the clay network is challenging. Therefore, keeping in view, the present study intended to functionalize the natural bentonite (BN) clay with 3-mercaptopropyl trimethoxy-silane (MPTS) and 3-aminopropyl triethoxysilane (APTES) to obtain BNMPTS and BNAPTES functionalized materials. Further, these materials were employed in the efficient elimination of toxic heavy metals such as As(III), As(V), Cu(II) and Cd(II), and the emerging micro-pollutants such as tetracycline hydrochloride (TC), Triclosan (TCS) and 17 α -ethynylestradiol (EE2) under batch and column reactor operations.

Bentonite was successfully functionalized with 3-mercaptopropyl trimethoxysilane and 3-aminopropyl triethoxysilane in a facile synthetic route conducted in nitrogen atmosphere using toluene as a solvent. The raw bentonite along with the functionalized materials were characterized by the fourier transform-infrared spectrometry (FT-IR), scanning electron microscope (SEM), transmission electron microscope (TEM) and the elemental spectra of solids was obtained by the energy-dispersive X-ray spectroscopy (EDX). X-ray diffraction method was used to evaluate structural property of the materials. Further, the BET surface area analyzer was employed to obtain the specific surface area, pore size and pore volume of the materials. Moreover, the functionalized materials before and after the sorption of Cu(II) and Cd(II) were analysed using the X-ray photoelectron spectroscopy (XPS).

The FT-IR data showed the successful introduction of organosilane within the clay network. The SEM image showed that BNMPTS and BNAPTES materials

possessed more compact structures compared to the pristine bentonite. The XRD data showed that intensity of diffraction signal is reduced significantly after the immobilization of organosilane on the bentonite clay. The TEM images of raw bentonite and functionalized materials clearly showed straight lattice fringes without deflection and the basal spacing of raw bentonite and functionalized clay obtained by TEM analyses were similar to that obtained by XRD analyses. The BET analysis revealed that all the materials possessed type IV isotherm with mesoporous structure and the specific surface area of the functionalized materials is reduced significantly after the incorporation of organosilane.

The functionalized materials along with the pristine bentonite were employed for the removal of As(III) and As(V) under batch study. Results showed that the functionalized materials possessed significantly enhanced percentage removal of As(III) and As(V) at wide range of pH 4.0 to 7.0. An increase in concentration of As(III) or As(V) showed a slight decrease in the percentage removal of these pollutants using the functionalized materials and the isotherm is fitted well to the Langmuir adsorption isotherm. A rapid uptake of As(III) and As(V) by these functionalized materials followed the pseudo-second-order rate kinetics. Increasing the concentrations of background electrolyte concentrations from 0.001 to 0.1mol/L NaCl, the percentage removal of these two pollutants was not affected which inferred that sorbate species forming an 'inner sphere complex' at the surface of functionalized solid. The presence of co-existing cations and anions except, EDTA and phosphate did not affect the percentage removal of As(III) and As(V) by these functionalized materials.

Further, the functionalized materials were employed in the removal of Cu(II) and Cd(II) using BNMPTS. The pH study showed that the very high percentage removal of Cu(II) and Cd(II) was almost unaffected within the studied pH range which showed greater affinity of Cu(II) and Cd(II) towards the composite material. Increasing the initial concentration of Cu(II) and Cd(II), background electrolyte concentrations (1000 times) and the presence of cations and anions, except EDTA did not affect the percentage removal of Cu(II) and Cd(II) using BNMPTS. The sorption isotherm performed for Cu(II) and Cd(II) followed Langmuir adsorption isotherm. A very fast uptake of these metal cations by BNMPTS solid followed

pseudo-second order rate kinetics. The XPS analysis confirmed that the adsorption of Cu(II)/or Cd(II) predominantly occurred through the hydroxyl groups present on the surface of BNMPTS. Moreover, the column reactor experiments result showed that very high breakthrough volume were obtained for the attenuation of Cu(II) and Cd(II) using 0.2 g and 0.5 g of the BNMPTS material. Moreover, the non-linear least square fitting were conducted using the Thomas equation and results indicated that very high loading capacity of Cu(II) and Cd(II) was achieved by the BNMPTS solid under the dynamic conditions; which further reaffirmed the affinity of BNMPTS towards the Cu(II) and Cd(II).

Furthermore, the BNMPTS and BNAPTES solids were effectively and efficiently employed in the elimination of micro-pollutants viz., tetracycline, triclosan and EE2 from aqueous solutions under the batch and column reactor operations. The pH dependent studies for these micro-pollutants using the BNMPTS and BNAPTES materials were conducted at a wide range of pH ~3.0 to 10.0. The percentage uptake of tetracycline by BNMPTS was very high in the pH range 3.2 to 7.0 and decreased sharply and reached to a very low removal at pH 10. On the other hand, the percentage uptake of tetracycline by BNAPTES showed almost a constant removal efficiency up until the pH 7-8 and then a noticeably decrease was observed. However, the decrease in efficiency using the BNAPTES was not that significant for tetracycline even at pH>7.3. This further inferred the potential applicability of BNMPTS and BNAPTES towards the attenuation of tetracycline from aqueous solutions using these materials. The effect of pH in the removal of triclosan by raw bentonite showed very limited implications in the elimination of triclosan from aqueous solution. However, the uptake of triclosan by BNMPTS and BNAPTES was remained almost constant from pH 3.21 to 7.01 but further increase in pH (pH>7.0), caused significant decrease in the uptake of triclosan by these two composite materials. The removal of triclosan was almost unaffected using BNMPTS and BNAPTES as the pH was increased from *Ca.* pH 3.21 to 7.01. However, the removal of triclosan was decreased abruptly at pH>7.0 and attained to a very low removal percentage at pH ~10. Therefore, a high uptake of triclosan around neutral pH conditions is providing an optimum pH conditions indicating BNMPTS and BNAPTES in the treatment processes for efficient removal of triclosan from aqueous

at neutral pH conditions. The pH dependent study of EE2 showed that the uptake of EE2 by the BNMPTS and BNAPTES was increased significantly with an increase in pH from 3.0 to 10.0. The high uptake of micro-pollutants by the BNMPTS and BNAPTES materials at wide range of pH was demonstrated due to the hydrophobic interaction between the micro-pollutant molecules and BNMPTS/or BNAPTES solids. Moreover, the dense grafted structure of BNMPTS and BNAPTES has enabled to trap significantly the micro-pollutants from the aqueous solutions and enhanced the elimination of micro-pollutants. On the other hand, it was observed that the pristine bentonite showed significantly low sorption efficiency as compared to the composite solids viz., BNMPTS or BNAPTES. This further inferred the greater applicability of these novel solids in the removal of micro-pollutants from aqueous solutions.

The initial sorptive concentration dependent study of tetracycline, triclosan and EE2 showed that BNMPTS and BNAPTES exhibited strong affinity towards the removal of these micro-pollutants. Further, the sorption isotherm of these micro-pollutants was obtained from the concentration dependence data showed that the sorption equilibrium of these micro-pollutants followed Langmuir adsorption isotherm. The effect of contact time in the removal of these micro-pollutants showed that rapid uptake of these pollutants was achieved and apparent equilibrium between the solid/solution phases was obtained within 120 minutes of contact for triclosan and EE2 and 180 minutes for tetracycline using these two solids. The kinetic modelling was conducted for these pollutants and results showed that the uptake of these micro-pollutants by the BNMPTS or BNAPTES fitted well to the PSO model compared to the PFO model. The applicability of PSO model showed that the tetracycline, triclosan and EE2 were bound onto the surface of the BNMPTS and BNAPTES materials by relatively stronger forces. Increasing the background electrolyte concentrations of NaCl (1000 times) had unaffected the removal percentage of these micro-pollutants by the BNMPTS and BNAPTES solids. This further inferred that the tetracycline, triclosan and EE2 were forming 'inner-sphere-complexes' at surface of solids having relatively stronger forces. Similarly, the presence of diverse co-existing cations viz., Mg(II), Mn(II), Ca(II) and Ni(II) and anions viz., ethylenediaminetetraacetate (EDTA), oxalic acid, phosphate and glycine

did not affect the percentage uptake of these micro-pollutants except the presence of EDTA. The presence of EDTA significantly affected the removal of tetracycline, triclosan and EE2 using BNMPTS and BNAPTES.

The column reactor operations showed that very high breakthrough volumes were obtained for the elimination of these micro-pollutants using 0.25 g and 0.5 g of the BNMPTS or BNAPTES materials. Moreover, the break through data was utilized to the Thomas equation and the Thomas constants were estimated using the least square non-linear fitting of column data. Result showed that on increasing the amount of the modified solids in the column, an increased in the loading capacity of these pollutants was obtained by BNMPTS and BNAPTES under the continuous flow systems. This again reaffirmed greater affinity of these solids towards the tetracycline, triclosan and EE2.

Additionally, applicability of these novel materials in the removal of micro-pollutants viz., tetracycline, triclosan and EE2 in real matrix sample (River water samples) was conducted under varied pH values. Results showed that the removal of these micro-pollutants was not affected as compared to the results obtained with purified water. These results showed the selectivity of solids towards these micro-pollutants and possible implacability in real matrix treatment.

Furthermore, the reusability of BNMPTS in the removal of Cu(II) showed that the percentage removal of Cu(II) was decreased from 97.8 to 88.9% after six replicates of adsorption-desorption cycles. Moreover, the reusability of BNMPTS and BNAPTES for the removal of tetracycline, triclosan and EE2 showed that the percentage removal of tetracycline decreased from 85.3 to 75.1% using BNMPTS and 82.4 to 73.1% using BNAPTES. Similarly, the percentage removal of triclosan was decreased from 96.4 to 85.3% using BNMPTS and from 96.5 to 84.2% using BNAPTES. The percentage removal of EE2 was decreased from 82.8 to 60.7.3% using BNMPTS and from 72.1 to 54.8% using BNAPTES while the materials were intended for six replicates adsorption-desorption cycles. Therefore, the studies indicated that BNMPTS and BNAPTES possessed greater stability and could be reutilized for successive operations in the removal of Cu(II), tetracycline, triclosan and EE2 from aqueous solutions. The studies showed that the novel and, possibly cost-effective functionalized solids possessed reasonably good suitability and

selectively in the removal of several heavy metal toxic ions along with several micro-pollutants from aqueous solutions. The materials could be further employed in the large-scale treatment of wastewaters contaminated with these pollutants at least at the 'Pilot Scale' treatment and the treatment process would be, possibly, sustainable and extended implacability.